Assessing the capacity of unoccupied aerial systems Structure-from-Motion (UAS-SfM) for monitoring forest and fuel attributes in California, USA for improved fire hazard land management



A thesis presented for the degree of Doctor of Philosophy

School of Geography and the Environment

Sean Reilly

Supervisors: Dr Imma Oliveras and Prof Yadvinder Mahli

Disturbance Ecology Lab





Looking out across the fire-shaped landscape at Pepperwood Preserve

Summary

Forest wildfires in California, USA historically played a beneficial ecological role in shaping landscape heterogeneity and driving ecological diversity. However, exacerbated by climate change and the expansion of the wilderness urban interface, over a century of federal wildfire suppression policies has given rise to elevated fuel loads in forests throughout the state such that half of California's forestlands now require restoration. The successful application of fuels reduction treatments on such a broad landscape scale depends highly upon targeting management efforts using accurate maps of fuel loading. This thesis, therefore, seeks to support these efforts through the development and assessment of an area-based machine learning modelling approach to predicting canopy fuel loads using data from unoccupied aerial system Structure-from-Motion (UAS-SfM). This thesis is comprised of four studies.

In the first study, I aimed to provide context for assessing the development of future fuels mapping methods. In this study, I conducted fuzzy cognitive mapping (FCM) with land managers to capture their decision-making around fire hazard mitigation and the role of information in these processes. From the FCM results, priority setting emerged as the most significant driver of management outcomes. While information consistently contributed to decision-making, and priority setting specifically, little agreement existed between interviewees on what information sources they utilize. However, they consistently identified accessibility and timeliness as the critical criteria for determining the utility of an information source.

In the second study, I developed a workflow for UAS-SfM data processing in the complex mixed forests of California and applied these data to monitoring the long-term impacts from a significant fire event. From this workflow, canopy metrics extracted from the UAS-SfM point cloud demonstrated strong relationships with airborne lidar (ALS) for the upper canopy with diminishing agreement at lower heights. In the fire impact testing, while upper canopy structure only exhibited minor changes with burn severity, spectral data from UAS-SfM captured significant persistent declines in vegetation health as measured by NDVI.

In the third study, I conducted area-based machine learning modelling of canopy fuel loads at sites across California using UAS-SfM predictors. These models performed well for the vertical fuel parameters of canopy base height (CBH), mean canopy height, and biomass, but displayed lower accuracy for the horizontal fuel parameters of leaf area index (LAI), canopy bulk density (CBD), and canopy cover. Variable selection proved consistent within each fuel parameter group, with the models for the vertical fuel parameters utilizing predictors related to the structure of the UAS-SfM data and predictors from the multispectral data and spectral indices for the horizontal parameters.

In the final study, I extended this area-based modelling approach to other remote sensing technologies, specifically terrestrial laser scanning (TLS), handheld mobile laser scanning (HMLS), and PlanetScope satellite spectral. This study sought to determine the greatest achievable performance of machine learning modelling of canopy fuels to provide context for the accuracies obtained from more accessible methods such as UAS-SfM. While TLS provided the highest accuracy across all parameters, UAS-SfM performance consistently came within 10% of TLS. Likewise, only 5% difference existed for any fuel parameter between the multispectral UAS-SfM data and the spectral data obtained from PlanetScope.

Together, these results demonstrate the utility of UAS-SfM as a potential mapping technology of forest fuel canopy loads. Further work should focus on removing the remaining technical barriers for the implementation of this technique in order to render it fully operationalizable in land management decision-making.

Acknowledgements

I owe this thesis to many people and my words here cannot sufficiently express my gratitude to each of them. First off, to Imma, for being the best supervisor I can imagine. Thank you for always being so supportive and understanding. I have grown tremendously as a researcher under your guidance, and it has been an honor to work with you. Likewise, to Dr. Matthew Clark and Dr. Lisa Bentley, at Sonoma State University. Thank you first and foremost for welcoming me into your project and trusting me with this work. I cannot thank you enough for providing me with this opportunity. I have loved every minute of getting to work with you and I am incredibly thankful for all that you have taught me. Together, the three of you shaped me into the researcher I am today and for that I am incredibly grateful.

Thank you as well to the Rhodes Trust. You have gone above and beyond in supporting me through this journey. The opportunities you have provided for me have surpassed anything of which I ever could have hoped.

To my mom and dad, you have given me so much that a thank you here can never capture. Thank you for always believing in me, encouraging me, and for a lifetime of support.

And most of all, to Maggie. Thank you for being by my side throughout all of this. You are my guiding light and I love you mountains.

Table of Contents

Chapter 1

Introduction 11
1. Mediterranean biomes and fire 12
2. Fire in California, USA 13
3. Land management for fire hazard mitigation 15
4. Social dynamics of fire management 18
5. Fuzzy cognitive mapping and thematic analysis for analyzing stakeholder decision-making 21
6. Fuel mapping methods 23
7. Machine learning 27
8. Thesis overview 29

Chapter 2

Promoting collective land management for wildfire mitigation through the identification of shared decision-making practices and barriers 54
Abstract 54
1. Introduction 55
2. Methods 57
2.1 Land manager stakeholder interviews 57
2.2 Fuzzy cognitive mapping (FCM) 59
2.3 Thematic analysis 62
3. Results 63
3.1 Fuzzy cognitive mapping 63
3.2 Social dynamics 66
3.3 Objectives, methods, and priority setting 68
3.4 Management planning and decision-making 71
3.5 Information and consultation 73
3.6 Funding and resources 76
4. Discussion 78
5. Conclusion 81
Supplement 87

Chapter 3

The Potential of Multispectral Imagery and 3D Point Clouds from Unoccupied Aerial Systems (UAS) for Monitoring Forest Structure and the Impacts of Wildfire in Mediterranean-Climate Forests 94
Abstract 94
1. Introduction 95
2. Methods 98
2.1 Study site 98
2.2. Data Sources 99
2.3. Data Analysis 101
3. Results 107
3.1. DTM and CHM Generation Capability Comparisons 107
3.2. Comparison of Forest Structure from UAS-SfM and ALS Point Clouds 110
3.3. Utility of UAS-SfM for Detecting Post-Fire Forest Change 113

4. Discussion 115
4.1. DTM and CHM Generation Capability Comparisons 115
4.2. Comparison of Forest Structure from UAS-SfM and ALS Point Clouds 117
4.3. Utility of UAS-SfM for Detecting Post-Fire Forest Change 118
5. Conclusions 120

Chapter 4

Unoccupied aerial system (UAS) Structure-from-Motion canopy fuel parameters: Multisite area-based modelling across forests in California, USA 131
Abstract 131
1. Introduction 133
2. Methods 137
2.1 Study sites 137
2.2 Data sources 139
2.3 Machine learning modelling 145
3. Results 149
3.1 Field-based plot-level aboveground biomass and canopy fuel parameters 149
3.2 Model comparison 151
3.3 Random forest model analysis 153
3.3 ALS comparison to UAS-SfM data 157
3.4 Model testing at novel site 158
4. Discussion 159
4.1 Vertical structure: Biomass, CBH, mean height 160
4.2 Horizontal structure: LAI, CBD, canopy cover 161
5. Conclusion 165
Supplement 182

Chapter 5

Area-based random forest modelling of canopy fuels across the forests of California, USA: Assessment of structural and spectral remote sensing performance 189
Abstract 189
1. Introduction 191
2. Methods 196
2.1 Study sites 196
2.2 Data sources 197
2.3 Data processing 201
2.4 Random forest modelling 205
3. Results 207
3.1 Datasets 207
3.2 Model testing 209
3.3 Structural data fusion ..... **Error! Bookmark not defined.**
4. Discussion 213
4.1 Structural remote sensing methods 213
4.2 Spectral remote sensing methods 215
5. Conclusion 217
Supplement 230

Chapter 6

Synthesis 235
1. Thesis motivation 236
2. Results 236
3. Limitations and future directions 241
3.1 Connecting research to practitioners 241
3.2 Tree delineation 242
3.3 Subcanopy fuels and other data sources 244
4. Conclusion 245

List of Study Figures and Tables

Promoting collective land management for wildfire mitigation through the identification of shared decision-making practices and barriers 54
Fig. 2.1 Fuzzy cognitive mapping (FCM) workflow diagram. 60
Table 2.1 Social cognitive map (SCM) qualitative aggregation category groupings 61
Fig. 2.2 Component accumulation curve. 63
Table 2.2 SCM component metrics 64
Fig. 2.3 Cognitive interpretation diagram (CID) for social cognitive map (SCM) with aggregated components 65
Table 2.3 Social cognitive map (SCM) aggregate component metrics 66
Fig. 2.4 Objectives, methods, and priority setting cognitive interpretation diagram (CID) 68
Fig. 2.5 Management planning and decision-making cognitive interpretation diagram (CID) 71
Fig. 2.6 Information and consultation cognitive interpretation diagram (CID) 73
Fig. 2.7 Funding and resources cognitive interpretation diagram (CID) 76
Table 2.S1 FCM participant component recoding 87

The Potential of Multispectral Imagery and 3D Point Clouds from Unoccupied Aerial Systems (UAS) for Monitoring Forest Structure and the Impacts of Wildfire in Mediterranean-Climate Forests 94
Fig. 3.1 Study site location at Pepperwood Preserve in California, USA 98
Table 3.1 Cloth simulation filter (CSF) parameter and Normalized Difference Vegetation Index (NDVI) threshold testing ranges 102
Fig. 3.2 Point cloud processing workflow. 104
Fig. 3.3 CSF parameter effect on DTM accuracy 107
Fig. 3.4 Boxplot of UAS-SfM DTM 1-m cell error by vegetation type for DTM obtained from optimized CSF parameters as compared to the ALS DTM 109
Fig. 3.5 Aboveground point cloud height distributions from complete study site data by forest type as measured by ALS and UAS-SfM height normalized using the ALS DTM 110
Table 3.2 Regression slope coefficients and Pearson's r correlation coefficient for point cloud grid metrics comparison between airborne laser scanner (ALS) data and unoccupied aerial system Structure-from-Motion (UAS-SfM) height normalized using the UAS-SfM digital terrain model (DTM) 111
Table 3.3 Regression slope coefficients and Pearson's r correlation coefficient for point cloud grid metrics comparison between ALS data and UAS-SfM height normalized using an ALS DTM 111
Fig. 3.6 Comparison of Pearson correlations for point cloud height metrics extracted from UAS-SfM height normalized using either UAS-SfM DTM or ALS DTM 112
Table 3.4 Kruskal–Wallis one-way analysis of variance results for 2017 Tubbs fire burn severity impact metrics 113
Fig. 3.7 Relationship among pre-fire ladder fuels derived from 2013 ALS data and 2017 Tubbs fire burn severity by forest types 113
Fig. 3.8 The impact of the 2017 Tubbs Fire on 95th percentile (P_{95}) and 75th percentile heights (P_{75}) and P_{75} mean NDVI by MTBS fire severity in forest types 114

Unoccupied aerial system (UAS) Structure-from-Motion canopy fuel parameters: Multisite area-based modelling across forests in California, USA 131
Fig. 4.1 Map of study sites 137
Fig. 4.2 Data processing workflow 139
Table 4.1 UAS-SfM structural and spectral predictors. 143

Table 4.2 Cross validation spatially-blocked group distance thresholds from spatial variogram partial sill range 145
Fig. 4.3 Field-based plot-level aboveground biomass and canopy fuel parameter estimates across all sites and for each individual site 149
Fig. 4.4 Field-based plot-level parameter relationships 150
Table 4.3 Models of canopy fuel parameters across all study sites 151
Fig. 4.5 Model cross validation error density 152
Fig. 4.6 Random Forest cross-validated predictions versus observed values 153
Fig. 4.7 Pepperwood random forest fuels prediction maps 154
Fig. 4.8 Relative scaled importance of top five predictors for random forest models 155
Fig. 4.9 Random forest all-sites model accuracy produced using different predictor variable subsets, including the full-predictor dataset. 156
Fig. 4.10 UAS-SfM vs ALS model performance 157
Table 4.4 Model accuracy when applied to a novel site withheld from training 158
Fig. 4.11 Saddle Mountain random forest model transfer accuracy 158
Table 4.S1 Anova testing mean differences in R^2 and RMSE among modelling methods 182
Fig. 4.S1 Individual site model comparisons 183
Fig. 4.S2 Relative scaled importance of top five predictors for SVM models 184
Fig. 4.S3 Relative scaled importance of top five predictors for LM with forward selection 185
Fig. 4.S4 Random forest variable importance for vertical distribution data subset models 185
Fig. 4.S5 Random forest variable importance for raster-based spectral data subset models 186
Fig. 4.S6 Random forest variable importance for height band spectral data subset models 186

Area-based random forest modelling of canopy fuels across the forests of California, USA: Assessment of structural and spectral remote sensing performance 189
Fig. 5.1 Location of study sites within California, USA 196
Table 5.1 Structural predictors 201
Fig. 5.2 Demonstration of the influence of dimension on voxelization for a conifer tree extracted from UAS-SfM at Pepperwood 202
Fig. 5.3 Demonstration of fusion, decimation, and voxelization processes for a 3 m wide transect from a plot at Saddle Mountain 203
Table 5.2 Spectral predictors computed per band and spectral index 204
Table 5.3 Cross validation spatially-blocked group distance thresholds from spatial variogram partial sill range 205
Fig. 5.4 Comparison of vertical distributions among strutural data methods 207
Fig. 5.5 Comparison of NDVI distributions between spectral data methods 208
Fig. 5.7 Mean R^2 model performance metrics among structural and spectral predictor combinations 209
Fig. 5.8. Comparison of model relative variable performance for fuel parameters using TLS, HMLS, and UAS-SfM structural sensors and UAS and Planet spectral sensors 211
Fig. 5.S1 Distribution of field measurements of fuel parameters by site 230
Fig. 5.S2 Comparison of point cloud (pnt) and voxel size model performance 231
Fig. 5.S3 Comparison of point cloud and voxel size model performance for lidar and UAS-SfM fusion data 232
Fig. 5.S4 Mean R^2 model performance metrics among structural and spectral predictor combinations, including structural fusion datasets 233

Chapter 1

Introduction

1. Mediterranean biomes and fire

Only five Mediterranean climate regions exist globally. These are found surrounding the Mediterranean Sea and in parts of Australia, California, Chile, and South Africa (Rundel et al., 2016). These regions all possess a strong seasonal climate, characterized by mild, wet winters and hot, dry summer droughts (Keeley et al., 2011). This climate pattern arose as early as the middle of the Miocene Epoch (~15 Ma) and has been largely stable since that time (Cowling et al., 2015; Rundel et al., 2016). The stability of this climate regime is thought to have fostered an explosion of plant development (Cowling et al., 2015). Consequently, all five Mediterranean biomes are among the top 25 global biodiversity hotspots (Myers et al., 2000).

The singular timing of precipitation in Mediterranean climate regions places unique stresses on the vegetation that inhabits these regions. During the summer drought period, which can last up to ten months, plants must maintain adequate water supplies for photosynthesis and productivity (Nardini et al., 2014). These pressures drive speciation and the high biodiversity of the region. However, on larger scales, local environmental variables, such as geology, alone are insufficient to explain the distribution of ecosystems and community assemblages (Keeley et al., 2011). Instead, regional diversity arose during the Quaternary Period primarily due to fire and climate change (Cowling et al., 1996). Fire plays a critical role in these landscapes due to the unique nature of the growing season and long summer drought. Vegetation grows early in the year to take advantage of the boundary conditions between the precipitation of the winter and the warmth of the summer, then subsequently dries during the summer, thus becoming increasingly flammable as the year progresses (Keeley et al., 2011). As a result of these seasonal patterns, many distant plant families have developed similar fire adaptations and life histories (Rundel et al., 2016).

In Mediterranean climates, fire serves as the moderator between different vegetation assemblages. This concept, known as alternative stable states, was first proposed by Lewontin (1969). He conceptualized ecosystems as multi-dimensional spaces defined by a series of environmental variables, such as precipitation, temperature, and, in this case, fire regime. For a given set of environmental

parameters, the vegetation community will shift in a specific, consistent direction until it reaches a place of stability. The question that arises, however, is if this stability point represents a globally stable state for the system or if alternative states may also exist. From this conceptualization arises the hypothesis that "communities can be found in one of several possible alternative stable states" (Beisner et al., 2003). A community will remain in one state until it is subjected to a sufficiently significant perturbation to shift it to a new stable position, at which point a new community assemblage will take its place (Beisner et al., 2003; Petraitis and Dudgeon, 2004).

Much of Mediterranean bioregions possess a continuum of alternative stable states from grassland to shrubland to forest, moderated by fire severity and frequency (Batllori et al., 2015). Globally, fire moderates between savannah and forest in areas with moderate rainfall and seasonality (Staver et al., 2011). Studies from Mediterranean regions around the world have demonstrated the relationship between fire and alternative vegetation assemblages (e.g., Acácio et al., 2009; Odion et al., 2010; Santana et al., 2010; Tsafrir et al., 2019). The unique fire attributes of different assemblages can generate self-maintaining fire regimes to perpetuate a specific species composition and preclude the colonization of others (Odion et al., 2010; Santana et al., 2010).

2. Fire in California, USA

While not all of California falls within the unique characteristics of the Mediterranean climate ecoregion, over half of the vegetation in California is fire maintained to some degree (Barbour and Major, 1988; Sugihara and Barbour, 2006) and California's unique flora developed following the emergence of its Mediterranean climate and fire regime (Rundel et al., 2016). Persistent dry air masses covering the state result in high fire risk for the entirety of the summer season (Minnich, 2006). The ensuing fire regime historically possessed high spatial variability which drove landscape ecosystem structure heterogeneity (Beaty and Taylor, 2008).

Fire return intervals ranged from seven to 610 years by vegetation assemblage (Van de Water and Safford, 2011). However, for California's dry productive forests, which include the widespread

conifer and mixed oak woodlands, fire return interval averaged around 12 years historically (Van de Water and Safford, 2011). Extensive research has been conducted to chart these historical fire return intervals using methods such as fire scare dendrochronology (e.g., Beaty and Taylor, 2008; Swetnam et al., 2009; Taylor and Skinner, 2003). From these reconstructions, it has been estimated that 1.8 million ha, or roughly 4% of the state, burned annually prior to 1800 (Stephens et al., 2007). As a result, smoky skies blanketed California for most of the year (Stephens et al., 2007). When burning occurs at this extent and regularity, fire becomes a self-limiting process. Fires reduce the amount of fuels available to successive fires, thus reducing their extent and severity (Collins et al., 2009). In the context of wildfires, fuels refer to any biomass, live or dead, available for a fire to consume (Husari et al., 2006; Reinhardt et al., 2008). Native Americans embraced this low-mixed severity frequent fire regime and employed fire as a tool to shape the landscape (Keeley, 2002; Klimaszewski-Patterson and Mensing, 2020). They employed fire for "keeping the country open, managing wildlife, manufacturing cultural items, and enhancing the growth of basketry material," among other purposes (Anderson, 2006).

All of this changed, however, when the area was colonized by Europeans. Fire return intervals began to lengthen immediately with the loss of these traditional burning practices, but the complete transformation of the fire regime occurred following the implementation of aggressive fire suppression policies in the 1900s (Forest Climate Action Team, 2018). Fire histories from conifer forests in Yosemite demonstrate the effective elimination of fire following fire suppression (Taylor and Scholl, 2012), while elsewhere fire return intervals increased by decades or centuries (Taylor, 2010; Taylor and Skinner, 1998). With the loss of fire, vegetation structure changed, growing denser, and wide scale beta diversity decreased (Perry et al., 2011; Taylor, 2010, 2000; Taylor and Skinner, 2003). Increased stand density has the secondary effect of increasing ecosystem water uptake, thereby exacerbating dry conditions (Perry et al., 2011). In some places, ongoing fire exclusion has allowed the community to shift towards an alternative stable state with more shade tolerant and fire intolerant species beginning to replace the historically occurring vegetation (Taylor, 2000; Taylor and Skinner, 2003).

As a result of these increasing stand densities, and, consequently, fuel loads, California has experienced an increase in large wildfires (Dennison et al., 2014; Miller et al., 2012). Many parts of the state observed increases in stand replacing high severity fires between 1984 and 2006 (Miller et al., 2009). Ongoing suppression drives a self-reinforcing feedback loop, the "firefighting trap," in which ever increasing fuel loads allow the few fires that do escape suppression to burn with ever increasing intensity and extent (Calkin et al., 2015; Moreira et al., 2020).

Ongoing climate change further exacerbates this cycle. Between 1984 and 2015, climate change is estimated to have nearly doubled the amount of area burned across the western United States (Abatzoglou and Williams, 2016). Since the mid-1990s, California has experienced a strong trend of increasing fire weather and exacerbated fuel conditions from earlier and warmer springs (Collins, 2014; Westerling, 2006). Fire weather arises from a combination of air temperature, low humidity, high wind speed, and low/no rainfall (Urbieta et al., 2015). Projections indicate California may experience as much as a 50% increase in extreme wildfire events by the end of the century as a result of ongoing climate change (Westerling, 2018). Increasing temperature and aridity, coupled with increased fire severity and frequency, pose a serious threat to woody species (Enright et al., 2015).

3. Land management for fire hazard mitigation

Simulations of large-scale fuels management programs indicate that taking management actions could substantially reduce the worst fire related impacts of climate change (Westerling, 2018). An estimated 15 million acres of forests in California, comprising approximately half of the state's forestlands, require restoration (Forest Climate Action Team, 2018). Two thirds of these forests lie on federal lands while the remaining five million acres consists of a mix of public and private lands (Forest Climate Action Team, 2018). Fortunately, despite the daunting scale of this challenge, there is significant political and public motivation to address these needs and California's state government has committed to treating one million acres per year by 2025 (Knight et al., 2022).

The primary objective of land management actions to mitigate fire hazard is to alter the behavior of potential future fires, rather than exclude fire. In particular, treatments aim to reduce fuel loads so fires burn predominantly along the ground and do not climb up into the canopy and kill trees (North et al., 2015b). Fire is able to leave the ground and ignite the canopy, an event known as torching, when surface flames reach a critical height, as determined by the forest canopy base height (CBH) and moisture content (Agee and Skinner, 2005). Once the crown torches, fire spreads between tree tops provided the crown is sufficiently dense, which is related to canopy bulk density (CBD), and has high canopy cover to enable the fire to travel sufficiently quickly to sustain ignition (Agee and Skinner, 2005).

The four main principles of fuels management, as established by Agee and Skinner (2005), are: (1) "reduce surface fuels," (2) "increase height to live crown," (3) "decrease crown density," and (4) "keep big trees of resistant species." Fuel loads can be modified through general reduction in their quantity or through disruption of their vertical and horizontal continuity (Husari et al., 2006). Fuels can be categorized by stratum, such as canopy, shrub, ground, etc. (Van Wagtendonk, 2006). However, for management purposes, they are usually separated into broader categories of surface, ladder, and canopy fuels (Husari et al., 2006). Ladder fuels, often comprised of vegetation such as small trees or shrubs, exist between the surface and canopy fuels and provide a conduit for fire to reach the canopy, thereby increasing the likelihood of torching (Menning and Stephens, 2007).

The principal methods for fuels reduction are thinning and prescribed fire. Thinning includes any method of mechanical or physical biomass removal, including for commercial purposes (Stephens et al., 2009). Thinning operations must consider what to do with the resulting biomass. If this biomass is left in the forest in slash piles, it can actually result in increased burn severity before the biomass degrades, a slow process which can take several years (Stephens et al., 2009; Wimberly et al., 2009). Consequently, treatments that include some form of post-thinning prescribed burning result in greater reduction in fire impact than thinning alone (Safford et al., 2009). For example, Ritchie et al. (2007) found the greatest post-fire tree survival in areas in which they had implemented both treatment methods, lower survival in areas with only thinning, and little to no survival in areas without treatment. Safford et al. (2009) found

canopy fires reduced to ground fires within 50 m of passing into a treatment block and tree survival increased by 60%.

Stephens et al. (2023) provides a comprehensive analysis of forest restoration treatment effectiveness from a 20 year study at an experimental forest in the Sierra Nevada mountains of California. They tested mechanical, fire, and combined treatments. They found that mechanical treatment could generate revenue through selective logging. Mechanical and fire treatment was essentially revenue neutral and produced biotic conditions most similar to historical conditions.

Carefully guided management must balance the limitations of treatment methods. In most forest conditions, both treatments produce negligible impacts on other ecosystem attributes (Stephens et al., 2012). However, the combination of mechanical thinning with prescribed burning can impact tree health and survival if ground fire heat intensity rises too high due to increased fuel loads from the thinning operation (Collins et al., 2014). Additionally, prescribed fire, in particular, faces many logistical barriers to implementation. Aside from the potential for escape and resulting liability, managers must carefully manage smoke impacts on neighbouring communities (Miller et al., 2019). Consequently, it can be prohibitively expensive to implement in proximity to residential areas (Florec et al., 2020). The key challenge with any such management action, however, is maintenance. As soon as a treatment is completed, the forest begins to grow again and fuels reaccumulate (Kauffman, 2004). This means that treatment effectiveness diminishes with the passage of time so, once initiated, managers must implement a plan for repeated management actions (Agee and Skinner, 2005; Stephens et al., 2023, 2012). Consequently, the long-term objective of management should be to establish restored firesheds in which ongoing managed fire can replicate historical fire regimes and preserve the reduced system fuel level without the need for ongoing costly mechanical intervention (North et al., 2015b, 2012).

Treatment effectiveness increases nonlinearly with scale and managers can employ treatments most successfully by targeting a percentage of the landscape. In fact, multiple studies have demonstrated that maximum reduction in fire intensity can be achieved through treatment of 10-20% of the landscape (Ager et al., 2010; Collins et al., 2013). In an assessment of the effectiveness of the California million

acre per year management objective, Daum et al. (2024) found significant differences in modelled fire severity depending on how well this effort could be targeted by fuel loading. Over a 100-year window, treating 1,000 km^2 per year randomly resulted in a 30% reduction in stand-replacing fires, which are fires that kill all trees within a given area. However, targeting this management to sites with the highest fuel loads increased this rate of reduction in stand-replacing fires to 90%. Due to terrain and other barriers to access, mechanical treatment cannot be realistically undertaken in all areas (North et al., 2015a). Even when limiting their model treatments by these constraints, Daum et al. (2024) still observed a significant improvement in the reduction of stand-replacement. In addition, through the integration of fire and land management processes, fuel treatments may actually enhance overall ecosystem health (Reinhardt et al., 2008). For example, fuel treatments can increase forest resilience to bark beetle infestations through lowered stand densities and removal of damaged trees (Moghaddas et al., 2018).

The challenge for land managers, therefore, centers on identifying where and how to implement treatments. Targeted treatments on this scale require comprehensive field data since fuel parameters significantly affect modelled fire behaviors, and, therefore, management targets (Collins et al., 2013). Even with good models, identifying the extent and location of strategic fuel treatments still presents a significant challenge (Agee and Skinner, 2005). Despite the previously mentioned cost-parity in treatment, management planning usually occurs under conditions of limited resources, rendering treatment cost-effectiveness a paramount consideration (Elia et al., 2016). Additionally, managers must frequently balance competing objectives, principally fuels reduction and carbon sequestration. Designing management practices to satisfy multiple objectives and prioritize where management occurs requires extensive information and decision-making tools (Ager et al., 2013; Driscoll et al., 2010).

4. Social dynamics of fire management

Management decisions do not occur in an ecological vacuum, separate from social dynamics. Instead, as a result of the risk fire poses to communities, fire and human landscapes need to be addressed as a coupled socio-ecological system (Moritz et al., 2014). Such a framework highlights the links between

human practices and the natural environment to aid in the development of pathways towards a "more sustainable coexistence with wildfire" and the development of fire-adapted communities (Moritz et al., 2014; Schoennagel et al., 2017). As mentioned previously, one-third of the forestlands requiring restoration in California are owned by private individuals, corporations, and/or local governments (Forest Climate Action Team, 2018).

Much of this private and locally owned area is classified as wilderness-urban interface (WUI). In the United States, the WUI is defined as areas with housing densities greater than one house per acre in close proximity to, or intermixed with, wildland vegetation (Stewart et al., 2007). It represents the fastest growing land use type in the United States and much of this growth is occurring within fire prone landscapes (Radeloff et al., 2018). The desire for deconcentrated housing and natural amenity access drives this expansion (Hammer et al., 2009). These development patterns have a significant impact on fire regimes. For example, patterns and densities of human development modulate the frequency of fire ignition, with moderate development levels resulting in the greatest number of ignitions (Syphard et al., 2007). Fires often cross between land tenures in the wilderness-urban interface (Ager et al., 2017), indicating the need for multi-actor management engagement to implement the landscape scale treatments previously discussed.

An important factor in WUI fire management considerations is community vulnerability to fire. The principle model of vulnerability in this context is developed from the "hazards-of-place" model proposed by Cutter (1996). This model merged prior conceptualizations of risk relating to exposure and biophysical conditions with social attributes that determine community response and capacity. By combining the two, fire vulnerability can be analysed as arising from the local holistic socio-ecological system. A community's vulnerability, therefore, constitutes the hazard due to local physical attributes, such as fuel loading, augmented by the "social fabric of the place" (Cutter et al., 2003). Kolden and Henson (2019) simplified their vulnerability analysis from this hazards-of-place model for fire to three main components: (1) "Exposure to the hazard," (2) "sensitivity of the population exposed (i.e., susceptibility to negative impacts)," and (3) "adaptive capacity (i.e., the ability to prepare for and/or

recover from a wildfire based on available resources).” Using this conceptualization, they demonstrated how community-wide fuels management can address all three components of vulnerability, especially as it relates to its most vulnerable and least capable members.

Residents of the WUI comprise a heterogenous group, which presents a significant barrier to such cohesive management. Paveglio et al. (2015) established four main archetypes for inhabitants of the WUI. These constitute a spectrum from formalized suburban communities to resource-dependent working landscapes. These four archetypes are differentiated primarily by increasing “ruralness” and decreasing formal structure. They also possess a spectrum of attributes related to management and governance capacity (Paveglio et al., 2015). As a result, specific efforts to foster community management must target the unique attributes of the community in question (Edgeley et al., 2020; Paveglio et al., 2019). The predisposition of residents to align themselves with others and groups sharing similar views on management and wildfire shape WUI social network capacity and structure (Fischer and Jasny, 2017). This can form a collaboration barrier between diverse organizations, individuals, and/or groups. In addition, the arrival of new landowners can disrupt the composition of archetypes and values within a given WUI community, especially if they possess divergent views on issues such as wildfire management (Butsic et al., 2015). This social heterogeneity tends to translate into an increased diversity of forest conditions as different landowners undertake varying degrees of management with different objectives (Charnley et al., 2017).

Overcoming this diversity and bringing collaborative management to WUI communities involves bridging community-individual scales (Meldrum et al., 2018). Collaborative action networks must unify the multiple objectives, capacities, and levels of trusts brought by the constituent members (Urgenson et al., 2017). Social capital and cohesion can be fostered through enhancing place attachment and management planning (Bihari and Ryan, 2012). An important aspect of fostering collective management is understanding individual motivations for undertaking, or foregoing, management actions. As a first order criteria, increased perception of wildfire risks corresponds with a higher likelihood of engaging in mitigation (Brenkert-Smith et al., 2012). Landowners’ perceptions of risk have been shown to be

positively related to real world conditions (Olsen et al., 2017), but they consistently perceive lower levels of risks than professionals given the same landscape conditions (Meldrum et al., 2015). Building upon risk perception, landowners weigh the significance of a certain risk in the context of the potential costs and benefits from undertaking mitigation measures (McFarlane et al., 2011). Other factors that promote individual engagement with wildfire management include community-wide risk and familiarity with community fire management planning (Wolters et al., 2017).

Management decision-making in the WUI does not take place solely between residents. Often professional land managers, either from government agencies or NGOs, drive management actions. The choice of mitigation treatment, and its ultimate success, depends heavily on public support (Brunson and Evans, 2005). This, in turn, hinges on public trust in managers and their ability to successfully implement a given treatment (Toman et al., 2011; Vogt et al., 2005). Managers and organizations, therefore, must invest in fostering this trust to increase their capacity. Perceived alignment of values between landowners and agencies significantly increases the public's perceptions of managers' trustworthiness and capacity (Ghasemi et al., 2020; Vaske and Absher, 2007). In addition, trust depends on the public perception of cohesion across agencies and scales (Rasch and McCaffrey, 2019). Therefore, increased alignment between agencies can serve to promote collaboration within communities. Consequently, further research is needed to identify "pathways" to fire adaption that function across local perspectives and values (Carroll and Paveglio, 2016).

5. Fuzzy cognitive mapping and thematic analysis for analyzing stakeholder decision-making

Since understanding pathways for enhanced collaboration plays a critical role in advancing collective management across WUI stakeholders, a more thorough understanding of decision-making commonalities across the network of actors is greatly needed. Participatory mapping, a process engaging stakeholders to capture systemic dynamics, provides a broad methodology through which these commonalities can be identified (Voinov and Bousquet, 2010). Fuzzy cognitive mapping (FCM) is one

such method that has been employed successfully in enhancing understanding of socio-ecological systems (Gray et al., 2015).

This technique involves capturing each participant's perceptions of causal relationships through cognitive maps which can then be aggregated to determine commonalities across groups and individuals (Özesmi and Özesmi, 2004). Axelrod (1976) first proposed the concept of cognitive mapping. He conceptualized that individual decision-making could be captured in graphical form using a network of concepts connected by arrows to depict causation. Kosko (1986) extended the work of Axelrod by integrating fuzzy, or uncertain, causality into the system. Using this method, participants identify all components which they associate with the research topic. They then draw connections between these to establish the relationship between components (Özesmi and Özesmi, 2004). Through the application of methods from graph theory, these participants' maps can be converted to matrices which permit further computational evaluation of component importance (Gray et al., 2015; Özesmi and Özesmi, 2004). Additionally, individual participants' maps can be combined through matrix addition to form a map representing the combined understanding of the system in question (Özesmi and Özesmi, 2004).

This technique captures "stakeholders' cognitive perceptions about complex ecosystem functions," thereby providing critical knowledge in guiding decision-making and management planning efforts (Kontogianni et al., 2012). FCM is well suited for usage across demographics due to its low complexity and ease of comprehension (Papageorgiou and Salmeron, 2013; van Vliet et al., 2010). FCM provides a means by which to assist communities in organising and communicating their collective opinions on management (Gray et al., 2015; Singer et al., 2017). FCM methods have been employed in natural hazard mitigation research (e.g., Samarasinghe and Strickert, 2013; Santoro et al., 2019) and in environmental decision making (e.g., Gray et al., 2014; Li et al., 2016). For wildfires, FCM has been applied to questions relating to social perceptions and drivers of wildfire risk, with the aim of modelling scenarios to target management actions (Devisscher et al., 2016). However, previously FCM had not been applied specifically to understanding decision-making processes on wildfire management among diverse stakeholders.

Qualitative narrative methods can deepen the meaning of FCM results by allowing participants to expand on the significance of specific connections or components (Gray et al., 2015). Thematic analysis is well suited for this purpose due to its flexibility (Clarke and Braun, 2017). Thematic analysis is a "method for identifying, analysing, and reporting patterns (themes) within data" (Braun and Clarke, 2006). The thematic analysis process involves coding each line of an interview by subject matter then identifying themes from these results (Thomas and Harden, 2008). From this process, common themes across participants may be identified from the manner in which they discuss components or connections within the system.

6. Fuel mapping methods

As discussed previously, in addition to more general attributes such as forest type and spatial scale, management optimization depends on fuel loading and structure (Reinhardt et al., 2008). Fire models, likewise, rely on accurate fuel spatial data (Andrews and Queen, 2001) and their outputs can be strongly influenced by fluctuations in fuel parameterization (Collins et al., 2013). Therefore, understanding the distribution of fuels within a forest is critical in any effort to utilize modelling or mapping in management decision-making (Arroyo et al., 2008; Chuvieco et al., 2020).

A spectrum of methods, reflecting the development of scientific capacity and technologies, exists for the quantification of fuels. Originally, fuels were mapped manually through exhaustive field survey campaigns that required excessive effort prohibiting widescale deployment (Arroyo et al., 2008). However, these field methods are still frequently utilized to accurately establish reference conditions to which other methods are compared (e.g., Filippelli et al., 2019). Fuels can also be modelled along environmental gradients, but the model building process requires a significant input of time and data to produce accurate results (Arroyo et al., 2008). These techniques have largely been replaced, however, with remote sensing methodologies. The spatial coverage of these methods means they are well suited for addressing the scale of information required for fuel management (Arroyo et al., 2008).

Remote sensing refers to the "acquisition and measurement of information about certain properties of phenomena, objects, or materials by a recording device not in physical contact with the features under surveillance" (Khorram et al., 2012). This term applies to technologies used in myriad fields, such as medical imaging. However, in environmental contexts, remote sensing generally refers to the use of sensors for measuring attributes of the Earth's surface (Khorram et al., 2012). Remote sensing methods are widely utilized to map fuel characteristics, including biomass and fuel continuity (Chuvieco et al., 2020).

Satellite passive sensors, such as the image sensors aboard the Landsat satellites, collect electromagnetic information about the Earth's surface (Arroyo et al., 2008; Khorram et al., 2012). These passive sensors cannot penetrate canopy cover or measure vertical structure (Arroyo et al., 2008; Riano et al., 2002). Therefore, fuel mapping using satellite data must employ inferential approaches to determine fuel loads. The two most common methods are vegetation index mapping (e.g., Jia et al., 2006) and landcover characterization (e.g., Stefanidou et al., 2022). The first method involves categorizing fuels into live and dead biomass using vegetation indices (Hernandez-Leal et al., 2006). More advanced methods attempt to extend the use of these indices further by grouping fuels by their seasonal phenology changes (Bajocco et al., 2015). The second method produces a map of fuel loads by classifying image pixels into vegetation types and then applying externally derived fuel density data to each class (Aragoneses and Chuvieco, 2021; e.g., Riano et al., 2002; Shaik et al., 2022; Stefanidou et al., 2022). While both methods can provide useful data, they are limited by their inability to measure fuel loads directly.

This role is filled by active sensors, the principle of which is lidar. Lidar, or light detection and ranging, sensors emit laser pulses at an object and record the time it takes the pulse to return to the sensor (Reutebuch et al., 2005). The object's precise 3D location in space can be ascertained from the length of this passage of time, the location of the sensor, and the scanner's orientation (Reutebuch et al., 2005). By scanning the laser across the object, a point cloud can be generated which captures the entire object's structure. For mapping of forest structure, lidar can either be collected aerially or on the ground ("terrestrial"). Lidar sensors mounted to airplanes (airborne lidar systems or ALS) sweep the forest and

produce continuous point clouds of forest 3D structure over large extents (Reutebuch et al., 2005). Accurate measurements of fuel metrics, including canopy base height and ladder fuel density, can be derived directly from these point clouds (e.g., Andersen et al., 2005; Forbes et al., 2022; Kramer et al., 2014; Mauro et al., 2021). However, the expense of ALS collection significantly limits the utility of this method for most management decision-making applications (Chuvieco et al., 2020).

Terrestrial lidar can be collected either with a tripod mounted sensor (TLS) or using a handheld mobile laser scanner (HMLS) (Forbes et al., 2022). TLS sensors are large and cumbersome units that collect single rotating scans from a fixed tripod point. Multiple scans can be registered to provide continuous coverage over a given area, but, due to the effort and time associated with this process, this extent is limited to the plot scale and, therefore, of limited utility for fuels mapping. However, TLS provides the highest resolution of any of the remote sensing data sources listed here, with the potential for accuracies measured in millimeters (Disney, 2019; Wilkes et al., 2017). TLS has been well demonstrated in its ability to measure forest attributes related to fire (Chen et al., 2016; García et al., 2011; Hillman et al., 2021; Taneja et al., 2023).

HMLS sensors, in contrast, are continuously walked through the forest by an operator, thereby allowing for faster collection of terrestrial lidar data, though data collection extent is still limited (Ryding et al., 2015). These sensors make use of a technology from robotics known as simultaneous localization and mapping (SLAM) which provides a means for the incremental construction of a map of an environment, and identification of one's location within that space, without prior information (Durrant-Whyte and Bailey, 2006). Though lower resolution than TLS, the produced point cloud still possess high resolution and at a fraction of the cost (Forbes et al., 2022). HMLS has been successfully employed in forest fuel studies and, as a relatively new technology, is still undergoing significant improvements in sensor power (e.g., Forbes et al., 2022; Hoffrén et al., 2024; Kang et al., 2024).

While not utilized in this thesis, spaceborne lidar, such as the Global Ecosystem Dynamics Investigation (GEDI) sensor aboard the International Space Station (ISS), presents an emerging technology with significant potential for future vegetation monitoring efforts (Potapov et al., 2021). This

sensor captures full-waveform lidar profiles and has been optimized for measuring forest structure, even under high canopy cover (Hoffrén et al., 2023; Lang et al., 2022). It collects 25 m diameter footprint samples at 60 m intervals along eight transects spaced 600 m apart to generate a 4 km wide measurement swath along the path of the ISS (Rishmawi et al., 2022). Studies have utilized GEDI data in a broad range of ecological applications such as canopy height mapping (e.g., Lang et al., 2022; Potapov et al., 2021; Rishmawi et al., 2022), fuels type classification (e.g., Hoffrén et al., 2023; Myroniuk et al., 2023), and biomass modelling (e.g, Silva et al., 2021). The GEDI instrument began sampling in 2018 and was temporarily decommissioned in 2023 but has resumed operation as of April 2024. Due to the nature of the spacing of the GEDI footprints and the ISS orbital path, GEDI does not provide continuous coverage, as compared to spectral satellite sensors, and temporal resolution varies by location (Blumenfeld, 2020).

Another emerging remote sensing technology, Structure-from-Motion photogrammetry, has arisen which may fill the void of low-cost 3D point cloud acquisition at spatial scales sufficient to inform management. Photogrammetry, the derivation of measurements from images, originated in the 1850s following the advent of photography (Konecny, 1985). In 1903, Sebastian Finsterwalder produced the first photogrammetric topographic map using images of a river valley (Konecny, 1985). Traditional photogrammetry methods determine the 3D location of points from overlapping images using stereo matching algorithms (Hirschmuller, 2008; Remondino et al., 2014; Scharstein and Szeliski, 2002). This method can quantify metrics such as above ground biomass (Filippelli et al., 2019) and vertical fuel structure (Marino et al., 2018) with similar accuracy to ALS.

The advent of Structure-from-Motion (SfM), however, has considerably advanced the practicality of photogrammetry (Westoby et al., 2012). Instead of using the camera position to determine 3D structure from overlapping images, the SfM algorithm identifies a series of points common to multiple images and constructs their 3D relationship based on their orientation across images (Lowe, 2004). Ullman (1979) established the underlying theorem in his proof that the precise structure and motion of as few as four points could be determined from three distinct views. The point matching process also determines the precise location of the camera (Westoby et al., 2012). As a result, significantly simpler and cheaper

systems with lower positional accuracy can be used to collect data for SfM then traditional photogrammetry (Westoby et al., 2012).

Due to these lower requirements, optical sensors mounted to unoccupied aerial systems (UAS) can efficiently and quickly capture the photographic data required to generate SfM point clouds. Increasing UAS capability over the past decade has significantly lowered data collection barriers (Aasen et al., 2018). Even more importantly, commercial SfM software packages, with highly automated workflows, have reduced the technical expertise required to produce point clouds (Fraser and Congalton, 2018). It is now possible to produce highly accurate point clouds using these technologies (e.g., Adjidjonu and Burgett, 2021; Agüera-Vega et al., 2017; Mancini et al., 2013). The utility of UAS-SfM has been well demonstrated in mapping ecosystem attributes such as forest structure (Alonzo et al., 2018; Belmonte et al., 2019; Cunliffe et al., 2016), changes in forest health (Campbell et al., 2020; Dash et al., 2018; Goodbody et al., 2018), phenology timing (Berra et al., 2019), and above ground biomass (Alonzo et al., 2020; Navarro et al., 2020).

7. Modelling approaches

While remote sensing datasets are impressive in their size and detail, these data have no intrinsic meaning on their own. As described by the consultant who taught me UAS-SfM data collection, these technologies and the data they produce are “shinny silver hammers” on their own. They look incredible but have no value unless analysis methods can connect their attributes to real world parameters of interest, such as canopy fuel loads. This can be done, on the simplest level, by finding single metric relationships. Shin et al. (2018) successfully measured individual ponderosa pine tree height with this technique using single UAS-SfM metrics, but only observed weak relationships between any individual point cloud metric and CBH. Instead, much higher accuracies can be obtained through the identification of more complex relationships between remote sensing metrics and field parameters using machine learning (Almeida et al., 2019). As defined by Heung et al. (2016), “machine learning is the automated process of uncovering patterns in large datasets using computer-based statistical models, where a fitted model may then be used

for prediction purposes on new data." The array of techniques that fall under the purview of machine learning is broad but three widely utilized methods are linear modelling, random forest, and support vector machines.

Linear modelling is the simplest of the modelling approaches utilized in this thesis. As the name suggests, this method generates linear relationships between predictors and outcomes, and can include multiple predictors (Comito and Pizzuti, 2022). As the only parametric method among those tested, linear models require input data to meet assumptions related to normality, linearity, homoscedasticity, and multicollinearity (Almeida et al., 2019). Optimal predictor sets are identified through stepwise regression, whereby a model is built through successive steps, either forwards from an empty model to which variables are added, backwards from a complete model from which variables are removed, or sequentially using a combination of these two approaches (Miller et al., 2022).

Random forest models fall under the spectrum of tree-based machine learning algorithms. Tree-based methods successively split a dataset at nodes to generate a final set of "leaf" nodes with the aim of maximizing the similarity of samples within a node while maximizing the difference between them (Heung et al., 2016). As a non-parametric approach, tree-based methods provide great flexibility in regards to non-normal data, mixture of data types, and the types of interactions between predictors (Talukdar et al., 2020). Developed by Breiman (2001), random forest extends the tree-based approach using a bootstrap ensemble of trees. Through this method, multiple trees are built, an "ensemble," and final predictions from each tree are averaged to generate an overall prediction (Sheykhmousa et al., 2020). Each tree is built with a randomized bootstrap sample (i.e., sampling with replacement) and restrictions on predictors available for node splitting (Almeida et al., 2019). Because of this approach, this method is robust to overfitting, outliers, and other data abnormalities (Belgiu and Drăguț, 2016).

Support vector machine (SVM) provides another non-parametric machine learning approach developed in the 1960s by Vapnik and colleagues (Smola and Schölkopf, 2004; Vapnik, 2006). This method centers on transforming the set of predictors and outcomes into higher dimensional spaces using a kernel function (Almeida et al., 2019). Originally developed for classification, SVM constructs a

hyperplane in that new higher dimensional space which serves as a decision boundary between groups (Mountrakis et al., 2011). The plane is defined by the samples closest to the decision boundary and these points are called the support vectors (Mountrakis et al., 2011). By substituting a linear function rather than a hyperplane decision boundary, SVM has been extended to perform regression as well (Heddam et al., 2022). Like random forest, SVM is non-parametric.

Both SVM and random forest utilize recursive feature elimination (RFE) for predictor selection. This method resembles backwards selection for linear models. RFE involves training the model using all predictors, ranking them by importance, removing the lowest ranking predictor, and then retraining the model using this reduced predictor subset (Guyon et al., 2002). This process is repeated until only two features remain. The best performing set of predictors is then used for training the final model.

8. Thesis overview

This thesis presents work from four papers aimed at informing better land management decision-making around fire hazard mitigation using UAS-SfM models of canopy fuel loads across the breadth of forests that characterize California, USA. The first study investigates how land managers consider information within their decision-making process to provide a framework for assessing the utility of UAS-SfM. The second paper develops a workflow for the processing of UAS-SfM and assesses the validity of metrics extracted from these data as they relate to forest structure. The third paper employs a range of machine learning techniques to model canopy fuels using UAS-SfM. The final paper extends this modelling analysis to a range of other remote sensing techniques.

References

Aasen, H., Honkavaara, E., Lucieer, A., Zarco-Tejada, P.J., 2018. Quantitative remote sensing at ultra-high resolution with UAV spectroscopy: A review of sensor technology, measurement procedures, and data correction workflows. Remote Sensing 10, 1091. https://doi.org/10.3390/rs10071091

Abatzoglou, J.T., Williams, A.P., 2016. Impact of anthropogenic climate change on wildfire across western US forests. Proc Natl Acad Sci USA 113, 11770–11775. https://doi.org/10.1073/pnas.1607171113

Acácio, V., Holmgren, M., Rego, F., Moreira, F., Mohren, G.M.J., 2009. Are drought and wildfires turning Mediterranean cork oak forests into persistent shrublands? Agroforest Syst 76, 389–400. https://doi.org/10.1007/s10457-008-9165-y

Adjidjonu, D., Burgett, J., 2021. Assessing the accuracy of unmanned aerial vehicles photogrammetric survey. International Journal of Construction Education and Research 17, 85–96. https://doi.org/10.1080/15578771.2020.1717683

Agee, J.K., Skinner, C.N., 2005. Basic principles of forest fuel reduction treatments. Forest Ecology and Management 211, 83–96. https://doi.org/10.1016/j.foreco.2005.01.034

Ager, A.A., Evers, C.R., Day, M.A., Preisler, H.K., Barros, A.M.G., Nielsen-Pincus, M., 2017. Network analysis of wildfire transmission and implications for risk governance. PLoS ONE 12, e0172867. https://doi.org/10.1371/journal.pone.0172867

Ager, A.A., Vaillant, N.M., Finney, M.A., 2010. A comparison of landscape fuel treatment strategies to mitigate wildland fire risk in the urban interface and preserve old forest structure. Forest Ecology and Management 259, 1556–1570. https://doi.org/10.1016/j.foreco.2010.01.032

Ager, A.A., Vaillant, N.M., McMahan, A., 2013. Restoration of fire in managed forests: A model to prioritize landscapes and analyze tradeoffs. Ecosphere 4, art29. https://doi.org/10.1890/ES13-00007.1

Agüera-Vega, F., Carvajal-Ramírez, F., Martínez-Carricondo, P., 2017. Accuracy of digital surface models and orthophotos derived from unmanned aerial vehicle photogrammetry. J. Surv. Eng. 143, 04016025. https://doi.org/10.1061/(ASCE)SU.1943-5428.0000206

Almeida, C.T.D., Galvão, L.S., Aragão, L.E.D.O.C.E., Ometto, J.P.H.B., Jacon, A.D., Pereira, F.R.D.S., Sato, L.Y., Lopes, A.P., Graça, P.M.L.D.A., Silva, C.V.D.J., Ferreira-Ferreira, J., Longo, M., 2019. Combining LiDAR and hyperspectral data for aboveground biomass modeling in the

Brazilian Amazon using different regression algorithms. Remote Sensing of Environment 232, 111323. https://doi.org/10.1016/j.rse.2019.111323

Alonzo, M., Andersen, H.-E., Morton, D., Cook, B., 2018. Quantifying boreal forest structure and composition using UAV Structure-from-Motion. Forests 9, 119. https://doi.org/10.3390/f9030119

Alonzo, M., Dial, R.J., Schulz, B.K., Andersen, H.-E., Lewis-Clark, E., Cook, B.D., Morton, D.C., 2020. Mapping tall shrub biomass in Alaska at landscape scale using Structure-from-Motion photogrammetry and lidar. Remote Sensing of Environment 245, 111841. https://doi.org/10.1016/j.rse.2020.111841

Andersen, H.-E., McGaughey, R.J., Reutebuch, S.E., 2005. Estimating forest canopy fuel parameters using LIDAR data. Remote Sensing of Environment 94, 441–449. https://doi.org/10.1016/j.rse.2004.10.013

Anderson, M.K., 2006. The use of fire by Native Americans in California, in: Sugihara, N. (Ed.), Fire in California's Ecosystems. University of California Press, pp. 416–430. https://doi.org/10.1525/california/9780520246058.003.0017

Andrews, P.L., Queen, Ll.P., 2001. Fire modeling and information system technology. Int. J. Wildland Fire 10, 343. https://doi.org/10.1071/WF01033

Aragoneses, E., Chuvieco, E., 2021. Generation and mapping of fuel types for fire risk assessment. Fire 4, 59. https://doi.org/10.3390/fire4030059

Arroyo, L.A., Pascual, C., Manzanera, J.A., 2008. Fire models and methods to map fuel types: The role of remote sensing. Forest Ecology and Management 256, 1239–1252. https://doi.org/10.1016/j.foreco.2008.06.048

Axelrod, R., 1976. The cognitive mapping approach to decision making, in: Axelrod, R. (Ed.), Structure of Decision: The Cognitive Maps of Political Elites. Princeton University Press, Princeton, pp. 3–17. https://doi.org/10.1515/9781400871957-004

Bajocco, S., Dragoz, E., Gitas, I., Smiraglia, D., Salvati, L., Ricotta, C., 2015. Mapping forest fuels through vegetation phenology: The role of coarse-resolution satellite time-series. PLoS One 10. https://doi.org/10.1371/journal.pone.0119811

Barbour, M.G., Major, J. (Eds.), 1988. Terrestrial vegetation of California, New expanded ed. ed, Special publication / California Native Plant Society. California Native Plant Society, Davis, Calif.

Batllori, E., Ackerly, D.D., Moritz, M.A., 2015. A minimal model of fire-vegetation feedbacks and disturbance stochasticity generates alternative stable states in grassland–shrubland–woodland systems. Environ. Res. Lett. 10, 034018. https://doi.org/10.1088/1748-9326/10/3/034018

Beaty, R.M., Taylor, A.H., 2008. Fire history and the structure and dynamics of a mixed conifer forest landscape in the northern Sierra Nevada, Lake Tahoe Basin, California, USA. Forest Ecology and Management 255, 707–719. https://doi.org/10.1016/j.foreco.2007.09.044

Beisner, B., Haydon, D., Cuddington, K., 2003. Alternative stable states in ecology. Frontiers in Ecology and the Environment 1, 376–382. https://doi.org/10.1890/1540-9295(2003)001[0376:ASSIE]2.0.CO;2

Belgiu, M., Drăguţ, L., 2016. Random forest in remote sensing: A review of applications and future directions. ISPRS Journal of Photogrammetry and Remote Sensing 114, 24–31. https://doi.org/10.1016/j.isprsjprs.2016.01.011

Belmonte, A., Sankey, T., Biederman, J.A., Bradford, J., Goetz, S.J., Kolb, T., Woolley, T., 2019. UAV-derived estimates of forest structure to inform ponderosa pine forest restoration. Remote Sensing in Ecology and Conservation n/a. https://doi.org/10.1002/rse2.137

Berra, E.F., Gaulton, R., Barr, S., 2019. Assessing spring phenology of a temperate woodland: A multiscale comparison of ground, unmanned aerial vehicle and Landsat satellite observations. Remote Sensing of Environment 223, 229–242. https://doi.org/10.1016/j.rse.2019.01.010

Bihari, M., Ryan, R., 2012. Influence of social capital on community preparedness for wildfires. Landscape and Urban Planning 106, 253–261. https://doi.org/10.1016/j.landurbplan.2012.03.011

Blumenfeld, J., 2020. Earth in the third dimension: first GEDI data available. URL https://www.earthdata.nasa.gov/learn/articles/first-gedi-data-available (accessed 8.2.24).

Braun, V., Clarke, V., 2006. Using thematic analysis in psychology. Qualitative Research in Psychology 3, 77–101. https://doi.org/10.1191/1478088706qp063oa

Breiman, L., 2001. Random forests. Machine Learning 45, 5–32. https://doi.org/10.1023/A:1010933404324

Brenkert-Smith, H., Champ, P.A., Flores, N., 2012. Trying not to get burned: Understanding homeowners' wildfire risk–mitigation behaviors. Environmental Management 50, 1139–1151. https://doi.org/10.1007/s00267-012-9949-8

Brunson, M.W., Evans, J., 2005. Badly burned? Effects of an escaped prescribed burn on social acceptability of wildland fuels treatments. Journal of Forestry 5.

Butsic, V., Kelly, M., Moritz, M., 2015. Land use and wildfire: A review of local interactions and teleconnections. Land 4, 140–156. https://doi.org/10.3390/land4010140

Calkin, D.E., Thompson, M.P., Finney, M.A., 2015. Negative consequences of positive feedbacks in US wildfire management. For. Ecosyst. 2, 9. https://doi.org/10.1186/s40663-015-0033-8

Campbell, M.J., Dennison, P.E., Tune, J.W., Kannenberg, S.A., Kerr, K.L., Codding, B.F., Anderegg, W.R.L., 2020. A multi-sensor, multi-scale approach to mapping tree mortality in woodland ecosystems. Remote Sensing of Environment 245, 111853. https://doi.org/10.1016/j.rse.2020.111853

Carroll, M., Paveglio, T., 2016. Using community archetypes to better understand differential community adaptation to wildfire risk. Phil. Trans. R. Soc. B 371, 20150344. https://doi.org/10.1098/rstb.2015.0344

Charnley, S., Spies, T.A., Barros, A.M.G., White, E.M., Olsen, K.A., 2017. Diversity in forest management to reduce wildfire losses: Implications for resilience. E&S 22, art22. https://doi.org/10.5751/ES-08753-220122

Chen, Y., Zhu, X., Yebra, M., Harris, S., Tapper, N., 2016. Strata-based forest fuel classification for wild fire hazard assessment using terrestrial LiDAR. J. Appl. Remote Sens 10, 046025. https://doi.org/10.1117/1.JRS.10.046025

Chuvieco, E., Aguado, I., Salas, J., García, M., Yebra, M., Oliva, P., 2020. Satellite remote sensing contributions to wildland fire science and management. Curr Forestry Rep 6, 81–96. https://doi.org/10.1007/s40725-020-00116-5

Clarke, V., Braun, V., 2017. Thematic analysis. The Journal of Positive Psychology 12, 297–298. https://doi.org/10.1080/17439760.2016.1262613

Collins, B.M., 2014. Fire weather and large fire potential in the northern Sierra Nevada. Agricultural and Forest Meteorology 189–190, 30–35. https://doi.org/10.1016/j.agrformet.2014.01.005

Collins, B.M., Das, A.J., Battles, J.J., Fry, D.L., Krasnow, K.D., Stephens, S.L., 2014. Beyond reducing fire hazard: Fuel treatment impacts on overstory tree survival. Ecological Applications 24, 1879–1886. https://doi.org/10.1890/14-0971.1

Collins, B.M., Kramer, H.A., Menning, K., Dillingham, C., Saah, D., Stine, P.A., Stephens, S.L., 2013. Modeling hazardous fire potential within a completed fuel treatment network in the northern Sierra Nevada. Forest Ecology and Management 310, 156–166. https://doi.org/10.1016/j.foreco.2013.08.015

Collins, B.M., Miller, J.D., Thode, A.E., Kelly, M., van Wagtendonk, J.W., Stephens, S.L., 2009. Interactions among wildland fires in a long-established Sierra Nevada Natural Fire Area. Ecosystems 12, 114–128. https://doi.org/10.1007/s10021-008-9211-7

Comito, C., Pizzuti, C., 2022. Artificial intelligence for forecasting and diagnosing COVID-19 pandemic: A focused review. Artificial Intelligence in Medicine 128, 102286. https://doi.org/10.1016/j.artmed.2022.102286

Cowling, R., Rundel, P., Lamont, B., Arroyo, M., Arianoutsou, M., 1996. Plant diversity in Mediterranean-climate regions. Trends in Ecology & Evolution 11, 362–366. https://doi.org/10.1016/0169-5347(96)10044-6

Cowling, R.M., Potts, A.J., Bradshaw, P.L., Colville, J., Arianoutsou, M., Ferrier, S., Forest, F., Fyllas, N.M., Hopper, S.D., Ojeda, F., Procheş, Ş., Smith, R.J., Rundel, P.W., Vassilakis, E., Zutta, B.R., 2015. Variation in plant diversity in Mediterranean-climate ecosystems: The role of climatic and topographical stability. J. Biogeogr. 42, 552–564. https://doi.org/10.1111/jbi.12429

Cunliffe, A.M., Brazier, R.E., Anderson, K., 2016. Ultra-fine grain landscape-scale quantification of dryland vegetation structure with drone-acquired Structure-from-Motion photogrammetry. Remote Sensing of Environment 183, 129–143. https://doi.org/10.1016/j.rse.2016.05.019

Cutter, S.L., 1996. Vulnerability to environmental hazards. Progress in Human Geography 20, 529–539. https://doi.org/10.1177/030913259602000407

Cutter, S.L., Boruff, B.J., Shirley, W.L., 2003. Social vulnerability to environmental hazards. Social Science Quarterly 84, 242–261. https://doi.org/10.1111/1540-6237.8402002

Dash, J.P., Pearse, G.D., Watt, M.S., 2018. UAV multispectral imagery can complement satellite data for monitoring forest health. Remote Sensing 10, 1216. https://doi.org/10.3390/rs10081216

Daum, K.L., Hansen, W.D., Gellman, J., Plantinga, A.J., Jones, C., Trugman, A.T., 2024. Do vegetation fuel reduction treatments alter forest fire severity and carbon stability in California forests? Earth's Future 12, e2023EF003763. https://doi.org/10.1029/2023EF003763

Dennison, P.E., Brewer, S.C., Arnold, J.D., Moritz, M.A., 2014. Large wildfire trends in the western United States, 1984-2011. Geophys. Res. Lett. 41, 2928–2933. https://doi.org/10.1002/2014GL059576

Devisscher, T., Boyd, E., Malhi, Y., 2016. Anticipating future risk in social-ecological systems using fuzzy cognitive mapping: The case of wildfire in the Chiquitania, Bolivia. E&S 21, art18. https://doi.org/10.5751/ES-08599-210418

Disney, M., 2019. Terrestrial lidar: a three-dimensional revolution in how we look at trees. New Phytologist 222, 1736–1741. https://doi.org/10.1111/nph.15517

Driscoll, D.A., Lindenmayer, D.B., Bennett, A.F., Bode, M., Bradstock, R.A., Cary, G.J., Clarke, M.F., Dexter, N., Fensham, R., Friend, G., Gill, M., James, S., Kay, G., Keith, D.A., MacGregor, C.,

Possingham, H.P., Russel-Smith, J., Salt, D., Watson, J.E.M., Williams, D., York, A., 2010. Resolving conflicts in fire management using decision theory: Asset-protection versus biodiversity conservation. Conservation Letters 3, 215–223. https://doi.org/10.1111/j.1755-263X.2010.00115.x

Durrant-Whyte, H., Bailey, T., 2006. Simultaneous localization and mapping: part I. IEEE Robot. Automat. Mag. 13, 99–110. https://doi.org/10.1109/MRA.2006.1638022

Edgeley, C.M., Paveglio, T.B., Williams, D.R., 2020. Support for regulatory and voluntary approaches to wildfire adaptation among unincorporated wildland-urban interface communities. Land Use Policy 91, 104394. https://doi.org/10.1016/j.landusepol.2019.104394

Elia, M., Lovreglio, R., Ranieri, N., Sanesi, G., Lafortezza, R., 2016. Cost-effectiveness of fuel removals in Mediterranean wildland-urban interfaces threatened by wildfires. Forests 7, 149. https://doi.org/10.3390/f7070149

Enright, N.J., Fontaine, J.B., Bowman, D.M., Bradstock, R.A., Williams, R.J., 2015. Interval squeeze: Altered fire regimes and demographic responses interact to threaten woody species persistence as climate changes. Frontiers in Ecology and the Environment 13, 265–272. https://doi.org/10.1890/140231

Filippelli, S.K., Lefsky, M.A., Rocca, M.E., 2019. Comparison and integration of lidar and photogrammetric point clouds for mapping pre-fire forest structure. Remote Sensing of Environment 224, 154–166. https://doi.org/10.1016/j.rse.2019.01.029

Fischer, A.P., Jasny, L., 2017. Capacity to adapt to environmental change: Evidence from a network of organizations concerned with increasing wildfire risk. E&S 22, art23. https://doi.org/10.5751/ES-08867-220123

Florec, V., Burton, M., Pannell, D., Kelso, J., Milne, G., 2020. Where to prescribe burn: The costs and benefits of prescribed burning close to houses. Int. J. Wildland Fire 29, 440. https://doi.org/10.1071/WF18192

Forbes, B., Reilly, S., Clark, M., Ferrell, R., Kelly, A., Krause, P., Matley, C., O'Neil, M., Villasenor, M., Disney, M., Wilkes, P., Bentley, L.P., 2022. Comparing remote sensing and field-based approaches to estimate ladder fuels and predict wildfire burn severity. Front. For. Glob. Change 5, 818713. https://doi.org/10.3389/ffgc.2022.818713

Forest Climate Action Team, 2018. California forest carbon plan: Managing our forest landscapes in a changing climate. Sacramento, CA.

Fraser, B.T., Congalton, R.G., 2018. Issues in unmanned aerial systems (UAS) data collection of complex forest environments. Remote Sensing 10, 908. https://doi.org/10.3390/rs10060908

García, M., Danson, F.M., Riaño, D., Chuvieco, E., Ramirez, F.A., Bandugula, V., 2011. Terrestrial laser scanning to estimate plot-level forest canopy fuel properties. International Journal of Applied Earth Observation and Geoinformation 13, 636–645. https://doi.org/10.1016/j.jag.2011.03.006

Ghasemi, B., Kyle, G.T., Absher, J.D., 2020. An examination of the social-psychological drivers of homeowner wildfire mitigation. Journal of Environmental Psychology 70, 101442. https://doi.org/10.1016/j.jenvp.2020.101442

Goodbody, T.R.H., Coops, N.C., Tompalski, P., Crawford, P., 2018. Assessing the status of forest regeneration using digital aerial photogrammetry and unmanned aerial systems. International Journal of Remote Sensing 39, 5246–5264. https://doi.org/10.1080/01431161.2017.1402387

Gray, S.A., Gray, S., De Kok, J.L., Helfgott, A.E.R., O'Dwyer, B., Jordan, R., Nyaki, A., 2015. Using fuzzy cognitive mapping as a participatory approach to analyze change, preferred states, and perceived resilience of social-ecological systems. E&S 20, art11. https://doi.org/10.5751/ES-07396-200211

Gray, S.R.J., Gagnon, A.S., Gray, S.A., O'Dwyer, B., O'Mahony, C., Muir, D., Devoy, R.J.N., Falaleeva, M., Gault, J., 2014. Are coastal managers detecting the problem? Assessing stakeholder perception of climate vulnerability using Fuzzy Cognitive Mapping. Ocean & Coastal Management 94, 74–89. https://doi.org/10.1016/j.ocecoaman.2013.11.008

Guyon, I., Weston, J., Barnhill, S., Vapnik, V., 2002. Gene selection for cancer classification using support vector machines. Machine Learning 46.

Hammer, R.B., Stewart, S.I., Radeloff, V.C., 2009. Demographic trends, the wildland–urban interface, and wildfire management. Society & Natural Resources 22, 777–782. https://doi.org/10.1080/08941920802714042

Heddam, S., Kim, S., Danandeh Mehr, A., Zounemat-Kermani, M., Elbeltagi, A., Malik, A., Kisi, O., 2022. A long short-term memory deep learning approach for river water temperature prediction, in: Current Trends and Advances in Computer-Aided Intelligent Environmental Data Engineering. Elsevier, pp. 243–270. https://doi.org/10.1016/B978-0-323-85597-6.00015-X

Hernandez-Leal, P.A., Arbelo, M., Gonzalez-Calvo, A., 2006. Fire risk assessment using satellite data. Advances in Space Research 37, 741–746. https://doi.org/10.1016/j.asr.2004.12.053

Heung, B., Ho, H.C., Zhang, J., Knudby, A., Bulmer, C.E., Schmidt, M.G., 2016. An overview and comparison of machine-learning techniques for classification purposes in digital soil mapping. Geoderma 265, 62–77. https://doi.org/10.1016/j.geoderma.2015.11.014

Hillman, S., Wallace, L., Reinke, K., Jones, S., 2021. A comparison between TLS and UAS LiDAR to represent eucalypt crown fuel characteristics. ISPRS Journal of Photogrammetry and Remote Sensing 181, 295–307. https://doi.org/10.1016/j.isprsjprs.2021.09.008

Hirschmuller, H., 2008. Stereo processing by semiglobal matching and mutual information. IEEE Trans. Pattern Anal. Mach. Intell. 30, 328–341. https://doi.org/10.1109/TPAMI.2007.1166

Hoffrén, R., Lamelas, M.T., De La Riva, J., Domingo, D., Montealegre, A.L., García-Martín, A., Revilla, S., 2023. Assessing GEDI-NASA system for forest fuels classification using machine learning techniques. International Journal of Applied Earth Observation and Geoinformation 116, 103175. https://doi.org/10.1016/j.jag.2022.103175

Hoffrén, R., Lamelas, M.T., De La Riva, J., 2024. Evaluation of handheld mobile laser scanner systems for the definition of fuel types in structurally complex Mediterranean forest stands. Fire 7, 59. https://doi.org/10.3390/fire7020059

Husari, S., Nichols, H.T., Sugihara, N.G., Stephens, S.L., 2006. Fire and fuel management, in: Sugihara, N. (Ed.), Fire in California's Ecosystems. University of California Press, pp. 444–465. https://doi.org/10.1525/california/9780520246058.003.0019

Jia, G.J., Burke, I.C., Goetz, A.F.H., Kaufmann, M.R., Kindel, B.C., 2006. Assessing spatial patterns of forest fuel using AVIRIS data. Remote Sensing of Environment 102, 318–327. https://doi.org/10.1016/j.rse.2006.02.025

Kang, P., Lin, S., Huang, C., Li, S., Wu, Z., Sun, L., 2024. Revealing three-dimensional variations in fuel structures in subtropical forests through backpack laser scanning. Forests 15, 155. https://doi.org/10.3390/f15010155

Kauffman, J.B., 2004. Death rides the forest: Perceptions of fire, land use, and ecological restoration of western forests. Conservation Biology 18, 878–882. https://doi.org/10.1111/j.1523-1739.2004.545_1.x

Keeley, J.E., 2002. Native American impacts on fire regimes of the California coastal ranges. J Biogeography 29, 303–320. https://doi.org/10.1046/j.1365-2699.2002.00676.x

Keeley, J.E., Bond, W.J., Bradstock, R.A., Pausas, J.G., Rundel, P.W., 2011. Fire in Mediterranean ecosystems: Ecology, evolution and management. Cambridge University Press, Cambridge. https://doi.org/10.1017/CBO9781139033091

Khorram, S., Nelson, S.A.C., Koch, F.H., van der Wiele, C.F., 2012. Remote Sensing, SpringerBriefs in Space Development. Springer US, Boston, MA. https://doi.org/10.1007/978-1-4614-3103-9

Klimaszewski-Patterson, A., Mensing, S., 2020. Paleoecological and paleolandscape modeling support for pre-Columbian burning by Native Americans in the Golden Trout Wilderness Area, California, USA. Landscape Ecol. https://doi.org/10.1007/s10980-020-01081-x

Knight, C.A., Tompkins, R.E., Wang, J.A., York, R., Goulden, M.L., Battles, J.J., 2022. Accurate tracking of forest activity key to multi-jurisdictional management goals: A case study in California. Journal of Environmental Management 302, 114083. https://doi.org/10.1016/j.jenvman.2021.114083

Kolden, C.A., Henson, C., 2019. A socio-ecological approach to mitigating wildfire vulnerability in the wildland urban interface: A case study from the 2017 Thomas Fire. Fire 2, 9. https://doi.org/10.3390/fire2010009

Konecny, G., 1985. Keynote address: The International Society for Photogrammetry and Remote Sensing, 75 years old, or 75 years young. Photogrammetric Engineering & Remote Sensing 15.

Kontogianni, A.D., Papageorgiou, E.I., Tourkolias, C., 2012. How do you perceive environmental change? Fuzzy Cognitive Mapping informing stakeholder analysis for environmental policy making and non-market valuation. Applied Soft Computing 12, 3725–3735. https://doi.org/10.1016/j.asoc.2012.05.003

Kosko, B., 1986. Fuzzy cognitive maps. International Journal of Man-Machine Studies 24, 65–75. https://doi.org/10.1016/S0020-7373(86)80040-2

Kramer, H., Collins, B., Kelly, M., Stephens, S., 2014. Quantifying ladder fuels: a new approach using LiDAR. Forests 5, 1432–1453. https://doi.org/10.3390/f5061432

Kuhn, M., Wing, J., Weston, S., Williams, A., Keefer, C., Engelhardt, A., Cooper, T., Mayer, Z., Kenkel, B., R Core Team, Benesty, M., Lescarbeau, R., Ziem, A., Scrucca, L., Tang, Y., Candan, C., Hunt, T., 2023. caret: Classification and Regression Training.

Lang, N., Kalischek, N., Armston, J., Schindler, K., Dubayah, R., Wegner, J.D., 2022. Global canopy height regression and uncertainty estimation from GEDI LIDAR waveforms with deep ensembles. Remote Sensing of Environment 268, 112760. https://doi.org/10.1016/j.rse.2021.112760

Lewontin, R.C., 1969. The meaning of stability. Brookhaven Symp Biol 22, 13–24.

Li, O., Gray, S.A., Sutton, S.G., 2016. Mapping recreational fishers' informal learning of scientific information using a fuzzy cognitive mapping approach to mental modelling. Fish Manag Ecol 23, 315–329. https://doi.org/10.1111/fme.12174

Lowe, D.G., 2004. Distinctive image features from scale-invariant keypoints. International Journal of Computer Vision 60, 91–110. https://doi.org/10.1023/B:VISI.0000029664.99615.94

Mancini, F., Dubbini, M., Gattelli, M., Stecchi, F., Fabbri, S., Gabbianelli, G., 2013. Using unmanned aerial vehicles (UAV) for high-resolution reconstruction of topography: The Structure-from-Motion approach on coastal environments. Remote Sensing 5, 6880–6898. https://doi.org/10.3390/rs5126880

Marino, E., Montes, F., Tomé, J.L., Navarro, J.A., Hernando, C., 2018. Vertical forest structure analysis for wildfire prevention: Comparing airborne laser scanning data and stereoscopic hemispherical images. International Journal of Applied Earth Observation and Geoinformation 73, 438–449. https://doi.org/10.1016/j.jag.2018.07.015

Mauro, F., Hudak, A.T., Fekety, P.A., Frank, B., Temesgen, H., Bell, D.M., Gregory, M.J., McCarley, T.R., 2021. Regional modeling of forest fuels and structural attributes using airborne laser scanning data in Oregon. Remote Sensing 13, 261. https://doi.org/10.3390/rs13020261

McFarlane, B.L., McGee, T.K., Faulkner, H., 2011. Complexity of homeowner wildfire risk mitigation: An integration of hazard theories. Int. J. Wildland Fire 20, 921. https://doi.org/10.1071/WF10096

Meldrum, J.R., Brenkert-Smith, H., Champ, P.A., Falk, L., Wilson, P., Barth, C.M., 2018. Wildland–urban interface residents' relationships with wildfire: Variation within and across communities. Society & Natural Resources 31, 1132–1148. https://doi.org/10.1080/08941920.2018.1456592

Meldrum, J.R., Champ, P.A., Brenkert-Smith, H., Warziniack, T., Barth, C.M., Falk, L.C., 2015. Understanding gaps between the risk perceptions of wildland-urban interface (WUI) residents and wildfire professionals. Risk Analysis 35, 1746–1761. https://doi.org/10.1111/risa.12370

Menning, K.M., Stephens, S.L., 2007. Fire climbing in the forest: A semiqualitative, semiquantitative approach to assessing ladder fuel hazards. Western Journal of Applied Forestry 22, 88–93. https://doi.org/10.1093/wjaf/22.2.88

Miller, A., Panneerselvam, J., Liu, L., 2022. A review of regression and classification techniques for analysis of common and rare variants and gene-environmental factors. Neurocomputing 489, 466–485. https://doi.org/10.1016/j.neucom.2021.08.150

Miller, C., O'Neill, S., Rorig, M., Alvarado, E., 2019. Air-quality challenges of prescribed fire in the complex terrain and wildland urban interface surrounding Bend, Oregon. Atmosphere 10, 515. https://doi.org/10.3390/atmos10090515

Miller, J.D., Safford, H.D., Crimmins, M., Thode, A.E., 2009. Quantitative evidence for increasing forest fire severity in the Sierra Nevada and Southern Cascade Mountains, California and Nevada, USA. Ecosystems 12, 16–32. https://doi.org/10.1007/s10021-008-9201-9

Miller, J.D., Skinner, C.N., Safford, H.D., Knapp, E.E., Ramirez, C.M., 2012. Trends and causes of severity, size, and number of fires in northwestern California, USA. Ecological Applications 22, 184–203. https://doi.org/10.1890/10-2108.1

Minnich, R.A., 2006. California climate and fire weather, in: Sugihara, N. (Ed.), Fire in California's Ecosystems. University of California Press, pp. 12–37. https://doi.org/10.1525/california/9780520246058.003.0002

Moghaddas, J.J., Roller, G.B., Long, J.W., Saah, D.S., Moritz, M.A., Stark, D.T., Schmidt, D., Buchholz, T., Freed, T.J., Alvey, E.C., Gunn, J.S., 2018. Fuel treatment for forest resilience and climate mitigations: A critical review for coniferous forests of the Sierra Nevada, Southern Cascade, Coast, Klamath, and Transverse Ranges (No. CCCA4- CNRA-2018– 017). California Natural Resources Agency.

Moreira, F., Ascoli, D., Safford, H., Adams, M.A., Moreno, J.M., Pereira, J.M.C., Catry, F.X., Armesto, J., Bond, W., González, M.E., Curt, T., Koutsias, N., McCaw, L., Price, O., Pausas, J.G., Rigolot, E., Stephens, S., Tavsanoglu, C., Vallejo, V.R., Van Wilgen, B.W., Xanthopoulos, G., Fernandes, P.M., 2020. Wildfire management in Mediterranean-type regions: Paradigm change needed. Environ. Res. Lett. 15, 011001. https://doi.org/10.1088/1748-9326/ab541e

Moritz, M.A., Batllori, E., Bradstock, R.A., Gill, A.M., Handmer, J., Hessburg, P.F., Leonard, J., McCaffrey, S., Odion, D.C., Schoennagel, T., Syphard, A.D., 2014. Learning to coexist with wildfire. Nature 515, 58–66. https://doi.org/10.1038/nature13946

Mountrakis, G., Im, J., Ogole, C., 2011. Support vector machines in remote sensing: A review. ISPRS Journal of Photogrammetry and Remote Sensing 66, 247–259. https://doi.org/10.1016/j.isprsjprs.2010.11.001

Myers, N., Mittermeier, R.A., Mittermeier, C.G., da Fonseca, G.A.B., Kent, J., 2000. Biodiversity hotspots for conservation priorities. Nature 403, 853–858. https://doi.org/10.1038/35002501

Myroniuk, V., Zibtsev, S., Bogomolov, V., Goldammer, J.G., Soshenskyi, O., Levchenko, V., Matsala, M., 2023. Combining Landsat time series and GEDI data for improved characterization of fuel types and canopy metrics in wildfire simulation. Journal of Environmental Management 345, 118736. https://doi.org/10.1016/j.jenvman.2023.118736

Nardini, A., Lo Gullo, M.A., Trifilò, P., Salleo, S., 2014. The challenge of the Mediterranean climate to plant hydraulics: Responses and adaptations. Environmental and Experimental Botany 103, 68–79. https://doi.org/10.1016/j.envexpbot.2013.09.018

Navarro, A., Young, M., Allan, B., Carnell, P., Macreadie, P., Ierodiaconou, D., 2020. The application of Unmanned Aerial Vehicles (UAVs) to estimate above-ground biomass of mangrove ecosystems. Remote Sensing of Environment 242, 111747. https://doi.org/10.1016/j.rse.2020.111747

North, M., Brough, A., Long, J., Collins, B., Bowden, P., Yasuda, D., Miller, J., Sugihara, N., 2015a. Constraints on mechanized treatment significantly limit mechanical fuels reduction extent in the Sierra Nevada. Journal of Forestry 113, 40–48. https://doi.org/10.5849/jof.14-058

North, M., Collins, B.M., Stephens, S., 2012. Using fire to increase the scale, benefits, and future maintenance of fuels treatments. Journal of Forestry 110, 392–401. https://doi.org/10.5849/jof.12-021

North, M., Stephens, S.L., Collins, B.M., Agee, J.K., Aplet, G., Franklin, J.F., Fule, P.Z., 2015b. Reform forest fire management. Science 349, 1280–1281. https://doi.org/10.1126/science.aab2356

Odion, D.C., Moritz, M.A., DellaSala, D.A., 2010. Alternative community states maintained by fire in the Klamath Mountains, USA. Journal of Ecology 98, 96–105. https://doi.org/10.1111/j.1365-2745.2009.01597.x

Olsen, C.S., Kline, J.D., Ager, A.A., Olsen, K.A., Short, K.C., 2017. Examining the influence of biophysical conditions on wildland–urban interface homeowners' wildfire risk mitigation activities in fire-prone landscapes. E&S 22, art21. https://doi.org/10.5751/ES-09054-220121

Özesmi, U., Özesmi, S.L., 2004. Ecological models based on people's knowledge: a multi-step fuzzy cognitive mapping approach. Ecological Modelling 176, 43–64. https://doi.org/10.1016/j.ecolmodel.2003.10.027

Papageorgiou, E.I., Salmeron, J.L., 2013. A review of fuzzy cognitive maps research during the last decade. IEEE Trans. Fuzzy Syst. 21, 66–79. https://doi.org/10.1109/TFUZZ.2012.2201727

Paveglio, T.B., Edgeley, C.M., Carroll, M., Billings, M., Stasiewicz, A.M., 2019. Exploring the influence of local social context on strategies for achieving fire adapted communities. Fire 2, 26. https://doi.org/10.3390/fire2020026

Paveglio, T.B., Moseley, C., Carroll, M.S., Williams, D.R., Davis, E.J., Fischer, A.P., 2015. Categorizing the social context of the wildland urban interface: Adaptive capacity for wildfire and community "archetypes." Forest Science 61, 298–310. https://doi.org/10.5849/forsci.14-036

Perry, D.A., Hessburg, P.F., Skinner, C.N., Spies, T.A., Stephens, S.L., Taylor, A.H., Franklin, J.F., McComb, B., Riegel, G., 2011. The ecology of mixed severity fire regimes in Washington, Oregon, and Northern California. Forest Ecology and Management 262, 703–717. https://doi.org/10.1016/j.foreco.2011.05.004

Petraitis, P.S., Dudgeon, S.R., 2004. Detection of alternative stable states in marine communities. Journal of Experimental Marine Biology and Ecology 300, 343–371. https://doi.org/10.1016/j.jembe.2003.12.026

Potapov, P., Li, X., Hernandez-Serna, A., Tyukavina, A., Hansen, M.C., Kommareddy, A., Pickens, A., Turubanova, S., Tang, H., Silva, C.E., Armston, J., Dubayah, R., Blair, J.B., Hofton, M., 2021. Mapping global forest canopy height through integration of GEDI and Landsat data. Remote Sensing of Environment 253, 112165. https://doi.org/10.1016/j.rse.2020.112165

Radeloff, V.C., Helmers, D.P., Kramer, H.A., Mockrin, M.H., Alexandre, P.M., Bar-Massada, A., Butsic, V., Hawbaker, T.J., Martinuzzi, S., Syphard, A.D., Stewart, S.I., 2018. Rapid growth of the US wildland-urban interface raises wildfire risk. Proc Natl Acad Sci USA 115, 3314–3319. https://doi.org/10.1073/pnas.1718850115

Rasch, R., McCaffrey, S., 2019. Exploring wildfire-prone community trust in wildfire management agencies. Forest Science 65, 652–663. https://doi.org/10.1093/forsci/fxz027

Reinhardt, E.D., Keane, R.E., Calkin, D.E., Cohen, J.D., 2008. Objectives and considerations for wildland fuel treatment in forested ecosystems of the interior western United States. Forest Ecology and Management 256, 1997–2006. https://doi.org/10.1016/j.foreco.2008.09.016

Remondino, F., Spera, M.G., Nocerino, E., Menna, F., Nex, F., 2014. State of the art in high density image matching. Photogram Rec 29, 144–166. https://doi.org/10.1111/phor.12063

Reutebuch, S.E., Andersen, H.-E., McGaughey, R.J., 2005. Light detection and ranging (LIDAR): An emerging tool for multiple resource inventory. Journal of Forestry 7.

Riano, D., Chuvieco, E., Ustin, S., Zomer, R., Dennison, P., Roberts, D., Salas, J., 2002. Assessment of vegetation regeneration after fire through multitemporal analysis of AVIRIS images in the Santa Monica Mountains. Remote Sensing of Environment 79, 60–71. https://doi.org/10.1016/S0034-4257(01)00239-5

Rishmawi, K., Huang, C., Schleeweis, K., Zhan, X., 2022. Integration of VIIRS observations with GEDI-Lidar measurements to monitor forest structure dynamics from 2013 to 2020 across the conterminous United States. Remote Sensing 14, 2320. https://doi.org/10.3390/rs14102320v

Ritchie, M.W., Skinner, C.N., Hamilton, T.A., 2007. Probability of tree survival after wildfire in an interior pine forest of northern California: Effects of thinning and prescribed fire. Forest Ecology and Management 247, 200–208. https://doi.org/10.1016/j.foreco.2007.04.044

Rundel, P.W., Arroyo, M.T.K., Cowling, R.M., Keeley, J.E., Lamont, B.B., Vargas, P., 2016. Mediterranean biomes: Evolution of their vegetation, floras, and climate. Annu. Rev. Ecol. Evol. Syst. 47, 383–407. https://doi.org/10.1146/annurev-ecolsys-121415-032330

Ryding, J., Williams, E., Smith, M., Eichhorn, M., 2015. Assessing Handheld Mobile Laser Scanners for Forest Surveys. Remote Sensing 7, 1095–1111. https://doi.org/10.3390/rs70101095

Safford, H.D., Schmidt, D.A., Carlson, C.H., 2009. Effects of fuel treatments on fire severity in an area of wildland–urban interface, Angora Fire, Lake Tahoe Basin, California. Forest Ecology and Management 258, 773–787. https://doi.org/10.1016/j.foreco.2009.05.024

Samarasinghe, S., Strickert, G., 2013. Mixed-method integration and advances in fuzzy cognitive maps for computational policy simulations for natural hazard mitigation. Environmental Modelling & Software 39, 188–200. https://doi.org/10.1016/j.envsoft.2012.06.008

Santana, V.M., Jaime Baeza, M., Marrs, R.H., Ramón Vallejo, V., 2010. Old-field secondary succession in SE Spain: Can fire divert it? Plant Ecol 211, 337–349. https://doi.org/10.1007/s11258-010-9793-y

Santoro, S., Pluchinotta, I., Pagano, A., Pengal, P., Cokan, B., Giordano, R., 2019. Assessing stakeholders' risk perception to promote Nature Based Solutions as flood protection strategies: The case of the Glinščica river (Slovenia). Science of The Total Environment 655, 188–201. https://doi.org/10.1016/j.scitotenv.2018.11.116

Scharstein, D., Szeliski, R., 2002. A taxonomy and evaluation of dense two-frame stereo correspondence algorithms. International Journal of Computer Vision 17, 35.

Schoennagel, T., Balch, J.K., Brenkert-Smith, H., Dennison, P.E., Harvey, B.J., Krawchuk, M.A., Mietkiewicz, N., Morgan, P., Moritz, M.A., Rasker, R., Turner, M.G., Whitlock, C., 2017. Adapt to more wildfire in western North American forests as climate changes. Proc Natl Acad Sci USA 114, 4582–4590. https://doi.org/10.1073/pnas.1617464114

Shaik, R.U., Laneve, G., Fusilli, L., 2022. An automatic procedure for forest fire fuel mapping using hyperspectral (PRISMA) imagery: A semi-supervised classification approach. Remote Sensing 14, 1264. https://doi.org/10.3390/rs14051264

Sheykhmousa, M., Mahdianpari, M., Ghanbari, H., Mohammadimanesh, F., Ghamisi, P., Homayouni, S., 2020. Support vector machine versus random forest for remote sensing image classification: a

meta-analysis and systematic review. IEEE J. Sel. Top. Appl. Earth Observations Remote Sensing 13, 6308–6325. https://doi.org/10.1109/JSTARS.2020.3026724

Shin, P., Sankey, T., Moore, M., Thode, A., 2018. Evaluating unmanned aerial vehicle images for estimating forest canopy fuels in a ponderosa pine stand. Remote Sensing 10, 1266. https://doi.org/10.3390/rs10081266

Silva, C.A., Duncanson, L., Hancock, S., Neuenschwander, A., Thomas, N., Hofton, M., Fatoyinbo, L., Simard, M., Marshak, C.Z., Armston, J., Lutchke, S., Dubayah, R., 2021. Fusing simulated GEDI, ICESat-2 and NISAR data for regional aboveground biomass mapping. Remote Sensing of Environment 253, 112234. https://doi.org/10.1016/j.rse.2020.112234

Singer, A., Gray, S., Sadler, A., Schmitt Olabisi, L., Metta, K., Wallace, R., Lopez, M.C., Introne, J., Gorman, M., Henderson, J., 2017. Translating community narratives into semi-quantitative models to understand the dynamics of socio-environmental crises. Environmental Modelling & Software 97, 46–55. https://doi.org/10.1016/j.envsoft.2017.07.010

Smola, A.J., Schölkopf, B., 2004. A tutorial on support vector regression. Statistics and Computing 14, 199–222. https://doi.org/10.1023/B:STCO.0000035301.49549.88

Staver, A.C., Archibald, S., Levin, S.A., 2011. The global extent and determinants of savanna and forest as alternative biome states. Science 334, 230–232. https://doi.org/10.1126/science.1210465

Stefanidou, A., Gitas, I.Z., Katagis, T., 2022. A national fuel type mapping method improvement using sentinel-2 satellite data. null 37, 1022–1042. https://doi.org/10.1080/10106049.2020.1756460

Stephens, S.L., Foster, D.E., Battles, J.J., Bernal, A.A., Collins, B.M., Hedges, R., Moghaddas, J.J., Roughton, A.T., York, R.A., 2023. Forest restoration and fuels reduction work: Different pathways for achieving success in the Sierra Nevada. Ecological Applications e2932. https://doi.org/10.1002/eap.2932

Stephens, S.L., Martin, R.E., Clinton, N.E., 2007. Prehistoric fire area and emissions from California's forests, woodlands, shrublands, and grasslands. Forest Ecology and Management 251, 205–216. https://doi.org/10.1016/j.foreco.2007.06.005

Stephens, S.L., McIver, J.D., Boerner, R.E.J., Fettig, C.J., Fontaine, J.B., Hartsough, B.R., Kennedy, P.L., Schwilk, D.W., 2012. The effects of forest fuel-reduction treatments in the United States. BioScience 62, 549–560. https://doi.org/10.1525/bio.2012.62.6.6

Stephens, S.L., Moghaddas, J.J., Edminster, C., Fiedler, C.E., Haase, S., Harrington, M., Keeley, J.E., Knapp, E.E., McIver, J.D., Metlen, K., Skinner, C.N., Youngblood, A., 2009. Fire treatment effects on vegetation structure, fuels, and potential fire severity in western U.S. forests. Ecological Applications 19, 305–320. https://doi.org/10.1890/07-1755.1

Stewart, S.I., Radeloff, V.C., Hammer, R.B., Hawbaker, T.J., 2007. Defining the wildland–urban interface. Journal of Forestry 105, 7.

Sugihara, N.G., Barbour, M.G., 2006. Fire and California vegetation, in: Sugihara, N. (Ed.), Fire in California's Ecosystems. University of California Press, pp. xvi–9. https://doi.org/10.1525/california/9780520246058.003.0001

Swetnam, T.W., Baisan, C.H., Caprio, A.C., Brown, P.M., Touchan, R., Anderson, R.S., Hallett, D.J., 2009. Multi-millennial fire history of the Giant Forest, Sequoia National Park, California, USA. fire ecol 5, 120–150. https://doi.org/10.4996/fireecology.0503120

Syphard, A.D., Radeloff, V.C., Keeley, J.E., Hawbaker, T.J., Clayton, M.K., Stewart, S.I., Hammer, R.B., 2007. Human influence on California fire regimes. Ecological Applications 17, 1388–1402. https://doi.org/10.1890/06-1128.1

Talukdar, S., Singha, P., Mahato, S., Shahfahad, Pal, S., Liou, Y.-A., Rahman, A., 2020. Land-use land-cover classification by machine learning classifiers for satellite observations — a review. Remote Sensing 12, 1135. https://doi.org/10.3390/rs12071135

Taneja, R., Wallace, L., Hillman, S., Reinke, K., Hilton, J., Jones, S., Hally, B., 2023. Up-scaling fuel hazard metrics derived from terrestrial laser scanning using a machine learning model. Remote Sensing 15, 1273. https://doi.org/10.3390/rs15051273

Taylor, A.H., 2010. Fire disturbance and forest structure in an old-growth Pinus ponderosa forest, southern Cascades, USA. Journal of Vegetation Science 21, 561–572. https://doi.org/10.1111/j.1654-1103.2009.01164.x

Taylor, A.H., 2000. Fire regimes and forest changes in mid and upper montane forests of the southern Cascades, Lassen Volcanic National Park, California, U.S.A. J Biogeography 27, 87–104. https://doi.org/10.1046/j.1365-2699.2000.00353.x

Taylor, A.H., Scholl, A.E., 2012. Climatic and human influences on fire regimes in mixed conifer forests in Yosemite National Park, USA. Forest Ecology and Management 267, 144–156. https://doi.org/10.1016/j.foreco.2011.11.026

Taylor, A.H., Skinner, C.N., 2003. Spatial patterns and controls on historical fire regimes and forest structure in the Klamath Mountains. Ecological Applications 13, 704–719. https://doi.org/10.1890/1051-0761(2003)013[0704:SPACOH]2.0.CO;2

Taylor, A.H., Skinner, C.N., 1998. Fire history and landscape dynamics in a late-successional reserve, Klamath Mountains, California, USA. Forest Ecology and Management 111, 285–301. https://doi.org/10.1016/S0378-1127(98)00342-9

Thomas, J., Harden, A., 2008. Methods for the thematic synthesis of qualitative research in systematic reviews. BMC Med Res Methodol 8, 45. https://doi.org/10.1186/1471-2288-8-45

Toman, E., Stidham, M., Shindler, B., McCaffrey, S., 2011. Reducing fuels in the wildland - urban interface: Community perceptions of agency fuels treatments. Int. J. Wildland Fire 20, 340. https://doi.org/10.1071/WF10042

Tsafrir, A., Osem, Y., Shemesh, H., Carmel, Y., Soref, C., Ovadia, O., 2019. Fire season modifies the perennial plant community composition through a differential effect on obligate seeders in eastern Mediterranean woodlands. Appl Veg Sci 22, 115–126. https://doi.org/10.1111/avsc.12408

Ullman, S., 1979. The interpretation of Structure-from-Motion. Proceedings of the Royal Society of London. Series B, Containing papers of a Biological character. Royal Society (Great Britain) 203, 405–426. https://doi.org/10.1098/rspb.1979.0006

Urbieta, I.R., Zavala, G., Bedia, J., Gutiérrez, J.M., Miguel-Ayanz, J.S., Camia, A., Keeley, J.E., Moreno, J.M., 2015. Fire activity as a function of fire–weather seasonal severity and antecedent climate across spatial scales in southern Europe and Pacific western USA. Environ. Res. Lett. 10, 114013. https://doi.org/10.1088/1748-9326/10/11/114013

Urgenson, L.S., Ryan, C.M., Halpern, C.B., Bakker, J.D., Belote, R.T., Franklin, J.F., Haugo, R.D., Nelson, C.R., Waltz, A.E.M., 2017. Visions of restoration in fire-adapted forest Landscapes: Lessons from the collaborative forest landscape restoration program. Environmental Management 59, 338–353. https://doi.org/10.1007/s00267-016-0791-2

Van de Water, K.M., Safford, H.D., 2011. A summary of fire frequency estimates for California vegetation before Euro-American Settlement. fire ecol 7, 26–58. https://doi.org/10.4996/fireecology.0703026

van Vliet, M., Kok, K., Veldkamp, T., 2010. Linking stakeholders and modellers in scenario studies: The use of Fuzzy Cognitive Maps as a communication and learning tool. Futures 42, 1–14. https://doi.org/10.1016/j.futures.2009.08.005

Van Wagtendonk, J.W., 2006. Fire as a physical process, in: Sugihara, N. (Ed.), Fire in California's Ecosystems. University of California Press, pp. 38–57. https://doi.org/10.1525/california/9780520246058.003.0003

Vapnik, V., 2006. Estimation of dependences based on empirical data, Information Science and Statistics. Springer New York, New York, NY. https://doi.org/10.1007/0-387-34239-7

Vaske, J.J., Absher, J.D., 2007. Salient value similarity, social trust and attitudes toward wildland fire management strategies. Human Ecology Review 14, 10.

Vogt, C.A., Winter, G., Fried, J.S., 2005. Predicting homeowners' approval of fuel management at the wildland–urban interface using the theory of reasoned action. Society & Natural Resources 18, 337–354. https://doi.org/10.1080/08941920590915242

Voinov, A., Bousquet, F., 2010. Modelling with stakeholders. Environmental Modelling & Software 25, 1268–1281. https://doi.org/10.1016/j.envsoft.2010.03.007

Westerling, A., 2018. Wildfire simulations for California's Fourth Climate Change Assessment: Projecting changes in extreme wildfire events with a warming climate (No. CCCA4- CEC-2018–014). California's Fourth Climate Change Assessment, California Energy Commission.

Westerling, A.L., 2006. Warming and earlier spring increase western U.S. forest wildfire activity. Science 313, 940–943. https://doi.org/10.1126/science.1128834

Westoby, M.J., Brasington, J., Glasser, N.F., Hambrey, M.J., Reynolds, J.M., 2012. 'Structure-from-Motion' photogrammetry: A low-cost, effective tool for geoscience applications. Geomorphology 179, 300–314. https://doi.org/10.1016/j.geomorph.2012.08.021

Wilkes, P., Lau, A., Disney, M., Calders, K., Burt, A., Gonzalez de Tanago, J., Bartholomeus, H., Brede, B., Herold, M., 2017. Data acquisition considerations for Terrestrial Laser Scanning of forest plots. Remote Sensing of Environment 196, 140–153. https://doi.org/10.1016/j.rse.2017.04.030

Wimberly, M.C., Cochrane, M.A., Baer, A.D., Pabst, K., 2009. Assessing fuel treatment effectiveness using satellite imagery and spatial statistics. Ecological Applications 19, 1377–1384. https://doi.org/10.1890/08-1685.1

Wolters, E.A., Steel, B.S., Weston, D., Brunson, M., 2017. Determinants of residential Firewise behaviors in Central Oregon. The Social Science Journal 54, 168–178. https://doi.org/10.1016/j.soscij.2016.12.004

Chapter 2

Preface

In this first study, I sought to understand how land managers make decisions around fire fuel hazard mitigation and the role that information plays in this process. This paper was motivated by a desire to better inform my future work in developing tools for mapping forest fire fuels.

I conceptualized this study and developed the methods with Imma. I conducted the interviews and analyses presented here, along with drafting the manuscript. This paper has not yet been submitted for publication.

The primary limitation of this study is the limited sample size. I had intended to conduct a larger sampling campaign, including advertising through community centers, churches, and local social organizations, but these efforts had to be abandoned with the onset of Covid. Furthermore, the fuzzy cognitive mapping (FCM) exercise worked very well in person but translated poorly to a digital platform. When conducted in person, participants became deeply involved in the mapping process and generated diagrams that captured a deep level of meaning for them. For example, one participant requested to take a photograph of their product and planned to use it for future organizational purposes. None of the online participants exhibited this level of engagement and two failed to produce maps altogether.

Despite this significant limitation, this study did achieve variable saturation, which is the standard used for determining if a population has been sufficiently sampled in FCM studies. Consequently, the findings from this study can be said to provide a sufficiently representative sample from which to draw meaningful conclusions. Additionally, the conversations with the interview participants generated clear

and consistent themes that are broadly applicable to this region and the problem of fire hazard mitigation. Fuzzy cognitive mapping, being a highly intensive interview process, will always struggle with capturing large sample sizes, even without the limitations of Covid. Therefore, the clarity and consistency of themes captured across groups must be given weight even if sample sizes are small. However, future work would do well to assess the findings presented here through other methodologies with broader reach, such as online surveys, by presenting the results from this FCM study to a broad range of diverse stakeholder groups and assessing their level of agreement with the findings presented herein.

Promoting collective land management for wildfire mitigation through the identification of shared decision-making practices and barriers

Sean Reilly [1] and Imma Oliveras Menor [1,2]

[1] Environmental Change Institute, University of Oxford, Oxford OX1 3QY, UK

[2] AMAP (Botanique et Modélisation de l'Architecture des Plantes et des Végétations), CIRAD, CNRS, INRA, IRD, Université de Montpellier, Montpellier, France

Abstract

Fire management in the wildland-urban interface (WUI) presents a significant challenge due to the complex land tenure that makes up the landscape. Effective management requires cohesive action between private landowners, government agencies, NGOs, and other actors. This study sought to identify common decision-making processes and barriers to the implementation of land management across the core demographics that comprise the WUI. To that end, we employed a mixed-method approach combining fuzzy cognitive mapping and thematic analysis to interviews with land managers, fire professionals, and private landowners in Napa and Sonoma Counties, California, United States. Priority setting emerged as the most important aspect of participants' fuzzy cognitive maps for driving change towards desired outcomes. Information plays a key role in guiding the process but only if it is timely and highly accessible. Improved cohesive action can be achieved through the reduction of barriers to private landowners to allow them to engage with land managers and fire professionals as equal collaborators. Therefore, we suggest collective fire hazard management priority setting is the key to fostering community action in the WUI.

1. Introduction

As wildfires continue to increase in size and number across the western United States (Schoennagel et al., 2017), the region requires an improved approach to reducing social fire vulnerability. Fire serves an important ecological role throughout this region and, historically, fire regimes consisted of frequent, low severity fires (Beaty and Taylor, 2008; Cowling et al., 1996; Odion et al., 2010; Sugihara and Barbour, 2006). Unfortunately, over the last 100 years, fire has been viewed as a catastrophe needing to be suppressed (Kauffman, 2004). These suppression and exclusion efforts have led to forest structural changes and, critically, changes in the amount of combustible material, or fuels, available to future fires (Dennison et al., 2014; Miller et al., 2009; Steel et al., 2015). Fires now burn less frequently but with greater intensity (Agee and Skinner, 2005; Miller et al., 2012), increasing hazard to society and, in particular, those who live in the wildland-urban interface (WUI). During the second half of the 20th century, the expansion and further development of the WUI was the greatest driver of fire regimes shifts (Syphard et al., 2007). In conjunction with climate change, the growth of the WUI intensifies the prevalence of destructive fires by increasing both fuel loading from heightened suppression efforts and social risk exposure (Brown et al., 2020; Calkin et al., 2015).

The WUI is defined as locations where homes and other developments “meet or intermingle” with undeveloped vegetated wildlands (Radeloff et al., 2005). In the United States, this definition has been codified as areas with low housing density and proximity to wildland areas (Syphard et al., 2007). The WUI in the United States grew faster than any other land use type from 1990 to 2010 and is projected to continue to expand significantly over the coming decade (Hammer et al., 2009; Radeloff et al., 2018; Theobald and Romme, 2007). Social shifts in desire for lower density housing and increased proximity to surrounding natural amenities drive this expansion (Hammer et al., 2009). Unfortunately, to date, the majority of this development has occurred in areas with historically high fire severities (Radeloff et al., 2018; Theobald and Romme, 2007). As a result, national fire fuel management efforts currently predominantly target WUI areas (Charnley et al., 2015).

The complex ownership landscape of the WUI presents serious challenges to cohesive management for fire hazard reduction. Nationally, approximately 90% of properties in the WUI are privately owned (Theobald and Romme, 2007) and large fires regularly cross between land tenures (Ager et al., 2017; Palaiologou et al., 2019). In addition, wildfire transmission from national forest lands threaten over half of the WUI in the western United States (Ager et al., 2019). As a result, management and hazard mitigation responsibility involves every level of land ownership, including federal agencies, state and local governments, as well as private industry and land holders (Ager et al., 2017; Mockrin et al., 2018). In addition, effective fire hazard management requires the application of targeted treatments across the landscape and across land tenures (Ager et al., 2010). Consequently, WUI fire hazard management requires widespread collective action across all levels of land ownership (Paveglio et al., 2019). This cohesive management also provides the only means by which to protect the most vulnerable and least resilient members of society who would otherwise be unable to protect themselves (Kolden and Henson, 2019).

Social wildfire vulnerability arises through the interplay of level of exposure, sensitivity to impact, and post-fire adaptive capacity (Kolden and Henson, 2019). By addressing these three, communities can become more fire adapted and, therefore, resilient. Fuel treatments and improved wildlands management directly reduce exposure, and, by extension, impact sensitivity (Kolden and Henson, 2019). These treatments aim to reduce the amount of combustible material in a forest so that subsequent fires burn with lower intensity (Reinhardt et al., 2008). However, optimal management actions for forest health and fire hazard reduction often do not align (Ager et al., 2010; Charnley et al., 2015). Likewise, aesthetic and resource changes as a result of treatment may conflict with local perceptions and valuation of optimal natural forest structure and values (Depietri and Orenstein, 2020; Jahn et al., 2020). The implementation of forest management treatments largely depends on public perception (Brunson and Evans, 2005; Charnley et al., 2015). This perception, in turn, arises from trust in land managers and the effectiveness of treatments (Toman et al., 2011; Vogt et al., 2005).

One understudied component of effective collective management in the WUI is how a cohesive decision-making process can be implemented across social and governance levels. The WUI presents a challenging management task due to the complexity of managing such a multi-layered and multi-actor system. Resident of the WUI often form a highly heterogenous group across spectrums of land management motivation, capacity, and desired outcomes (Nielsen-Pincus et al., 2015; Paveglio and Edgeley, 2017; Paveglio et al., 2015). While local social differences render it impossible to generalize a blanket management approach to all WUI landscapes, a critical piece of missing research is identifying commonalities between management decision-making processes across actors in the WUI. Through an understanding of what different groups in the WUI perceive as common aspects and challenges to decision-making, a more unified approach can be implemented which will facilitate future collective action. This paper aims at filling this knowledge gap by addressing the following question: What common approaches and perceived barriers exist between decision-making processes across actors and institutions engaged in fire hazard mitigation land management in the WUI? Using a combined fuzzy cognitive mapping and thematic analysis approach, this study applies this question to a case study of Napa and Sonoma Counties in the state of California.

2. Methods

2.1 Land manager stakeholder interviews

Anyone engaged in land management in Napa and/or Sonoma Counties in the state of California, United States, was eligible to participate in this study. These counties both lie just north of San Francisco and have experienced repeated severe fires over the last decade. As of 2005, California had the highest number of WUI properties among any state in the United States (Radeloff et al., 2005) and these two counties contain especially high WUI densities in highly fire prone areas. In particular, we sought individuals from three demographics: Land managers, defined as any individuals engaged in land management in a professional capacity; fire personnel, defined as any individuals engaged in combatting

wildfires; and private landowners, defined as any individuals who own forested lands but are not professional managers. These demographics encompass all individuals directly engaged in land management in these counties. We identified participants using snowball sampling, whereby each participant was asked to identify other potential candidates. Our initial pool of potential interview candidates was taken from among the attendees at a fire workshop at Pepperwood Preserve in Sonoma County. We contacted 56 potential participants and successfully interviewed 19. Of these 19, two were private land owners, two were fire personnel and 15 were land managers. Among the land managers, three worked in private land management or the forest industry, three were professional foresters, four worked for local government agencies, two worked in academic advising, and three worked for NGOs.

We contacted participants via email and asked them to participate in a one-hour long interview. We initially conducted the interviews in person but were forced to switch to video interviews due to the implementation of Covid-19 socially distancing guidelines midway through the data collection process. Interviews were conducted under ethical permission from the University of Oxford (reference SOGE 1A-2020-10). Participants provided either written consent or, following the transfer to video interviews, recorded verbal consent to be interviewed.

We conducted semi-structured interviews that consisted of three parts. To begin, we asked each participant about their background and experience with land management. We then asked them about what role, if any, does fire hazard play in their decision-making. For the second part of the interview, we invited participants to create a fuzzy cognitive map of their decision-making process (explained in Section 2.2). The final portion of the interview involved a discussion of the map they had generated. We asked participants to describe the strengths, limitations, choke points, and other areas of improvement for the decision-making model. In order to further explore the topics, we then asked follow-up questions. We concluded by asking participants about the role of information in guiding the decision-making process.

2.2 Fuzzy cognitive mapping (FCM)

Fuzzy cognitive mapping is a method for capturing causal relationships in a manner that can be analysed and compared concretely between multiple participants (Özesmi and Özesmi, 2004). In this study, we asked participants to create maps identifying key components in their decision-making process and the connections between these components.

We followed the method of Özesmi and Özesmi (2004) in guiding our participants through the drawing of their own maps, known as participant cognitive maps (PCMs). To explain the exercise, we presented them a map of an arbitrary decision process, in this case a parent deciding to buy ice cream for their child. Once participants understood the purpose of the exercise, they were invited to identify components of their decision-making process and the connections between them. Unlike Özesmi and Özesmi (2004), we did not ask our participants to weight the strength of individual connections. We found this additional task confused our initial participants and diminished the quality of their maps. Additionally, during initial testing, participants' assignment of weights appeared arbitrary, rather than reflecting a deeply held perception of importance, so did not provide additional trustworthy significance to the data. We provided as minimal of input as possible, only engaging with the participant if they asked for guidance.

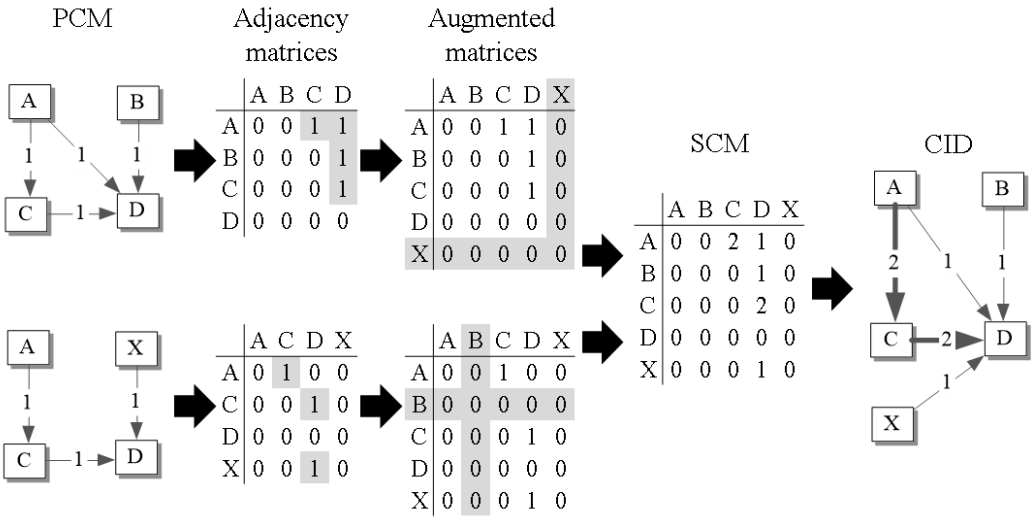


Fig. 2.1 Fuzzy cognitive mapping (FCM) workflow diagram including participant cognitive maps (PCM), social cognitive maps (SCM), and cognitive interpretation diagram (CID).

From the hand drawn PCMs, we generated adjacency matrices to analyse the relationship between components (Fig. 2.1, Özesmi and Özesmi, 2004). Adjacency matrices are square matrices with row and columns for every component. A connection between two components (e.g., A to C) in the PCM is captured in the adjacency matrix with a value in the corresponding row and column (e.g., row A column C). Since participants did not assign weights to individual connections, we assigned each connection a value of one. Many participants used slightly different terms to refer to the same concept. Therefore, we recoded variables in PCMs in order to standardize the language used across maps (Table 2.S1). For example, we standardized the participant variables of "cost," "funding," "grants," and "what can I afford to do" into one variable of "funding." We incorporated participants' description of a component and what occurs during that step in evaluating how to group them. We generated a series of augmented matrices for each recoded PCM. Augmented matrices contain the full set of components identified across all participants, rather than just the ones identified by a specific participant as included in the smaller adjacency matrix. We then combined these through matrix addition to form one social cognitive map (SCM) to represent the entire system (Özesmi and Özesmi, 2004). Connection weights for the SCM are the result of the number of PCMs containing that connection. Weights, therefore, represent the level of consensus between PCMs on the existence of a particular connection. For each variable, we computed the indegree, outdegree, and centrality. The indegree and outdegree are the total combined weights of all connections to and from a component, respectively. The centrality of a component is given by the sum of the indegree and outdegree. Together, these three provide a measure of the importance of a component in the network (Özesmi and Özesmi, 2004).

Table 2.1 Social cognitive map (SCM) qualitative aggregation category groupings

Aggregate component	Original components
Information and consultation	'Compile site data', 'External data', 'Research', 'Site attributes', 'Parcel size', 'Record of success', 'Expert consultation', 'Field survey', 'Outreach', 'Community safety', 'Fire hazard', 'Environmental health'
Stakeholder engagement and capacity	'Stakeholder engagement', 'Stakeholder capacity building'
Institutional knowledge and capacity	'Institutional capacity', 'Institutional knowledge', 'Strategic plan'
Objectives, methods, and priority setting	'Establish objectives', 'Management methods', 'Priority setting'
Management planning and decision-making	'Decision-making', 'Plan development', 'Feasibility'
Funding and resources	'Funding', 'Resources'
Implementation	'Implementation', 'Monitoring and upkeep'

We condensed the SCM variables through qualitative aggregation. Qualitative aggregation involves identifying components with similar qualities that can be represented by a larger aggregate component (Table 2.1). Initially, we removed any variable which contained both an indegree and outdegree of one or fewer. Subsequently, we grouped components by similarity in content and the manner in which participants discussed them. For example, we grouped “decision-making” and “plan development” together because different participants referred to the same aspects of their planning process with these two similar labels. We computed weights for the new aggregate components by summing the connections to and from their constituent components. We removed any connection with a weight of one, meaning it had only been included by one participant. From these weights and connections, we produced a cognitive interpretation diagram (CID) for the full network (Özesmi and Özesmi, 2004). For each aggregate variable, we once again computed the indegree, outdegree, and centrality.

We then separately disaggregated each of the components with the highest centrality into their original constituent variables. From the resulting SCM, we produced modified a CID depicting only the connections to and from each component to highlight the flow through those pieces. As before, we omitted connections identified by only one participant.

2.3 Thematic analysis

We employed thematic analysis to analyse the interviewees' verbal responses using the process described in Braun and Clarke (2006). This method allows for a flexible approach to capturing key themes across participants, regardless of sample size and research question (Clarke and Braun, 2017). We focused the thematic analysis on extracting further information relating to the four main components of the SCM. In addition, we added an additional area of focus, social dynamics, since every interview participant addressed this topic but none included it in their PCM. These five topics represent the most important aspects of the system, as described by the interviewees.

To conduct the thematic analysis, the lead author coded each line of the interviews based on their relevance to the five key topics. Subsequently, these were further separated by content to identify thematically similar groups from within each topic. We then summarized the key information and content from each group to extract the core attributes of these themes. With this method, we sought to capture the common experiences and defining themes across all participants.

3. Results

3.1 Fuzzy cognitive mapping

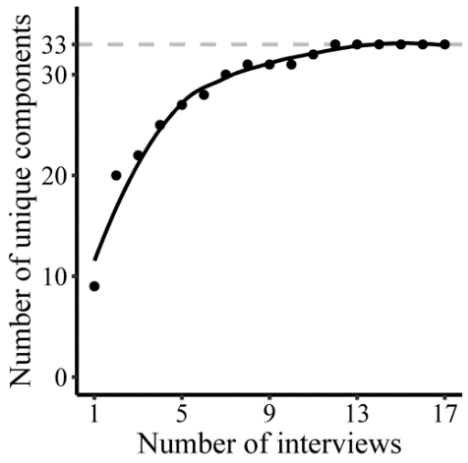


Fig. 2.2 Component accumulation curve.

Of the 19 participants in this study, 17 successfully produced maps. Two participants failed to complete the exercises due to technical challenges of administering the interview via a digital platform. After recoding, participant maps had an average of 8.5 components with a range from six to fourteen components. Variable saturation was reached after twelve interviews at a total of 33 identified variables, and no new variables were mentioned thereafter (Fig. 2.2). Consequently, we can conclude that the population was sufficiently sampled (Özesmi and Özesmi, 2004).

Table 2.2 SCM component metrics. Indegree and outdegree calculated as the sum of all connections leading to and from a component, respectively. Centrality calculated as the sum of indegree and out degree. *n* denotes number of PCMs which contained the component.

Component	Indegree	Outdegree	Centrality	*n*
Plan development	24	15	39	11
Funding	15	19	34	14
Priority setting	17	11	28	9
Decision-making	14	8	22	5
Stakeholder engagement	11	8	19	8
Implementation	14	5	19	8
Institutional capacity	7	8	15	7
Partnerships	6	6	12	9
Establish objectives	5	7	12	6
Resources	5	6	11	7
Permission and compliance	5	5	10	6
Field survey	3	7	10	6
Feasibility	5	5	10	3
Expert consultation	2	7	9	8
External data	2	6	8	4
Environmental health	4	4	8	3
Record of success	3	4	7	2
Management methods	2	5	7	3
Stakeholder capacity building	4	2	6	1
Fire hazard	2	3	5	3
Compile site data	3	2	5	2
Community safety	2	3	5	2
Site attributes	1	3	4	2
Strategic plan	1	2	3	2
Research	1	2	3	2
Parcel size	1	2	3	1
Outreach	1	2	3	2
Monitoring and upkeep	2	1	3	2
Stakeholder capacity	1	1	2	1
Institutional knowledge	0	2	2	2
Adaptive management	1	1	2	1
Project proposal	0	1	1	1
Modelling	0	1	1	1

From the PCMs, we generated an SCM with 33 components and 130 connections (Table 2.2). While funding was included in the highest number of PCMs, plan development emerged as the most

important component in terms of centrality. When referring to difficult or complex aspects of their decision-making process in the generation of their PCMs, participants tended to utilize broad component names to capture multiple actions or steps. To take the top component as an example, participants who included "plan development" in their PCM often proceeded to verbally explain the multiple steps involved in its generation. Participants tended to use a higher level of specificity when referring to tangible details such as specific information sources.

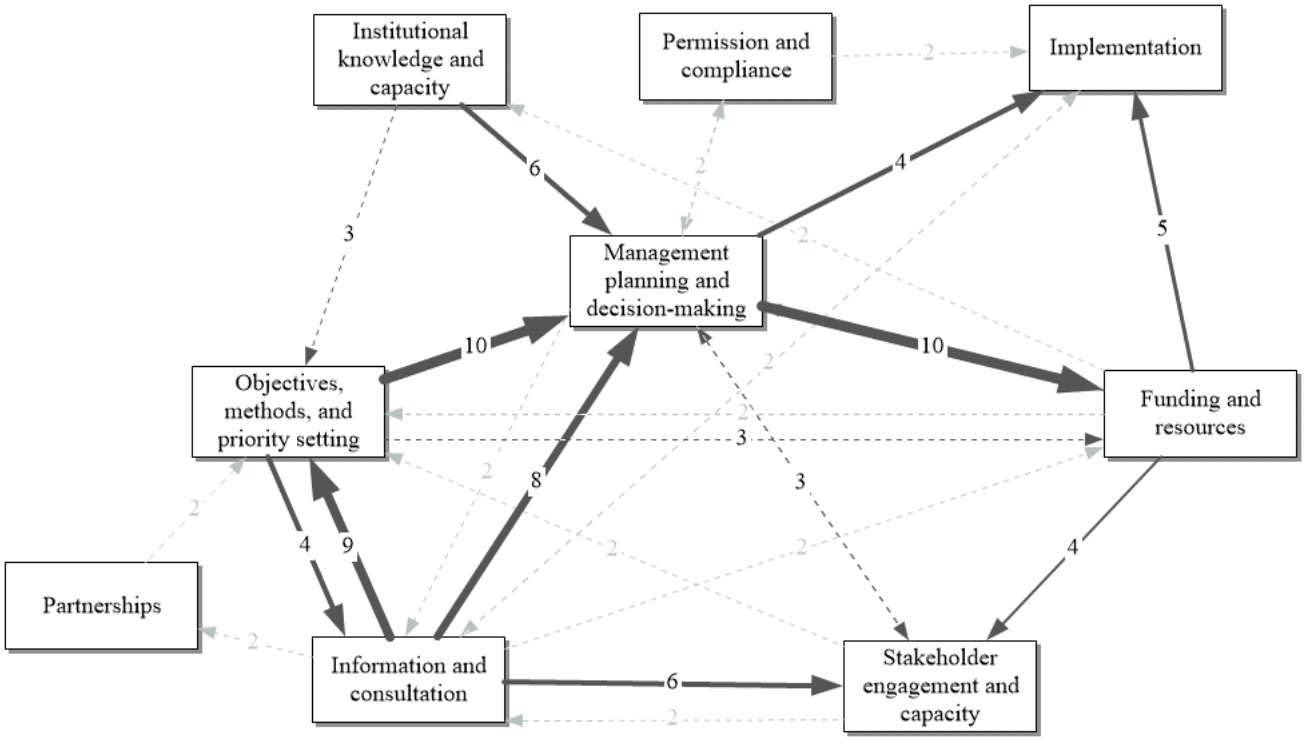


Fig. 2.3 Cognitive interpretation diagram (CID) for social cognitive map (SCM) with aggregated components. The directionality of each relationship is indicated by the arrowhead and the weight of the relationship is indicated by the line thickness and number label. Line width and label represents the weight of the connection as determined by the number of participants ($N = 17$) who identified it. Low weight connections displayed with a dashed line and grey coloration.

Table 2.3 Social cognitive map (SCM) aggregate component metrics. Indegree and outdegree calculated as the sum of all connections leading to and from a component, respectively. Centrality calculated as the sum of indegree and out degree.

Component	Indegree	Outdegree	Centrality
Management planning and decision-making	37	21	58
Information and consultation	10	29	39
Funding and resources	15	21	36
Objectives, methods, and priority setting	18	17	35
Stakeholder engagement and capacity	13	7	20
Implementation	13	2	15
Institutional knowledge and capacity	2	9	11
Permission and compliance	2	4	6
Partnerships	2	2	4

Following qualitative aggregation, the resulting SCM contained nine components (Fig. 2.3). The largest number of components were aggregated under the new component of "information and expert consultation" (Table 2.1). Based on centrality values, "management planning and decision-making" is the most important component of this system (Table 2.3). The strongest pathway extends from "objectives, methods, and priority setting" into "management planning and decision-making" and finally to "funding and resources." "Information and consultation" served as a strong driver with respect to the components of "objectives, methods, and priority setting" and "management planning and decision-making."

3.2 Social dynamics

The most common theme related to social dynamics, mentioned in nine interviews across all demographic groups, was the substantial shift in mentality following the severe fires that swept through the region in 2017. Nine of the interviewees stressed how their thinking and focus on fire changed dramatically following the events. For managers, fire management became a top priority, regardless of background or prior focus. One land manager, describing this paradigm shift, stated:

> "*If you had asked me [about fire hazard management] in September of 2017, I would have said I don't know anything about fire, I don't work with fire. As of October 2017, when the Nuns and the Tubbs came through, my focus completely changed. Again, I am not a fire science person*

but the focus on fire, the focus of recovery, and the focus of reducing vegetation that is a fire fuel became my top priority."

Among private landholders, these fires served as a watershed moment in terms of recognition of the potential fire hazard which has only been amplified in the last few years with repeated fire events, smoke filled days, and power outages. These events have served to increase awareness of management needs and motivation to undertake treatment.

The second most common theme, mentioned in eight interviews across all demographic groups, was the challenges of management in an area with such complex landownership. Respondents commented on the high number of small parcels, many of which are owned by older residents or by individuals who cannot afford to undertake recommended fire prevention actions. They reported that many residents moved to this area from urban locations, such as San Francisco, for aesthetic reasons and do not have any land management experience or awareness. Land managers engaged in assisting private landholders observed frustration from community members that, while they undertook forest treatment efforts, their neighbours neglected to do so and, therefore, put all surrounding properties at increased risk. Many respondents shared frustration over this lack of cohesive action. One land manager summarized the need for collective action as "*how are you [at fuel management] as a community because your community is going to burn as a community*."

The third key theme with respect to social dynamics, which emerged from seven of the interviews across all demographic groups, was the importance of community buy-in for successful treatment implementation. One interviewee in local government stressed that all fuels management efforts are "*going to die if people forget and they stop supporting it*." Several land managers and one landowner engaged in a community organization indicated that they often plan their management efforts based on which members of the community appear to be most engaged at that moment. As an example, widespread community buy-in plays a particularly critical role in prescribed burning since even one concerned neighbour can derail a planned burn.

The last key social dynamic element involves language barriers faced by private landowners. While they seek to obtain the necessary technical and financial assistance to assist them in protecting their properties from future fires, private landowners often struggle with grant applications, reports, and other documents written in technical jargon. One participant described this as "*fire world language*" and emphasized the need for translations into language accessible to private landowners. This "language," and the divide it creates between professional and private individuals, reportedly extends to interpersonal interactions as well. One private landowner, describing an encounter with fire personnel, recounted:

> "*Just recently I was in a meeting with some of the fire organizations. We're sitting at the same table with them and they refer to us as the public. It was a small group. They could have used our names, but it was like oh my gosh there it is, right there, that's the divide. You know it feels like we're viewed as our job is just to get out of the way so they can come in and put out the fire, protect us, or whatever, instead of it really being seen as a partnership.*"

3.3 Objectives, methods, and priority setting

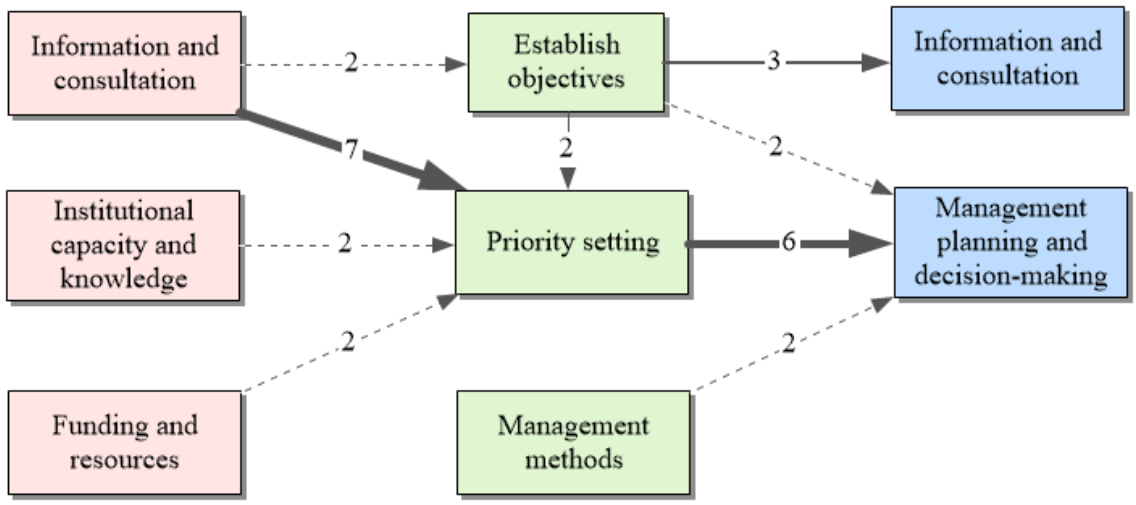


Fig. 2.4 Objectives, methods, and priority setting cognitive interpretation diagram (CID). Depicts drivers (red) and receivers (blue) for the components (green) that comprise this group. The directionality of each relationship is indicated by the arrowhead. Line width and label represents the weight of the connection as determined by the number of participants who identified it. Connections identified by only two participants displayed by a dashed line. Connections identified by only one participant omitted.

All interviewees discussed the importance and difficulty of priority setting. More than 50% of the participants included it in their PCM (Table 2.2). A third of PCMs included priority setting as a connecting element between "information and consultation" and "management planning and decision-making" (Fig. 2.4). Participants sought to identify best feasible management opportunities, "*not just triage them*." However, the primary challenge of prioritization, as identified in every interview, was the need to balance urgency of acting with limitations in resources and capacity. One land manager summarized this challenge as "*you have to take these things in steps and you have to identify what is a viable chunk that I can actually get done and will have the most bang for the buck*." In order to maximize resources, interviewees typically prioritized projects which returned multiple benefits or required lower financial investments. Fire personnel and private landowners stressed that their top priority projects always focus on community safety. The importance all participants placed on priority setting in their narratives strongly reflects the centrality of this variable. It has the third highest centrality and number of PCM inclusions of all components in the full SCM (Table 2.1).

Despite its minimal role in the SCM, two-thirds of participants stressed the importance of the process and challenges of establishing objectives in their narratives (Table 2.2, Fig. 2.4). This discrepancy in importance was largely due to the fact that participants often discussed the establishment of objectives as the starting point of their priority setting process, rather than as a separate step to be included in their PCM. For this reason, we formed these variables into a group for the aggregated SCM. All demographic groups discussed the need for, and lack of, wide scale cohesive objectives to help guide local actions. For example, one land manager stated:

> "*It would be nice if there was a county-wide plan identifying priorities. Not every bloody road necessarily but you know where [the state wildfire fighting agency] thinks a shaded fuel break would be particularly important, instead of each individual landowner trying to ring their own property*."

This issue primarily arose in the context of working with private landowners. Among land managers engaged in assisting private landowners, all participants indicated that their process began with

assisting the landowner in establishing their own objectives. However, while the land managers viewed their role as primarily supporting the landowners on the promotion of these objectives, the landowners discussed their need for assistance throughout the entire process since they felt unequipped to develop appropriate objectives alone.

Management methods appeared in three PCMs and five of the participants discussed different options (Table 2.2). With respect to the majority of participants, vegetation structure and management objectives appeared to dictate specific management options, and, therefore, did not constitute a discrete decision point. The one participant who discussed management options at most length stressed the social challenges associated with prescribed burning. They indicated that prescribed burning could play a significant role in ongoing fuels management but that each burn currently requires a great deal of coordinated education and outreach due to significant social distrust of the practice.

3.4 Management planning and decision-making

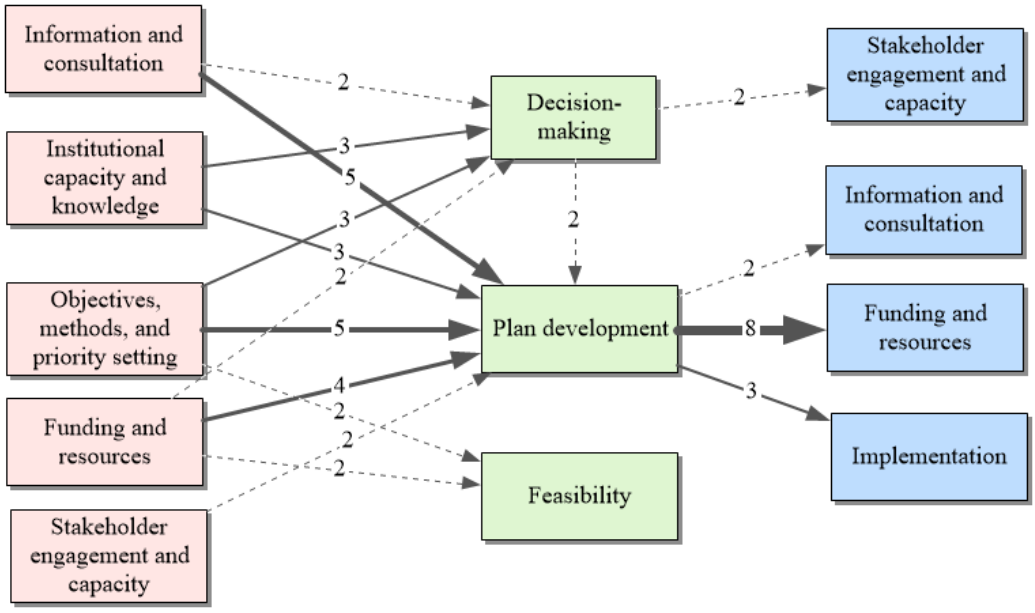


Fig. 2.5 Management planning and decision-making cognitive interpretation diagram (CID). Depicts drivers (red) and receivers (blue) for the components (green) that comprise this group. The directionality of each relationship is indicated by the arrowhead. Line width and label represents the weight of the connection as determined by the number of participants who identified it. Connections identified by only two participants displayed by a dashed line. Connections identified by only one participant omitted.

As mentioned previously, plan development emerged as the most important element by centrality in the SCM (Table 2.2). Consequently, plan development had more drivers than any other component in the SCM (Fig 2.5) and it served as the principle driver for funding and resources, the most discussed component in the SCM. Despite this apparent importance from the SCM, those participants who were not landowners did not discuss plan development in any depth. Most land managers simply indicated at which point in the process they create their management plan. They discussed inputs in detail, as captured by the high number of drivers for the component, but not how these pieces combined to create the plan. To generate plans for private landowners, they consistently described the plan development as a simple matter of combining the landowner's objectives with available site information.

Much of the land managers' decision-making occurred in the process of generating this plan. As with prioritization, urgency emerged again as the most common factor in decision-making, especially with respect to deciding what actions should be undertaken from the planning stage through

implementation. Fire personnel identified project upkeep as a key decision-making criterion. In order for them to proceed with the planning and implementation of a project, they needed demonstrable ability to upkeep the project after its completion.

In contrast to the clear understanding of plan development and management decision-making voiced by participants engaged in such activities in a professional capacity, private landowners struggled with these steps of the management process. One landowner reported working with a forester on a management plan but not fully understanding its scope and significance until after attending an educational workshop. In particular, the workshop helped them to connect their personal goals to potential management actions, which they describe as "*a much better experience for me, to have a plan that means something to me personally*." Private landowners and land managers agreed that a critical component in assisting private landowners is that the final decisions must be made by the landowner. They may rely on expert advice but the final understanding and decision must come from said landowner. As one land manager remarked, the role of professional input should be to educate the landowner about available options in order to "*empower them to say hey, I can actually do something that will make a difference here*."

3.5 Information and consultation

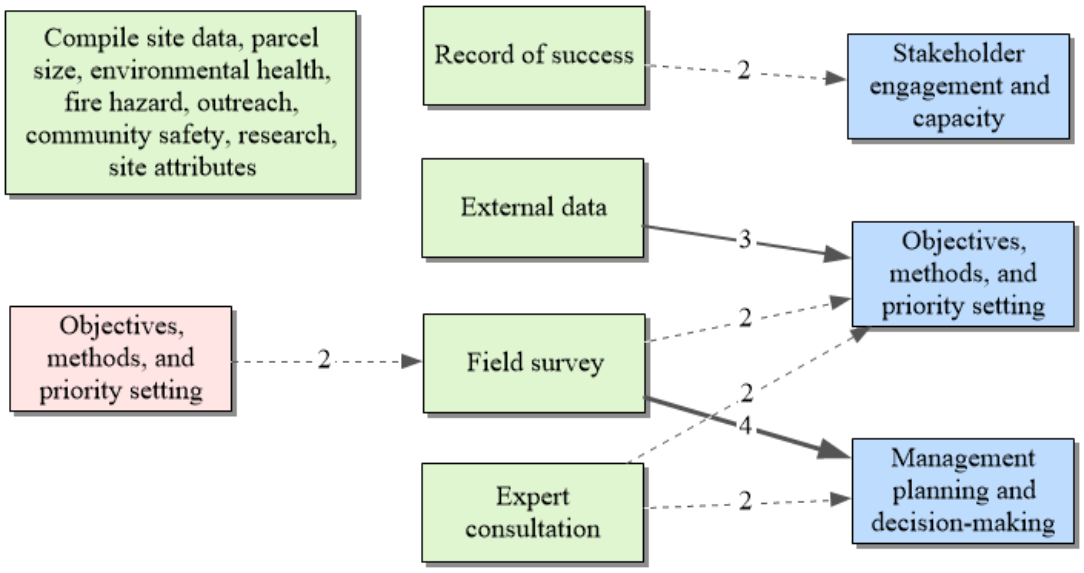


Fig. 2.6 Information and consultation cognitive interpretation diagram (CID). Depicts drivers (red) and receivers (blue) for the components (green) that comprise this group. The directionality of each relationship is indicated by the arrowhead. Line width and label represents the weight of the connection as determined by the number of participants who identified it. Connections identified by only two participants displayed by a dashed line. Connections identified by only one participant omitted. Large green box contains all components with no remaining connections after the removal of single PCM connections.

The component of information and consultation emerged as a strong driver of the decision-making process with the highest outdegree of any aggregated component (Table 2.3). However, when these components are disaggregated and the weakest connections removed, few components retain any connections (Fig. 2.6). Field surveys emerged as the most important element but even its connections have low weights. Information and expert consultation, therefore, played an important role in the functioning of the entire system but little consensus exists between participants in their sourcing or utilization of this data in their decision-making.

Despite this heterogeneity, two key themes emerged that determine the value of an information source. Information accessibility and ease of use emerged as the key determinant of information utility, mentioned by almost half of participants. Private landowners heavily stressed the need for information to be available and communicated in a way that they can access. One landowner voiced their frustration over their perception of the jargon laden opacity of data availability by stating:

"*Just seems like if [the state wildfire fighting agency] could tell us their modelling and tell us what their priorities are, and if the scientific community could translate the data in a way that it's transferable down at the level of parcels and then have the fire community help us look at it… You know it seems like all the pieces are there*."

Several interviewees reported frustration over the lack of a centralized repository for site data. They acknowledged that data are available online, but not in a format that facilitates its utilization. Discussing this challenge, one land manager stated, "*I find out about stuff all the time where I'm like I wished I had known that. If there was a more centralized location to go looking for data products that were regionally applicable, that would be incredibly helpful*." With respect to field data collection, both land managers and private landowners highlighted the utility of smartphone-based information gathering, such as Avenza.

Information acquisition timeframe and scale was mentioned in more than a third of the interviews. Due to the frequency of fire occurrence, participants reported that significant wildland vegetation changes occur regularly. Consequently, information sources that require significant time to collect and process may provide little utility, since there is a high probability of sufficient vegetation change to render the information useless before it is even available. One land manager described this challenge as "*we don't want to do this haphazardly. At the same time, if we are paralyzed by needing to have the most precise data possible that could cost homes and lives and wildlands. I think you have to walk in the middle*." Therefore, participants highlighted data scale as an important factor in considering information. Due to the small parcel size of the majority of properties in the area, low effort field visits often prove sufficient to inform management. This scale of information gathering also ranks highly with respect to the first theme, particularly as it relates to ease of use. One participant described this, stating, fire hazard is "*often very obvious on the ground. We might not be able to quantify it but we can at least point at it and say here's something that needs a treatment*."

When discussing the importance of information sources, manual field surveys and expert consultations emerged as the two most important information sources utilized by participants. Many land

managers, in particular, stressed the importance of in-person field observations, regardless of other available data. One private landowner stressed the importance of assistance from professionals in guiding them through this process. In addition, most land managers utilize publicly available GIS databases for property information, such as site slope.

Participants did not identify remote sensing data as a useful information source in land management decision-making. Instead, they viewed broad scale information sources to be primarily useful as communication tools. Several participants highlighted the power of aerial imagery to communicate larger landscape connectivity and management options to private landowners and policy makers. All participants who discussed these methods stressed the amount of effort and technical capacity required to extract meaningful information from aerial imagery and lidar data. They believed such information could be useful for widespread management planning but all interviewees said such an effort was beyond their reach. In the end, most land managers professed a lack of interest in these more complicated data sources due to its expense and effort. More simple data collection methods, primarily field sampling, provided sufficient information for their needs and allowed more time for actual management. One land manager, describing lidar, stated:

> "*We've been able to look at some of that but I'm not sure how terribly useful it is. Although some people have gone in and been able to do some reasonably decent fuel modelling, at the end of the day, if there isn't somebody who has got the money and time to work on the fuel issue, it does not matter.*"

3.6 Funding and resources

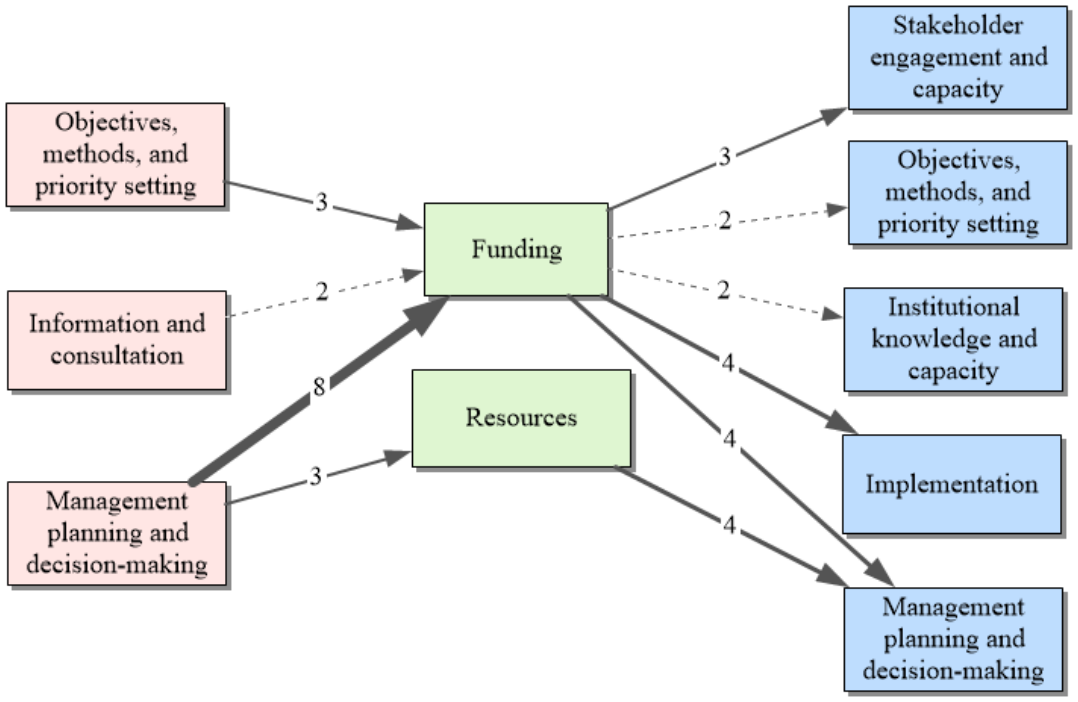


Fig. 2.7 Funding and resources cognitive interpretation diagram (CID). Depicts drivers (red) and receivers (blue) for the components (green) that comprise this group. The directionality of each relationship is indicated by the arrowhead. Line width and label represents the weight of the connection as determined by the number of participants who identified it. Connections identified by only two participants displayed by a dashed line. Connections identified by only one participant omitted.

More participants included funding in their PCM than any other component (Table 2.2) and, in the SCM, the main connective pathway terminates at funding (Fig. 2.3). This reflects the manner in which every participant described funding. Across all demographics, funding served as, by far, the largest barrier to implementation of management plans. With the exception of two individuals, interviewees discussed the challenge of grant funding for this work. With the exception of some state agencies and wealthy landowners, none of the participants or the people with whom they worked could afford to complete the treatments they had identified through their decision-making process without outside sources of grant funding. One land manager described the grant process as "*like swimming in shark infested waters. Everybody is chomping trying to get at it. To me that's not a good situation.*" Landowners reported being repeatedly denied grants, despite receiving extensive input and support from both land managers and fire professionals. Many participants discussed the challenges of navigating available grants which often

provide funding for specific goals. As a result, participants had to modify their goals and treatment plans to match available funding sources. As one land manager explained, this forces a shift towards "*incremental pieces as project descriptions when really you need the energy to create a program that can move forward over time.*" Additionally, many participants voiced frustration with respect to the one-time nature of these grants, whereby the funding body will support the initial work but not ongoing upkeep. To achieve lasting fuels mitigation outcomes at a landscape scale, many participants advocated for an alternative approach with more consistent funding streams that lowered barriers for land managers and private landowners to undertake larger scale projects and to support the ongoing work required to maintain them.

More than a third of participants identified the challenge of insufficient resources in their PCMs and their narratives. Resources, as used here, refers to work crews and equipment required to actually conduct a management treatment. As with funding, participants discussed the lack of resources as a serious barrier to project implementation. In particular, these participants stressed the intensive workload placed on their staff and personnel capacities in order to conduct fuels management projects. They also discussed limited equipment availability. As one land manager reported, "*sometimes we have to drop a project for the year just because we simply do not have time to manage it.*" In addition, land managers indicated that many private landowners do not have the personal capacity to seek out funding, even when it is available. Several participants stressed that these resource limitations particularly impacted the ability to conduct prescribed burns. One land manager, who worked on connecting organizations with grants, summarized the human resource capacity limitation as:

> "*Champions [to lead projects] are humans. They only have so much time and energy. Especially under constrained budget conditions, having enough humans that know how to manage projects, that have the right expertise, and that actually know how to manage grants... [Some organizations] had very little knowledge of what that would entail and it was very daunting for them to agree to be a champion even if it was a great fit... I'll call it successful delivery challenges.*"

4. Discussion

This study sought to determine the common decision-making processes and barriers related to wildfire hazard reduction experienced by professional land managers, fire personnel, and private landowners. Through the usage of fuzzy cognitive mapping (FCM), we identified a core decision-making chain across demographic groups. This chain begins with the establishment and prioritization of land management objectives. Participants then applied these objectives to the formation of a land management plan, either through their own abilities or through the engagement of an outside knowledgeable professional. Finally, participants sought funding for their intended management actions. This funding stage determined if a plan could be successfully implemented. Information and professional consultation helped drive both the priority setting and management plan phases of this chain.

When considering how to inspire change within this system, priority setting emerged as the critical stage for intervention. Participants across all demographics identified this phase as the primary point in which they engaged in actual decision-making. Subsequent actions, regardless of land tenure, focused simply on the realization of these priorities. Even plan development, the most important component in the map based on centrality, followed entirely from the priority setting process. Therefore, any attempt to influence this system towards a desired outcome should focus on the priority setting process of all involved actors.

To effectively reduce fire hazard in WUI landscapes, all actors must engage in aligned land management efforts (Dombeck et al., 2004). The results from this study suggest that collective priority setting may be the most effective way to achieve this goal. Through this collective process, individual actors, both private landowners and institutions, could ensure their personal priorities align with the actions being taken across the landscape. Therefore, any management planning and implementation they undertake that is consistent with these collective priorities would be amplified across the landscape through collective action. The willingness of individual actors, and private landowners in particular, to undertake management actions depends on their perception of personal responsibility and the efficacy of

their actions (Ghasemi et al., 2020; Martin et al., 2009). Therefore, individual engagement in management should increase just through the perception of priority alignment.

Achieving equitable collective priority setting will require the creation of inclusive spaces and processes, especially those targeted at private landowners. Government agencies, fire professionals and land managers need to view private landowners as key partners in the process, rather than a hurdle to confront. As stated by one participant, they can no longer view private landowners as simply "the public." Private landowners in this study wanted to engage with wider priority setting and decision-making processes but confronted barriers to doing so. Beyond simply priority setting, removing these barriers is critical for promoting public buy-in. The importance of public buy-in identified in this study is in agreement with previous research which found that public acceptance of, and willingness to engage in, fuels management depends on perceived competence of land managers and ongoing relationship building (Rasch and McCaffrey, 2019; Shindler and Toman, 2003; Toman et al., 2011).

Improved collective management outcomes could be promoted through the development of more integrative information systems. Participants across all demographics voiced their frustration over the fragmentation and inconsistency of information sources. Information appeared as the primary driver of priority setting and plan development so merits careful consideration. To be useful, we found that information must be accessible, timely, and of a relevant scale. Private landowners identified accessibility as a key issue. For them to be able to appropriately engage in any cohesive management efforts, information must be delivered to them in a manner which they can understand. They preferred to have professional assistance in interpreting data for their situation. This corroborates previous research which found landowners benefited most from education coupled with personal interaction (Brenkert-Smith et al., 2012; McCaffrey, 2004).

Interview participants do not utilize information from remote sensing in its current form. In general, they professed a lack of resources to enable them to develop the capabilities required for its implementation in their decision-making process. This stems from the widely held view that these information sources are overly complicated or difficult to access. In its current form, it violates the criteria

for information utility highlighted above. However, remote sensing methodologies have an extremely high potential to facilitate large scale management, especially when attempting to integrate efforts across land tenures. This disconnect between potential utility and current perceived barriers could be addressed through the addition of remote sensing experts on management teams or the development of an information repository where scientists could provide remote sensing data to the land management community in a more accessible and readily interpretable format.

As could be anticipated, the final piece of the puzzle is funding. Regardless of the success of priority alignment and management planning, it is impossible to implement solutions without funding. The current "shark infested waters" of the grant-based system frustrated participants in all demographics. Participants called for a more sustainable system whose goal is to support larger and more long-term projects. To achieve long-term resiliency, management must encourage a safe return of fire to the landscape (Reinhardt et al 2008). This cannot be achieved through the one-time local level management projects that currently exist via the grant system.

This study focused on identifying common ground in decision-making across a range of core demographics in the WUI. Our sample size was small but did achieve variable saturation, suggesting we sufficiently sampled the population to draw meaningful conclusions about this research question and this population. However, we did not achieve variable saturation for each demographic group (i.e., private landowners, fire professionals, etc.). Consequently, our results may be missing perspectives within these groups which would diminish the generalizability of these findings. Furthermore, our study focused on a specific region in California. Other WUI regions, such as those dominated by working lands, may present different social dynamics and decision-making processes. Future studies, therefore, should seek to expand this study to encompass larger sample sizes across broader geographic regions to identify the differences in decision-making approaches between demographic groups and ensure the generalizability of the findings presented here. Additionally, these results should be validated through alternative methods capable of capturing large sample sizes, such as online surveys.

5. Conclusion

Collective management action in the WUI for wildfire hazard reduction should focus on fostering cohesive priority setting. We demonstrated that all other management outcomes follow directly from this initial process. This can best be achieved through the removal of information and funding barriers to enable private landowners to engage with the management process as equal partners with professional land managers and fire personnel. Through this process, community resilience and ecosystem health may be promoted simultaneously.

Authorship contribution statement

Conceptualization, S.R. and I.O.; methodology, S.R. and I.O.; investigation, S.R.; software, S.R.; formal analysis, S.R.; resource, S.R.; writing—original draft preparation, S.R.; writing—review and editing, I.O.; visualization, S.R.; supervision, I.O.; funding acquisition, S.R. All authors have read and agreed to the published version of the manuscript.

Acknowledgements

SR was funded by the Rhodes Trust and through the University of Oxford Environmental Change Institute Small Grant Scheme.

References

Agee, J.K., Skinner, C.N., 2005. Basic principles of forest fuel reduction treatments. Forest Ecology and Management 211, 83–96. https://doi.org/10.1016/j.foreco.2005.01.034

Ager, A.A., Evers, C.R., Day, M.A., Preisler, H.K., Barros, A.M.G., Nielsen-Pincus, M., 2017. Network analysis of wildfire transmission and implications for risk governance. PLoS ONE 12, e0172867. https://doi.org/10.1371/journal.pone.0172867

Ager, A.A., Houtman, R.M., Day, M.A., Ringo, C., Palaiologou, P., 2019. Tradeoffs between US national forest harvest targets and fuel management to reduce wildfire transmission to the wildland urban

interface. Forest Ecology and Management 434, 99–109. https://doi.org/10.1016/j.foreco.2018.12.003

Ager, A.A., Vaillant, N.M., Finney, M.A., 2010. A comparison of landscape fuel treatment strategies to mitigate wildland fire risk in the urban interface and preserve old forest structure. Forest Ecology and Management 259, 1556–1570. https://doi.org/10.1016/j.foreco.2010.01.032

Beaty, R.M., Taylor, A.H., 2008. Fire history and the structure and dynamics of a mixed conifer forest landscape in the northern Sierra Nevada, Lake Tahoe Basin, California, USA. Forest Ecology and Management 255, 707–719. https://doi.org/10.1016/j.foreco.2007.09.044

Brenkert-Smith, H., Champ, P.A., Flores, N., 2012. Trying not to get burned: Understanding homeowners' wildfire risk–mitigation behaviors. Environmental Management 50, 1139–1151. https://doi.org/10.1007/s00267-012-9949-8

Brown, T., Leach, S., Wachter, B., Gardunio, B., 2020. The extreme 2018 northern California fire season. Bulletin of the American Meteorological Society 101, S1–S4. https://doi.org/10.1175/BAMS-D-19-0275.1

Brunson, M.W., Evans, J., 2005. Badly burned? Effects of an escaped prescribed burn on social acceptability of wildland fuels treatments. Journal of Forestry 5.

Calkin, D.E., Thompson, M.P., Finney, M.A., 2015. Negative consequences of positive feedbacks in US wildfire management. For. Ecosyst. 2, 9. https://doi.org/10.1186/s40663-015-0033-8

Charnley, S., Poe, M.R., Ager, A.A., Spies, T.A., Platt, E.K., Olsen, K.A., 2015. A burning problem: Social dynamics of disaster risk reduction through wildfire mitigation. Human Organization 74, 329–340. https://doi.org/10.17730/0018-7259-74.4.329

Cowling, R., Rundel, P., Lamont, B., Arroyo, M., Arianoutsou, M., 1996. Plant diversity in Mediterranean-climate regions. Trends in Ecology & Evolution 11, 362–366. https://doi.org/10.1016/0169-5347(96)10044-6

Dennison, P.E., Brewer, S.C., Arnold, J.D., Moritz, M.A., 2014. Large wildfire trends in the western United States, 1984-2011. Geophys. Res. Lett. 41, 2928–2933. https://doi.org/10.1002/2014GL059576

Depietri, Y., Orenstein, D.E., 2020. Managing fire risk at the wildland-urban interface requires reconciliation of tradeoffs between regulating and cultural ecosystem services. Ecosystem Services 44, 101108. https://doi.org/10.1016/j.ecoser.2020.101108

Dombeck, M.P., Williams, J.E., Wood, C.A., 2004. Wildfire policy and public lands: Integrating scientific understanding with social concerns across landscapes. Conservation Biology 18, 883–889. https://doi.org/10.1111/j.1523-1739.2004.00491.x

Ghasemi, B., Kyle, G.T., Absher, J.D., 2020. An examination of the social-psychological drivers of homeowner wildfire mitigation. Journal of Environmental Psychology 70, 101442. https://doi.org/10.1016/j.jenvp.2020.101442

Hammer, R.B., Stewart, S.I., Radeloff, V.C., 2009. Demographic trends, the wildland–urban interface, and wildfire management. Society & Natural Resources 22, 777–782. https://doi.org/10.1080/08941920802714042

Jahn, J.L.S., White, M.S., Brenkert-Smith, H., 2020. My place or yours? Using spatial frames to understand the role of place in forest management conflicts. Society & Natural Resources 33, 329–346. https://doi.org/10.1080/08941920.2019.1709003

Kauffman, J.B., 2004. Death rides the forest: Perceptions of fire, land use, and ecological restoration of western forests. Conservation Biology 18, 878–882. https://doi.org/10.1111/j.1523-1739.2004.545_1.x

Kolden, C.A., Henson, C., 2019. A socio-ecological approach to mitigating wildfire vulnerability in the wildland urban interface: A case study from the 2017 Thomas Fire. Fire 2, 9. https://doi.org/10.3390/fire2010009

Martin, W.E., Martin, I.M., Kent, B., 2009. The role of risk perceptions in the risk mitigation process: The case of wildfire in high risk communities. Journal of Environmental Management 91, 489–498. https://doi.org/10.1016/j.jenvman.2009.09.007

McCaffrey, S., 2004. Thinking of wildfire as a natural hazard. Society & Natural Resources 17, 509–516. https://doi.org/10.1080/08941920490452445

Miller, J.D., Safford, H.D., Crimmins, M., Thode, A.E., 2009. Quantitative evidence for increasing forest fire severity in the Sierra Nevada and Southern Cascade Mountains, California and Nevada, USA. Ecosystems 12, 16–32. https://doi.org/10.1007/s10021-008-9201-9

Miller, J.D., Skinner, C.N., Safford, H.D., Knapp, E.E., Ramirez, C.M., 2012. Trends and causes of severity, size, and number of fires in northwestern California, USA. Ecological Applications 22, 184–203. https://doi.org/10.1890/10-2108.1

Mockrin, M.H., Fishler, H.K., Stewart, S.I., 2018. Does wildfire open a policy window? Local government and community adaptation after fire in the United States. Environmental Management 62, 210–228. https://doi.org/10.1007/s00267-018-1030-9

Nielsen-Pincus, M., Ribe, R.G., Johnson, B.R., 2015. Spatially and socially segmenting private landowner motivations, properties, and management: A typology for the wildland urban interface. Landscape and Urban Planning 137, 1–12. https://doi.org/10.1016/j.landurbplan.2014.11.020

Odion, D.C., Moritz, M.A., DellaSala, D.A., 2010. Alternative community states maintained by fire in the Klamath Mountains, USA. Journal of Ecology 98, 96–105. https://doi.org/10.1111/j.1365-2745.2009.01597.x

Özesmi, U., Özesmi, S.L., 2004. Ecological models based on people's knowledge: a multi-step fuzzy cognitive mapping approach. Ecological Modelling 176, 43–64. https://doi.org/10.1016/j.ecolmodel.2003.10.027

Palaiologou, P., Ager, A.A., Nielsen-Pincus, M., Evers, C.R., Day, M.A., 2019. Social vulnerability to large wildfires in the western USA. Landscape and Urban Planning 189, 99–116. https://doi.org/10.1016/j.landurbplan.2019.04.006

Paveglio, T., Edgeley, C., 2017. Community diversity and hazard events: Understanding the evolution of local approaches to wildfire. Nat Hazards 87, 1083–1108. https://doi.org/10.1007/s11069-017-2810-x

Paveglio, T.B., Edgeley, C.M., Carroll, M., Billings, M., Stasiewicz, A.M., 2019. Exploring the influence of local social context on strategies for achieving fire adapted communities. Fire 2, 26. https://doi.org/10.3390/fire2020026

Paveglio, T.B., Moseley, C., Carroll, M.S., Williams, D.R., Davis, E.J., Fischer, A.P., 2015. Categorizing the social context of the wildland urban interface: Adaptive capacity for wildfire and community "archetypes." Forest Science 61, 298–310. https://doi.org/10.5849/forsci.14-036

Radeloff, V.C., Hammer, R.B., Stewart, S.I., Fried, J.S., Holcomb, S.S., McKeefry, J.F., 2005. The wildland-urban interface in the United States. Ecological Applications 15, 799–805. https://doi.org/10.1890/04-1413

Radeloff, V.C., Helmers, D.P., Kramer, H.A., Mockrin, M.H., Alexandre, P.M., Bar-Massada, A., Butsic, V., Hawbaker, T.J., Martinuzzi, S., Syphard, A.D., Stewart, S.I., 2018. Rapid growth of the US wildland-urban interface raises wildfire risk. Proc Natl Acad Sci USA 115, 3314–3319. https://doi.org/10.1073/pnas.1718850115

Rasch, R., McCaffrey, S., 2019. Exploring wildfire-prone community trust in wildfire management agencies. Forest Science 65, 652–663. https://doi.org/10.1093/forsci/fxz027

Reinhardt, E.D., Keane, R.E., Calkin, D.E., Cohen, J.D., 2008. Objectives and considerations for wildland fuel treatment in forested ecosystems of the interior western United States. Forest Ecology and Management 256, 1997–2006. https://doi.org/10.1016/j.foreco.2008.09.016

Schoennagel, T., Balch, J.K., Brenkert-Smith, H., Dennison, P.E., Harvey, B.J., Krawchuk, M.A., Mietkiewicz, N., Morgan, P., Moritz, M.A., Rasker, R., Turner, M.G., Whitlock, C., 2017. Adapt to more wildfire in western North American forests as climate changes. Proc Natl Acad Sci USA 114, 4582–4590. https://doi.org/10.1073/pnas.1617464114

Shindler, B., Toman, E., 2003. Fuel reduction strategies in forest communities: A longitudinal analysis of public support. j for 101, 8–15. https://doi.org/10.1093/jof/101.6.8

Steel, Z.L., Safford, H.D., Viers, J.H., 2015. The fire frequency-severity relationship and the legacy of fire suppression in California forests. Ecosphere 6, art8. https://doi.org/10.1890/ES14-00224.1

Sugihara, N.G., Barbour, M.G., 2006. Fire and California vegetation, in: Sugihara, N. (Ed.), Fire in California's Ecosystems. University of California Press, pp. xvi–9. https://doi.org/10.1525/california/9780520246058.003.0001

Syphard, A.D., Radeloff, V.C., Keeley, J.E., Hawbaker, T.J., Clayton, M.K., Stewart, S.I., Hammer, R.B., 2007. Human influence on California fire regimes. Ecological Applications 17, 1388–1402. https://doi.org/10.1890/06-1128.1

Theobald, D.M., Romme, W.H., 2007. Expansion of the US wildland–urban interface. Landscape and Urban Planning 83, 340–354. https://doi.org/10.1016/j.landurbplan.2007.06.002

Toman, E., Stidham, M., Shindler, B., McCaffrey, S., 2011. Reducing fuels in the wildland - urban interface: Community perceptions of agency fuels treatments. Int. J. Wildland Fire 20, 340. https://doi.org/10.1071/WF10042

Vogt, C.A., Winter, G., Fried, J.S., 2005. Predicting homeowners' approval of fuel management at the wildland–urban interface using the theory of reasoned action. Society & Natural Resources 18, 337–354. https://doi.org/10.1080/08941920590915242

Supplement

Table 2.S1 FCM participant component recoding.

Recoded component name	Original component name
Adaptive management	Reflect and change
Community safety	Community safety
Compile site data	Map
	Parcel map
Decision making	Briefings and meetings sorting through opportunities
	Decision point from landowner if they want to proceed to try to do something
	Focused strategic conversation
	Management team
	Manager retreats
	Weekly managers meeting
Environmental health	Ecology
	Ecosystem services
	Ecosystem services lost
	Environmental concerns
Establish objectives	Aesthetic backdrop
	Aesthetics
	Concerns about wildfire
	Discuss resource concerns, goals, and objectives
	Forest health and stewardship
	Produce certain future condition
	Safety
	Site visit + goals
	Top level sets goals
	What are objectives/goals for the land
	Wildlife
	Work with landowner to identify
Expert consultation	Consult experts for advice
	Consult with [state wildfire fighting agency] and other fire experts
	Consultants
	Consultants professional training and experience
	Consultation
	Direct observation from contractors/consultants

	Forest plan required for some financial options
	Hire consultant
	State agency WERT reports (priority setting)
	Talk to colleagues to find consultant
External data	Data collected by other parties (field surveys/studies) - spatial and written
	Information sources
	Outside information
	What objective information available to describe needs?
Feasibility	Can it be implemented?
	Does it make sense?
	What do I need right now?
Field survey	Conduct forest/road inventory
	Direct observation from field visits
	Identify lands needing treatment
	Inventory sealed appropriately
	Looking for burn units
	Physical field experience
	Site visits
Fire hazard	Fire risk
	Fire weather
	Hazardous conditions
	Losses from fire
	Regional fuel break
Funding	Cost factors
	Cost/benefit analysis
	County approaching RCD for assistance after 2017 fires - giving us $ for technical assistance
	External funding sources (patchwork)
	Finding funding and navigating specific language for each agency
	Funded
	Funding
	Funding sources
	Funding/grant opportunity
	Identify possible funding sources
	Interested if financial system available
	Secure funding
	What can I afford to do?
Implementation	Action

	Conduct burn
	Implement
	Implementation
	Implementation timeline
	On-the-ground
	Pre-burn prep
	Proceed with fuel reduction
	Project implementation
	Site/unit prep
	Work
Institutional capacity	Can you support it?
	Consult with staff
	County kept $ in our contract for cash match to fed grant to hire forester
	Formal training
	Internal
	New associate director will help us build program
	Staff on hand
	Training and experience
	What can I do myself?
Institutional knowledge	Informal stories from peers
	Past fire experience
Management methods	Access
	Economic/commercial harvest
	Fuel reduction
	General fuels reduction
	Grazing
	Identify options
	Improve firefighting access
	Limbing and stopping spread
	Mechanical/manual and chemical removal
	Personal prep
	Prescribed fire
	Pre-suppression
	Safe construction in WUI
	Strategic areas where fire would stop
	Tool box
Modelling	Future projections
Monitoring and upkeep	Monitoring

	Mop/clean up
	Ongoing maintenance
	Post-fire stewardship
Outreach	Community outreach
	Media
	Messaging
	Neighbours
	Outreach
	Talk to decision-makers
Parcel size	< 20 forested acres
	> 20 forested acres
Partnerships	Associate director [of outside organization] led transformation and invited me to weigh in
	Organization
	Partnerships with [state wildfire fighting agency] etc.
	Partners
	Partnership
	Refer to [partner organization]
	Research other organizations
	What do I need outside help to do?
	What had county already committed to do?
Permission and compliance	Environmental compliance
	Environmental impact report
	Legal? If not, amend
	Permission
	Permits
Plan development	Burn boss final review
	Compile and communicate to elected
	Develop treatment plan
	Figure out appropriate time frame (Seasonal, phenology, nesting birds, hazards, conditions, permitting) - When do we do them? What do we actually have the resources to do?
	Finalize logistics
	[Organization] second draft
	Fire risk report
	Land owner first draft
	Management plan
	Proposal development
	Start burn plan and mapping

	Unit management plan
	Updating strategic plan now with new forester's input and more detail on forest health program
	Write management plan/prescribe treatments to meet goals and objectives
Priority setting	Areas of consideration
	Consider management priorities and objectives
	Get information about what people are already worried about, etc?
	Identify partial project aims with high bang for the buck value
	Report prioritization
	Set priorities
	Strategic location (fire prone, ridgelines, etc.)
	Values conflicts
	Watershed priority lists (local)
	We could, but should we?
	What can we undertake that meets multiple goals simultaneously? What is the greatest risk? Urgency with feasibility
Project proposal	Proposed project
Record of success	Previous successful project
	Track record of success in other communities
Research	Research
	Research completed project
	Studies of outcomes
Resources	Contractors
	Equipment
	Infrastructure
	Insurance
	List other professional services, contacts, and funding sources to meet goals
	Outside
	Resources
Site attributes	Properties
	Property values and neighbours
	Public lands
	Site history
Stakeholder capacity	Start on their own
Stakeholder capacity building	Add understanding
	Capacity development
	Training

Stakeholder engagement	Ability to get local buy-in
	[Organization] had grant $ left over from [fire management] project - Used it for [meeting] convening with many stakeholders
	Client calls/referred
	Community
	Community support
	Dissatisfaction with status quo
	Empowered to do something
	Identify project champion and matchmaking
	Input from other stakeholders, CDFW, community members
	Surveys and focus groups
Strategic plan	Our strategic plan included forest health as a goal from board of directors
	Previous strategic plans

Chapter 3

Preface

In this second study, I explored the capability of unoccupied aerial system Structure-from-Motion (UAS-SfM) as a remote sensing method in the forests of California, USA and, specifically, to determine if this approach could provide meaningful measurements of canopy structure. From the criteria for an informational input to be useful as identified by the interviewees in my first paper, it appeared that UAS-SfM would have the greatest potential for meeting these needs among the available remote sensing techniques. However, before I could attempt to measure fuel loads, I needed to perform the analyses presented in this chapter to develop a workflow for processing UAS-SfM data and validate the accuracy of this sensor for California forests.

This study began my collaboration with Dr. Matt Clark and Dr. Lisa Bentley at Sonoma State University. The data included in this study comes from their 3D Forests research project, with which I assisted. Dr. Clark and I flew the UAS flights at Pepperwood in this study. I also assisted Dr. Bentley's graduate students with the collection of TLS, HMLS, and field data that will appear in later chapters.

Dr. Clark, Imma, and I developed this paper. I performed the analyses and drafted the manuscript, with editing assistance from my coauthors. Dr. Clark performed processing steps involving commercial software licenses (e.g., PIX4D, Lidar360). This study was published in *Remote Sensing*:

Reilly, S., Clark, M.L., Bentley, L.P., Matley, C., Piazza, E., Oliveras Menor, I., 2021. The potential of multispectral imagery and 3D point clouds from unoccupied aerial systems (UAS) for monitoring forest structure and the impacts of wildfire in Mediterranean-climate forests. Remote Sensing 13, 3810. https://doi.org/10.3390/rs13193810

The Potential of Multispectral Imagery and 3D Point Clouds from Unoccupied Aerial Systems (UAS) for Monitoring Forest Structure and the Impacts of Wildfire in Mediterranean-Climate Forests

Sean Reilly [1], Matthew L. Clark [2], Lisa Patrick Bentley [3], Corbin Matley [2,3], Elise Piazza [4] and Imma Oliveras Menor [1,5]

[1] Environmental Change Institute, University of Oxford, Oxford OX1 3QY, UK

[2] Center for Interdisciplinary Geospatial Analysis, Department of Geography, Environment, and Planning, Sonoma State University, Rohnert Park, CA 94928, USA

[3] Department of Biology, Sonoma State University, Rohnert Park, CA 94928, USA

[4] US Army Corps of Engineers, Regulatory Division, South Branch, San Francisco, CA 94102, USA

[5] AMAP (Botanique et Modélisation de l'Architecture des Plantes et des Végétations), CIRAD, CNRS, INRA, IRD, Université de Montpellier, Montpellier, France

Abstract

Wildfire shapes vegetation assemblages in Mediterranean ecosystems, such as those in the state of California, United States. Successful restorative management of forests in-line with ecologically beneficial fire regimes relies on a thorough understanding of wildfire impacts on forest structure and fuel loads. As these data are often difficult to comprehensively measure on the ground, remote sensing approaches can be used to estimate forest structure and fuel load parameters over large spatial extents. Here, we analyze the capabilities of one such methodology, unoccupied aerial system Structure-from-Motion (UAS-SfM) from digital aerial photogrammetry, for mapping forest structure and wildfire impacts in the Mediterranean forests of northern California. To determine the ability of UAS-SfM to map the structure of mixed oak and conifer woodlands and to detect persistent changes caused by fire, we compared UAS-SfM derived metrics of terrain height and canopy structure to pre-fire airborne laser scanning (ALS) measurements. We found that UAS-SfM was able to accurately capture the forest's

upper-canopy structure, but was unable to resolve mid- and below-canopy structure. The addition of a normalized difference vegetation index (NDVI) ground point filter to the DTM generation process improved DTM root mean square error (RMSE) by ~1 m with an overall DTM RMSE of 2.12 m. Upper-canopy metrics (max height, 95th percentile height, and 75th percentile height) were highly correlated between ALS and UAS-SfM ($r > +0.9$), while lower-canopy metrics and metrics of density and vertical variation had little to no similarity. Two years after the 2017 Sonoma County Tubbs fire, we found significant decreases in UAS-SfM metrics of bulk canopy height and NDVI with increasing burn severity, indicating the lasting impact of the fire on vegetation health and structure. These results point to the utility of UAS-SfM as a monitoring tool in Mediterranean forests, especially for post-fire canopy changes and subsequent recovery.

Keywords

UAS, Structure-from-Motion, Mediterranean, California, fire, forest structure, fire management, airborne laser scanner, ALS, lidar

1. Introduction

While widespread, mixed-severity wildfire regimes play a crucial role in shaping the ecosystems of Mediterranean climatic regions (Beaty and Taylor, 2008; Cowling et al., 1996; Odion et al., 2010; Rundel et al., 2016), current climate change (Westerling, 2018) and historic wildfire suppression have increased the frequency of high-intensity and stand-replacing fires (Miller et al., 2009), as well as 90th percentile fire size (Dennison et al., 2014), in California (United States). Consequently, there is a pressing need to quantify forest structure and fuel loading at multiple spatial scales to understand and forecast relationships between wildfire hazards and forest structure attributes (Filippelli et al., 2019; Flannigan et al., 2009; Westerling and Bryant, 2008). While ground-based surveys may provide accurate data, their limited spatial coverage hampers their usefulness at broader scales (Alonzo et al., 2018; Berra et al., 2019). Remote sensing methods for mapping forest structure and fuels provide a useful alternative since

they have high temporal resolution and large spatial coverage. However, due to its passive, top-down collection method, imagery from multispectral satellite sensors generally fail to detect forest properties below the canopy, nor is it optimal for determining vegetation height (Arroyo et al., 2008), particularly in forests with high canopy cover. Therefore, mapping forest structure from multispectral satellite data is often done indirectly. For example, in the case of estimating the spatial distribution of fire fuels, fuel density models are applied to satellite-derived maps of vegetation characteristics (Stefanidou et al., 2022). However, this indirect method cannot detect variations in vertical forest structure or fuel continuity masked below the canopy within an area possessing similar overstory vegetation characteristics.

Airborne laser scanners (ALS), or lidar sensors, provide an alternative remote sensing method not hindered by these shortcomings as they actively send energy pulses that penetrate below the canopy (Arroyo et al., 2008). Canopy structure metrics derived from ALS point clouds have a strong relationship with field measurements (Andersen et al., 2005) and can be used to determine vertical fuel structures (Marino et al., 2018). Notably, ALS can detect the presence of ladder fuels (Kramer et al., 2014). Ladder fuels are live and dead vegetation that exists between ground vegetation and the base of the canopy above, allowing fire to climb from the forest floor and ignite the canopy (Menning and Stephens, 2007). However, management of yearly or seasonal events such as wildfires require frequent repeated monitoring (Filippelli et al., 2019). While the advent of the NASA Surface Topography and Vegetation program and future lidar satellite systems may address this shortcoming (e.g., Donnellan et al., 2021), ALS is currently excessively cost prohibitive and effort intensive to be conducted with sufficient regularity for this purpose (Chuvieco et al., 2020).

As opposed to the expense and effort required for an ALS survey, forest structure metrics can also be obtained relatively inexpensively from digital aerial photogrammetry (DAP) using unoccupied aerial systems (UAS) carrying commercially available cameras (e.g., Dandois et al., 2015). Three-dimensional point clouds can be generated from overlapping aerial images using Structure-from-Motion (SfM) processing techniques, providing an alternative method for mapping forest structure at a potentially lower cost than ALS depending on spatial extent (e.g., Alonzo et al., 2020; Dandois and Ellis, 2013;

Tompalski et al., 2019), as well as UAS lidar at stand scales (Hu et al., 2020). The low cost and relative ease of the UAS DAP SfM (hereafter UAS-SfM) method make it particularly useful for repeated monitoring during rapidly changing events at plot to stand scales (Campbell et al., 2020), such as interannual wildfires. Of additional benefit over ALS, when used with a multispectral or hyperspectral sensor and downwelling irradiance sensor, UAS-SfM can provide calibrated spectral measurements as well as structural data. However, UAS-SfM technology is not without its own limitations. Due to the passive nature of an imaging sensor and the need for a point to appear in multiple overlapping photographs for its spatial location to be determined, DAP has minimal ability to detect structure below canopy cover as compared to ALS (Cunliffe et al., 2016; White et al., 2018). Therefore, DAP may be limited in the assessment of terrain height, which is needed for accurate point cloud height normalization, and detection of below-canopy forest structure.

To the best of our knowledge, the capabilities of multispectral UAS-SfM for mapping forest structure and below-canopy fuels in the mixed-oak and conifer woodlands of California have not been explored. Focused on a study site in a Mediterranean-climate mixed forest of Northern California, USA, this study seeks to address this research gap with the following objectives:

1. Evaluate the accuracy, as compared with ALS, of multispectral UAS-SfM in estimating ground elevation, a fundamental component of estimating accurate forest heights.
2. Determine the ability, as compared with ALS, of UAS-SfM to measure different metrics of canopy structure.
3. Demonstrate the utility of multispectral UAS-SfM in assessing the impact of wildfire on changes in photosynthetic productivity (greenness) and canopy height relative to ALS baseline conditions.

Findings from these objectives seek to answer the broad question: Can accurate measurements of forest attributes be obtained from UAS-SfM so it can be used as a stand-scale (e.g., 1 to 500 ha) remote-sensing monitoring tool to assess fire fuels and post-fire changes?

2. Methods

2.1 Study site

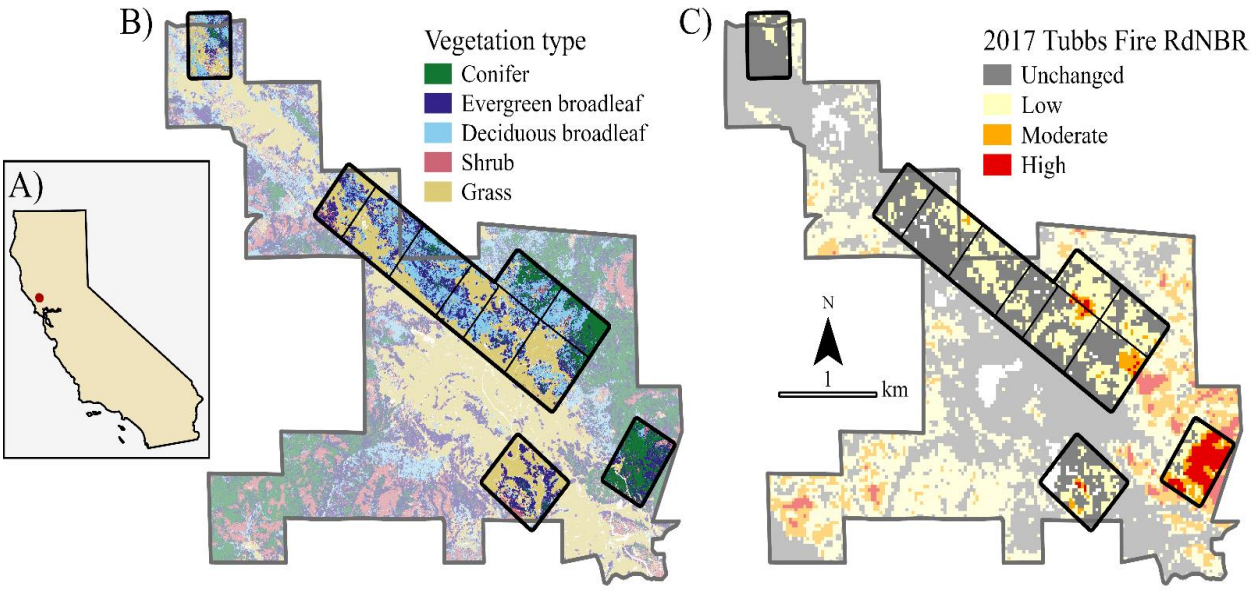


Fig. 3.1 (A) Study site location at Pepperwood Preserve (red point) in California, USA. Maps of (B) vegetation assemblages and (C) the 2017 Tubbs Fire burn severity (MTBS) across the study site. Unoccupied aerial systems Structure-from-Motion (UAS-SfM) data collection extent is represented by black boxes.

This study took place at Pepperwood Preserve (38.57º N, 122.68º W), a 1,261-ha nature preserve in Sonoma County, California, USA (Fig. 1A). Located in the northern Coast Range, the property has predominantly rolling hills (61 - 475 m elevation) vegetated with a mosaic of Douglas-fir forest, oak woodland, chaparral, and grassland (Fig. 1B; Ackerley et al., 2020; Evett et al., 2013). The area is characterized by a Mediterranean climate with dry, hot summers (April to October) reaching over 37˚C and mild, wet winters (November to March) infrequently dropping below 0˚C. The preserve experiences high interannual precipitation variability but receives, on average, around 86 cm of precipitation per year.

As is common throughout California, this climatic regime generates conditions for wildfires by late summer, due to sustained drying of fuels and vegetation, that are further exacerbated by strong autumnal winds (Nauslar et al., 2018). In 2017, the Tubbs Fire swept through Pepperwood (Fig. 3.1C), burning over 95% of the preserve (Pepperwood Preserve, 2019). This fire was the fourth deadliest and second most destructive in California history prior to 2020 (CalFire, 2019a, 2019b). The fire ignited on 9

October 2017 4:45 UTC as part of a complex of fires in the region north of San Francisco, CA. Strong easterly Diablo winds rapidly spread the fire during the first 12 h after ignition (Nauslar et al., 2018). During its 23-day span, the Tubbs fire burned 14,895 ha across all vegetation types in the region.

2.2. Data Sources

2.2.1 Unoccupied Aerial System (UAS) Structure-from-Motion (SfM) Multispectral Data Collection and Processing

This study employed a SenseFly eBee X fixed-wing UAS platform with a MicaSense RedEdge-MX sensor onboard. This multispectral sensor collects five spectral bands: blue (475 nm center, 20 nm bandwidth), green (560 nm center, 20 nm bandwidth), red (668 nm center, 10 nm bandwidth), red edge (717 nm center, 10 nm bandwidth), and near-IR (840 nm center, 40 nm bandwidth). Additionally, an onboard MicaSense Downwelling Light Sensor (DLS) 2 collected ambient sunlight and sun angle. Due to variations in solar light intensity, sensor radiance values must be standardized to reflectance and calibrated based on a sample of known reflectance values in order for multispectral measurements to be comparable across flight missions performed on different days or under varying light conditions, as well as to be compared against reflectance data from other sensors, such as multispectral satellite images. Radiance data were converted to reflectance using downwelling radiance measured from the DLS2 and calibrated with images of a MicaSense calibration panel (RP04-1926247-OB) captured on the ground immediately before or after each flight.

We flew the UAS for 13 days between 27 September 2019 and 8 October 2019 under leaf-on conditions (i.e., leaves present on deciduous trees) and clear-sky conditions, almost exactly two years after the Tubbs fire. All flights were conducted within two hours of solar noon to minimize shadowing. We divided the study coverage area (Fig. 3.1B,C, black boxes) into 11 flight mission zones based on battery flight-time limitations. These 11 boxes had an average size of 33 ha and total area of 332 ha. SenseFly's eMotion 3 software (version 3.7) and a ground station controlled the UAS. The UAS flew autonomously using preplanned missions to ensure consistent coverage and flight characteristics. Flight plans utilized eMotion's built-in flight control function and a raster digital surface model (DSM) from the

2013 ALS mission (Section 2.2.2). This function adjusts flight altitude in order to maintain a 122-m (400-ft) flying height above the DSM. Flights were conducted with a 75% latitudinal and longitudinal image overlap. We flew each mission zone twice, employing a perpendicular "lawn mower" pattern to form a crosshatch grid. To improve georeferencing, at least three ground control points (GCPs, i.e., visible targets) were distributed throughout the mission zone prior to each flight. We obtained GPS coordinates of each GCP from >100 readings using a Trimble Juno SB and differential correction with Pathfinder Office. GCPs had a mean horizontal accuracy of 2.35 m and vertical accuracy of 2.65 m.

We processed the resulting images using Pix4Dmapper (Pix4D, Lausanne, Switzerland, version 4.4.12), which performed the reflectance calibration and generated reflectance orthomosaics for each spectral band with an 8 cm pixel size and a three-dimensional point cloud from the green spectral band. The point cloud had an average point density of 180 points/m2. The resulting point clouds had a mean RMS error from the GCPs of 1.5 m, with the exception of one highly erroneous GCP. This point was not found to affect the overall georeferencing of the resulting point cloud. We calculated pixel-level Normalized Difference Vegetation Index (NDVI) values using the red and near-IR orthomosaic images and merged the spectral data, including NDVI, with the point cloud in R (version 3.6.3) using the lidR and raster packages (Hijmans et al., 2019; R Core Team, 2019; Roussel et al., 2020).

2.2.2. Airborne Laser Scanner (ALS) Data

We obtained ALS data from the 2013 Sonoma County Vegetation Mapping and Lidar Program website (www.sonomavegmap.org, accessed Sept 2019). Watershed Sciences, Inc. (Portland, OR, USA) collected these data between 28 September 2013 and 26 November 2013 using aircraft-mounted ALS50 and ALS70 sensors at a pulse density of >8 pulses/m2 (Watershed Sciences, 2016). The point cloud had an average point density of 15 points/m2 and an average point density in vegetation of 9.2 points/m2. The survey employed 9685 GCPs with a maximum x, y, z RMSE of 0.2 cm. Watershed Sciences conducted ground point classification using TerraSolid software and refined the point classification using a subsequent statistical surface algorithm.

2.2.3. Vegetation Distribution Data

We obtained vegetation distribution data for Pepperwood Preserve from Ackerly et al. (2020). They generated their vegetation distribution map from imagery obtained by the National Aeronautics and Space Administration's Jet Propulsion Lab using the Airborne Visible Infrared Spectrometer-Next Generation (AVIRIS-NG) on 5 June 2014. Ackerly et al. classified this hyperspectral imagery with a support vector machine algorithm, first with broad landcover classes, then at the tree species level in forest pixels. For the purposes of this study, we grouped tree species pixels into three generalized forest types: conifer (*Pseudotsuga menziesii* and *Sequoia sempervirens*), evergreen broadleaf (*Arbutus menziesii*, *Notholithocarpus densiflorus*, *Quercus agrifolia*, and *Umbellularia californica*), and deciduous broadleaf (*Acer macrophyllum*, *Aesculus california*, *Quercus douglasii*, *Quercus garryana*, *Quercus kelloggii*, and *Quercus lobata*).

2.2.4. 2017 Tubbs Fire Burn Severity Data

We obtained burn severity data for the 2017 Tubbs Fire from the Monitoring Trends in Burn Severity (MTBS) 2017 burn severity mosaic (Eidenshink et al., 2007; Picotte et al., 2020) (Fig. 3.1C). This dataset utilizes the relative delta normalized burn ratio (RdNBR) (Miller and Thode, 2007) which analysts classify by fire into burn severity categories (Eidenshink et al., 2007; Picotte et al., 2020).

2.3. Data Analysis

2.3.1. Digital Terrain Model (DTM) Generation Capability Analysis

DTMs are commonly generated from point cloud data by filtering for ground points and then interpolating a raster surface from these points (Bigdeli et al., 2018). A number of ground-filtering methods and algorithms exist and perform comparably well (Klápště et al., 2020), including the cloth simulation filter (CSF) from Zhang et al. (2016). The CSF classifies ground points based on the behavior of a simulated cloth draped over an inverted version of the point cloud. Four parameters determine the performance of the cloth: rigidness, the ability of the cloth to bend; grid resolution, the spacing of cloth particles; distance threshold, the maximum distance from the cloth for a point to be classified as ground;

and, time step, the movement between iterations. Rigidness only has three possible states, corresponding to the number of times a simulated cloth particle can be moved per step, while the other parameters can take any positive value. Compared to other ground-finding algorithms, the accessible parameters of the CSF algorithm render it well suited to applications in challenging forest environments where algorithm optimization must be conducted to reduce DTM generation error.

In our study site, the ground in September to October is generally covered with dirt or senesced grass, both of which have low NDVI values relative to understory vegetation. We employed the CSF in conjunction with a novel post-processing NDVI filter that takes advantage of the NDVI contrast between ground and understory components. After CSF classification of ground points, we applied a filter to reclassify all ground points with an NDVI above a threshold value. This filter removes misclassified photosynthetic understory vegetation points from the preexisting set of ground points. We generated DTMs from the identified and filtered ground points using a triangulated irregular network (TIN) to grid interpolation at one-meter resolution. Ground finding and DTM generation were conducted using the lidR package in R (R Core Team, 2019; Roussel et al., 2020).

Table 3.1 Cloth simulation filter (CSF) parameter and Normalized Difference Vegetation Index (NDVI) threshold testing ranges. Range and step define the limits and spacing of the values over which each parameter was iterated.

Parameter	Round One			Round Two			Final
	Constant	Range	Step	Constant	Range	Step	Constant
Rigidness	1	1–3	1	3			3
Grid resolution	0.5	0.1–2.5	0.1	1	0.5–1.1	0.01	0.45
Distance threshold	0.5	0.1–2.5	0.1	0.1	0–0.2	0.01	0.01
Time step	0.65	0.1–2.5	0.1	0.6	0.5–1	0.01	0.58
NDVI threshold	off	0.1–1	0.1	0.5	0.4–0.6	0.01	0.55

To optimize DTM generation for the varied forests of Pepperwood, we iterated each CSF parameter and the post-processing NDVI filter threshold over an extreme range of values while holding all other parameters constant (Table 3.1). Due to the relatively high accuracy of ALS DTMs, we considered any deviation of the UAS-SfM DTM from the ALS DTM to be erroneous. We produced error rasters comparing the resulting sequence of DTMs to the ALS-derived benchmark. We registered the UAS-SfM point cloud to the ALS data using the iterative closest point (ICP) algorithm in the software

Lidar360 (GreenValley International, Berkeley, CA, USA, version 4.0; RMSE range: 1.57–2.34 m), and applied the resulting transformation matrices to the UAS-SfM point cloud in R. This ICP step was conducted prior to DTM error analysis using the complete UAS-SfM and ALS point clouds in order to align the ground and ensure any detected deviance in the UAS-SfM DTM produced was due to ground finding error and the DTM generation process, rather than due to a systematic offset between the point clouds. We limited this analysis to flight mission interiors at least 50 m from the mission edge to reduce the effect of edge artifacts. We calculated root mean squared error (RMSE) for the entirety of the study site as well as by vegetation type.

We conducted a second round of CSF parameter testing across the range of minimum RMSE values from the first round using a smaller step between iterations to further refine parameter values. As in round one, each parameter was run through its range while the other parameters were held constant. As mentioned previously, rigidness only has three distinct levels. Therefore, we did not repeat the iteration process for rigidness in round two. Unlike the first round, we conducted this second round in a stepwise manner, whereby the constant value for a parameter was updated to its newly identified optimum before proceeding with the next parameter assessment. A parameter's relative effect on RMSE in round one determined the order of optimization for this second round. We optimized grid resolution first, holding the other parameters at the constant corresponding to the minimum RMSE obtained in round one. Time step was optimized second, using the updated round two optimized grid resolution value, along with the other constants from round one. Distance threshold was parameterized third and NDVI threshold last, again updating parameters to their new values before proceeding. Final optimized CSF parameter values corresponded to the minimum RMSE obtained in round two. We produced a final UAS-SfM DTM from this set of optimized parameters using TIN-to-grid interpolation. We then calculated absolute error (relative to the ALS DTM) for each raster cell and separated this error by vegetation type.

2.3.2. Comparison of Forest Structure from UAS-SfM and ALS Point Clouds

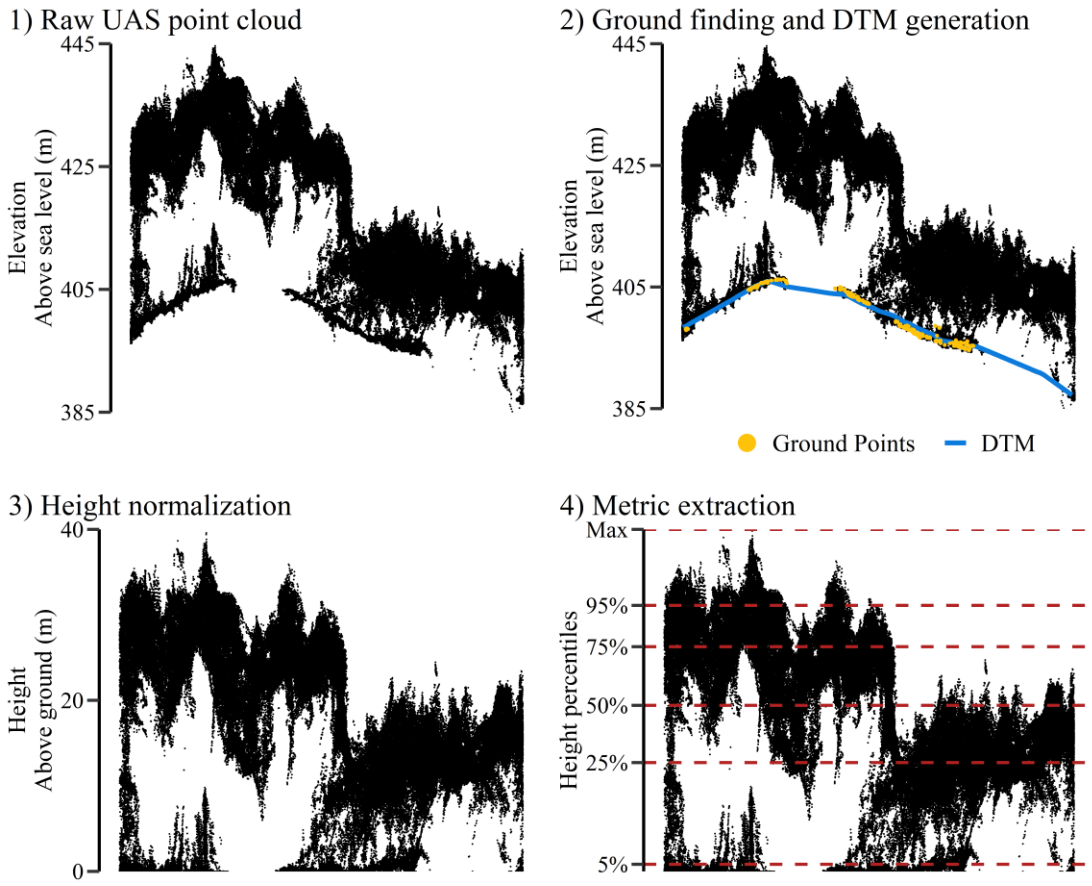


Fig. 3.2 Point cloud processing workflow.

We first compared the actual vertical height point cloud structures of UAS-SfM and ALS height-normalized point cloud data for each forest type. We then compared vertical height structure metrics between these data types. The general workflow for extracting vegetation structure metrics from point cloud data involves: (1) height normalizing the data against a digital terrain model (DTM) to isolate canopy height from terrain features, and (2) extracting metrics from these normalized data (Fig. 3.2). We conducted this height normalization process on the original, unregistered UAS-SfM point cloud in two ways. First, to determine the capability of UAS-SfM as a standalone method for measuring forest structure, we height normalized the UAS-SfM point cloud using the UAS-SfM DTM produced through the previously described CSF optimization (Section 2.3.1). Second, to determine the enhanced capability of UAS-SfM in areas with preexisting high-resolution DTMs, we height normalized the UAS-SfM point

cloud using the ALS DTM. To correct for any systematic vertical and horizontal location bias separating the UAS-SfM point cloud and the ALS DTM, we registered the UAS-SfM ground points to the ALS DTM prior to height normalization. We generated transformation matrices for the alignment of the UAS-SfM ground points to the ALS DTM using the ICP algorithm in Lidar360, and applied the matrices to the entire UAS-SfM point cloud in R. This method allowed for registration based solely on the ground points to avoid overfitting of canopy metric comparisons as would occur if the entire point clouds had been used for registration purposes.

Using these height normalized data, we compared area-based height metrics between both UAS-SfM datasets and ALS. A subset of metrics from Filippelli et al. (2019) were computed at a 20 × 20-m grid scale. While the high resolution of UAS-SfM data permits analysis at finer spatial scales, this larger grid scale was selected to align with a preexisting plot network at Pepperwood. Additionally, the MTBS burn severity dataset is assessed at 30 m resolution, limiting finer scale analysis of differences between burn severities. Density metrics represented the percentage of 3D points within a grid cell that fell within a particular vertical height band. Other metrics from each cell included height percentiles (P_5, P_{25}, P_{50}, P_{75}, and P_{95}), mean, maximum, standard deviation, skewness, and kurtosis of point cloud heights. To reduce confounding factors of mixed species and structural change due to fire, respectively, we filtered grid cells for only those cells covered by at least 75% of one forest type and with a burn severity of unchanged or low. From this filtered dataset, we computed the slope linear regression coefficient and Pearson's correlation coefficient for the relationship between UAS-SfM and ALS values for each of these metrics. This was done using 10,000 bootstrap replicates of 100 grid cells per forest type to correct for spatial autocorrelation and maintain balanced sample sizes. In addition to these standard metrics of point cloud height, we compared the ladder fuel metric from Green et al. (2020) between the two datasets in the same way as the other metrics. This metric is calculated as the number of points between 1 and 4 m divided by the total number of points below 4 m and was shown to significantly contribute to canopy damage in local non-wind-driven fires, including the Tubbs Fire.

2.3.3. Utility of UAS-SfM for Detecting Post-Fire Forest Change

We took a random sample of 20 grid cells per forest type (conifer, broadleaf evergreen, broadleaf deciduous) from each of the four burn severity classes (none, low, medium, and high). High burn severity data in deciduous broadleaf forest was excluded from all Tubbs Fire analysis due to insufficient sample size (n = 8 grid cells). These data were found to violate normality, so nonparametric statistical tests were implemented in subsequent analyses.

We determined the influence of ladder fuels on Tubbs Fire burn severity by forest type. Ladder fuels from the ALS data were used in this analysis since these data represented pre-fire conditions (four-year difference). We conducted a Kruskal–Wallis one-way analysis of variance to test differences in mean rank ladder fuel density among burn severity classes for the three forest types. Significant results were followed by Dunn's post-hoc test to examine the nature of between-group differences. We adjusted p-values via the Bonferroni method to account for multiple comparisons.

We determined the impact of fire severity in the Tubbs Fire on forest canopy structure using the 95th percentile height (P_{95}) metric and 75th percentile height (P_{75}) metrics. Since these metrics are highly positively correlated between UAS-SfM and ALS data with regression coefficients close to one (Table 3.2), the two can be directly compared for assessing change in canopy structure (Filippelli et al., 2019). In this case, ALS represents pre-fire canopy conditions and UAS-SfM represents post-fire conditions. We also tested differences in mean rank of P_{95} and P_{75} canopy metrics, respectively, among burn severity classes by forest type using a Kruskal–Wallis one-way analysis of variance test. Significant results were followed by Dunn's post-hoc tests to examine the nature of between-group differences. We adjusted p-values via the Bonferroni method to account for multiple comparisons. For this analysis, we used the UAS-SfM dataset height normalized using the ALS DTM.

Lastly, we used mean NDVI at the P_{75} canopy height to determine the impact of fire severity on canopy health. In the absence of pre-fire NDVI values, we used the unburned forest stands as the control reference for the purpose of detecting the fire's impact. As before, we tested the differences in mean rank

P75 canopy metrics among burn severity classes by forest type using a Kruskal–Wallis test with a Dunn's post-hoc test for between-group differences and Bonferroni adjusted p-values.

3. Results

3.1. DTM and CHM Generation Capability Comparisons

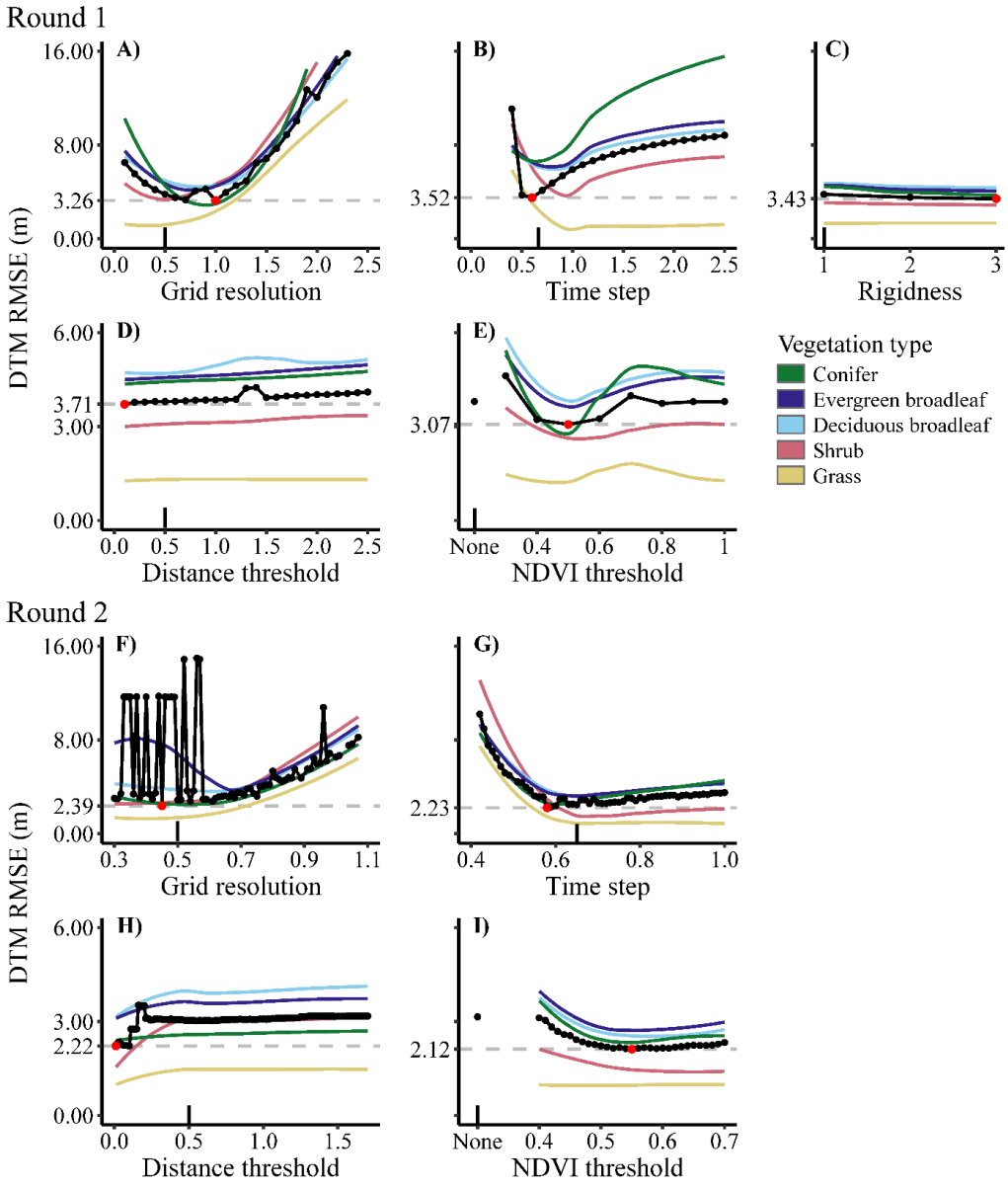


Fig. 3.3 CSF parameter effect on DTM accuracy for Round 1 (top) and Round 2 (bottom) of optimization. The DTM root mean square error (RMSE, m) for the entire study site is shown by black points and black line. Colored lines depict RMSE by vegetation type smoothed using local polynomial regression. Red dot and horizontal grey dashed line denote minimum achieved RMSE. Vertical black line intersecting the x-axis indicates default parameter value.

Compared to the baseline ALS DTM, two rounds of CSF parameter optimization achieved a UAS-SfM-derived DTM with a minimum RMSE of 2.12 m across the study site (Fig. 3.3I). This was a reduction of 1.68 m of error relative to the DTM generated from CSF default parameters (Fig. 3.3A). Responses to parameter changes were largely consistent among vegetation types. Therefore, parameter optimization could be conducted across the full study site without sacrificing accuracy in any given vegetation type. Across the wide range of the first round of parameter testing, the rigidness and distance threshold parameters had minimal effect (Fig. 3.3C,D), while the grid resolution and time step parameters greatly affected both DTM accuracy and processing time (Fig. 3.3A,B). In particular, grid resolution processing times rose sharply as the resolution approached zero.

The post-processing NDVI threshold filter reduced UAS-SfM DTM error in both rounds of processing (Fig. 3.3E,I). Compared to the DTM produced from the CSF default parameters alone, the NDVI filter reduced sitewide RMSE by 0.73 m, down to 3.07 m (Fig. 3.3E). In comparison, two rounds of parameter optimization without the NDVI filter reduced sitewide RMSE by only 0.66 m. The performance of the NDVI filter was even more pronounced in the second round. With optimal values for other CSF parameters in place, the addition of the NDVI filter reduced sitewide RMSE by 1.02 m (Fig. 3.3I). Therefore, of the final achieved optimization improvement of 1.68 m, ~61% was due to the NDVI threshold filter. Additional processing time for this filter was negligible. When the error analysis was limited from the entire DTM to just the identified ground points, regression results between these ground points and the corresponding elevation of the ALS DTM show a strong positive relationship ($r \approx +1$, slope $\approx +1$). This confirms the CSF process accurately identifies ground points.

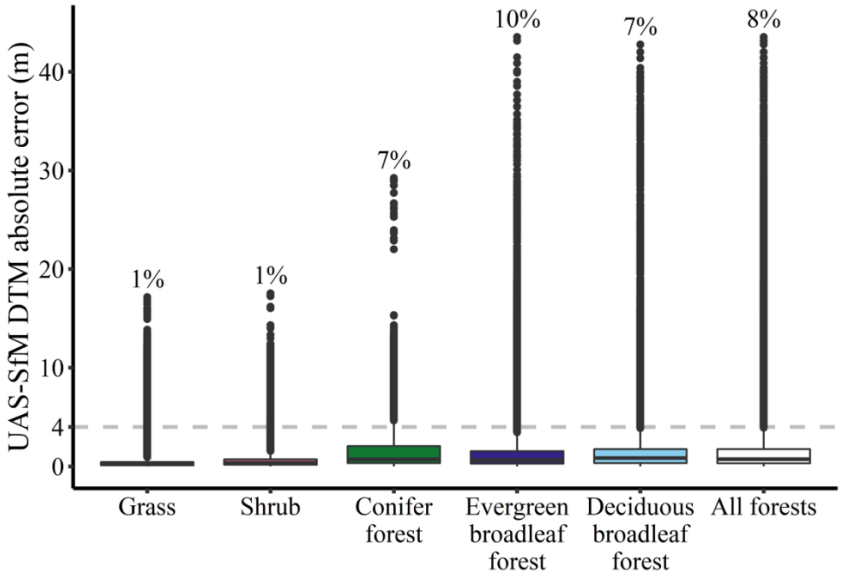


Fig. 3.4 Boxplot of UAS-SfM DTM 1-m cell error by vegetation type for DTM obtained from optimized CSF parameters as compared to the ALS DTM. Numbers above each boxplot represent percentage of DTM cells with greater than 4 m of error.

However, the distribution of absolute error from all 1 m cells of the UAS-SfM DTM, when compared to an ALS DTM, showed a substantial number of extreme outliers across all vegetation types, and, in some cases, higher than the canopy height (Fig. 3.4). While the ground finding process improved overall DTM accuracy, the measurement limitations of UAS-SfM meant that it was unable to detect any ground points in some regions with substantial changes in terrain height, subsequently resulting in DTM errors observed in those areas. Based on their respective interquartile ranges, UAS-SfM DTM generation appears to demonstrate greater consistency in accuracy for grasslands than forested areas. However, due to the number of outliers across vegetation types, statistical analyses could not be conducted to differentiate DTM accuracy by vegetation type. Errors over 15 m were observed even in a few grasslands, indicating that large errors can appear even in areas without canopy cover. Errors over 4 m represent locations where the DTM inaccuracy would be so great as to render detection of ladder fuels largely impossible. Eight percent of the combined forest UAS-SfM DTM cells had errors greater than 4 m, while only 1% of grass and shrub cells had errors above this threshold, respectively. When separated by forest type, the forest cell error percentages ranged from 7–10%.

3.2. Comparison of Forest Structure from UAS-SfM and ALS Point Clouds

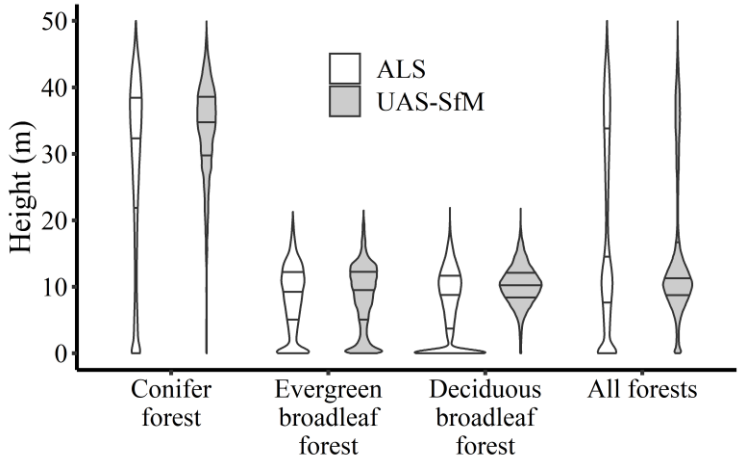


Fig. 3.5 Aboveground point cloud height distributions (meters) from complete study site data by forest type as measured by ALS (white) and UAS-SfM height normalized using the ALS DTM (shaded). Plots scaled for equal area. Horizontal lines represent 25%, 50% and 75% percentiles, respectively.

The vertical structure of UAS-SfM and ALS point clouds reflect the ability of each sensor to detect structure below the canopy. Across all forest types for the complete sitewide dataset, ALS point clouds had a negatively tapered vertical density from the middle to lower part of forest canopies and a high density of ground points (Fig. 3.5). The UAS-SfM point cloud upper-canopy density structure closely resembled that of ALS data, reaching a maximum canopy point density at a similar height. However, the lower canopy structure for UAS data tapered rapidly, indicating that the UAS point cloud was generally unable to detect the ground under heavy tree canopy. An exception to this pattern was observed in the evergreen broadleaf forest, which exhibited an increased point density at ground level. The unburned stand of evergreen broadleaf forest in this analysis contained trees spatially separated from one another, and it is from these gaps between the trees that the ground points were measured. Therefore, the increase in ground points does not actually represent an increased ability of UAS-SfM to detect below canopy structure in this forest type.

Table 3.2 Regression slope coefficients and Pearson's r correlation coefficient for point cloud grid metrics comparison between airborne laser scanner (ALS) data and unoccupied aerial system Structure-from-Motion (UAS-SfM) height normalized using the UAS-SfM digital terrain model (DTM). Metrics P_5, P_{25}, etc. represent height percentiles. Values given are mean (standard error) of 10,000 bootstrap replicas of 100 unburned plots per forest type. Coefficient and r values greater than 0.8 are shown in bold.

	Conifer		Evergreen Broadleaf		Deciduous Broadleaf		All Forest Types	
Height Metric	**Coefficient**	**r**	**Coefficient**	**r**	**Coefficient**	**r**	**Coefficient**	**r**
Ladder fuels	+0.09 (0.07)	+0.13 (0.10)	+0.05 (0.09)	+0.08 (0.13)	+0.16 (0.04)	+0.39 (0.07)	+0.16 (0.04)	+0.23 (0.06)
Density								
2–5 m	+0.12 (0.18)	+0.07 (0.08)	+0.09 (0.05)	+0.24 (0.11)	+0.07 (0.06)	+0.18 (0.12)	+0.08 (0.04)	+0.16 (0.08)
5–10 m	+0.36 (0.13)	+0.45 (0.13)	+0.21 (0.05)	+0.39 (0.09)	+0.25 (0.04)	+0.61 (0.09)	+0.33 (0.03)	+0.63 (0.04)
10–15 m	+0.38 (0.08)	+0.64 (0.10)	+0.22 (0.05)	+0.47 (0.10)	+0.21 (0.04)	+0.53 (0.09)	+0.32 (0.02)	+0.67 (0.04)
Distribution								
Max	+0.52 (0.12)	+0.67 (0.07)	+0.64 (0.08)	+0.76 (0.07)	+0.62 (0.11)	+0.69 (0.11)	**+0.81 (0.03)**	**+0.89 (0.02)**
Mean	+0.52 (0.06)	**+0.80 (0.05)**	+0.38 (0.08)	+0.60 (0.10)	+0.35 (0.09)	+0.56 (0.11)	+0.66 (0.02)	**+0.88 (0.02)**
P_5	+0.01 (0.01)	+0.17 (0.12)	−0.00 (0.02)	+0.00 (0.13)	+0.00 (0.00)	+0.07 (0.10)	+0.01 (0.01)	+0.19 (0.08)
P_{25}	+0.44 (0.06)	+0.66 (0.07)	+0.12 (0.11)	+0.17 (0.15)	+0.03 (0.04)	+0.09 (0.12)	+0.53 (0.04)	+0.74 (0.04)
P_{50}	+0.62 (0.08)	**+0.80 (0.05)**	+0.39 (0.08)	+0.58 (0.10)	+0.41 (0.12)	+0.41 (0.12)	+0.73 (0.03)	**+0.86 (0.02)**
P_{75}	+0.61 (0.09)	+0.77 (0.05)	+0.44 (0.07)	+0.68 (0.09)	+0.47 (0.11)	+0.59 (0.12)	+0.75 (0.03)	**+0.89 (0.02)**
P_{95}	+0.56 (0.10)	+0.73 (0.06)	+0.55 (0.07)	+0.75 (0.07)	+0.55 (0.11)	+0.67 (0.11)	+0.78 (0.03)	**+0.89 (0.02)**
Variation								
SD	+0.24 (0.08)	+0.29 (0.09)	+0.47 (0.05)	+0.72 (0.07)	+0.28 (0.12)	+0.33 (0.15)	+0.71 (0.04)	+0.72 (0.03)
Skewness	+0.29 (0.04)	+0.63 (0.08)	+0.16 (0.09)	+0.28 (0.11)	+0.05 (0.04)	+0.15 (0.11)	+0.15 (0.04)	+0.33 (0.07)
Kurtosis	+0.05 (0.02)	+0.42 (0.12)	−0.02 (0.04)	−0.05 (0.08)	−0.03 (0.01)	−0.33 (0.08)	+0.01 (0.01)	+0.04 (0.08)

Table 3.3 Regression slope coefficients and Pearson's r correlation coefficient for point cloud grid metrics comparison between ALS data and UAS-SfM height normalized using an ALS DTM. Metrics P_5, P_{25}, etc. represent height percentiles. Values given are mean (standard error) of 10,000 bootstrap replicas of 100 unburned plots per forest type. Coefficient and r values greater than 0.8 are shown in bold.

	Conifer		Evergreen Broadleaf		Deciduous Broadleaf		All Forest Types	
Height Metric	**Coefficient**	**r**	**Coefficient**	**r**	**Coefficient**	**r**	**Coefficient**	**r**
Ladder fuels	+0.16 (0.06)	+0.26 (0.10)	+0.02 (0.10)	+0.04 (0.14)	+0.08 (0.04)	+0.19 (0.10)	+0.08 (0.04)	+0.13 (0.07)
Density								
2–5 m	+0.40 (0.13)	+0.35 (0.10)	+0.16 (0.08)	+0.33 (0.14)	+0.18 (0.07)	+0.43 (0.10)	+0.20 (0.05)	+0.40 (0.08)
5–10 m	+0.54 (0.08)	+0.74 (0.07)	+0.35 (0.05)	+0.61 (0.07)	+0.23 (0.04)	+0.61 (0.07)	+0.36 (0.03)	+0.70 (0.03)
10–15 m	+0.62 (0.06)	**+0.83 (0.04)**	+0.35 (0.04)	+0.72 (0.07)	+0.26 (0.03)	+0.68 (0.07)	+0.39 (0.02)	**+0.80 (0.03)**
Distribution								
Max	+0.72 (0.18)	**+0.81 (0.09)**	+0.71 (0.10)	+0.79 (0.08)	+0.73 (0.11)	**+0.85 (0.12)**	**+0.92 (0.04)**	**+0.93 (0.02)**
Mean	+0.65 (0.09)	**+0.84 (0.07)**	+0.41 (0.10)	+0.60 (0.15)	+0.49 (0.06)	**+0.81 (0.06)**	+0.75 (0.03)	**+0.91 (0.03)**
P_5	+0.01 (0.01)	+0.23 (0.05)	−0.01 (0.03)	−0.03 (0.15)	−0.00 (0.01)	−0.03 (0.11)	+0.01 (0.01)	+0.17 (0.10)
P_{25}	+0.57 (0.10)	+0.67 (0.08)	+0.13 (0.12)	+0.17 (0.15)	+0.02 (0.02)	+0.11 (0.10)	+0.60 (0.05)	+0.75 (0.04)
P_{50}	+0.76 (0.12)	**+0.82 (0.07)**	+0.41 (0.10)	+0.57 (0.13)	+0.66 (0.09)	+0.70 (0.07)	**+0.83 (0.04)**	**+0.89 (0.03)**
P_{75}	+0.78 (0.14)	**+0.83 (0.07)**	+0.49 (0.10)	+0.69 (0.12)	+0.64 (0.08)	**+0.82 (0.08)**	**+0.86 (0.03)**	**+0.92 (0.02)**
P_{95}	+0.75(0.16)	**+0.84(0.08)**	+0.61(0.10)	+0.77(0.09)	+0.69(0.10)	**+0.85(0.10)**	**+0.89(0.03)**	**+0.93(0.02)**
Variation								
SD	+0.22(0.10)	+0.21(0.10)	+0.50(0.06)	+0.69(0.07)	+0.26(0.10)	+0.35(0.14)	**+0.80(0.05)**	+0.67(0.03)
Skewness	+0.30(0.07)	+0.48(0.09)	+0.25(0.05)	+0.45(0.07)	+0.12(0.04)	+0.35(0.11)	+0.18(0.03)	+0.34(0.05)
Kurtosis	+0.06(0.02)	+0.28(0.10)	−0.01(0.03)	−0.04(0.08)	−0.02(0.01)	−0.25(0.15)	−0.01(0.01)	−0.03(0.06)

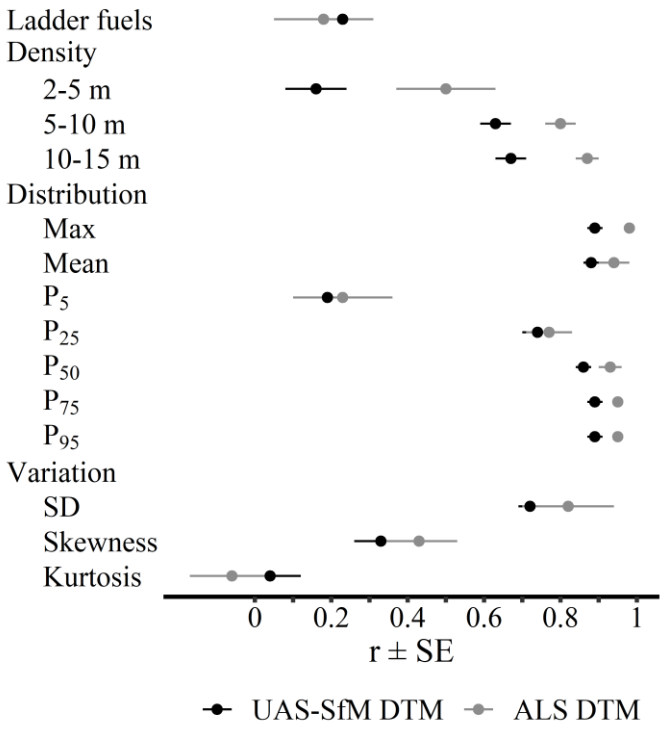


Fig. 3.6 Comparison of Pearson correlations for point cloud height metrics extracted from UAS-SfM height normalized using either UAS-SfM DTM or ALS DTM across all forest types. Coefficients and their standard errors computed using 10,000 bootstrap replicates between UAS-SfM and ALS

The area-based metric comparisons between UAS-SfM and ALS data reflect the preceding observations on subcanopy detection across vegetation types (Table 3.2 and 3.3). For both the UAS-SfM height metrics extracted using the UAS-SfM derived DTM and the ALS DTM for height normalization, only metrics associated with the upper half of the canopy (e.g., P_{50}, P_{75}, P_{95}, mean height, and max height) exhibited Pearson's $r > +0.80$. No relationships of this type exist between UAS-SfM and ALS for any of the metrics of height variation, nor those of height density for either of the height normalization approaches, with the exception of upper-canopy density (10–15 m) from the ALS DTM normalized dataset. As expected from the errors identified during the UAS-SfM DTM generation analysis (Section 3.1), the metrics extracted from the UAS-SfM data height normalized using the ALS DTM systematically performed better than the UAS-SfM data height normalized using the UAS-SfM DTM. However, these differences were small, especially for percentile metrics associated with the upper half of the canopy (Fig. 3.6).

Table 3.4 Kruskal–Wallis one-way analysis of variance results for 2017 Tubbs fire burn severity impact metrics. Significance at the 95% level denoted in bold.

Metric and Sample	χ^2	*p*	df	N
Pre-fire ladder fuel				
All forests	18.99	**<0.001**	3	220
Conifer	2.59	0.46	3	80
Evergreen broadleaf	13.68	**0.003**	3	80
Deciduous broadleaf	0.41	0.82	2	60
ΔP_{95}				
All forests	7.16	0.06	3	220
Conifer	0.79	0.85	3	80
Evergreen broadleaf	10.82	**0.01**	3	80
Deciduous broadleaf	0.73	0.69	2	60
ΔP_{75}				
All forests	35.01	**<0.001**	3	220
Conifer	10.98	**0.01**	3	80
Evergreen broadleaf	30.41	**<0.001**	3	80
Deciduous broadleaf	1.17	0.56	2	60
P_{75} NDVI				
All forests	89.81	**<0.001**	3	220
Conifer	54.49	**<0.001**	3	80
Evergreen broadleaf	35.31	**<0.001**	3	80
Deciduous broadleaf	9.21	0.01	2	60

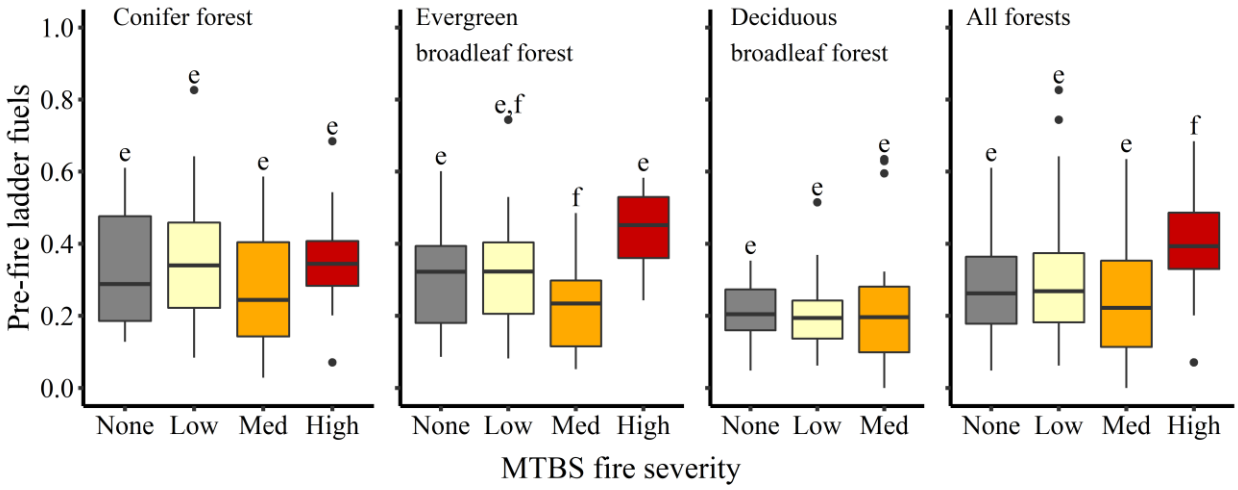


Fig. 3.7 Relationship among pre-fire ladder fuels derived from 2013 ALS data and 2017 Tubbs fire burn severity by forest types. Lower case letters represent statistically similar groups at the 95% confidence level using a Dunn's post-hoc test.

Ladder fuels: Across all forest types, the mean rank ladder fuel density was significantly higher in the high burn severity class, as compared to all other areas (Table 3.4, Fig. 3.7). In evergreen broadleaf forests, the mean rank ladder fuel density was significantly lower in the medium burn severity class, as

compared to the unburned and high burn severities classes (Table 3.4, Fig. 3.7). The ladder fuel densities did not differ among burn severities for the other forest types.

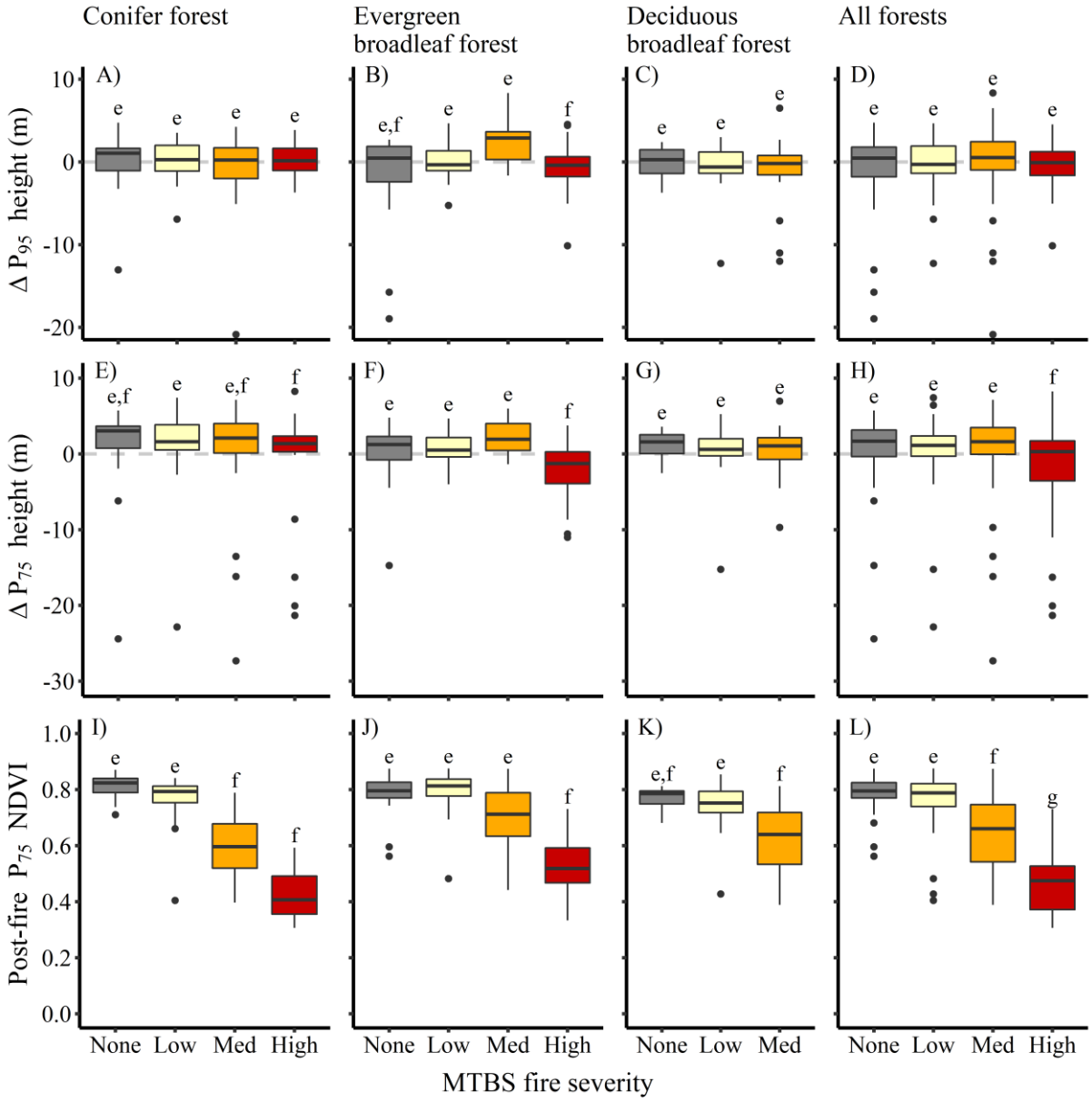


Fig. 3.8 The impact of the 2017 Tubbs Fire on 95th percentile (P_{95}) and 75th percentile heights (P_{75}) and P_{75} mean NDVI by MTBS fire severity in forest types. Lower case letters represent statistically similar groups at the 95% confidence level. Change in canopy height metrics calculated as pre-fire ALS percentile height minus post-fire UAS-SfM percentile height.

ΔP_{95}: In evergreen broadleaf forests, the mean rank in pre-fire (ALS) to post-fire (UAS-SfM) P_{95} canopy height change (ΔP_{95}) was significantly more negative (i.e., greater decrease in heights) in the high burn severity class as compared to the low and medium burn severity classes (Table 3.4, Figure 8B). The

mean rank ΔP_{95} was not significantly different across burn severities in the other forest types or for all forests combined (Table 3.4, Fig. 3.8B–D).

ΔP_{75}: Across all forest types and in evergreen broadleaf forests, the mean rank ΔP_{75} was significantly more negative in the high burn severity class as compared to all others (Table 3.4, Fig. 3.8F,H). In conifer forests, the mean rank ΔP_{75} was significantly more negative in the high burn severity class as compared to the low burn severity (Table 3.4, Fig. 3.8E). The mean rank ΔP_{75} did not differ in deciduous broadleaf forests.

P_{75} NDVI: Across all forest types and in evergreen broadleaf forests, the mean rank in NDVI at post-fire (UAS) P_{75} canopy height (P_{75} NDVI) was significantly lower in the high burn severity class as compared to all others (Table 3.4, Fig. 3.8L,J). In addition, across all forest types, the mean rank P_{75} was significantly lower in the medium burn severity class as compared to the low and unburned classes (Table 3.4, Fig. 3.8L). In conifer forests, the mean rank in P_{75} NDVI was significantly lower in the medium and high burn severity classes as compared to all others (Table 3.4, Fig. 3.8I). In deciduous broadleaf forests, the mean rank in P_{75} NDVI was significantly lower in the medium burn severity class as compared to the low burn severity class (Table 3.4, Fig. 3.8K).

In summary, only evergreen broadleaf forests exhibited a change in 95th percentile canopy height at higher burn severities. Bulk canopy height, represented by the 75th height percentile, decreased at high burn severity when considering all forests together, and within evergreen broadleaf and conifer forests. We also found that NDVI values in the bulk canopy decreased (i.e., lower greenness) with increasing burn severity, regardless of forest type.

4. Discussion

4.1. DTM and CHM Generation Capability Comparisons

This study sought to assess the capacity of UAS-SfM as a standalone forest monitoring tool to be employed in Mediterranean forests without preexisting ALS data. This requires that a sufficiently accurate DTM can be estimated from UAS-SfM 3D point clouds, considering both detection of ground

points and the classification of these points as ground relative to understory vegetation. This terrain finding process enables the isolation of canopy height from topography. While it is possible to achieve sub-centimeter DTM accuracy from UAS-SfM for bare ground conditions (Adjidjonu and Burgett, 2021), increasing vegetation cover heavily impacts DTM accuracy (Goodbody et al., 2018a; Graham et al., 2019; Wallace et al., 2019). Through two rounds of ground finding parameter optimization, we achieved a site wide DTM RMSE of 2.12 m. However, 8% of DTM coverage in forest areas contained errors over 4 m. This height threshold represents the upper limit of the ladder fuel metric from Green et al. (2020), so errors of this magnitude connote an inability to detect surface or ladder fuels.

While the proliferation of error of this magnitude is serious, deciding whether this represents an unacceptable level of error largely depends on the context in which these data will be used. To determine canopy height and other metrics in areas of dense forest, having a baseline DTM from a more reliable source, such as airborne or UAS lidar, will always be best practice (Jayathunga et al., 2018; Prata et al., 2020), assuming terrain does not change considerably over a study time period. However, in situations where these data do not exist, 8% error coverage may have to represent an acceptable margin. Of perhaps more importance among this erroneous area are the individual DTM sites with extreme errors, linked with gaps in the distribution of detected ground points. Future research should analyze the role of topography and canopy type in producing these areas of extreme error magnitude in order to determine conditions under which UAS-SfM cannot function without a preexisting DTM. Another future avenue of research to avoid these errors entirely is to determine if DTM-independent methods for extraction of forest metrics, which have been validated in forestry growing stock volume measurements (Giannetti et al., 2018), can be applied to the mapping of fuel loads.

This study employed the Cloth Simulation Filter (CSF) from Zhang et al. (2016) in conjunction with a subsequent NDVI filter to classify ground points from which a DTM could be generated through interpolation. In Mediterranean shrublands, Carvajal-Ramirez et al. (2019b) found the CSF performance was weaker relative to an NDVI classifier, and the authors called for the need to assess the impact of CSF parameter setting on ground-finding accuracy. In this study, CSF parameter optimization alone only

marginally improved RMSE over the default parameters. However, the addition of our NDVI threshold filter resulted in a large (>60%) improvement in RMSE. Drawing on the concept of the NDVI classifier from Carvajal-Ramirez et al. (2019b), the combination of CSF with an NDVI filter leverages the strengths of both methods. The CSF identifies an initial set of ground points from which the NDVI filter removes misclassified vegetation. When multispectral data exist, this filter provides a computationally simple way to improve ground finding based on point cloud structure alone. While methods for ground finding are continually being developed or improved (e.g., Cai et al., 2019), this filter provides an additional tool in mitigating the subcanopy detection shortcomings of UAS-SfM. However, one important caveat to our results is that our study area benefits from relatively low senesced grass (depending on cattle rotations and deer grazing) and higher live shrubs in late summer, thereby providing a strong NDVI contrast that aids the ground filter. Further tests of the CSF and NDVI filter combination in other ecosystems are certainly warranted.

4.2. Comparison of Forest Structure from UAS-SfM and ALS Point Clouds

Linear regression comparisons between UAS-SfM and ALS confirm past findings from other forest types and applications that UAS-SfM can only reliably resolve upper-canopy structure, but does so with a high degree of accuracy (Vastaranta et al., 2013; e.g., Wallace et al., 2019). The analysis presented here closely matches Filippelli et al. (2019), who found similar relationships in a montane coniferous and lodgepole pine forest between ALS and SfM DAP collected using an airplane flown at high altitude and with lower image overlap than used in this study. This suggests that SfM DAP has the same strength and limitations irrespective of image acquisition method and forest type. In particular, SfM DAP provides a powerful tool for measuring upper-canopy forest structure. The strength of this tool is dependent on the accuracy of the DTM underlying the analysis. While the use of the ALS DTM for height normalization systematically improved the accuracy of extracted canopy metrics as compared to the UAS-SfM, both methods performed well in measuring all metrics associated with the upper half of the canopy.

For SfM DAP to determine a point's 3D location, it must appear in multiple overlapping images. Therefore, the technique often fails to detect gaps in canopy cover, let alone resolve what lies below the canopy (White et al., 2018). In our study, this shortcoming was most acutely demonstrated in our attempt to measure ladder fuels. No relationship existed between the ALS and UAS-SfM derived metrics. SfM DAP overestimates metrics of density, such as the ladder fuels metric, and canopy cover due to this lack of subcanopy detection (Jayathunga et al., 2018). The analysis of the point cloud's respective vertical structure lends additional weight to the conclusion that UAS-SfM cannot measure ladder fuels using the same metric as is employed for ALS. However, this study was limited in this analysis due to the six years between the collection of ALS and UAS-SfM data. While we restricted this analysis to areas of the study site unaffected by the Tubbs Fire, forest structure may have changed during the interim period (e.g., tree growth, disease, or mortality), which may account for some of the measured UAS-SfM error relative to the ALS baseline. Despite the subcanopy detection limitations of SfM DAP, Filippelli et al. (2019) found DAP models of canopy structure performed comparably to those derived from ALS. Future studies with coincident ALS and UAS-SfM data should investigate this relationship further to determine if other methods can measure ladder fuel density from UAS-SfM despite its limitations under high canopy cover.

4.3. Utility of UAS-SfM for Detecting Post-Fire Forest Change

Two years after the Tubbs Fire swept through Pepperwood, UAS-SfM found minimal changes in canopy height relative to pre-fire metrics. In the aggregate analysis of all forest types, measures of maximum height (95th percentile) did not change, while bulk canopy height (75th percentile) decreased significantly in regions with the highest burn severity. We observed significant decreases in NDVI with increasing burn severity across all forests regardless of structural change. While we did not have calibrated pre-fire measures of NDVI on the same spatial scale to which we could compare, the unburned areas were used as a control reference in this comparison. This demonstrates the long-lasting impact a severe wildfire has on Mediterranean forest health.

The role of NDVI in understanding forest health indicates that multispectral sensors have an important role in forest monitoring for fire hazard and post-fire recovery. Change in NDVI can detect fine-scale forest physiological stress (Dash et al., 2018). Change in NDVI also provides the best estimator of post-fire severity in Mediterranean vegetation (Carvajal-Ramírez et al., 2019a; Green et al., 2020). The long-term trend of NDVI over a stand or ecosystem can be used to measure the degree to which different vegetation types manage to recover from a severe fire event (Díaz-Delgado et al., 2003). In our study ecosystem, UAS-SfM-based measures of NDVI or other greenness indices over multiple times post-fire could provide valuable crown-scale information on tree response to fire (Larrinaga and Brotons, 2019; Pádua et al., 2020), such as initiation of epicormic sprouting and subsequent canopy growth. As demonstrated here, this information can provide insight on impacts beyond what structural information alone could provide. In addition, since multispectral UAS-SfM provides coupled spectral and structural information, it offers a means to target analysis at particular levels of the canopy in a way that is not possible with aerial or satellite imagery alone. For example, here we were able to use this technology to disentangle bulk canopy changes in NDVI from other post-fire ecosystem changes, such as ground vegetation recovery. While our results targeted change detection at the 20 m grid level, future studies should leverage the high resolution of this technology to analyze change at finer scales or even at the individual tree level.

The analysis of post-fire canopy changes would not have been possible without the existence of the pre-fire ALS data. While the unburned areas could be used as a control in the absence of such data, as done here with the NDVI analysis, change analysis of this type greatly benefits from ongoing monitoring. It is in this capacity that UAS-SfM provides a particularly strong benefit due to the ease of data acquisition at plot to stand scales.

Although UAS-SfM could not estimate ladder fuels, our analysis with ALS-based pre-fire ladder fuels and burn severity revealed a pattern that merits further investigation. In the aggregate analysis of all forest types, the high burn severity class exhibited greater pre-fire ladder fuel density than the low burn severity class. We found a significant relationship between increasing pre-fire ladder fuel densities and

medium to high burn severity in evergreen broadleaf forest, but not in the conifer forest. Neither forest type had a significant difference between low and high burn severities. Conifers in particular showed no relationship between burn severity and ladder fuel density. Two explanations are possible for this. First, the majority of conifer forest that burned at high severity during the Tubbs Fire did so during the initial "Diablo" wind-driven portion of the event. Green et al. (2020) identified these winds to be an even stronger driver of burn severity than ladder fuels. Therefore, the mixed signal across forest types and in conifer forests may be attributable to wind strength overwhelming any difference that ladder fuel densities may have otherwise caused in burn severity (Keeley and Syphard, 2019). An alternative explanation, however, is that the ladder fuel metric employed here performs well in shorter evergreen broadleaf forests, especially in determining if higher intensities fires are able to cross the high severity threshold, but does not apply in tall conifer forests where canopy base height may be well above 4 m. Further work is needed to investigate the utility of different measures of vertical fuel continuity, such as ladder fuel metrics, in different forest types. Furthermore, the estimation of such subcanopy metrics at a stand scale using UAS may best be achieved with an attached lidar sensor instead of the SfM approach used here (Hillman et al., 2021). Although UAS-SfM is currently more economical, prices for UAS lidar are expected to decrease over time (Hu et al., 2020).

5. Conclusions

For fire hazard mitigation land management treatments to be effective, land managers must implement them at broad spatial scales, from single forest stands to larger regions (Collins et al., 2013). This requires an improved understanding of forest structure and fuel loading to inform management practices.

Due to the comparatively low investment in time or resources involved in conducting repeated data collection missions, UAS-SfM provides a unique opportunity to monitor ongoing changes and recovery of forest structure and physiological health following major disturbance events at plot to stand scales (Campbell et al., 2020; Goodbody et al., 2018b). Our study in a Mediterranean forest site in

Northern California found UAS-SfM able to accurately detect ground points. However, ground points in some areas were too sparsely distributed to reliably estimate ground elevation, a limitation that affects subsequent canopy height retrieval and limits its use in these areas as a standalone tool in the absence of more accurate terrain data. This shortcoming arose from UAS-SfM's limited subcanopy detection ability, which also hindered its ability to detect ladder fuels and other below-canopy metrics. Across the study site, UAS-SfM excelled at mapping the upper canopy of forests and, when combined with a multispectral sensor, can provide information on vegetation productivity and physiological stress. This accuracy can be improved further when the UAS-SfM is paired with an accurate baseline measurement of ground elevation (e.g., from an airborne lidar sensor). UAS-SfM, therefore, provides a valuable tool for monitoring post-fire impacts and recovery through the use of upper-canopy metrics of structure and health, especially at sites with pre-fire data as presented here. Much work remains to be done in the evaluation of UAS-SfM as a fire fuel monitoring tool in Mediterranean ecosystems. Future work should focus on leveraging the strengths of this method to improve management outcomes.

Authorship contribution statement

Conceptualization, S.R., M.L.C., L.P.B. and I.O.; methodology, S.R., M.L.C., L.P.B. and I.O.; investigation, S.R., M.L.C., L.P.B., C.M. and E.P.; software, S.R. and M.L.C.; formal analysis, S.R. and M.L.C.; resources, M.L.C. and L.P.B.; writing—original draft preparation, S.R.; writing—review and editing, I.O., M.L.C., L.P.B., C.M. and E.P.; visualization, S.R.; supervision, I.O., M.L.C. and L.P.B.; funding acquisition, L.P.B. and M.L.C. All authors have read and agreed to the published version of the manuscript.

Acknowledgments

Funding for this research was supported by CAL FIRE Forest Health and Forest Legacy (8GG18806) and California State University, Agricultural Research Institute (20-01-106) awards. SR was funded by the Rhodes Trust and through the University of Oxford Environmental Change Institute Small

Grant Scheme. We thank the staff of Pepperwood Preserve for allowing us access to their beautiful site. This work is a product of the 3D Forests research group.

References

Ackerly, D.D., Kling, M.M., Clark, M.L., Papper, P., Oldfather, M.F., Flint, A.L., Flint, L.E., 2020. Topoclimates, refugia, and biotic responses to climate change. Front Ecol Environ 18, 288–297. https://doi.org/10.1002/fee.2204

Adjidjonu, D., Burgett, J., 2021. Assessing the accuracy of unmanned aerial vehicles photogrammetric survey. International Journal of Construction Education and Research 17, 85–96. https://doi.org/10.1080/15578771.2020.1717683

Alonzo, M., Andersen, H.-E., Morton, D., Cook, B., 2018. Quantifying boreal forest structure and composition using UAV Structure-from-Motion. Forests 9, 119. https://doi.org/10.3390/f9030119

Alonzo, M., Dial, R.J., Schulz, B.K., Andersen, H.-E., Lewis-Clark, E., Cook, B.D., Morton, D.C., 2020. Mapping tall shrub biomass in Alaska at landscape scale using Structure-from-Motion photogrammetry and lidar. Remote Sensing of Environment 245, 111841. https://doi.org/10.1016/j.rse.2020.111841

Andersen, H.-E., McGaughey, R.J., Reutebuch, S.E., 2005. Estimating forest canopy fuel parameters using LIDAR data. Remote Sensing of Environment 94, 441–449. https://doi.org/10.1016/j.rse.2004.10.013

Arroyo, L.A., Pascual, C., Manzanera, J.A., 2008. Fire models and methods to map fuel types: The role of remote sensing. Forest Ecology and Management 256, 1239–1252. https://doi.org/10.1016/j.foreco.2008.06.048

Beaty, R.M., Taylor, A.H., 2008. Fire history and the structure and dynamics of a mixed conifer forest landscape in the northern Sierra Nevada, Lake Tahoe Basin, California, USA. Forest Ecology and Management 255, 707–719. https://doi.org/10.1016/j.foreco.2007.09.044

Berra, E.F., Gaulton, R., Barr, S., 2019. Assessing spring phenology of a temperate woodland: A multiscale comparison of ground, unmanned aerial vehicle and Landsat satellite observations. Remote Sensing of Environment 223, 229–242. https://doi.org/10.1016/j.rse.2019.01.010

Bigdeli, B., Amini Amirkolaee, H., Pahlavani, P., 2018. DTM extraction under forest canopy using LiDAR data and a modified invasive weed optimization algorithm. Remote Sensing of Environment 216, 289–300. https://doi.org/10.1016/j.rse.2018.06.045

Cai, S., Zhang, W., Liang, X., Wan, P., Qi, J., Yu, S., Yan, G., Shao, J., 2019. Filtering airborne LiDAR data through complementary cloth simulation and progressive TIN densification filters. Remote Sensing 11, 1037. https://doi.org/10.3390/rs11091037

CalFire, 2019a. Top 20 deadliest California wildfires.

CalFire, 2019b. Top 20 most destructive California wildfires.

Campbell, M.J., Dennison, P.E., Tune, J.W., Kannenberg, S.A., Kerr, K.L., Codding, B.F., Anderegg, W.R.L., 2020. A multi-sensor, multi-scale approach to mapping tree mortality in woodland ecosystems. Remote Sensing of Environment 245, 111853. https://doi.org/10.1016/j.rse.2020.111853

Carvajal-Ramírez, F., Marques da Silva, J.R., Agüera-Vega, F., Martínez-Carricondo, P., Serrano, J., Moral, F.J., 2019a. Evaluation of fire severity indices based on pre- and post-fire multispectral imagery sensed from UAV. Remote Sensing 11, 993. https://doi.org/10.3390/rs11090993

Carvajal-Ramírez, F., Serrano, J.M.P.R., Agüera-Vega, F., Martínez-Carricondo, P., 2019b. A comparative analysis of phytovolume estimation methods based on UAV-photogrammetry and multispectral imagery in a Mediterranean forest. Remote Sensing 11, 2579. https://doi.org/10.3390/rs11212579

Chuvieco, E., Aguado, I., Salas, J., García, M., Yebra, M., Oliva, P., 2020. Satellite remote sensing contributions to wildland fire science and management. Curr Forestry Rep 6, 81–96. https://doi.org/10.1007/s40725-020-00116-5

Collins, B.M., Kramer, H.A., Menning, K., Dillingham, C., Saah, D., Stine, P.A., Stephens, S.L., 2013. Modeling hazardous fire potential within a completed fuel treatment network in the northern Sierra Nevada. Forest Ecology and Management 310, 156–166. https://doi.org/10.1016/j.foreco.2013.08.015

Cowling, R., Rundel, P., Lamont, B., Arroyo, M., Arianoutsou, M., 1996. Plant diversity in Mediterranean-climate regions. Trends in Ecology & Evolution 11, 362–366. https://doi.org/10.1016/0169-5347(96)10044-6

Cunliffe, A.M., Brazier, R.E., Anderson, K., 2016. Ultra-fine grain landscape-scale quantification of dryland vegetation structure with drone-acquired Structure-from-Motion photogrammetry. Remote Sensing of Environment 183, 129–143. https://doi.org/10.1016/j.rse.2016.05.019

Dandois, J.P., Ellis, E.C., 2013. High spatial resolution three-dimensional mapping of vegetation spectral dynamics using computer vision. Remote Sensing of Environment 136, 259–276. https://doi.org/10.1016/j.rse.2013.04.005

Dandois, J.P., Olano, M., Ellis, E.C., 2015. Optimal altitude, overlap, and weather conditions for computer vision UAV estimates of forest structure. Remote Sensing 7, 13895–13920. https://doi.org/10.3390/rs71013895

Dash, J.P., Pearse, G.D., Watt, M.S., 2018. UAV multispectral imagery can complement satellite data for monitoring forest health. Remote Sensing 10, 1216. https://doi.org/10.3390/rs10081216

Dennison, P.E., Brewer, S.C., Arnold, J.D., Moritz, M.A., 2014. Large wildfire trends in the western United States, 1984-2011. Geophys. Res. Lett. 41, 2928–2933. https://doi.org/10.1002/2014GL059576

Díaz-Delgado, R., Lloret, F., Pons, X., 2003. Influence of fire severity on plant regeneration by means of remote sensing imagery. International Journal of Remote Sensing 24, 1751–1763. https://doi.org/10.1080/01431160210144732

Donnellan, A., Harding, D., Lundgren, P., Wessels, K., Gardner, A., Simard, M., Parrish, C., Jones, C., Lou, Y., Stoker, J., Ranson, K., Osmanoglu, B., Lavalle, M., Luthcke, S., Saatchi, S., Treuhaft,

R., 2021. Observing Earth's changing surface topography and vegetation structure: A framework for the decade. NASA Suface Topography and Vegetation Incubation Study.

Eidenshink, J., Schwind, B., Brewer, K., Zhu, Z.-L., Quayle, B., Howard, S., 2007. A project for monitoring trends in burn severity. fire ecol 3, 3–21. https://doi.org/10.4996/fireecology.0301003

Evett, R.R., Dawson, A., Bartolome, J.W., 2013. Estimating vegetation reference conditions by combining historical source analysis and soil phytolith analysis at Pepperwood Preserve, Northern California Coast Ranges, U.S.A: Estimating vegetation reference conditions. Restor Ecol 21, 464–473. https://doi.org/10.1111/j.1526-100X.2012.00912.x

Filippelli, S.K., Lefsky, M.A., Rocca, M.E., 2019. Comparison and integration of lidar and photogrammetric point clouds for mapping pre-fire forest structure. Remote Sensing of Environment 224, 154–166. https://doi.org/10.1016/j.rse.2019.01.029

Flannigan, M.D., Krawchuk, M.A., de Groot, W.J., Wotton, B.M., Gowman, L.M., 2009. Implications of changing climate for global wildland fire. Int. J. Wildland Fire 18, 483–507. https://doi.org/10.1071/WF08187

Giannetti, F., Chirici, G., Gobakken, T., Næsset, E., Travaglini, D., Puliti, S., 2018. A new approach with DTM-independent metrics for forest growing stock prediction using UAV photogrammetric data. Remote Sensing of Environment 213, 195–205. https://doi.org/10.1016/j.rse.2018.05.016

Goodbody, T.R.H., Coops, N.C., Hermosilla, T., Tompalski, P., Pelletier, G., 2018a. Vegetation phenology driving error variation in digital aerial photogrammetrically derived terrain models. Remote Sensing 10, 1554. https://doi.org/10.3390/rs10101554

Goodbody, T.R.H., Coops, N.C., Tompalski, P., Crawford, P., 2018b. Assessing the status of forest regeneration using digital aerial photogrammetry and unmanned aerial systems. International Journal of Remote Sensing 39, 5246–5264. https://doi.org/10.1080/01431161.2017.1402387

Graham, A., Coops, N.C., Wilcox, M., Plowright, A., 2019. Evaluation of ground surface models derived from Unmanned Aerial Systems with Digital Aerial Photogrammetry in a disturbed conifer forest. Remote Sensing 11, 84. https://doi.org/10.3390/rs11010084

Green, K., Tukman, M., Loudon, D., Schichtel, A., Gaffney, K., Clark, M., 2020. Sonoma County Complex Fires of 2017: Remote sensing data and modeling to support ecosystem and community resiliency. California Fish and Wildlife Journal 14–45.

Hijmans, R.J., Etten, J. van, Sumner, M., Cheng, J., Bevan, A., Bivand, R., Busetto, L., Canty, M., Forrest, D., Ghosh, A., Golicher, D., Gray, J., Greenberg, J.A., Hiemstra, P., Geosciences, I. for M.A., Karney, C., Mattiuzzi, M., Mosher, S., Nowosad, J., Pebesma, E., Lamigueiro, O.P., Racine, E.B., Rowlingson, B., Shortridge, A., Venables, B., Wueest, R., 2019. raster: Geographic Data Analysis and Modeling.

Hillman, S., Wallace, L., Lucieer, A., Reinke, K., Turner, D., Jones, S., 2021. A comparison of terrestrial and UAS sensors for measuring fuel hazard in a dry sclerophyll forest. International Journal of Applied Earth Observation and Geoinformation 95, 102261. https://doi.org/10.1016/j.jag.2020.102261

Hu, T., Sun, X., Su, Y., Guan, H., Sun, Q., Kelly, M., Guo, Q., 2020. Development and performance evaluation of a very low-cost UAV-Lidar System for forestry applications. Remote Sensing 13, 77. https://doi.org/10.3390/rs13010077

Jayathunga, S., Owari, T., Tsuyuki, S., 2018. Evaluating the performance of photogrammetric products using fixed-wing UAV imagery over a mixed conifer–broadleaf forest: Comparison with airborne laser scanning. Remote Sensing 10, 187. https://doi.org/10.3390/rs10020187

Keeley, J.E., Syphard, A.D., 2019. Twenty-first century California, USA, wildfires: fuel-dominated vs. wind-dominated fires. fire ecol 15, 1–15. https://doi.org/10.1186/s42408-019-0041-0

Klápště, P., Fogl, M., Barták, V., Gdulová, K., Urban, R., Moudrý, V., 2020. Sensitivity analysis of parameters and contrasting performance of ground filtering algorithms with UAV photogrammetry-based and LiDAR point clouds. International Journal of Digital Earth 13, 1–23. https://doi.org/10.1080/17538947.2020.1791267

Kramer, H., Collins, B., Kelly, M., Stephens, S., 2014. Quantifying ladder fuels: a new approach using LiDAR. Forests 5, 1432–1453. https://doi.org/10.3390/f5061432

Larrinaga, A.R., Brotons, L., 2019. Greenness indices from a low-cost UAV imagery as tools for monitoring post-fire forest recovery. Drones 3, 6. https://doi.org/10.3390/drones3010006

Marino, E., Montes, F., Tomé, J.L., Navarro, J.A., Hernando, C., 2018. Vertical forest structure analysis for wildfire prevention: Comparing airborne laser scanning data and stereoscopic hemispherical images. International Journal of Applied Earth Observation and Geoinformation 73, 438–449. https://doi.org/10.1016/j.jag.2018.07.015

Menning, K.M., Stephens, S.L., 2007. Fire climbing in the forest: A semiqualitative, semiquantitative approach to assessing ladder fuel hazards. Western Journal of Applied Forestry 22, 88–93. https://doi.org/10.1093/wjaf/22.2.88

Miller, J.D., Safford, H.D., Crimmins, M., Thode, A.E., 2009. Quantitative evidence for increasing forest fire severity in the Sierra Nevada and Southern Cascade Mountains, California and Nevada, USA. Ecosystems 12, 16–32. https://doi.org/10.1007/s10021-008-9201-9

Miller, J.D., Thode, A.E., 2007. Quantifying burn severity in a heterogeneous landscape with a relative version of the delta Normalized Burn Ratio (dNBR). Remote Sensing of Environment 109, 66–80. https://doi.org/10.1016/j.rse.2006.12.006

Nauslar, N., Abatzoglou, J., Marsh, P., 2018. The 2017 North Bay and Southern California fires: A case study. Fire 1, 18. https://doi.org/10.3390/fire1010018

Odion, D.C., Moritz, M.A., DellaSala, D.A., 2010. Alternative community states maintained by fire in the Klamath Mountains, USA. Journal of Ecology 98, 96–105. https://doi.org/10.1111/j.1365-2745.2009.01597.x

Pádua, L., Guimarães, N., Adão, T., Sousa, A., Peres, E., Sousa, J.J., 2020. Effectiveness of Sentinel-2 in multi-temporal post-fire monitoring when compared with UAV imagery. IJGI 9, 225. https://doi.org/10.3390/ijgi9040225

Pepperwood Preserve, 2019. What does resilience look like after two fires in two years? Pepperwood Field Notes. URL https://www.pepperwoodpreserve.org/2019/11/18/what-does-resilience-look-like-after-two-fires-in-two-years/ (accessed 1.21.20).

Picotte, J.J., Bhattarai, K., Howard, D., Lecker, J., Epting, J., Quayle, B., Benson, N., Nelson, K., 2020. Changes to the Monitoring Trends in Burn Severity program mapping production procedures and data products. fire ecol 16, 16. https://doi.org/10.1186/s42408-020-00076-y

Prata, G.A., Broadbent, E.N., de Almeida, D.R.A., St. Peter, J., Drake, J., Medley, P., Corte, A.P.D., Vogel, J., Sharma, A., Silva, C.A., Zambrano, A.M.A., Valbuena, R., Wilkinson, B., 2020. Single-pass UAV-borne GatorEye LiDAR sampling as a rapid assessment method for surveying forest structure. Remote Sensing 12, 4111. https://doi.org/10.3390/rs12244111

R Core Team, 2019. R: A language and environment for statistical computing.

Roussel, J.-R., Auty, D., De Boissieu, F., Sánchez Meador, A., Jean-François, B., 2020. lidR: Airborne LiDAR data manipulation and visualization for forestry applications.

Rundel, P.W., Arroyo, M.T.K., Cowling, R.M., Keeley, J.E., Lamont, B.B., Vargas, P., 2016. Mediterranean biomes: Evolution of their vegetation, floras, and climate. Annu. Rev. Ecol. Evol. Syst. 47, 383–407. https://doi.org/10.1146/annurev-ecolsys-121415-032330

Stefanidou, A., Gitas, I.Z., Katagis, T., 2022. A national fuel type mapping method improvement using sentinel-2 satellite data. null 37, 1022–1042. https://doi.org/10.1080/10106049.2020.1756460

Tompalski, P., White, J.C., Coops, N.C., Wulder, M.A., 2019. Quantifying the contribution of spectral metrics derived from digital aerial photogrammetry to area-based models of forest inventory attributes. Remote Sensing of Environment 234, 111434. https://doi.org/10.1016/j.rse.2019.111434

Vastaranta, M., Wulder, M.A., White, J.C., Pekkarinen, A., Tuominen, S., Ginzler, C., Kankare, V., Holopainen, M., Hyyppä, H., 2013. Airborne laser scanning and digital stereo imagery measures of forest structure: Comparative results and implications to forest mapping and inventory update. Canadian Journal of Remote Sensing 39, 382–395.

Wallace, L., Bellman, C., Hally, B., Hernandez, J., Jones, S., Hillman, S., 2019. Assessing the ability of image based point clouds captured from a UAV to measure the terrain in the presence of canopy cover. Forests 10, 284. https://doi.org/10.3390/f10030284

Watershed Sciences, 2016. Sonoma County vegetation mapping and lidar program: Technical data report.

Westerling, A., 2018. Wildfire simulations for California's Fourth Climate Change Assessment: Projecting changes in extreme wildfire events with a warming climate (No. CCCA4- CEC-2018–014). California's Fourth Climate Change Assessment, California Energy Commission.

Westerling, A.L., Bryant, B.P., 2008. Climate change and wildfire in California. Climatic Change 87, 231–249. https://doi.org/10.1007/s10584-007-9363-z

White, J.C., Tompalski, P., Coops, N.C., Wulder, M.A., 2018. Comparison of airborne laser scanning and digital stereo imagery for characterizing forest canopy gaps in coastal temperate rainforests. Remote Sensing of Environment 208, 1–14. https://doi.org/10.1016/j.rse.2018.02.002

Zhang, W., Qi, J., Wan, P., Wang, H., Xie, D., Wang, X., Yan, G., 2016. An easy-to-use airborne LiDAR data filtering method based on cloth simulation. Remote Sensing 8, 501. https://doi.org/10.3390/rs8060501

Chapter 4

Preface

In this third study, I utilized the UAS-SfM processing and metric extraction workflow from the previous study to generate machine learning models of canopy fire fuels using data from sites across California. This paper, for me, is the heart of my thesis, wherein I demonstrate for the first time the ability of UAS-SfM to model fuels in a way that could be of value to land managers, owners, and state personnel.

The research in this study was developed by me, Imma, Dr. Clark, and Dr. Bentley. I was not involved in the further field data collection at the sites beyond Pepperwood. That work was conducted by the 3D Forests team led by Dr. Clark and Dr. Bentley. They gave me access to the raw field data and PIX4D SfM outputs and I conducted all further analyses and manuscript preparation. All coauthors assisted with editing the final text. This paper was submitted to Remote Sensing of Environment and has been accepted with minor revisions.

Unoccupied aerial system (UAS) Structure-from-Motion canopy fuel parameters: Multisite area-based modelling across forests in California, USA

Sean Reilly [1], Matthew L. Clark [2], Lika Loechler [2], Jack Spillane [2], Melina Kozanitas [3], Paris Krause [4], David Ackerly [3], Lisa Patrick Bentley [4], and Imma Oliveras Menor [1,5]

[1] Environmental Change Institute, University of Oxford, Oxford OX1 3QY, UK

[2] Center for Interdisciplinary Geospatial Analysis, Department of Geography, Environment, and Planning, Sonoma State University, Rohnert Park, CA 94928, USA

[3] Departments of Integrative Biology and Environmental Science, Policy, and Management, University of California, Berkeley, CA 94720, USA

[4] Department of Biology, Sonoma State University, Rohnert Park, CA 94928, USA

[5] AMAP (Botanique et Modélisation de l'Architecture des Plantes et des Végétations), CIRAD, CNRS, INRA, IRD, Université de Montpellier, Montpellier, France

Abstract

There is a pressing need for well-informed management to reduce wildfire hazard and restore fire's beneficial ecological role in the Mediterranean- and temperate-climate forests of California, USA. These efforts rely upon the accessibility of high spatial and temporal resolution data on biomass and canopy fuel parameters such as canopy base height (CBH), mean canopy height, canopy bulk density (CBD), canopy cover, and leaf area index (LAI). Remote sensing using unoccupied aerial system Structure-from-Motion (UAS-SfM) presents a promising technology for this application due to its accessibility, relatively low cost, and possibility for high temporal cadence. However, to date, this method has not been studied in the complex mosaic of forest types found across California. In this study we

examined the capacity of structural and multispectral information obtained from UAS-SfM, in conjunction with machine learning methods, to model aboveground biomass and forest canopy fuel structural parameters using an area-based approach across multiple sites representing a diversity of forest types in California.

Based on correlations with field measurements, fuel parameters separated into vertical (biomass, CBH, and mean height) and horizontal (LAI, CBD, canopy cover) groups. UAS-SfM random forest models performed well for modelling the vertical structure canopy fuels parameters (R^2 0.69 – 0.75). These models exhibited strong performance in comparison to ALS, as well as when transferred to a novel site. Vertical structure predictors were prominent in these models, and did not improve with the addition of spectral predictors. UAS-SfM random forest models of horizontal structure parameters mainly used raster-based spectral indices (primarily NDVI) and had relatively low performance (R^2 0.49 – 0.59). In addition, these models underperformed ALS and had poor performance when applied to a novel site. When applied to a region with widespread UAS-SfM data coverage, models from both groups successfully produced contiguous maps that could be used for modelling fire behavior or in management decision making and monitoring.

These findings indicate that UAS-SfM, without the need for multispectral sensors, is well suited for mapping area-based vertical-structure canopy parameters across diverse landscapes supporting a wide range of forest types. In contrast, the identification of spectral mean variables for modelling horizontal structure canopy fuels suggests the potential of multi- or hyperspectral sensors or high-resolution satellite imagery for meeting management information needs.

Keywords

UAS, SfM, machine learning, canopy fuels, biomass, California forests

1. Introduction

Wildfires shape many ecosystems across the globe, giving rise to highly heterogeneous landscapes due to the spatial and temporal variation inherent in natural wildfire behavior (Beaty and Taylor, 2008; Hessburg et al., 2015; Staver et al., 2011). Fire is a naturally self-limiting process whereby previous burns act as barriers to subsequent fires due to the removal of fuels, defined as biomass available for consumption (Collins et al., 2009; Husari et al., 2006; Keeley et al., 1999; Minnich, 1983; Park et al., 2021; Parks et al., 2015). However, when fire is suppressed or excluded, fuel loads continually rise, eventually surpassing historical levels and eliminating controls on future fire spread or intensity (Prichard et al., 2021; Stephens and Ruth, 2005). As a result of historical suppression practices in the United States, fires now burn at higher severity and on broader scales, despite intensifying suppression efforts (Dennison et al., 2014; Miller et al., 2012, 2009).

Fuel loads in forests of California, USA are a key driver of high-severity fire and are the only parameter governing fire behavior over which managers may exert influence (Duff et al., 2017; Parks et al., 2018). Forest treatments, such as mechanical thinning of the understory, fire breaks, and prescribed fire, can reduce overall fuel quantities and disrupt the spatial continuity of fuels (Agee and Skinner, 2005; Prichard et al., 2021; Stephens and Moghaddas, 2005). To achieve widespread fire hazard mitigation benefits, decision making for treatment optimization and targeting relies upon detailed understanding of fire behavior across the landscape, which, in turn, depends on spatially explicit maps of fuels and/or fuels-related forest structural parameters (Collins et al., 2010; Gale et al., 2021). For example, the initiation of crown torching depends upon vertical forest structural components, such as canopy base height (CBH), while horizontal canopy structural attributes, such as canopy bulk density (CBD) and canopy cover (CC), govern sustained canopy ignition and spread among crowns (Agee and Skinner, 2005; Van Wagner, 1977). Aboveground tree biomass presents an additional parameter of interest for informing treatment selection due to the high imperative for maximizing stable carbon sequestration in the face of climate change (Foster et al., 2020; Hunter and Robles, 2020; Moghaddas et al., 2018).

Measuring these forest attributes presents a significant challenge due to their inherent spatial and temporal variability (Alonso-Rego et al., 2021; Arellano-Pérez et al., 2018). Consequently, remote sensing approaches provide an advantage over traditional field-based manual sampling approaches in that they can estimate continuous fuels parameters over broad extents and are unencumbered by terrain or vegetative barriers to site access. Spaceborne passive sensors generally approximate fuel distributions through the application of fuel density models to observed vegetation classes (Aragoneses and Chuvieco, 2021; Arroyo et al., 2008; Shaik et al., 2022; Stefanidou et al., 2022). These methods are constrained by their reliance on externally-derived fuel models with irregular updates, vegetation maps derived from coarse resolution satellite-based optical imagery, and their inability to account for variation in canopy structure or fuel distribution within a vegetation class, a significant limitation in the structurally-complex forests of California. Alternatively, methods utilizing active sensors, namely airborne laser scanners (ALS) or lidar, provide a means to measure forest structure and fuel loads directly over regional spatial scales (Alonso-Rego et al., 2021; Andersen et al., 2005; García-Cimarras et al., 2021; Hillman et al., 2021b; Kramer et al., 2014; Rocha et al., 2023). However, high cost and equipment requirements of ALS severely limit the capacity of this approach to provide either the spatial coverage or the frequency of repeated measurements required to inform ongoing management of dynamic fuel loads and recurrent fire events at plot to stand scales (Chuvieco et al., 2020; Filippelli et al., 2019; Szpakowski and Jensen, 2019). While lidar mounted on an unoccupied aerial system (UAS) could reduce this barrier, these systems cannot provide spectral data and are not yet sufficiently cost effective to be readily operationalizable in management settings (Gale et al., 2021; Hillman et al., 2021a).

UAS Structure-from-Motion (SfM), the photogrammetric derivation of 3D spatial information from overlapping images, presents a promising technology that could fill this need for readily-acquirable spatial data that directly measures canopy structure and fuel loads at the stand scale (Lowe, 2004; Westoby et al., 2012). The advent of commercial SfM software, coupled with the development of UAS platforms, has significantly reduced the barriers to obtaining and processing highly accurate structural data (Aasen et al., 2018; Adjidjonu and Burgett, 2021; Agüera-Vega et al., 2017; Fraser and Congalton,

2018). At the stand scale, the relatively low cost and ease of imagery acquisition make UAS-SfM well suited for mapping dynamic ecological forces like fuel load accumulation and interannual wildfire events (Campbell et al., 2020), as well as effects of management activities (e.g., prescribed burns, thinning). This method has been successfully employed in a variety of ecological applications that measure vegetation structure (e.g., Fu et al., 2021; Navarro et al., 2020; Swayze et al., 2021), including aspects of fire ecology and management (Szpakowski and Jensen, 2019). When coupled with the appropriate sensor, the capacity of UAS-SfM to collect coincidental multispectral data provides additional capability in measuring forest structure and health beyond the limits of lidar data or Red-Green-Blue UAS-SfM (e.g., Abdollahnejad and Panagiotidis, 2020; Reilly et al., 2021).

The capacity of UAS-SfM to measure canopy fuel parameters has only received limited investigation to date (e.g., Shin et al., 2018), especially in California forests (e.g., Forbes et al., 2022; Lamping et al., 2021). The majority of previous related research has focused on coniferous forests (e.g., Alonzo et al., 2018; Sun et al., 2023) or plantation sites (e.g., Chandrasekaran et al., 2022) to measure specific canopy parameters. These studies have achieved strong results due to the ease of tree segmentation under these forest conditions. However, current tree segmentation algorithms fail to segregate individual tree crowns when applied to more complex mosaic canopies, such as oak woodlands (e.g., Chávez-Durán et al., 2024). Consequently, there is a large research gap for UAS-SfM methods, such as area-based approaches that are capable of modelling canopy fuel loads across the wide range of complex forest types without the prerequisite step of tree segmentation.

In our past research in California forests, we found UAS-SfM possesses the capacity to measure upper-canopy structure and to detect the persistent influence of burn severity on ecosystem structure and vegetation recovery (Reilly et al., 2021). However, our and other research has found the passive sensor mainly detects upper-canopy photons, which hampers UAS-SfM's ability to detect subcanopy structure or directly measure key fuel attributes related to internal structure or lower-canopy strata, such as ladder fuels, CBD, or CBH (Forbes et al., 2022; Reilly et al., 2021; Shin et al., 2018). Modelling approaches to estimate stand parameters can overcome these limitations in photogrammetric techniques by leveraging

inherent relationships among distinct components of canopy structure (Filippelli et al., 2019). To address the research gap described above, this paper explores the capability of multispectral UAS- and area-based machine learning to model tree aboveground biomass and canopy fuel parameters across a diverse and complex range of forest types found in California.

Specifically, we address the following objectives:

1. Evaluate the accuracy of machine learning models produced using UAS-SfM data to estimate tree aboveground biomass and five important canopy fuel structural parameters: mean height, canopy base height (CBH), canopy cover (CC), canopy bulk density (CBD), and leaf area index (LAI).
2. Compare the accuracy of the best modelling technique produced using UAS-SfM data with the same models produced using ALS data, which has deeper canopy penetration.
3. Using the best modelling technique, evaluate model variable selection and importance.
4. Demonstrate the mapping capability of this modelling approach when utilized in conjunction with wide coverage UAS-SfM data.
5. Evaluate the accuracy of machine learning models produced using UAS-SfM data when applied to a novel site.

2. Methods

2.1 Study sites

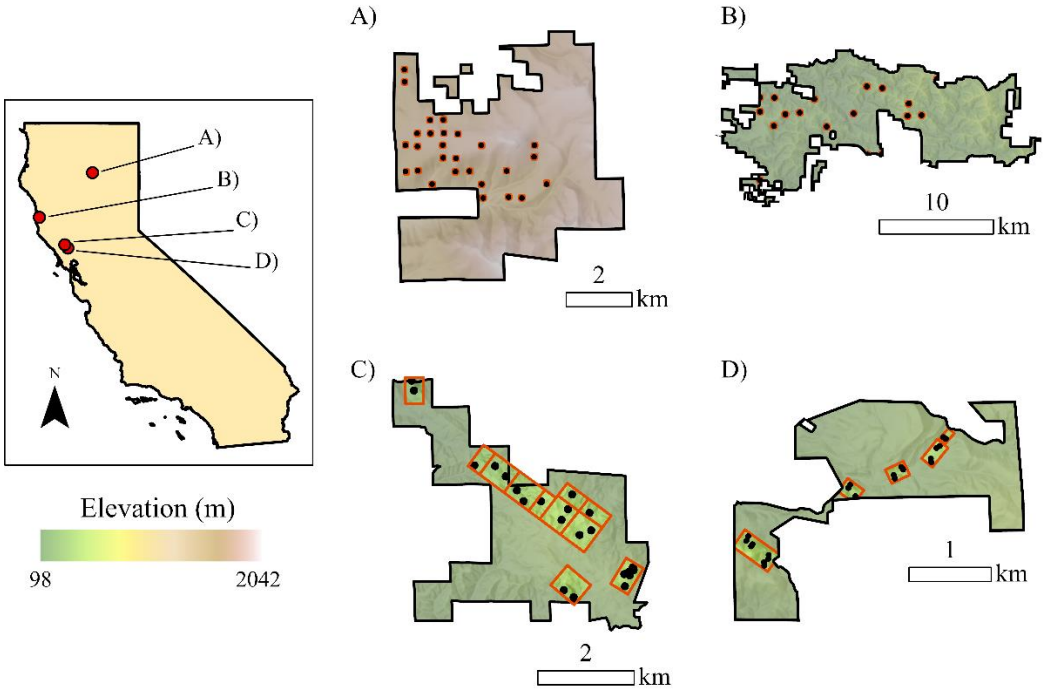


Fig. 4.1 Map of study sites (a) LaTour, (b) Jackson, (c) Pepperwood, and (d) Saddle Mountain within California, USA. Red boxes denote UAS flight zone perimeters. Black points represent field sites.

We collected UAS-SfM and field data at four sites across northern California that span a wide range of ecosystem types. Data were collected in the summer from 2018 through 2021. LaTour Demonstration State Forest covers 3,550 ha in the Cascade mountains of Shasta County ranging in elevation from 1,150 m to 2,050 m (Fig. 4.1A). The site is in the Cascades ecoregion (Level 3; Shasta County; Griffith et al., 2016), and populated by mixed conifer forests, with white fir (*Abies concolor*) as the most prevalent species especially at higher elevations (Berbach et al., 1995). The site has active stand thinning and some plots had open canopies. We sampled 27 preexisting 0.04-ha circular California Forest Inventory (CFI) plots between 7 July and 17 July 2020. Jackson Demonstration State Forest covers 19,700 ha acres in the Coast Range ecoregion (Mendocino County) ranging in elevation from 24 m to 670 m (Fig. 4.1B). The site predominantly contains second-growth coast redwood (*Sequoia sempervirens*) and Douglas fir (*Pseudotsuga menziesii*) that are less than 120 years old with some isolated remaining old-

growth groves and residual trees (Eng, 2015). Most plots had dense, closed canopies. We sampled 10 0.04-ha circular CFI plots between 15 June and 2 July 2020 and an additional 17 CFI plots between 8 July and 12 July 2021. Pepperwood Preserve covers 1,261 ha in the Central California Foothills and Coastal Mountains ecoregion (Sonoma County) ranging in elevation from 61 m to 475 m elevation. The site is vegetated with a diverse mosaic of species assemblages including Douglas fir forest, oak woodlands, chaparral, and grasslands (Ackerly et al., 2020; Evett et al., 2013). Note that Pepperwood was almost completely burned in the 2017 Tubbs Fire, with a range from low to high severity across the site. We sampled 22 plots between 1 Sept and 15 Oct 2019. These 0.04-ha square plots have been sampled since 2013 as part of a Sentinel plot network at the site, and the ground truth data for this study were taken from summer 2018 field work (Ackerly et al., 2013; Oldfather et al., 2016). The final site, Saddle Mountain Open Space Preserve, covers 390 ha and is 8 km southeast of Pepperwood. The site has a similar vegetation assemblage to its neighboring Pepperwood site. We established and sampled 22 0.04-ha circular plots between 4 August and 9 August 2020. These plots were established within 60-m of the road and collected as paired points in different forest types. Pepperwood and Saddle Mountain have a Mediterranean climate, whereas Latour and Jackson have a climate associated with temperate coniferous forests. For the sites with preexisting networks of plots (CFI for Jackson and LaTour, Sentinel plot network at Pepperwood), we used a stratified random sampling of plots near roads and away from powerlines, with strata determined by a Principal Components Analysis on ALS structure metrics, adding in an additional consideration of Tubbs burn severity for Pepperwood.

Our plot size was dictated by the preexisting sampling network employed by managers and researchers at our sites for their long-term studies. For management applications and understanding of fire behavior, study plot resolution needs to capture fine-scale forest variation and connectivity. Our small plot size of 0.04-ha, therefore, is well suited for mapping the heterogeneity of biomass and fuels across a site as required to address our research aims (Shugart et al., 2010). The data collected from this scale of plot, however, should be understood to represent local conditions, rather than provide representative measurements of the site as a whole.

2.2 Data sources

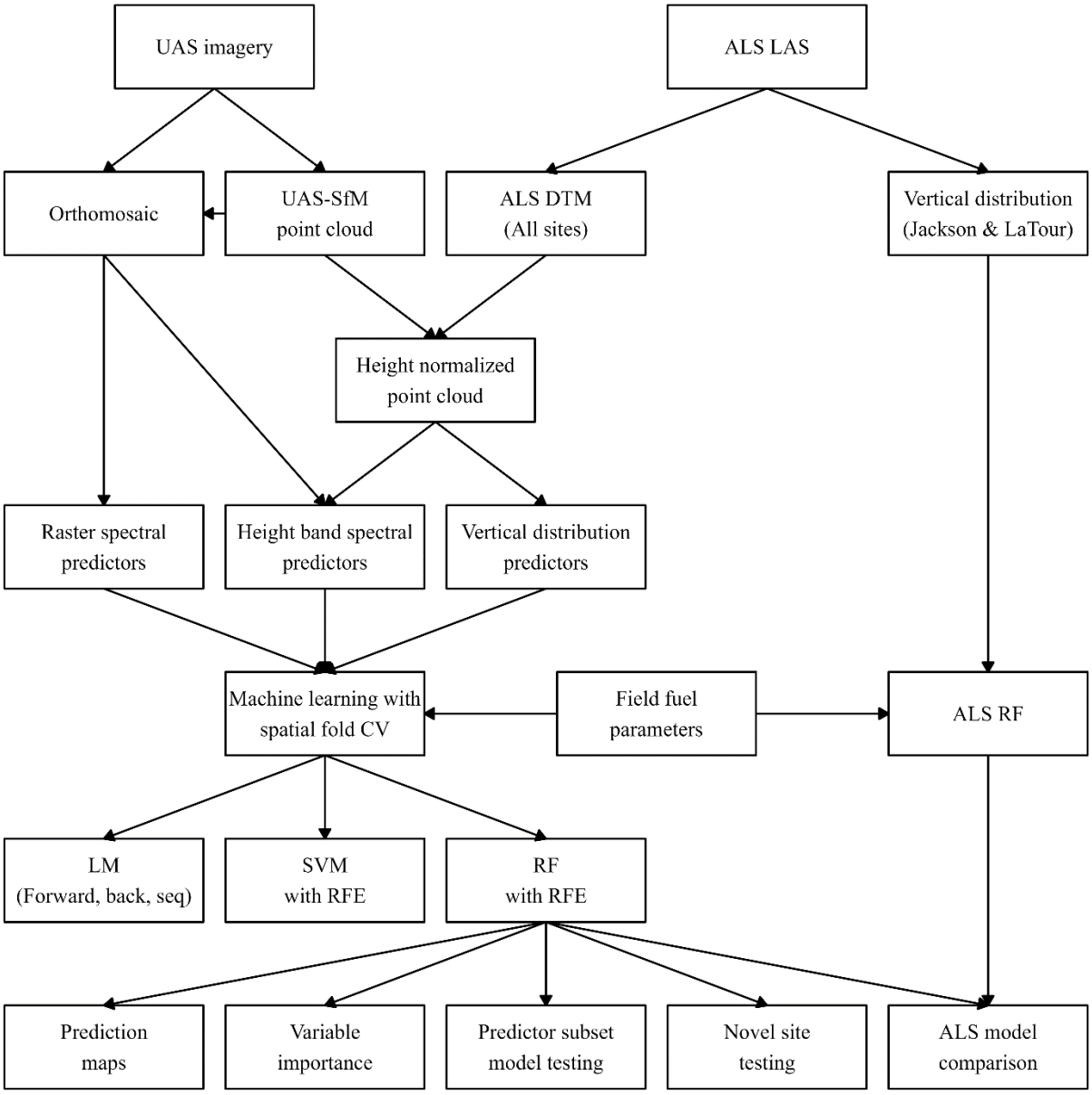


Fig. 4.2 Data processing workflow

2.2.1 Field-based measurements

For this study, we collected tree-level measurements of diameter at breast height (DBH), tree height, and lowest live crown for all stems with DBH greater than 10 cm. We measured DBH at 1.37 m above the ground on the uphill side of the trunk. We employed a Laser Technology Impulse 200 LR

Rangefinder to determine tree height. Lowest live crown was defined as the height above the ground of the lowest branch supporting live vegetation within 2 m of the next highest branch and was measured with either a tape measure or laser rangefinder, as practical. At Saddle Mountain, we collected all field measurements. At Pepperwood, we utilized DBH measurements previously collected in 2018 as part of the Sentinel site monitoring program. At LaTour, we utilized preexisting DBH and height measurements from a California Department of Forestry and Fire Protection (CAL FIRE) survey conducted in 2020, supplementing as needed with field measurements for plots that had not been included in their campaign. At Jackson, we also utilized preexisting DBH and tree height measurements from CAL FIRE collected in 2020. However, due to the extreme tree height and high canopy cover of the redwood forests at that site, tree heights at Jackson cannot be measured directly. Tree heights, therefore, were estimated from DBH measurements using preexisting CAL FIRE models of the relationship between DBH and tree height (J. Leddy, personal communication, May 17, 2021). We computed individual tree aboveground biomass from DBH and height measurements using the California Air Resource Board's carbon offset protocols based on the U.S. Forest Service's Forest Inventory and Analysis Program volume and biomass equations (FIA, 2014). We took the mean of individual tree measurements for height, aboveground biomass, and lowest live crown to determine plot-level mean height, total aboveground biomass, and canopy base height (CBH), respectively.

We calculated the mean of five measurements per plot (center and 7 m from center in cardinal directions) from the LI-COR LAI-2000 Plant Canopy Analyzer and Forestry Suppliers spherical crown densiometer to measure leaf area index (LAI) and canopy cover, respectively. Canopy cover was estimated in cardinal directions at each of the five locations within the plot, and all cover estimates were averaged for a plot-level measurement. The LAI-2000 uses a handheld wand to measure the percentage of radiation passing through the forest canopy in order to estimate canopy gap fraction and LAI (Keane et al., 2005; Welles and Norman, 1991). LAI-2000 gap fraction measurements were used to compute canopy bulk density (CBD) using the equations from Keane et al. (2005). Keane et al. (2005) conducted destructive sampling at five sites dominated by conifer trees in the western United States to directly

measure plot level CBD at varying levels of basal area removal. They modelled the relationship between these measurements and coincidentally collected LAI-2000 measurements as CBD = 0.2231 – 0.2012 LAI2000A, where LAI2000A represented the mean gap fraction across five zenith angles. This relationship was found to be significant, but with a modest R^2 of 0.56. When using the LAI-2000, we placed one wand in open-canopy areas to measure top-of-canopy radiance, and we strived to take measurements with a second wand within plots during early morning hours to avoid direct sunlight. Both wands had a 45° optic cover with the opening facing away from the sun. The five LAI estimates in a plot were averaged to create one plot-level measurement.

2.2.2 UAS-SfM data collection and processing

This study utilized a MicaSense RedEdge-MX multispectral sensor onboard two UAS platforms. The Micasense sensor detects five spectral bands: blue (475 nm center, 20 nm bandwidth), green (560 nm center, 20 nm bandwidth), red (668 nm center, 10 nm bandwidth), red edge (717 nm center, 10 nm bandwidth), and near-IR (840 nm center, 40 nm bandwidth). At Pepperwood and Saddle Mountain, the sensor was flown using a SenseFly eBee X fixed-wing UAS platform. We flew Pepperwood between September 27 to October 15, 2019 and Saddle Mountain on August 4 and 5, 2020. At Jackson and LaTour, we flew a DJI Matrice 200 (M200) quadcopter UAS platform. We flew Jackson on June 29 to July 2, 2020 and added more sites in July 8-12, 2021. We flew LaTour between July 11 to 16, 2020. UAS platform selection depended upon the availability of a suitable location for fixed-wing take-off and landing. The SenseFly allows for significantly greater mapping coverage per flight but requires a large soft-landing area free from obstructions. The M200 was used in heavily forested sites where these landings were not possible.

Additionally, we used an onboard MicaSense Downwelling Light Sensor (DLS) 2, along with a MicaSense calibration panel (RP04-1926247-OB), for radiometric calibration to convert raw radiance measurements to reflectance values that could be compared between flights across sites. We flew each flight box twice at a flight altitude of 122-m (400 ft) above ground level using a perpendicular crosshatch

pattern to ensure maximum coverage. SenseFly's eMotion 3 software (version 3.7) controlled the fixed-wing eBee to collect imagery at 75% latitudinal and longitudinal overlap while the Micasense Atlas app controlled the quadcopter M200 to collect imagery at 85% overlap.

We generated reflectance orthomosaics and SfM 3D point clouds from the collected imagery using Pix4Dmapper (Fig. 4.2, Pix4D, Lausanne, Switzerland, version 4.4.12). The resulting orthomosaics had 5-cm resolution at LaTour, Jackson, and Saddle Mountain, and 15-cm resolution at Pepperwood. Pepperwood had a lower resolution because of a change in sampling method to prioritize coverage over a larger area. Due to battery flight time restrictions, the eBee had to fly with lower overlap to cover the required area. This resulted in a drop in final orthomosaic resolution when processed through Pix4D. The SfM points clouds had a mean density of 320 points/m^2 with a range from 36 to 672 points/m^2 depending on site characteristics.

We calculated the following spectral indices from the multispectral orthomosaics (Dash et al., 2018):

$$\text{Normalized Difference Vegetation Index (NDVI)} = (\text{NIR} - \text{Red}) \,/\, (\text{NIR} + \text{Red})$$

$$\text{Normalized Difference Red Edge (NDRE)} = (\text{NIR} - \text{Red Edge}) \,/\, (\text{NIR} + \text{Red Edge})$$

$$\text{Green NDVI (GNDVI)} = (\text{NIR} - \text{Green}) \,/\, (\text{NIR} + \text{Green})$$

We calculated these spectral index rasters at the same resolution as the orthomosaic imagery from their respective site (i.e., 5 cm for LaTour, Jackson, and Saddle Mountain, and 15-cm for Pepperwood). These indices were selected based on the available Micasense Rededge MX spectral bands and their relationships with plant physiology (Dash et al., 2018). We then spatially-joined reflectance bands and spectral indices with the point cloud in R (version 4.2.3) using the lidR package (R Core Team, 2023; Roussel et al., 2023). Following the method of Reilly et al. (2021), we identified ground points within the point cloud with a cloth simulation filter and removed erroneously misclassified vegetation points using an NDVI filter (Zhang et al., 2016). We then used these ground points to register the point clouds to preexisting ALS digit terrain models (DTM) (Fig. 4.2., see section 2.2.3 below). For flight boxes with insufficient identified ground points due to high canopy cover, primarily at Jackson, we performed

registration on the complete UAS-SfM and ALS point clouds. Following registration, we height normalized the UAS-SfM point cloud using the ALS DTM and extracted the points within the field plot boundaries.

Table 4.1 UAS-SfM structural and spectral predictors.

Predictor label	Description	N
	Vertical Density	
Z_{max}	Max height	1
$\overline{Z}$	Mean height	1
P_x	Height percentiles in 5% increments (0% to 95 %)	20
Z_{SD}	Height standard deviation	1
Z_{CV}	Height coefficient of variation	1
Z_{Kurt}	Height kurtosis	1
Z_{Skew}	Height skewness	1
Z_{IQR}	Height interquartile range	1
CRR	Canopy relief ratio $(\overline{Z} - Z_{min}) \,/\, (Z_{max} - Z_{min})$	1
D_{Hx}	Height density bands	10
CC_{1m}	Percentage of points above 1m	1
CC_{Mean}	Percentage of points above mean	1
	Raster-based Spectral	
$\overline{SPECTRA}$	Orthomosaic mean for spectral bands and indices	8
$SPECTRA_{SD}$	Orthomosaic standard deviation for spectra bands and indices	8
	Height-band Spectral	
$\overline{SPECTRA}_{Hx}$	Height band mean for spectral bands and indices	80
$SPECTRA_{Hx}SD$	Height band standard deviation for spectral bands and indices	80
	Total	216

Note. Subscript *x* denotes index placeholder for multiple bands. SPECTRA denotes placeholder for individual spectral bands (blue, green, red, red-edge, NIR) and spectral indices (NDVI, GNDVI, NDRE).

This study utilized an area-based approach to extracting information from the UAS-SfM data. To summarize these data at the plot level, 216 predictors were generated for modelling inputs (Table 4.1, Fig. 4.2). We extracted these predictors directly from the point cloud, rather than from a digital surface model. We computed 40 vertical distribution predictors based on Filipelli et al. (2019) and Marino et al (2018). These included variables of the height profile, height variation, density bands, and cover. For the density band variables (D_{Hx}), we divided the vertical distribution of points at each plot into ten equal height bands and computed the percentage of points that fell within each of them. For the canopy cover bands, we

computed the percentage of points above either 1 m or the mean. Finally, we computed the canopy relief ratio as (mean height – minimum height) / (max height – minimum height) (Marino et al., 2018).

In addition to the vertical distribution predictors, we also generated 176 spectral predictors, divided into raster-based and height-band categories. We generated 16 raster-based spectral predictors by computing the mean and standard deviation from the orthomosaics for the five individual spectral bands (i.e., blue, green, red, red-edge, NIR) and the three spectral indices (i.e., NDVI, GNDVI, NDRE). We also generated an additional 160 height-band spectral predictors. To produce these, we divided the point cloud into ten vertical bins, as we did for the vertical density predictors, and isolated the related spectral information within each bin. For each of these ten slices of the spectral data, we computed the same set of 16 predictors (i.e., mean and standard deviation of the five spectral bands and three indices) to generate 160 height-band spectral predictors in total.

2.2.3 ALS data collection and processing

ALS data for Pepperwood and Saddle Mountain came from the 2013 Sonoma County Vegetation -Mapping and Lidar Program, which were collected by Watershed Science between 28 Sept 2013 and 26 Nov 2013 using aircraft-mounted Leica ALS50 and ALS70 sensors (Watershed Sciences, 2016). ALS data for Jackson were collected by Dewberry and Quantum Spatial between 3 Mar 2017 and 24 Aug 2017 using an aircraft-mounted Leica ALS70 sensor (Dewberry, 2018). ALS data for LaTour were collected by Quantum Spatial between 11 Oct 2019 and 27 Dec 2019 using a Riegl VQ1560i sensor (Quantum Spatial, 2020). Collected ALS data had a mean point density of 25 points/m^2 with a range from 6 to 49 points/m^2. ALS DTMs were generated from ground points within the data as classified following procedures by each company.

We constrained our comparisons between models using both UAS-SfM and ALS data to Jackson and LaTour. The ALS data at these sites were collected within a narrow window of our UAS-SfM campaign and no disturbance events occurred at the sites between collection times. Saddle Mountain and Pepperwood were excluded from this analysis because of the large temporal gap between collection times

and a significant disturbance event (the Tubbs fire) that significantly affected the area. Following the UAS-SfM procedure, we height normalized the ALS DTMs and extracted the points that fell within each plot boundary. Since ALS lacks spectral information, only the vertical density subset of variables was computed from these data for modelling input (Fig. 4.2).

2.3 Machine learning modelling

Following the methods of Almeida et al. (2019), we tested five regression modelling methods using the caret package in R (Kuhn et al., 2023). Caret, in turn, utilizes a suite of R packages to streamline model training for complex regression and classification algorithms (Cutler and Wiener, 2022; Karatzoglou et al., 2023; Miller, 2020). The models tested in this study comprised three linear models (LM), support vector machine (SVM), and random forest (RF). For each approach, we centered and scaled the predictor variables prior to training the model using caret's default method of subtracting the mean to center and dividing by the standard deviation to scale. Additionally, for the LM methods, we addressed multicollinearity in the predictor set by removing subsets of variables that surpassed a correlation of r = 0.9 using the internal caret function.

Table 4.2 Cross validation spatially-blocked group distance thresholds from spatial variogram partial sill range

Parameter	Abbreviation	Partial sill range
Biomass	-	44 m
Mean height	-	75 m
Canopy base height	CBH	266 m
Canopy cover	CC	513 m
Canopy bulk density	CBD	487 m
Leaf area index	LAI	103 m

We assessed model performance using cross validation with spatially-blocked groups. There has been ongoing debate in the literature about the accuracy of spatially-blind cross validation (Ploton et al., 2020; Pohjankukka et al., 2017; Wadoux et al., 2021). If neighboring plots are separated into testing and training sets, their inherent spatial autocorrelation could artificially inflate the reported performance of the model. Therefore, we computed a set of spatial variograms for each canopy fuel parameter and used the range of the partial sill as a distance threshold for data splitting (Table 4.2). The sill range of a spatial

variogram is the distance at which the model asymptotically levels out. The partial sill range is the distance at which the model reaches this asymptotic value minus the nugget, the variation in the model due to random or sampling error (Cressie, 1988). This range represents the distance at which spatial autocorrelation has ceased and, therefore, sites farther apart than this distance are appropriate for comparison (Ploton et al., 2020). All sites within this distance threshold comprised a spatially-blocked group that would be collectively assigned to either training or testing subsets at each cross validation split. At each cross validation split, R^2 and RMSE were computed on the held out spatially-blocked group. At the end, the error metrics from all of the cross-validation iterations were summarized into average metrics for the final model. Using this spatial cross validation, each model was optimized using the minimization of the root mean squared error (RMSE) of the fuel parameter predictions.

LM methods seek to establish linear relationships between the predictor variables and given fuel parameter response. LM feature selection occurs in a stepwise manner that can either be done forward, whereby the algorithm starts with an empty model and adds significant variables; backwards, whereby the algorithm starts with a complete model and removes nonsignificant variables; or sequentially, whereby both steps are conducted simultaneously. We tested all three approaches in this study.

SVM is a non-parametric modelling approach that uses a kernel to map predictor variables to higher dimensions in an attempt to generate a linear relationship from nonlinear inputs (Mountrakis et al., 2011; Vapnik, 2006). Based on the results of Almeida et al. (2019), we employed a radial kernel.

RF is an extension of tree based classifiers whereby an ensemble of individual classification trees generated from bootstrap subsamples of the input data cast votes on a prediction (Breiman, 2001). These models can be tuned by setting the number of randomly selected features per tree split or by selecting the number of trees. A grid search of these tuning parameters found negligible impact on model accuracy.

Prior to final model training, we conducted SVM and RF predictor selection using the Recursive Feature Elimination (RFE) function within caret. This process ranks each feature by importance and sequentially removes them until two remain. It then identifies the lowest number of predictors with an

RMSE within the 95% confidence interval of the overall lowest RMSE (Almeida et al., 2019). We then used this identified subset of predictor variables to train the final models.

For the individual site and ALS model analyses, we followed these same methods. However, due to the small spatial extent and limited sample sizes, we omitted the spatial blocking from the cross-validation process and used a smaller number of cross validation groups. For comparison with UAS-SfM, we modeled canopy fuel parameters with ALS only at Jackson and LaTour as these data were acquired within three years of UAS flights, thereby minimizing differences due to vegetation change in the intervening years. Further, these are conifer-dominated sites with relatively low seasonal variation in leaf phenology.

2.3.1 Pepperwood area-based mapping

We applied the final all-site model to a large contiguous region at Pepperwood to demonstrate the capability of this modelling approach, in conjunction with UAS-SfM, to generate continuous maps of canopy parameters as needed for fire behavior modelling and broad-scale evaluation of management practices. Pepperwood was selected for this demonstration because the site's terrain and interspersed grasslands provided adequate landing zones for the eBee fixed-wing drone. This allowed us to collect extensive overlapping flight boxes to generate data over a large region to which the model could be applied (Fig. 4.1 – Pepperwood).

Vegetation distribution data for Pepperwood was taken from Ackerly et al. (2020). In their study, they utilized a support vector machine (SVM) algorithm to generate maps of land cover classes and tree species distributions from 2-m hyperspectral imagery by the National Aeronautics and Space Administration's Jet Propulsion Lab Airborne Visible Infrared Spectrometer-Next Generation (AVIRIS-NG) on 5 June 2014. We aggregated tree species into three forest types, namely conifer, evergreen broadleaf, and deciduous broadleaf (Reilly et al., 2021).

2.3.2 Novel site testing

For the novel site testing, we generated a set of RF fuel parameter models using the data from all sites except for Saddle Mountain using the same methods described above, including spatially-blocked cross validation. We then applied these models to the withheld Saddle Mountain plots to generate a set of test predictions on samples to which the original model had been fully blind. Saddle Mountain was selected for this analysis since the values from Saddle Mountain for all field-based fuels parameters fell within the range defined by the other three sites. All other sites had at least one parameter in which their values exceeded those from the other sites. Since RF models cannot extrapolate beyond the limits of the training data, this would have inherently resulted in poor model performance if the other sites had been withheld and tested in this way.

3. Results

3.1 Field-based plot-level aboveground biomass and canopy fuel parameters

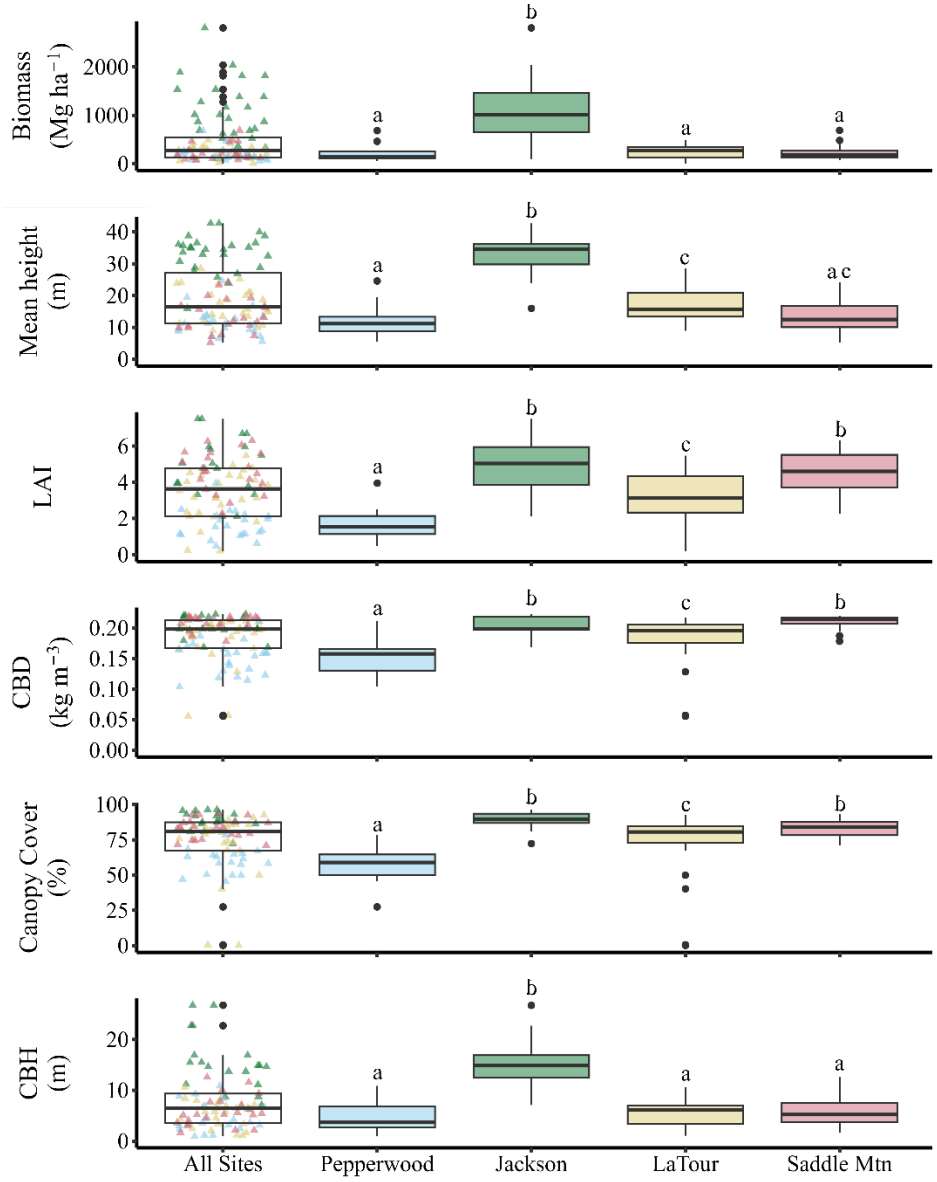


Fig. 4.3 Field-based plot-level aboveground biomass and canopy fuel parameter estimates across all sites and for each individual site. Lower case letters represent statistically similar groups as determined by ANOVA.

The distribution of canopy data measured in the field across sites followed expected patterns based on the dominant species compositions at each site (Fig. 4.3). Pepperwood, LaTour, and Saddle Mountain generally possessed similar parameter ranges, with Pepperwood consistently belonging to the

lowest statistically identified group. In contrast, Jackson, the only site predominantly populated by coastal redwood forests, consistently belonged to the highest value group for all field-based parameters.

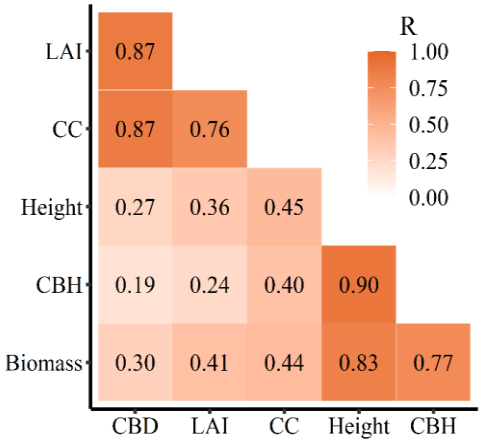


Fig. 4.4 Field-based plot-level parameter relationships. R values denote Pearson correlation coefficients.

Correlation results segregate field-based fuel parameters into two distinct groups which align with the conceptual structural organization of these parameters (Fig. 4.4). The first group of aboveground biomass, mean height, and CBH are principally vertical measurements of forest structure (biomass allometry leverages height-structure relationships). The second group consists of LAI, CBD, and canopy cover, which are horizontal measures of canopy structure. With the exceptions of the correlations between CBH and CBD ($p = 0.08$) and between CBH and LAI ($p = 0.053$), all correlations between fuel parameters were significant. Correlations within the identified groups were significant at $\alpha < 0.001$.

3.2 Model comparison

Table 4.3 Models of canopy fuel parameters across all study sites. Mean performance results obtained from 100 replicates of 10 cross validation using spatially-blocked groups. Underlined values denote the statistically most accurate models per canopy parameter as determined by ANOVA at $\alpha = 0.05$ (Table 4.S1). Multiple underlines per row denote statistically equivalent top performance metrics. Mean and standard deviation of all field measurements given as reference for magnitude of RMSE. SVM = Support Vector Machine; RF = Random Forest.

Fuel parameter	Linear methods			SVM	RF	Mean (SD)
	Forward	Sequential	Backwards			
			R^2			
Biomass	0.62	0.59	0.56	0.69	0.75	
Mean height	0.72	0.71	0.64	0.71	0.73	
CBH	0.68	0.68	0.63	0.66	0.69	
CC	0.50	0.45	0.41	0.48	0.49	
CBD	0.49	0.48	0.36	0.41	0.50	
LAI	0.38	0.40	0.36	0.45	0.59	
			RMSE			
Biomass	12.36	13.00	13.41	11.17	9.28	18.79 (21.04) Mg
Mean height	5.04	5.07	1535.30	5.16	4.85	19.64 (10.22) m
CBH	3.03	2.99	3.27	2.92	2.57	7.69 (5.59) m
CC	12.11	12.91	14.80	11.14	11.17	75.43 (18.61) %
CBD	0.02	0.02	2.27	0.03	0.02	0.19 (0.04) kg m^{-3}
LAI	1.51	35.10	575.9	1.34	1.13	3.54 (1.76)

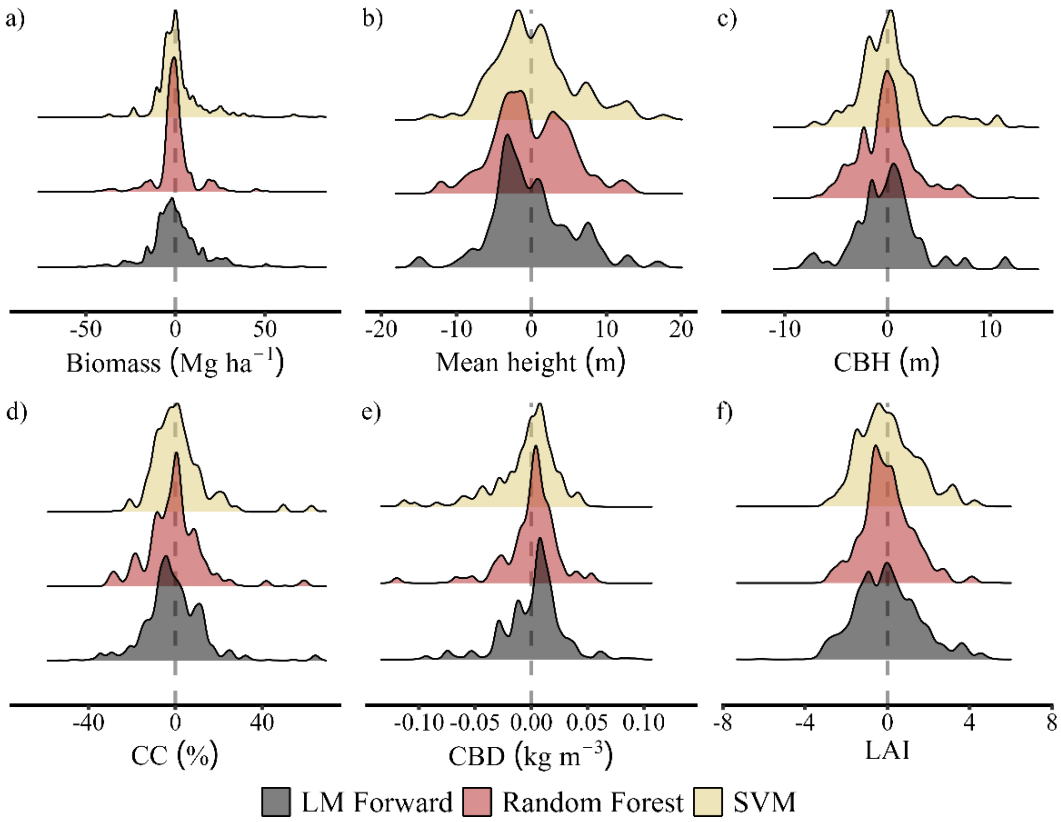


Fig. 4.5 Model cross validation error density. Individual error measurements taken from 9,600 estimates produced across 100 replicates of 10-fold cross validation using spatially-blocked groups.

While there were significant differences among observed model performances, in general, random forest, SVM, and forward linear regression models explained similar variance in the data for the majority of parameters (Tables 3 & S1). However, across all canopy fuel parameters, random forest did consistently outperform or match the accuracy, as given by R^2 and RMSE, of all other methods (Table 4.3, Fig. 4.5). Therefore, the remainder of the analysis in this paper will focus on random forest models. See supplement sections S1 and S2 for further analysis of model comparison and individual site model results.

3.3 Random forest model analysis

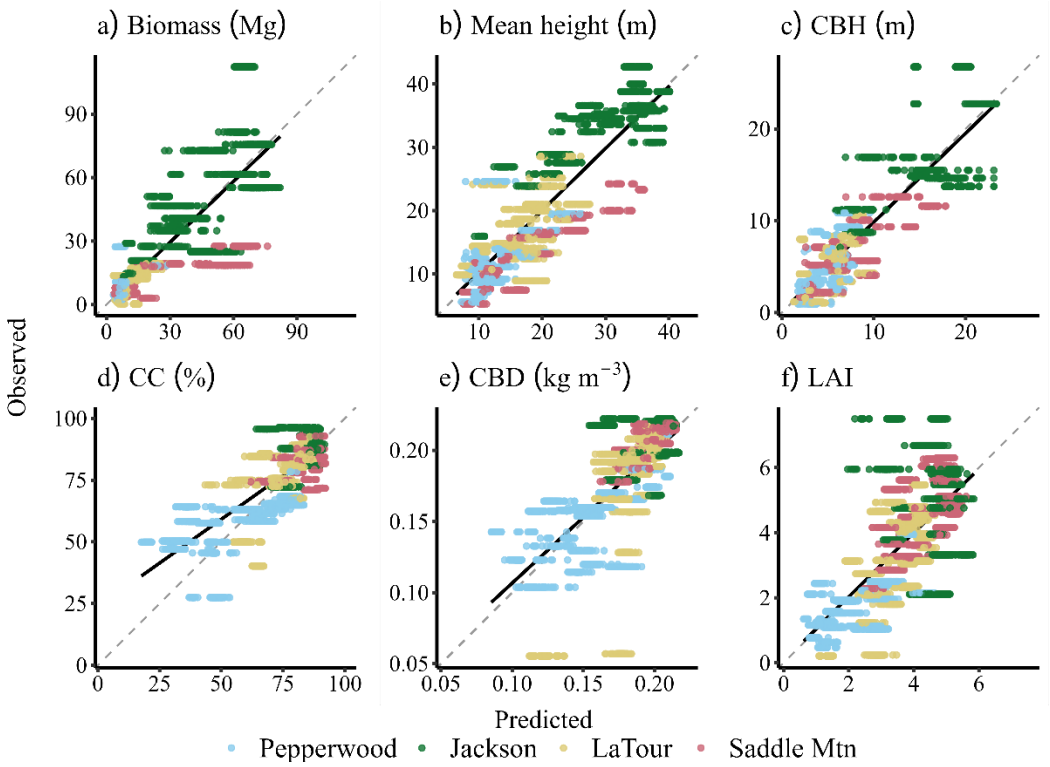


Fig. 4.6 Random Forest cross-validated predictions versus observed values for all-sites models (Table 4.3). Grey dashed reference line represents the one-to-one relationship between predicted and observed values. Black solid line denotes the regression best fit.

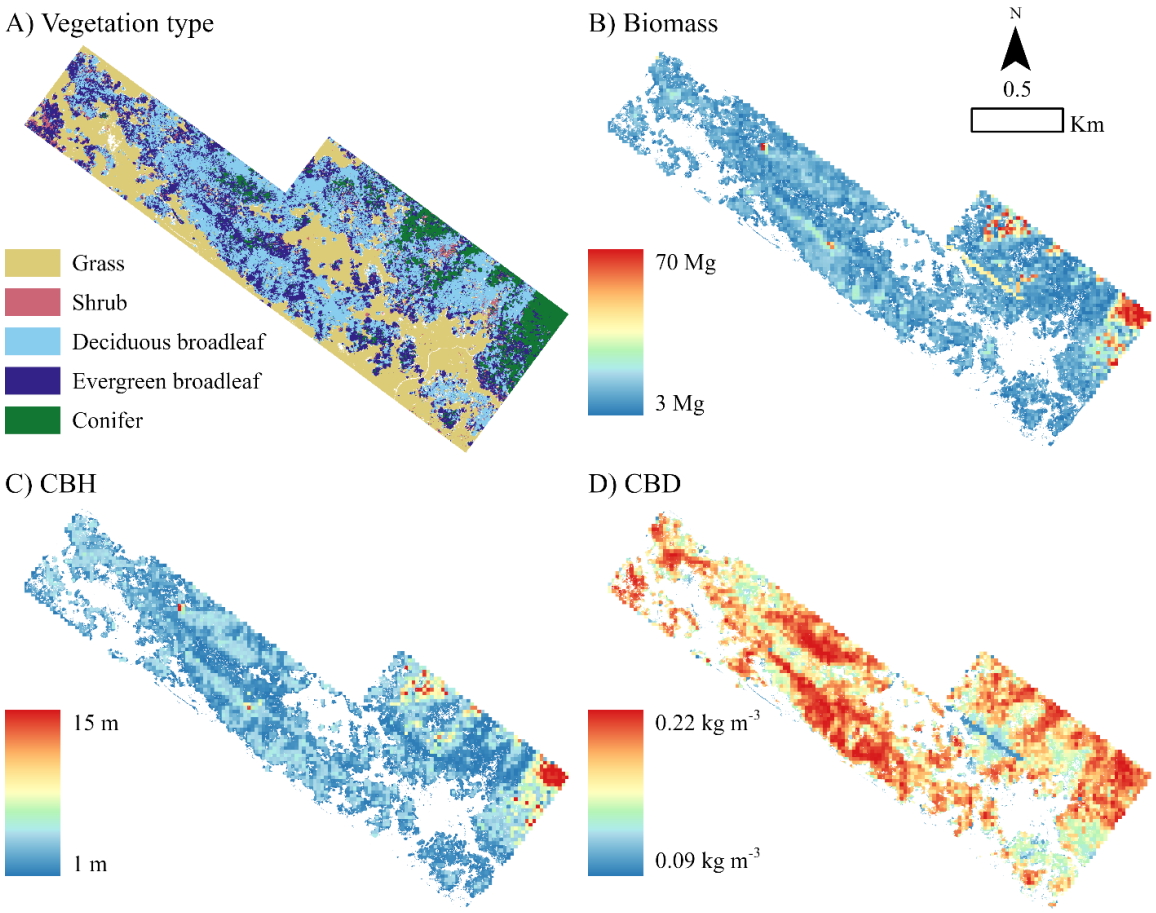


Fig. 4.7 Pepperwood random forest fuels prediction maps at 20 m resolution from the final all site model for each parameter. White areas are grasslands and shrublands, which were not analyzed.

Random forest all-sites model performance differed markedly between the vertical and horizontal groups of fuel parameters. The models for the vertical structure fuel parameters of biomass, mean height, and CBH returned R^2 values from 0.69 to 0.75 while the horizontal structure fuel parameters values ranged from 0.40 to 0.59 (Table 4.3). Apart from canopy cover, the average relationship between predicted versus observed values approximated a one-to-one relationship (Fig. 4.6). Random forest model error increased markedly for extreme values of each canopy fuel parameter (Fig. 4.6). We applied the all-sites random forest model to UAS-SfM spatial predictors at Pepperwood to produce estimated fuel loads (Fig. 4.7). These maps show strong relationships between vegetation classes and canopy fuel parameters (Fig. 4.7). As expected, coniferous regions demonstrate higher biomass and CBH as compared to broadleaf forest regions (Fig. 4.7b-c).

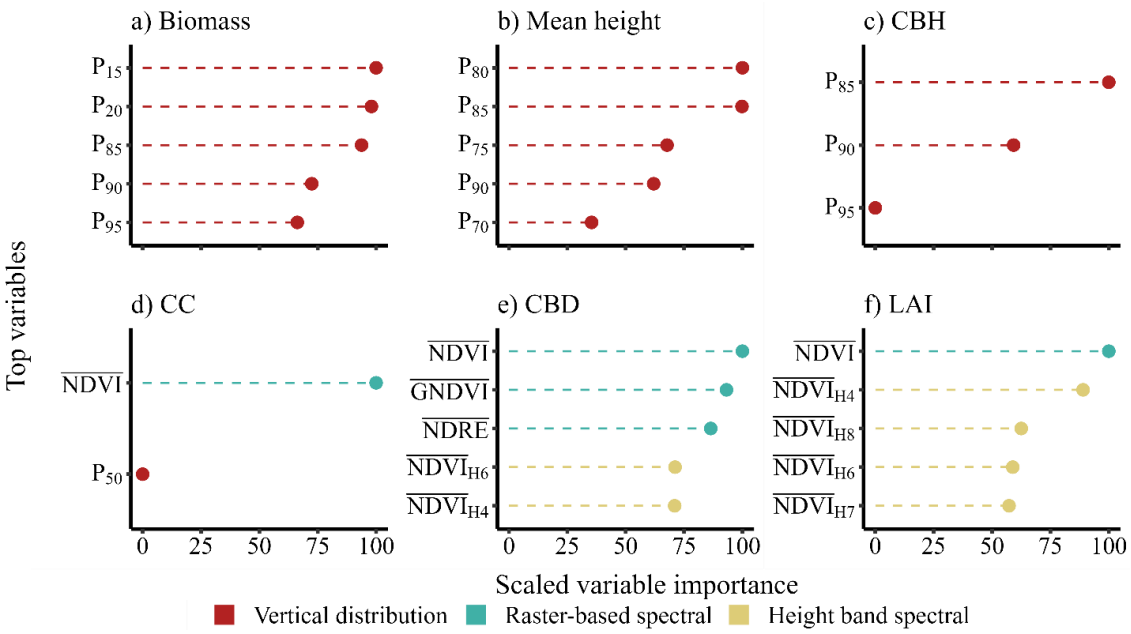


Fig. 4.8 Relative scaled importance of top five predictors for random forest models produced across all sites.

Height percentiles were consistently in the top five predictors for vertical structure fuel parameter models of biomass, mean height, and CBH (Fig. 4.8a-c). These predictors capture the vertical distribution of the forest canopy. The model for biomass relied upon a mixture of height percentiles from the lower and upper canopy while the models for both mean height and CBH exclusively utilized height percentiles from the upper canopy.

In contrast, the horizontal structure models of canopy cover, CBD, and LAI had top-five predictors based on spectral indices (Fig. 4.8d-f). The raster-based mean NDVI emerged as the top variable for all three fuel parameters. The model for canopy cover relied almost exclusively upon this index (Fig. 4.8d). The model for LAI also exclusively depended upon NDVI, augmenting the raster-based mean with a combination of NDVI height bands (Fig. 4.8f). The model for CBD supplemented NDVI with other spectral predictors (Fig. 4.8e). None of these models included individual spectral bands.

See supplement section S3 for SVM and LM variable selection. SVM variable selection closely matched that of random forest and exhibited the same separation between parameter groups. Linear models, in contrast, demonstrated less consistency in variable selection.

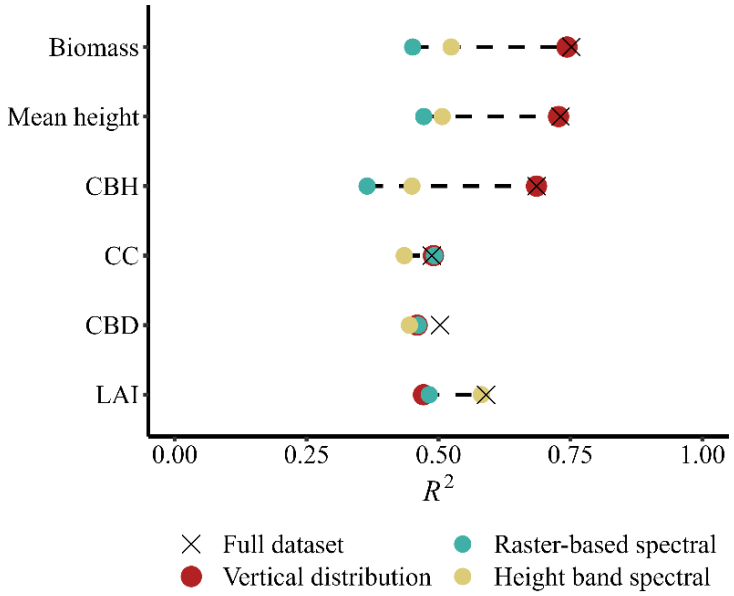


Fig. 4.9 Random forest all-sites model accuracy produced using different predictor variable subsets, including the full-predictor dataset. Performance results obtained from 100 replicates of 10-fold cross validation using spatially-blocked groups.

Testing the models by isolating predictor variables by data type resulted in distinct patterns between the vertical and horizontal fuel parameter groups (Fig. 4.9). Restricting the predictors to only the vertical distribution predictor subset resulted in models for the vertical fuel parameters biomass, mean height, and CBH with performance comparable to the model with all predictors, while performance for the spectral-based data subset models lagged significantly behind.

The horizontal parameter group demonstrated much lower variability among models produced with different predictor subsets (Fig. 4.9). The vertical distribution and raster-based spectral data subset models performed nearly identically for all three fuel parameters. Model performance for both predictor subsets matched that of the full-predictor model for canopy cover but lagged for CBD and LAI. For LAI, only the height band spectral subset model matched the full-predictor model performance, utilizing a set of mean NDVI height bands (Fig. 4.9, S6). This was the only canopy fuel parameter for which this data subset achieved the maximum accuracy. None of the variable subset models matched that of the CBD full-predictor model. While the performance loss was marginal, all other fuel parameters had at least one variable subset that returned comparable accuracy to the full-predictor model. See supplement section S4 for analysis of predictor subset model variable importance.

3.3 ALS comparison to UAS-SfM data

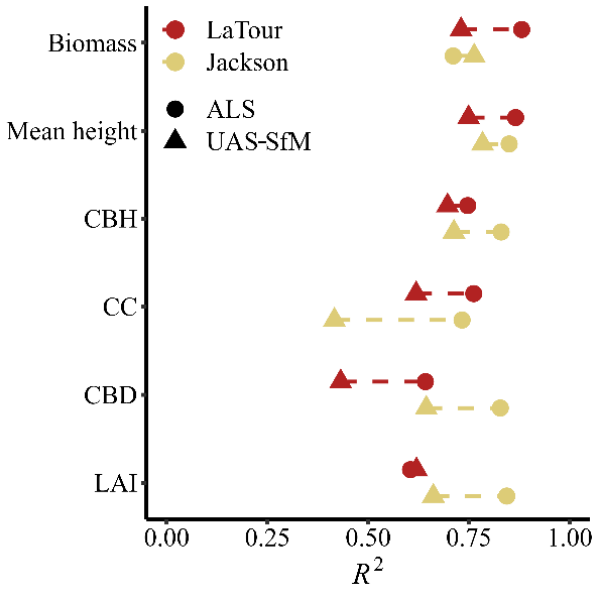


Fig. 4.10 UAS-SfM vs ALS model performance. Random forest individual site model results from 100 replicates of 5-fold cross validation without spatial blocking.

Apart from the models for biomass at Jackson and LAI at LaTour, ALS-based random forest models outperformed UAS-SfM models across sites and fuel parameters (Fig. 4.10). ALS performance displayed minimal variation among parameters. Consequently, the difference in accuracy between UAS and ALS was most pronounced for those horizontal structure fuels parameters, namely canopy cover and CBD, which had the largest decrease in UAS-SfM model performance relative to ALS, as compared to the vertical structure parameter group. These differences were particularly pronounced for Jackson, which had dense, closed-canopy coast redwood forests.

3.4 Model testing at novel site

Table 4.4 Model accuracy when applied to a novel site withheld from training. Model generated using 100 replicates of 10-fold cross validation using spatially-blocked groups from all sites except Saddle Mountain. Saddle Mountain accuracy metrics derived from the application of this model to the site without further training.

Canopy fuel parameter	R^2		RMSE	
	Model	Saddle Mtn	Model	Saddle Mtn
Biomass	0.82	0.74	8.89	14.71
Mean height	0.79	0.84	4.25	6.31
CBH	0.74	0.69	2.60	2.40
CC	0.65	0.05	11.01	8.20
CBD	0.55	0.20	0.020	0.010
LAI	0.60	0.31	1.18	1.15

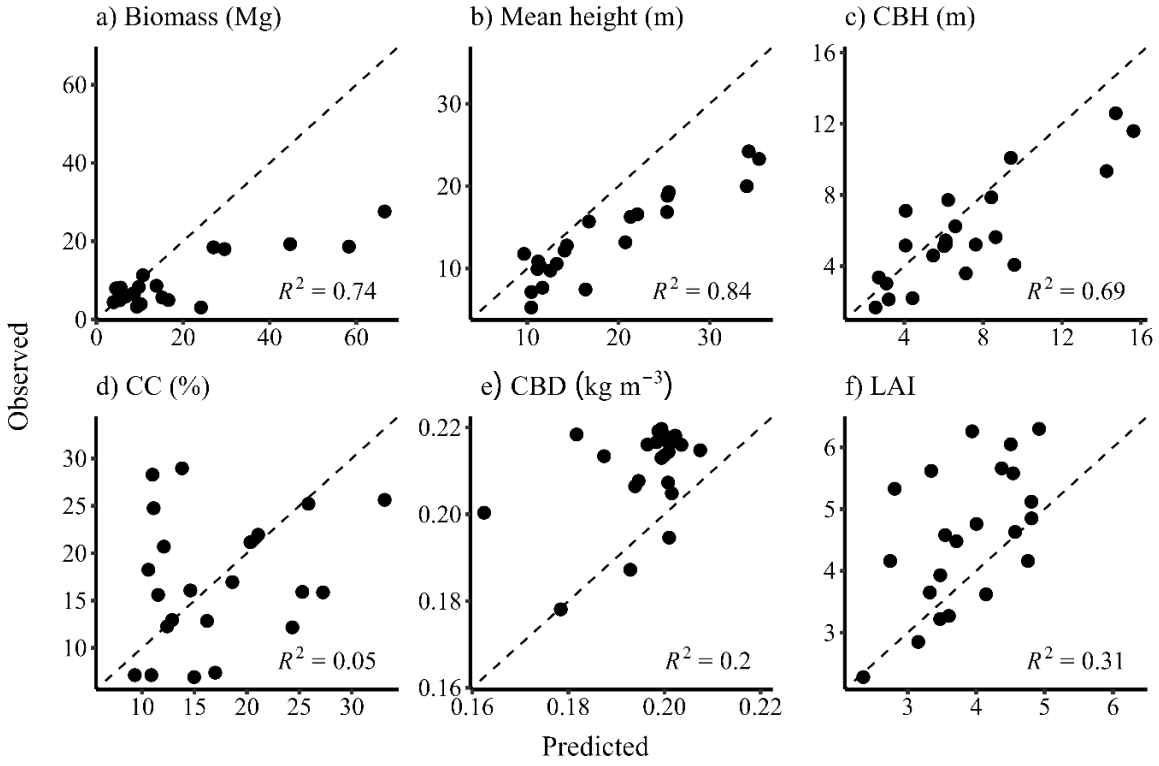


Fig. 4.11 Saddle Mountain random forest model transfer accuracy. Dotted reference line denotes idealized one-to-one relationship between measured and predicted values.

Model accuracy, when transferred to an independent site, differed by fuel parameter group (Table 4.4, Fig. 4.11). The vertical parameter group of biomass, mean height, and CBH retained adequate model accuracy at the independent site as compared to the original model cross-validation accuracy. In contrast,

the horizontal parameter group experienced significant drops in model performance, and none were well predicted.

4. Discussion

Reducing future forest fire hazard and restoring historical fire regimes relies upon the accessibility of accurate spatial information about aboveground biomass and fire fuel loads. Such data are difficult and time consuming to obtain using traditional field-based methods. Instead, the spatial complexity of these environmental attributes lends themselves well to remote sensing approaches. The use of UAS-SfM has the potential to provide a low-cost and flexible means of estimating fuels at stand scales. In a multisite analysis representing a broad range of forest types of California, this study found canopy fuel parameters segregate consistently into two distinct groups based on structural distribution. The first group is comprised of the vertical structure parameters biomass, mean height, and CBH. The second group contains the horizontal structure parameters canopy cover, CBD, and LAI. These groups emerged from strong correlations among field-based measurements across our study sites, and these patterns persisted in UAS-SFM based modelling performance and variable selection.

In models built using the combined data from all study sites, random forest consistently returned the highest overall accuracy, as defined by R^2 and RMSE, compared to SVM or linear regression methods. This is consistent with previous research identifying the performance of this method in similar applications (e.g., Almeida et al., 2019; Arellano-Pérez et al., 2018). Model accuracy differed between the vertical and horizontal groups, returning consistently higher performance for vertical fuel parameters. Since random forest is unable to extrapolate beyond the range of the data used to train the model, cross-validation error increased substantially for extreme parameter values. This limitation also restricted our novel site testing to the only site (Saddle Mountain) whose parameters fell within the range bounded by the other three sites. This challenge is not specific to random forest and highlights the importance of sampling breadth and distribution when targeting an area of interest or when applying a model to novel areas.

4.1 Vertical structure: Biomass, CBH, mean height

Our model for CBH exceeded previously published photogrammetric model accuracies by greater than 20% (Filippelli et al., 2019; Shin et al., 2018), and our models for biomass and mean canopy height fell within 2% of the highest previously published performance metrics for UAS-SfM or photogrammetry derived models from forest ecosystems around the world (Domingo et al., 2019; Filippelli et al., 2019; Ota et al., 2019; Shin et al., 2018), including previous work in California forests (Lamping et al., 2021).

The performance of the model for CBH demonstrates the powerful utility of combining machine learning with UAS-SfM to overcome SfM's inherent limited capacity to measure subcanopy forest structure (Forbes et al., 2022; Reilly et al., 2021) by exploiting inherent relationships in the canopy to model attributes that otherwise elude direct detection by photogrammetric methods (Filippelli et al., 2019). Shin et al. (2018) only achieved 33% accuracy in their attempt to model CBH using a single lower canopy height predictor derived from UAS-SfM data. In our study, however, the random forest model for CBH leveraged the observed relationship in the field data between CBH and mean height to achieve a high accuracy for a key canopy fuel parameter that it otherwise was unable to directly observe. Future research should investigate whether this indirect approach can detect the effects of targeted understory treatments, such as thinning or prescribed burns.

The UAS-SfM models for these three vertical fuel parameters demonstrated comparable accuracy to those using ALS predictors at the two sites included in this analysis. Our UAS-SfM models for CBH and mean height only marginally underperformed ALS models at the test sites of Jackson and LaTour, and fell within the range of globally reported ALS model accuracies for these parameters (Alonso-Rego et al., 2021; Andersen et al., 2005; Botequim et al., 2019; Bright et al., 2017; Chamberlain et al., 2021; Engelstad et al., 2019; Erdody and Moskal, 2010). Of note, the UAS-SfM model for biomass at Jackson outperformed its ALS counterpart and our full-predictor UAS-SfM biomass model outperformed previously published ALS-based models from California forest sites and from other Mediterranean-climate regions (Alonso-Rego et al., 2021; Lamping et al., 2021). This finding aligns with previous results demonstrating that UAS-SfM and photogrammetry based models of biomass match or outperform

ALS models in ponderosa pine forests in the western United States (Filippelli et al., 2019; Swayze et al., 2022). Since biomass is partially determined by canopy height, the higher point density of UAS-SfM (e.g., 320 points/m^2) at the top of canopy may render it particularly well suited for measuring total tree height, whereas lower ALS point density (e.g., 25 points/m^2) could result in missing maximum measurements of treetops. For this set of vertical canopy fuel parameters, these results suggest UAS-SfM area-based random forest models can provide comparable accuracy to ALS based methods and may outperform ALS under certain conditions.

Reflecting the vertical structural nature of these parameters, the top variables selected by the model for each parameter consisted solely of point cloud height percentiles and model performances were negligibly affected by the removal of spectral data in the predictor subset analysis. Other studies have reported similar structural variable selection for these parameters (e.g., Lamping et al., 2021; Swayze et al., 2022). Additionally, when applied to a novel site, these models retained a high level of performance. This suggests the vertical distribution predictor relationships identified by the random forest models persist across sites and among forest types. Consequently, these vertical structure canopy fuel parameters are well suited to 3D-based mapping approaches and the addition of spectral information does not significantly affect model accuracy. Future photogrammetric studies into this parameter set, therefore, should focus on sensors that prioritize image resolution and view angle (e.g., high-definition RGB cameras), rather than spectral resolution, to maximize canopy structure detection. Furthermore, this sensor selection could provide higher subcanopy structure detection, and therefore potentially greater model accuracy, through the collection of oblique imagery beyond the capabilities of the nadir restricted Micasense RedEdge-MX sensor employed in this study (Wallace et al., 2019).

4.2 Horizontal structure: LAI, CBD, canopy cover

The horizontal structure parameters of LAI, CBD, and canopy cover demonstrated consistently lower model accuracy than the vertical structure parameters, never exceeding R^2 of 0.60 for any of the random forest models. In contrast to the vertical parameters, the random forest models for these

horizontal parameters relied upon spectral attributes of the UAS-SfM data, with raster-based mean NDVI arising as the top contributor in all models. These horizontal parameters pertain directly to aspects of the forest canopy, namely its composition, spatial distribution, and density of live and dead leaves and branches. Consequently, it appears that these random forest models leveraged the relationships between spectral indices and live-canopy characteristics, such as concentration of photosynthetic activity, to model these plot-scale horizontal attributes.

Our canopy cover model accuracy falls below the lowest previously published UAS-SfM derived canopy cover models from forests around the globe (Belmonte et al., 2019; Shin et al., 2018; Wallace et al., 2019; Zahra et al., 2022). However, Belmonte et al. (2019) demonstrated a significant 30% decrease in model performance with increasing canopy cover in ponderosa pine forests, with accuracy dropping to match our results in their highest density stands. Considering that only the Pepperwood site contained a majority of plots below their high-density threshold, our results align with the Belmonte et al. finding that UAS-SfM struggles to model canopy cover under high-cover conditions. For this parameter, plot level mean NDVI appears to represent a proxy for percentage of live canopy in relation to ground and below-canopy senesced vegetation or exposed soil. This finding aligns with other studies that have identified NDVI as a highly accurate single predictor for canopy cover from UAS-SfM (Shin et al., 2018; Zahra et al., 2022). ALS, on the other hand, is particularly well suited for mapping canopy cover since it is able to actively detect subcanopy structure regardless of level of cover and, globally, has reported accuracies greater than 99% (Cai et al., 2021; Dai et al., 2022).

For CBD, our modelling approach utilizing spectral indices returned a significant improvement over previous literature. Few existing studies have modelled CBD using photogrammetric techniques and, to our knowledge, only Shin et al. (2018) utilized UAS-SfM for this purpose. Shin et al. (2018) only achieved an accuracy of <1% in ponderosa pine forest in their attempt to reconstruct CBD through allometric equations based on their UAS-SfM derived measurements of canopy height. Consequently, this study's demonstrated accuracy of 50% represents a significant improvement in performance over this previous UAS-SfM study and also exceeds the highest photogrammetric accuracy in the literature

(Filippelli et al., 2019). In accordance with our observed lower UAS-SfM performance compared to our ALS models of CBD, our UAS-SfM model accuracy is at the bottom end of published ALS CBD models from around the world (Alonso-Rego et al., 2021; Andersen et al., 2005; Bright et al., 2017; Chamberlain et al., 2021; Engelstad et al., 2019; García et al., 2017). We further note that CBD is difficult to measure in the field, and CBD model uncertainty is further increased by the weak relationship in the equations from Keane et al. (2005) used to estimate CBD from LAI-2000 gap fraction, and the model's focus on conifer forests.

While our model for LAI performed better than those of the other horizontal parameters, it underperformed compared to previously published photogrammetry models (Li et al., 2022; Liu and Wang, 2018; Stobbelaar et al., 2022; Zhang et al., 2019) and ALS models (e.g., Sumnall et al., 2021; Wang et al., 2023; Yin et al., 2022) from forests around the world. The previous photogrammetric studies were conducted within single forest types. Consequently, our lower performance may be due to the breadth of forest types represented in our multi-site analysis. Further, as with CBD, LAI was estimated based on an equation applied to LAI-2000 gap fraction measurements, and factors such as variable overhead sunlight conditions could add to model error. However, the saturation of spectral indices presents a much more likely mechanism for this decline in model accuracy. In models from forest sites around the globe, satellite-based NDVI has been demonstrated to possess the strongest relationship with LAI field measurements when LAI values are below two, and NDVI becomes asymptotically saturated when LAI rises further (Gao et al., 2023; Haboudane, 2004). Only Pepperwood had a majority of plots with LAI below this level. As a result, our model of LAI displayed a sharp prediction threshold as LAI increased above three, strongly suggesting the impact of this oversaturation effect influenced the performance of our models.

Models for all three canopy fuel parameters followed a similar trend in performance, exhibiting prediction clustering and loss of accuracy at the highest end of their respective ranges, suggesting this impact of oversaturation to be ubiquitous. In the novel site testing at Saddle Mountain, model performance declined considerably for all three parameters. The Saddle Mountain plots fall at the top end

of the observed range for this group. Since random forest cannot extrapolate, this error at the end of the range could be an artifact of insufficient training data at elevated fuel parameter levels such as high canopy cover. Additionally, since our novel site testing was limited to a single site, this decline in model performance could also be due to some undetected irregularity of the plots at Saddle Mountain. However, the most likely explanation for this failure is the aforementioned loss of information due to the oversaturation of spectral indices.

In the predictor subset analysis, both the spectral-based vertical distribution and raster-based models returned comparable accuracy to one another for all three horizontal fuel parameters. The raster-based model variable selection resembled the top variables from the full predictor models and, once again, all models identified mean NDVI as the key predictor. The model with vertical distribution predictors selected top variables relating to the point distribution within the middle third of the canopy, pointing to the relationship between the bulk distribution of the point cloud and these horizontal canopy fuel parameters. However, despite their performance in subset models, the combination of the spectral and vertical data in the full-predictor model did not significantly improve the accuracy beyond that of the subset models for canopy cover or CBD. LAI was the only fuel parameter for which the combined structural and spectral capacity of UAS-SfM appeared to significantly impact overall model performance. Based on these findings, future studies into horizontal canopy fuel parameters should prioritize the multispectral capabilities of UAS-SfM.

Since the models for CBD and canopy cover solely utilized mean raster-based spectral indices, modelling using satellite-based spectral data may be able to provide comparable accuracies to those observed in this study. The 0.04 ha scale of the ground validation plots underlying this study dictated the spatial resolution at which the UAS-SfM modelling could be performed. Consequently, despite its high-resolution, reducing the UAS-SfM data to a matching spatial resolution could have resulted in potentially significant loss of detail and accuracy, potentially exacerbating an already weak information signal due to the oversaturation of spectral indices. The 0.04 ha resolution at which these analyses were conducted is comparable to that provided by modern satellite multispectral sensors, such as Landsat 8-9 and Sentinel 2.

(e.g., Drusch et al., 2012). In post-fire mapping applications, Sentinel-2 derived NDVI has been demonstrated to correspond to coincidental measurements obtained from multispectral UAS-SfM (Pádua et al., 2020). Consequently, models built using these satellite-based spectral indices could match the performance accuracy to the methods employed in this study (Arellano-Pérez et al., 2018; Chuvieco et al., 2020; Gale et al., 2021), with the advantage of greater temporal frequency and spatial extent for lower monetary cost. For example, while they failed to model vertical canopy fuels, Pierce et al (2012) successfully modelled CBD and canopy cover at a site neighboring LaTour using Landsat derived indices. The additional spectral bands, and therefore potential indices, available via satellite sensors could assist in mitigating the oversaturation that may have hampered our models (Gao et al., 2023). Future studies should further investigate the capacity of these direct modelling approaches using satellite spectral indices for horizontal canopy fuels since the accessibility of these data would render them of high value to land managers, particularly in tracking change over larger areas or with greater frequency than is feasible with UAS-SfM. However, the decreased accuracy of our spectra-based models when applied to a novel site testing scenario suggests that the spatial and temporal consistency of these methods requires extensive validation prior to being employed for operational applications.

5. Conclusion

This study presents novel analysis of UAS-SfM structural and multispectral area-based machine learning models of biomass and canopy fuel parameters across a broad range of complex forest types characteristic of California and other Mediterranean regions. We found the following:

- Fuel parameters segregate into vertical (biomass, CBH, and mean height) and horizontal (LAI, CBD, canopy cover) groups based on correlations between field measurements and these relationships persist throughout model results.
- UAS-SfM random forest models are well suited for modelling the vertical structure canopy fuels parameters. These models retained high performance in comparison to ALS and when transferred to a novel site.

- Models for vertical fuel parameters rely exclusively upon UAS-SfM vertical structure predictors and exhibit no model improvement with the addition of spectral predictors. Future studies on this group, therefore, should focus on image resolution to improve structural information gathering, rather than spectral resolution.
- UAS-SfM random forest models provided less accurate estimates of the horizontal structure parameters. In addition, these models exhibited significant loss in accuracy in comparison to ALS and in the novel site transfer.
- Models for horizontal fuel parameters rely primarily upon raster-based spectral indices, primarily NDVI. Due to the similarity between the plot size in this study and satellite imagery resolution, future work should explore if models using satellite-based spectral data can provide comparable performance to the UAS-SfM spectral results presented here.

The mitigation of wildfire hazard and restoration of historical fire regimes in the forests of California, USA relies upon the accessibility of accurate data on the spatial distribution of fuel loads to inform management decision making. Canopy fuel parameters present a critical component of forest structure for these purposes since they moderate crown torching and sustained ignition, hallmarks of high severity fire events. Future work should expand on these results to ascertain better methods for performing widespread mapping coverage and developing models that are robust to transfer to novel sites. These two factors will significantly improve the operational use of these methods by land managers. In our case, our ability to generate widespread maps was limited to Pepperwood due to the landing requirements of the fixed-wing drone and the battery limitations of the quadcopter. However, future research using new UAS technology such as vertical takeoff and landing fixed-wing drones will be able to overcome these limitations and generate meaningfully large maps for ongoing management monitoring and decision making around fire hazard mitigation.

Authorship contribution statement

Conceptualization: S.R. and M.L.C.; Methodology: S.R., M.L.C., and I.O.; Investigation: S.R., M.L.C., L.L., P.K., M.K., and J.S.; Software: S.R. and M.L.C.; Formal analysis: S.R. and M.L.C.; Resources: M.L.C., D.A., and L.P.B.; Writing—original draft preparation: S.R.; Writing—review and editing: I.O., M.L.C., L.P.B., M.K., L.L., J.S., P.K., and D.A.; Visualization: S.R.; Supervision: I.O. and M.L.C.; Funding acquisition: L.P.B. and M.L.C. All authors have read and agreed to the published version of the manuscript.

Acknowledgements

Funding for this research was supported by CAL FIRE Forest Health and Forest Legacy (8GG18806) and California State University, Agricultural Research Institute (20-01-106) awards to L.P.B and M.L.C. S.R. was funded by the Rhodes Trust and through the University of Oxford Environmental Change Institute Small Grant Scheme. Pepperwood ground data collection was supported by funding from the Gordon and Betty Moore Foundation and National Science Foundation grants 1754475 and 1835086. We thank Lisa Micheli (Pepperwood Preserve), Monica Delmartini (Saddle Mountain), Jason Poburko (LaTour), and Lynn Webb (Jackson) for granting us use of their sites and facilitating access to their datasets. We thank Ryan Ferrell, Michael O'Neil, Allison Kelly, Brieanne Forbes, Catherine Seel, Corbin Matley in collecting field data and Corbin Matley, Michelle Villasenor, and Natalie Hoover for their assistance in collecting UAS data. We also thank Andrew Peters for his work on the study site map.

References

Aasen, H., Honkavaara, E., Lucieer, A., Zarco-Tejada, P.J., 2018. Quantitative remote sensing at ultra-high resolution with UAV spectroscopy: A review of sensor technology, measurement procedures, and data correction workflows. Remote Sensing 10, 1091. https://doi.org/10.3390/rs10071091

Abdollahnejad, A., Panagiotidis, D., 2020. Tree species classification and health status assessment for a mixed broadleaf-conifer forest with UAS multispectral imaging. Remote Sensing 12, 3722. https://doi.org/10.3390/rs12223722

Ackerly, D., Oldfather, M., Halbur, M., Micheli, L., 2013. Establishment of woodland vegetation research plots at Pepperwood Preserve (Technical report for the Gordon and Betty Moore Foundation). Dwight Center for Conservation Science, Pepperwood, Santa Rosa, CA.

Ackerly, D.D., Kling, M.M., Clark, M.L., Papper, P., Oldfather, M.F., Flint, A.L., Flint, L.E., 2020. Topoclimates, refugia, and biotic responses to climate change. Front Ecol Environ 18, 288–297. https://doi.org/10.1002/fee.2204

Adjidjonu, D., Burgett, J., 2021. Assessing the accuracy of unmanned aerial vehicles photogrammetric survey. International Journal of Construction Education and Research 17, 85–96. https://doi.org/10.1080/15578771.2020.1717683

Agee, J.K., Skinner, C.N., 2005. Basic principles of forest fuel reduction treatments. Forest Ecology and Management 211, 83–96. https://doi.org/10.1016/j.foreco.2005.01.034

Agüera-Vega, F., Carvajal-Ramírez, F., Martínez-Carricondo, P., 2017. Accuracy of digital surface models and orthophotos derived from unmanned aerial vehicle photogrammetry. J. Surv. Eng. 143, 04016025. https://doi.org/10.1061/(ASCE)SU.1943-5428.0000206

Almeida, C.T.D., Galvão, L.S., Aragão, L.E.D.O.C.E., Ometto, J.P.H.B., Jacon, A.D., Pereira, F.R.D.S., Sato, L.Y., Lopes, A.P., Graça, P.M.L.D.A., Silva, C.V.D.J., Ferreira-Ferreira, J., Longo, M., 2019. Combining LiDAR and hyperspectral data for aboveground biomass modeling in the Brazilian Amazon using different regression algorithms. Remote Sensing of Environment 232, 111323. https://doi.org/10.1016/j.rse.2019.111323

Alonso-Rego, C., Arellano-Pérez, S., Guerra-Hernández, J., Molina-Valero, J.A., Martínez-Calvo, A., Pérez-Cruzado, C., Castedo-Dorado, F., González-Ferreiro, E., Álvarez-González, J.G., Ruiz-González, A.D., 2021. Estimating stand and fire-related surface and canopy fuel variables in pine

stands using low-density airborne and single-scan terrestrial laser scanning data. Remote Sensing 13, 5170. https://doi.org/10.3390/rs13245170

Alonzo, M., Andersen, H.-E., Morton, D., Cook, B., 2018. Quantifying boreal forest structure and composition using UAV Structure-from-Motion. Forests 9, 119. https://doi.org/10.3390/f9030119

Andersen, H.-E., McGaughey, R.J., Reutebuch, S.E., 2005. Estimating forest canopy fuel parameters using LIDAR data. Remote Sensing of Environment 94, 441–449. https://doi.org/10.1016/j.rse.2004.10.013

Aragoneses, E., Chuvieco, E., 2021. Generation and mapping of fuel types for fire risk assessment. Fire 4, 59. https://doi.org/10.3390/fire4030059

Arellano-Pérez, S., Castedo-Dorado, F., López-Sánchez, C., González-Ferreiro, E., Yang, Z., Díaz-Varela, R., Álvarez-González, J., Vega, J., Ruiz-González, A., 2018. Potential of Sentinel-2A data to model surface and canopy fuel characteristics in relation to crown fire hazard. Remote Sensing 10, 1645. https://doi.org/10.3390/rs10101645

Arroyo, L.A., Pascual, C., Manzanera, J.A., 2008. Fire models and methods to map fuel types: The role of remote sensing. Forest Ecology and Management 256, 1239–1252. https://doi.org/10.1016/j.foreco.2008.06.048

Beaty, R.M., Taylor, A.H., 2008. Fire history and the structure and dynamics of a mixed conifer forest landscape in the northern Sierra Nevada, Lake Tahoe Basin, California, USA. Forest Ecology and Management 255, 707–719. https://doi.org/10.1016/j.foreco.2007.09.044

Belmonte, A., Sankey, T., Biederman, J.A., Bradford, J., Goetz, S.J., Kolb, T., Woolley, T., 2019. UAV-derived estimates of forest structure to inform ponderosa pine forest restoration. Remote Sensing in Ecology and Conservation n/a. https://doi.org/10.1002/rse2.137

Berbach, M., Cafferata, P., Schlosser, J., Eng, H., Robards, T., McDonald, S., Walters, D., Dreesmann, K., 1995. Latour Demonstration State Forest sustained yield plan. California Department of Forestry and Fire Protection.

Botequim, B., Fernandes, P.M., Borges, J.G., González-Ferreiro, E., Guerra-Hernández, J., 2019. Improving silvicultural practices for Mediterranean forests through fire behaviour modelling using LiDAR-derived canopy fuel characteristics. Int. J. Wildland Fire 28, 823. https://doi.org/10.1071/WF19001

Breiman, L., 2001. Random forests. Machine Learning 45, 5–32. https://doi.org/10.1023/A:1010933404324

Bright, B., Hudak, A., Meddens, A., Hawbaker, T., Briggs, J., Kennedy, R., 2017. Prediction of forest canopy and surface fuels from lidar and satellite time series data in a bark beetle-affected forest. Forests 8, 322. https://doi.org/10.3390/f8090322

Cai, S., Zhang, W., Jin, S., Shao, J., Li, L., Yu, S., Yan, G., 2021. Improving the estimation of canopy cover from UAV-LiDAR data using a pit-free CHM-based method. International Journal of Digital Earth 14, 1477–1492. https://doi.org/10.1080/17538947.2021.1921862

Chamberlain, C.P., Sánchez Meador, A.J., Thode, A.E., 2021. Airborne lidar provides reliable estimates of canopy base height and canopy bulk density in southwestern ponderosa pine forests. Forest Ecology and Management 481, 118695. https://doi.org/10.1016/j.foreco.2020.118695

Chandrasekaran, A., Shao, G., Fei, S., Miller, Z., Hupy, J., 2022. Automated inventory of broadleaf tree plantations with UAS imagery. Remote Sensing 14, 1931. https://doi.org/10.3390/rs14081931

Chávez-Durán, Á.A., García, M., Olvera-Vargas, M., Aguado, I., Figueroa-Rangel, B.L., Trucíos-Caciano, R., Rubio-Camacho, E.A., 2024. Forest canopy fuel loads mapping using unmanned aerial vehicle high-resolution red, green, blue and multispectral imagery. Forests 15, 225. https://doi.org/10.3390/f15020225

Chuvieco, E., Aguado, I., Salas, J., García, M., Yebra, M., Oliva, P., 2020. Satellite remote sensing contributions to wildland fire science and management. Curr Forestry Rep 6, 81–96. https://doi.org/10.1007/s40725-020-00116-5

Collins, B.M., Miller, J.D., Thode, A.E., Kelly, M., van Wagtendonk, J.W., Stephens, S.L., 2009. Interactions among wildland fires in a long-established Sierra Nevada Natural Fire Area. Ecosystems 12, 114–128. https://doi.org/10.1007/s10021-008-9211-7

Collins, B.M., Stephens, S.L., Moghaddas, J.J., Battles, J., 2010. Challenges and approaches in planning fuel treatments across fire-excluded forested landscapes. Journal of Forestry.

Cressie, N., 1988. Spatial prediction and ordinary kriging. Mathematical Geology 20.

Cutler, F. original by L.B. and A., Wiener, R. port by A.L. and M., 2022. randomForest: Breiman and Cutler's Random Forests for Classification and Regression.

Dai, W., Guan, Q., Cai, S., Liu, R., Chen, R., Liu, Q., Chen, C., Dong, Z., 2022. A comparison of the performances of unmanned-aerial-vehicle (UAV) and terrestrial laser scanning for forest plot canopy cover estimation in Pinus massoniana forests. Remote Sensing 14, 1188. https://doi.org/10.3390/rs14051188

Dash, J.P., Pearse, G.D., Watt, M.S., 2018. UAV multispectral imagery can complement satellite data for monitoring forest health. Remote Sensing 10, 1216. https://doi.org/10.3390/rs10081216

Dennison, P.E., Brewer, S.C., Arnold, J.D., Moritz, M.A., 2014. Large wildfire trends in the western United States, 1984-2011. Geophys. Res. Lett. 41, 2928–2933. https://doi.org/10.1002/2014GL059576

Dewberry, 2018. California FEMA F9 lidar report (No. G17PD00044).

Domingo, Ørka, Næsset, Kachamba, Gobakken, 2019. Effects of UAV image resolution, camera type, and image overlap on accuracy of biomass predictions in a tropical woodland. Remote Sensing 11, 948. https://doi.org/10.3390/rs11080948

Drusch, M., Del Bello, U., Carlier, S., Colin, O., Fernandez, V., Gascon, F., Hoersch, B., Isola, C., Laberinti, P., Martimort, P., Meygret, A., Spoto, F., Sy, O., Marchese, F., Bargellini, P., 2012. Sentinel-2: ESA's optical high-resolution mission for GMES operational services. Remote Sensing of Environment 120, 25–36. https://doi.org/10.1016/j.rse.2011.11.026

Duff, T., Keane, R., Penman, T., Tolhurst, K., 2017. Revisiting wildland fire fuel quantification methods: The challenge of understanding a dynamic, biotic entity. Forests 8, 351. https://doi.org/10.3390/f8090351

Eng, H., 2015. Jackson Demonstration State Forest, California, United States of America, in: Forest Plans of North America. Elsevier, pp. 177–187. https://doi.org/10.1016/B978-0-12-799936-4.00021-7

Engelstad, P.S., Falkowski, M., Wolter, P., Poznanovic, A., Johnson, P., 2019. Estimating canopy fuel attributes from low-density LiDAR. Fire 2, 38. https://doi.org/10.3390/fire2030038

Erdody, T.L., Moskal, L.M., 2010. Fusion of LiDAR and imagery for estimating forest canopy fuels. Remote Sensing of Environment 114, 725–737. https://doi.org/10.1016/j.rse.2009.11.002

Evett, R.R., Dawson, A., Bartolome, J.W., 2013. Estimating vegetation reference conditions by combining historical source analysis and soil phytolith analysis at Pepperwood Preserve, Northern California Coast Ranges, U.S.A: Estimating vegetation reference conditions. Restor Ecol 21, 464–473. https://doi.org/10.1111/j.1526-100X.2012.00912.x

FIA, 2014. Regional biomass equations used by FIA to estimate bole, bark, and branches. U.S. Department of Agriculture Forest Service, Pacific Northwest Research Station.

Filippelli, S.K., Lefsky, M.A., Rocca, M.E., 2019. Comparison and integration of lidar and photogrammetric point clouds for mapping pre-fire forest structure. Remote Sensing of Environment 224, 154–166. https://doi.org/10.1016/j.rse.2019.01.029

Forbes, B., Reilly, S., Clark, M., Ferrell, R., Kelly, A., Krause, P., Matley, C., O'Neil, M., Villasenor, M., Disney, M., Wilkes, P., Bentley, L.P., 2022. Comparing remote sensing and field-based approaches to estimate ladder fuels and predict wildfire burn severity. Front. For. Glob. Change 5, 818713. https://doi.org/10.3389/ffgc.2022.818713

Foster, D.E., Battles, J.J., Collins, B.M., York, R.A., Stephens, S.L., 2020. Potential wildfire and carbon stability in frequent-fire forests in the Sierra Nevada: trade-offs from a long-term study. Ecosphere 11. https://doi.org/10.1002/ecs2.3198

Fraser, B.T., Congalton, R.G., 2018. Issues in unmanned aerial systems (UAS) data collection of complex forest environments. Remote Sensing 10, 908. https://doi.org/10.3390/rs10060908

Fu, X., Zhang, Z., Cao, L., Coops, N.C., Goodbody, T.R.H., Liu, H., Shen, X., Wu, X., 2021. Assessment of approaches for monitoring forest structure dynamics using bi-temporal digital aerial photogrammetry point clouds. Remote Sensing of Environment 255, 112300. https://doi.org/10.1016/j.rse.2021.112300

Gale, M.G., Cary, G.J., Van Dijk, A.I.J.M., Yebra, M., 2021. Forest fire fuel through the lens of remote sensing: Review of approaches, challenges and future directions in the remote sensing of biotic determinants of fire behaviour. Remote Sensing of Environment 255, 112282. https://doi.org/10.1016/j.rse.2020.112282

Gao, Si, Zhong, R., Yan, K., Ma, X., Chen, X., Pu, J., Gao, Sicong, Qi, J., Yin, G., Myneni, R.B., 2023. Evaluating the saturation effect of vegetation indices in forests using 3D radiative transfer simulations and satellite observations. Remote Sensing of Environment 295, 113665. https://doi.org/10.1016/j.rse.2023.113665

García, M., Saatchi, S., Casas, A., Koltunov, A., Ustin, S., Ramirez, C., Balzter, H., 2017. Extrapolating forest canopy fuel properties in the California Rim Fire by combining airborne lidar and Landsat OLI data. Remote Sensing 9, 394. https://doi.org/10.3390/rs9040394

García-Cimarras, A., Manzanera, J.A., Valbuena, R., 2021. Analysis of Mediterranean vegetation fuel type changes using multitemporal LiDAR. Forests 12, 335. https://doi.org/10.3390/f12030335

Griffith, G.E., Omernik, J.M., Smith, D.W., Cook, T.D., Tallyn, E., Moseley, K., Johnson, C.B., 2016. Ecoregions of California (Report No. 2016–1021), Open-File Report. Reston, VA. https://doi.org/10.3133/ofr20161021

Haboudane, D., 2004. Hyperspectral vegetation indices and novel algorithms for predicting green LAI of crop canopies: Modeling and validation in the context of precision agriculture. Remote Sensing of Environment 90, 337–352. https://doi.org/10.1016/j.rse.2003.12.013

Hessburg, P.F., Churchill, D.J., Larson, A.J., Haugo, R.D., Miller, C., Spies, T.A., North, M.P., Povak, N.A., Belote, R.T., Singleton, P.H., Gaines, W.L., Keane, R.E., Aplet, G.H., Stephens, S.L., Morgan, P., Bisson, P.A., Rieman, B.E., Salter, R.B., Reeves, G.H., 2015. Restoring fire-prone Inland Pacific landscapes: seven core principles. Landscape Ecol 30, 1805–1835. https://doi.org/10.1007/s10980-015-0218-0

Hillman, S., Wallace, L., Lucieer, A., Reinke, K., Turner, D., Jones, S., 2021a. A comparison of terrestrial and UAS sensors for measuring fuel hazard in a dry sclerophyll forest. International Journal of Applied Earth Observation and Geoinformation 95, 102261. https://doi.org/10.1016/j.jag.2020.102261

Hillman, S., Wallace, L., Reinke, K., Jones, S., 2021b. A comparison between TLS and UAS LiDAR to represent eucalypt crown fuel characteristics. ISPRS Journal of Photogrammetry and Remote Sensing 181, 295–307. https://doi.org/10.1016/j.isprsjprs.2021.09.008

Hunter, M.E., Robles, M.D., 2020. Tamm review: The effects of prescribed fire on wildfire regimes and impacts: A framework for comparison. Forest Ecology and Management 475, 118435. https://doi.org/10.1016/j.foreco.2020.118435

Husari, S., Nichols, H.T., Sugihara, N.G., Stephens, S.L., 2006. Fire and fuel management, in: Sugihara, N. (Ed.), Fire in California's Ecosystems. University of California Press, pp. 444–465. https://doi.org/10.1525/california/9780520246058.003.0019

Karatzoglou, A., Smola, A., Hornik, K., Australia (NICTA), N.I., Maniscalco, M.A., Teo, C.H., 2023. kernlab: Kernel-Based Machine Learning Lab.

Keane, R.E., Reinhardt, E.D., Scott, J., Gray, K., Reardon, J., 2005. Estimating forest canopy bulk density using six indirect methods. Can. J. For. Res. 35, 724–739. https://doi.org/10.1139/x04-213

Keeley, J.E., Fotheringham, C.J., Morais, M., 1999. Reexamining fire suppression impacts on brushland fire regimes. Science 284, 1829–1832. https://doi.org/10.1126/science.284.5421.1829

Kramer, H., Collins, B., Kelly, M., Stephens, S., 2014. Quantifying ladder fuels: a new approach using LiDAR. Forests 5, 1432–1453. https://doi.org/10.3390/f5061432

Kuhn, M., Wing, J., Weston, S., Williams, A., Keefer, C., Engelhardt, A., Cooper, T., Mayer, Z., Kenkel, B., R Core Team, Benesty, M., Lescarbeau, R., Ziem, A., Scrucca, L., Tang, Y., Candan, C., Hunt, T., 2023. caret: Classification and Regression Training.

Lamping, J.E., Zald, H.S.J., Madurapperuma, B.D., Graham, J., 2021. Comparison of low-cost commercial unpiloted digital aerial photogrammetry to airborne laser scanning across multiple forest types in California, USA. Remote Sensing 13, 4292. https://doi.org/10.3390/rs13214292

Li, C., Zheng, Y., Zhang, X., Wu, F., Li, L., Jiang, J., 2022. Comparison of canopy cover and leaf area index estimation from airborne lidar and digital aerial photogrammetry in tropical forests. Applied Sciences 12, 9882. https://doi.org/10.3390/app12199882

Liu, X., Wang, L., 2018. Feasibility of using consumer-grade unmanned aerial vehicles to estimate leaf area index in Mangrove forest. Remote Sensing Letters 9, 1040–1049. https://doi.org/10.1080/2150704X.2018.1504339

Lowe, D.G., 2004. Distinctive image features from scale-invariant keypoints. International Journal of Computer Vision 60, 91–110. https://doi.org/10.1023/B:VISI.0000029664.99615.94

Marino, E., Montes, F., Tomé, J.L., Navarro, J.A., Hernando, C., 2018. Vertical forest structure analysis for wildfire prevention: Comparing airborne laser scanning data and stereoscopic hemispherical images. International Journal of Applied Earth Observation and Geoinformation 73, 438–449. https://doi.org/10.1016/j.jag.2018.07.015

Miller, J.D., Safford, H.D., Crimmins, M., Thode, A.E., 2009. Quantitative evidence for increasing forest fire severity in the Sierra Nevada and Southern Cascade Mountains, California and Nevada, USA. Ecosystems 12, 16–32. https://doi.org/10.1007/s10021-008-9201-9

Miller, J.D., Skinner, C.N., Safford, H.D., Knapp, E.E., Ramirez, C.M., 2012. Trends and causes of severity, size, and number of fires in northwestern California, USA. Ecological Applications 22, 184–203. https://doi.org/10.1890/10-2108.1

Miller, T.L. based on F. code by A., 2020. leaps: Regression Subset Selection.

Minnich, R.A., 1983. Fire mosaics in southern California and northern Baja California. Science 219, 1287–1294. https://doi.org/10.1126/science.219.4590.1287

Moghaddas, J.J., Roller, G.B., Long, J.W., Saah, D.S., Moritz, M.A., Stark, D.T., Schmidt, D., Buchholz, T., Freed, T.J., Alvey, E.C., Gunn, J.S., 2018. Fuel treatment for forest resilience and climate mitigations: A critical review for coniferous forests of the Sierra Nevada, Southern Cascade, Coast, Klamath, and Transverse Ranges (No. CCCA4- CNRA-2018– 017). California Natural Resources Agency.

Mountrakis, G., Im, J., Ogole, C., 2011. Support vector machines in remote sensing: A review. ISPRS Journal of Photogrammetry and Remote Sensing 66, 247–259. https://doi.org/10.1016/j.isprsjprs.2010.11.001

Navarro, A., Young, M., Allan, B., Carnell, P., Macreadie, P., Ierodiaconou, D., 2020. The application of Unmanned Aerial Vehicles (UAVs) to estimate above-ground biomass of mangrove ecosystems. Remote Sensing of Environment 242, 111747. https://doi.org/10.1016/j.rse.2020.111747

Oldfather, M.F., Britton, M.N., Papper, P.D., Koontz, M.J., Halbur, M.M., Dodge, C., Flint, A.L., Flint, L.E., Ackerly, D.D., 2016. Effects of topoclimatic complexity on the composition of woody plant communities. AoB PLANTS 8, plw049. https://doi.org/10.1093/aobpla/plw049

Ota, T., Ahmed, O.S., Minn, S.T., Khai, T.C., Mizoue, N., Yoshida, S., 2019. Estimating selective logging impacts on aboveground biomass in tropical forests using digital aerial photography obtained before and after a logging event from an unmanned aerial vehicle. Forest Ecology and Management 433, 162–169. https://doi.org/10.1016/j.foreco.2018.10.058

Pádua, L., Guimarães, N., Adão, T., Sousa, A., Peres, E., Sousa, J.J., 2020. Effectiveness of Sentinel-2 in multi-temporal post-fire monitoring when compared with UAV imagery. IJGI 9, 225. https://doi.org/10.3390/ijgi9040225

Park, I.W., Mann, M.L., Flint, L.E., Flint, A.L., Moritz, M., 2021. Relationships of climate, human activity, and fire history to spatiotemporal variation in annual fire probability across California. PLoS ONE 16, e0254723. https://doi.org/10.1371/journal.pone.0254723

Parks, S.A., Holsinger, L.M., Miller, C., Nelson, C.R., 2015. Wildland fire as a self-regulating mechanism: The role of previous burns and weather in limiting fire progression. Ecological Applications 25, 1478–1492. https://doi.org/10.1890/14-1430.1

Parks, S.A., Holsinger, L.M., Panunto, M.H., Jolly, W.M., Dobrowski, S.Z., Dillon, G.K., 2018. High-severity fire: Evaluating its key drivers and mapping its probability across western US forests. Environ. Res. Lett. 13, 044037. https://doi.org/10.1088/1748-9326/aab791

Pierce, A.D., Farris, C.A., Taylor, A.H., 2012. Use of random forests for modeling and mapping forest canopy fuels for fire behavior analysis in Lassen Volcanic National Park, California, USA. Forest Ecology and Management 279, 77–89. https://doi.org/10.1016/j.foreco.2012.05.010

Ploton, P., Mortier, F., Réjou-Méchain, M., Barbier, N., Picard, N., Rossi, V., Dormann, C., Cornu, G., Viennois, G., Bayol, N., Lyapustin, A., Gourlet-Fleury, S., Pélissier, R., 2020. Spatial validation reveals poor predictive performance of large-scale ecological mapping models. Nat Commun 11, 4540. https://doi.org/10.1038/s41467-020-18321-y

Pohjankukka, J., Pahikkala, T., Nevalainen, P., Heikkonen, J., 2017. Estimating the prediction performance of spatial models via spatial k-fold cross validation. International Journal of Geographical Information Science 31, 2001–2019. https://doi.org/10.1080/13658816.2017.1346255

Prichard, S.J., Hessburg, P.F., Hagmann, R.K., Povak, N.A., Dobrowski, S.Z., Hurteau, M.D., Kane, V.R., Keane, R.E., Kobziar, L.N., Kolden, C.A., North, M., Parks, S.A., Safford, H.D., Stevens, J.T., Yocom, L.L., Churchill, D.J., Gray, R.W., Huffman, D.W., Lake, F.K., Khatri-Chhetri, P., 2021. Adapting western North American forests to climate change and wildfires: 10 common questions. Ecological Applications 31. https://doi.org/10.1002/eap.2433

Quantum Spatial, 2020. Carr Hirz Delta fires 2019 lidar processing report.

R Core Team, 2023. R: A language and environment for statistical computing.

Reilly, S., Clark, M.L., Bentley, L.P., Matley, C., Piazza, E., Oliveras Menor, I., 2021. The potential of multispectral imagery and 3D point clouds from unoccupied aerial systems (UAS) for monitoring

forest structure and the impacts of wildfire in Mediterranean-climate forests. Remote Sensing 13, 3810. https://doi.org/10.3390/rs13193810

Rocha, K.D., Silva, C.A., Cosenza, D.N., Mohan, M., Klauberg, C., Schlickmann, M.B., Xia, J., Leite, R.V., Almeida, D.R.A. de, Atkins, J.W., Cardil, A., Rowell, E., Parsons, R., Sánchez-López, N., Prichard, S.J., Hudak, A.T., 2023. Crown-Level Structure and Fuel Load Characterization from Airborne and Terrestrial Laser Scanning in a Longleaf Pine (Pinus palustris Mill.) Forest Ecosystem. Remote Sensing 15, 1002. https://doi.org/10.3390/rs15041002

Roussel, J.-R., Auty, D., De Boissieu, F., Sánchez Meador, A., Jean-François, B., Demetrios, G., Steinmeier, L., Adaszewski, S., 2023. lidR: Airborne LiDAR Data Manipulation and Visualization for Forestry Applications.

Shaik, R.U., Laneve, G., Fusilli, L., 2022. An automatic procedure for forest fire fuel mapping using hyperspectral (PRISMA) imagery: A semi-supervised classification approach. Remote Sensing 14, 1264. https://doi.org/10.3390/rs14051264

Shin, P., Sankey, T., Moore, M., Thode, A., 2018. Evaluating unmanned aerial vehicle images for estimating forest canopy fuels in a ponderosa pine stand. Remote Sensing 10, 1266. https://doi.org/10.3390/rs10081266

Shugart, H.H., Saatchi, S., Hall, F.G., 2010. Importance of structure and its measurement in quantifying function of forest ecosystems. J. Geophys. Res. 115, 2009JG000993. https://doi.org/10.1029/2009JG000993

Staver, A.C., Archibald, S., Levin, S.A., 2011. The global extent and determinants of savanna and forest as alternative biome states. Science 334, 230–232. https://doi.org/10.1126/science.1210465

Stefanidou, A., Gitas, I.Z., Katagis, T., 2022. A national fuel type mapping method improvement using sentinel-2 satellite data. null 37, 1022–1042. https://doi.org/10.1080/10106049.2020.1756460

Stephens, S.L., Moghaddas, J.J., 2005. Experimental fuel treatment impacts on forest structure, potential fire behavior, and predicted tree mortality in a California mixed conifer forest. Forest Ecology and Management 215, 21–36. https://doi.org/10.1016/j.foreco.2005.03.070

Stephens, S.L., Ruth, L.W., 2005. Federal forest-fire policy in the United States. Ecological Applications 15, 532–542. https://doi.org/10.1890/04-0545

Stobbelaar, P., Neinavaz, E., Nyktas, P., 2022. Prediction of leaf area index using thermal infrared data acquired by UAS over a mixed temperate forest. International Journal of Applied Earth Observation and Geoinformation 114, 103049. https://doi.org/10.1016/j.jag.2022.103049

Sumnall, M.J., Trlica, A., Carter, D.R., Cook, R.L., Schulte, M.L., Campoe, O.C., Rubilar, R.A., Wynne, R.H., Thomas, V.A., 2021. Estimating the overstory and understory vertical extents and their leaf area index in intensively managed loblolly pine (Pinus taeda L.) plantations using airborne laser scanning. Remote Sensing of Environment 254, 112250. https://doi.org/10.1016/j.rse.2020.112250

Sun, Z., Wang, Y., Ding, Z., Liang, R., Xie, Y., Li, R., Li, H., Pan, L., Sun, Y., 2023. Individual tree segmentation and biomass estimation based on UAV digital aerial photograph. J. Mt. Sci. 20, 724–737. https://doi.org/10.1007/s11629-022-7563-7

Swayze, N.C., Tinkham, W.T., Creasy, M.B., Vogeler, J.C., Hoffman, C.M., Hudak, A.T., 2022. Influence of UAS flight altitude and speed on aboveground biomass prediction. Remote Sensing 14, 1989. https://doi.org/10.3390/rs14091989

Swayze, N.C., Tinkham, W.T., Vogeler, J.C., Hudak, A.T., 2021. Influence of flight parameters on UAS-based monitoring of tree height, diameter, and density. Remote Sensing of Environment 263, 112540. https://doi.org/10.1016/j.rse.2021.112540

Szpakowski, D., Jensen, J., 2019. A review of the applications of remote sensing in fire ecology. Remote Sensing 11, 2638. https://doi.org/10.3390/rs11222638

Van Wagner, C.E., 1977. Conditions for the start and spread of crown fire. Can. J. For. Res. 7, 23–34. https://doi.org/10.1139/x77-004

Vapnik, V., 2006. Estimation of dependences based on empirical data, Information Science and Statistics. Springer New York, New York, NY. https://doi.org/10.1007/0-387-34239-7

Wadoux, A.M.J.-C., Heuvelink, G.B.M., de Bruin, S., Brus, D.J., 2021. Spatial cross-validation is not the right way to evaluate map accuracy. Ecological Modelling 457, 109692. https://doi.org/10.1016/j.ecolmodel.2021.109692

Wallace, L., Bellman, C., Hally, B., Hernandez, J., Jones, S., Hillman, S., 2019. Assessing the ability of image based point clouds captured from a UAV to measure the terrain in the presence of canopy cover. Forests 10, 284. https://doi.org/10.3390/f10030284

Wang, Y., Fang, H., Zhang, Y., Li, S., Pang, Y., Ma, T., Li, Y., 2023. Retrieval and validation of vertical LAI profile derived from airborne and spaceborne LiDAR data at a deciduous needleleaf forest site. GIScience & Remote Sensing 60, 2214987. https://doi.org/10.1080/15481603.2023.2214987

Watershed Sciences, 2016. Sonoma County vegetation mapping and lidar program: Technical data report.

Welles, J.M., Norman, J.M., 1991. Instrument for indirect measurement of canopy architecture. Agronomy Journal 83, 818–825. https://doi.org/10.2134/agronj1991.00021962008300050009x

Westoby, M.J., Brasington, J., Glasser, N.F., Hambrey, M.J., Reynolds, J.M., 2012. 'Structure-from-Motion' photogrammetry: A low-cost, effective tool for geoscience applications. Geomorphology 179, 300–314. https://doi.org/10.1016/j.geomorph.2012.08.021

Yin, T., Cook, B.D., Morton, D.C., 2022. Three-dimensional estimation of deciduous forest canopy structure and leaf area using multi-directional, leaf-on and leaf-off airborne lidar data. Agricultural and Forest Meteorology 314, 108781. https://doi.org/10.1016/j.agrformet.2021.108781

Zahra, N.F., Setiawan, Y., Prasetyo, L.B., 2022. Estimation of mangrove canopy cover using unmanned aerial vehicle (UAV) in Indramayu Regency, West Java. IOP Conf. Ser.: Earth Environ. Sci. 950, 012032. https://doi.org/10.1088/1755-1315/950/1/012032

Zhang, D., Liu, J., Ni, W., Sun, G., Zhang, Z., Liu, Q., Wang, Q., 2019. Estimation of forest leaf area index using height and canopy cover information extracted from unmanned aerial vehicle stereo imagery. IEEE J. Sel. Top. Appl. Earth Observations Remote Sensing 12, 471–481. https://doi.org/10.1109/JSTARS.2019.2891519

Zhang, W., Qi, J., Wan, P., Wang, H., Xie, D., Wang, X., Yan, G., 2016. An easy-to-use airborne LiDAR data filtering method based on cloth simulation. Remote Sensing 8, 501. https://doi.org/10.3390/rs8060501

Supplement

S1. Models for all study sites

Table 4.S1 Anova testing mean differences in R^2 and RMSE among modelling methods for fold error metrics from 100 replicates of 10-fold cross validation using spatially-blocked groups.

Fuel parameter	Df	R^2				RMSE			
		SS	MS	F	*p*	SS	MS	F	*p*
Biomass									
Method	4	23.5	5.89	80.13	<0.001	11004	2751	82.23	<0.001
Residuals	4995	366.8	0.07			1.7E+05	33.5		
Mean height									
Method	4	4.59	1.15	20.45	<0.001	1.9E+09	4.7E+08	6.91	<0.001
Residuals	4995	280.6	0.056			3.4E+11	6.8E+07		
CBH									
Method	4	2.3	0.56	7.61	<0.001	254	63.53	27.57	<0.001
Residuals	4975	368.3	0.07			11463	2.3		
CC									
Method	4	4.6	1.14	9.16	<0.001	8845	2211.2	31.86	<0.001
Residuals	4818	601.3	0.12			3.3E+05	69.4		
CBD									
Method	4	14.1	3.53	33.99	<0.001	3885	941.3	2.01	0.09
Residuals	4797	498.6	0.104			2.3E+06	483.7		
LAI									
Method	4	43.2	10.8	150.20	<0.001	2.6E+08	6.4E+07	2.96	0.02
Residuals	4985	358.3	0.072			1.1E+11	2.2E+07		

For aboveground biomass in particular, random forest was significantly more accurate than all other methods, with less spread of error (Fig. 4.5a). The model performance of SVM and LM forward were not significantly different from that of random forest for mean height or canopy cover, and error patterns were similar with longer tails and more negative bias (Fig. 4.5b,d). Additionally, the LM forward model for CBD was not significantly different from that of random forest, and both had a positive bias in error (Fig. 4.5e). Random forest significantly outperformed all other methods in modelling LAI and CBH as measured by either R^2 or RMSE, respectively, but not both fuel parameters.

S2. Individual study site models

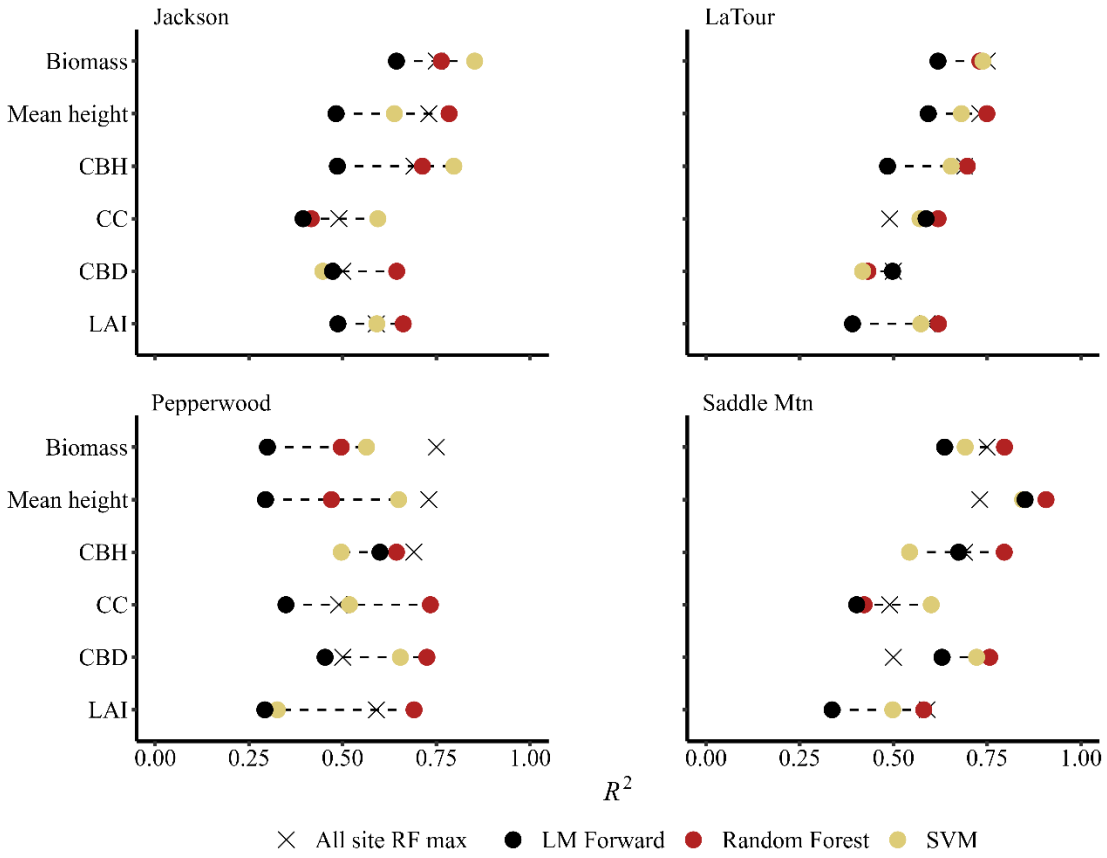


Fig. 4.S1 Individual site model comparisons. Performance results obtained from 100 replicates of 5-fold cross validation using spatially blocked groups.

Model performance differed among individual study sites (Figure S1). The top model performance at Jackson and LaTour roughly aligned with the accuracy distribution of the all-site random forest model. Saddle Mountain's top models also matched the all-site random forest model while overperforming for mean height and CBD. Pepperwood demonstrated the greatest departure in model accuracy. At this site, the accuracy distribution between the two groups of fuel parameters flipped, with CC, CBD, and LAI exhibiting greater model predictive power than those for biomass, mean height, or CBD. Few discernable patterns emerged among the different models by canopy fuel parameter across the sites (Figure S1).

For all fuel parameters across sites, random forest outperformed the other modelling methods in two thirds of cases. Only the models for LAI demonstrated a consistent relationship across sites between

the relative accuracies of modelling approaches, with random forest returning the maximum performance across all sites. No other fuel parameter was modelled with maximum accuracy by the same method across all four sites. SVM returned the top performance for 29% of the remaining fuel parameters, while linear methods lagged for all fuel parameters except for CBD at LaTour. The remainder of our analysis focused on random forests given its generally equal or higher accuracy than other techniques.

S3. SVM and LM variable importance

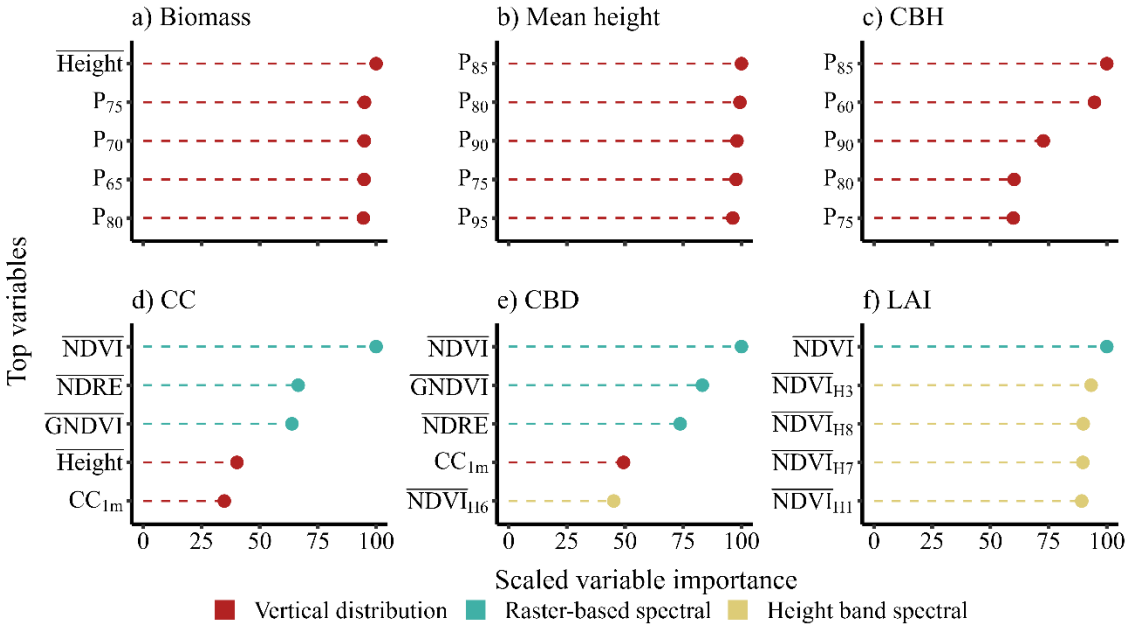


Fig. 4.S2 Relative scaled importance of top five predictors for SVM models produced across all sites.

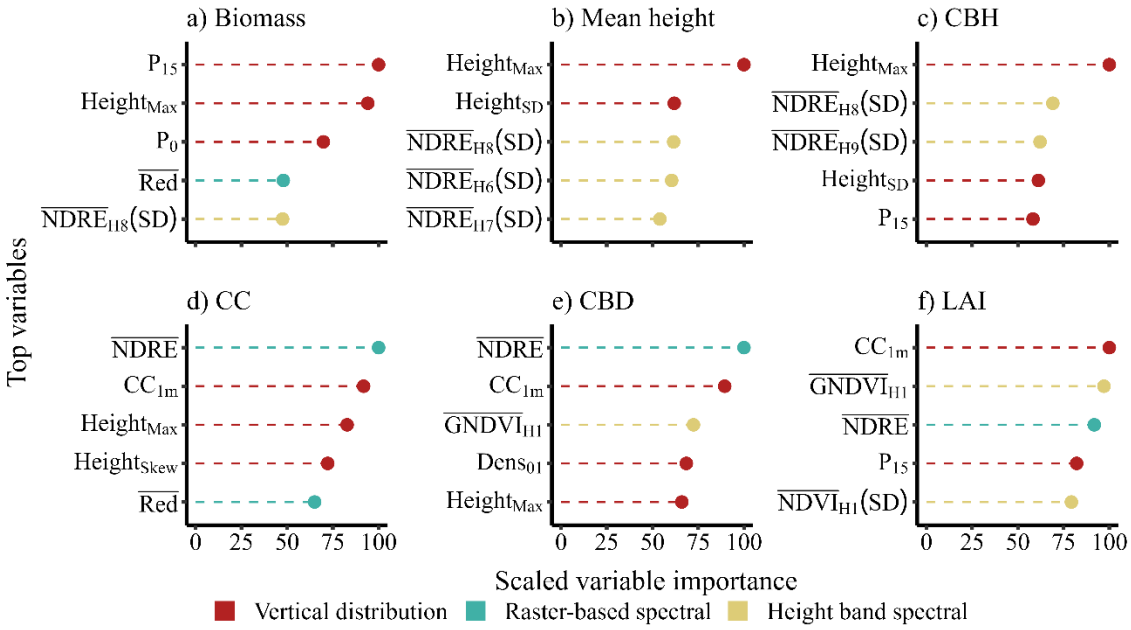


Fig. 4.S3 Relative scaled importance of top five predictors for LM with forward selection models produced across all sites.

S4. Predictor subset variable importance

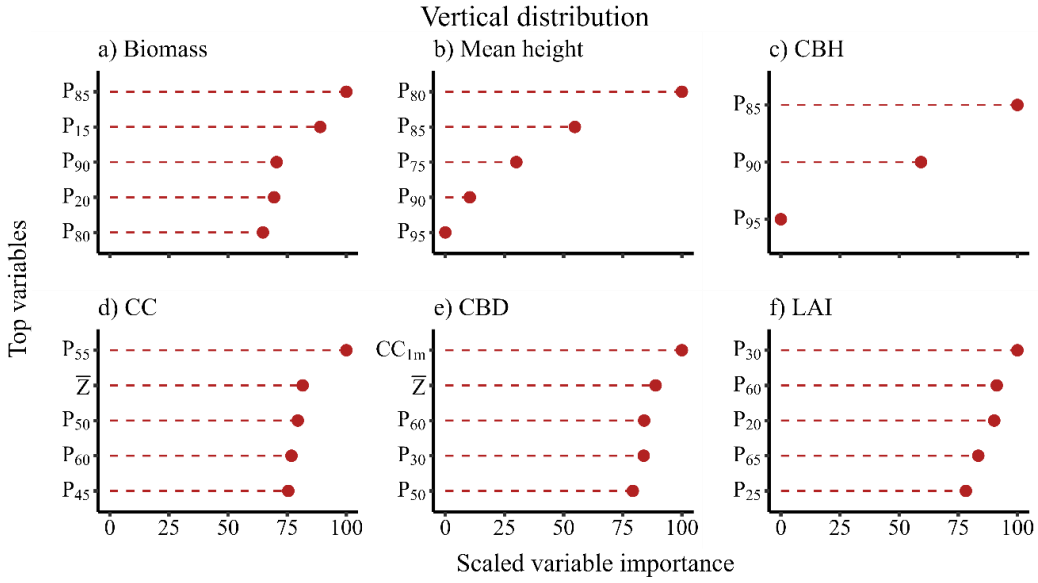


Fig. 4.S4 Random forest variable importance for vertical distribution data subset models. Relative scaled importance of top five variables for random forest models produced across all sites.

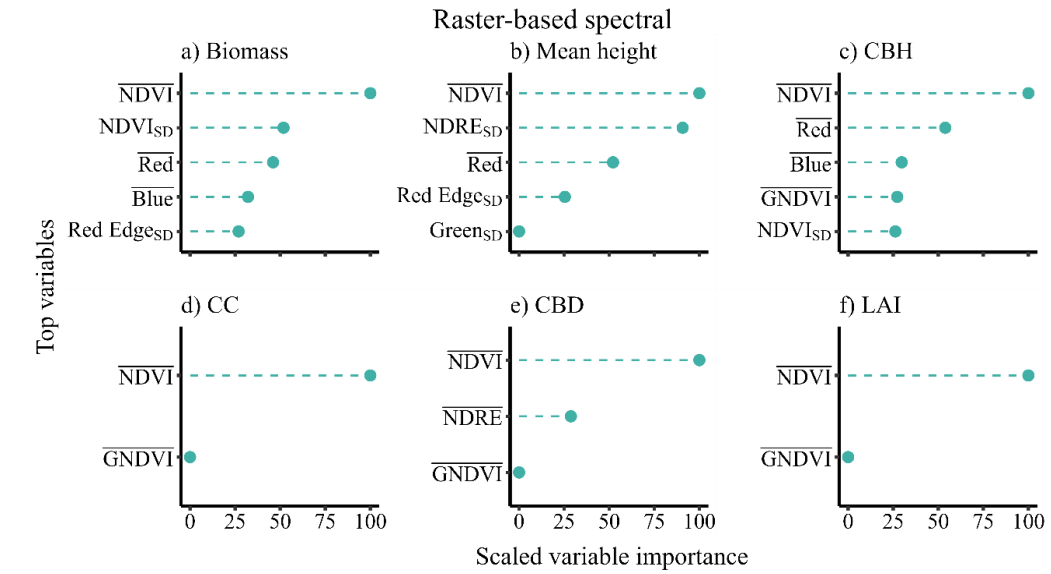


Fig. 4.S5 Random forest variable importance for raster-based spectral data subset models. Relative scaled importance of top five variables for random forest models produced across all sites.

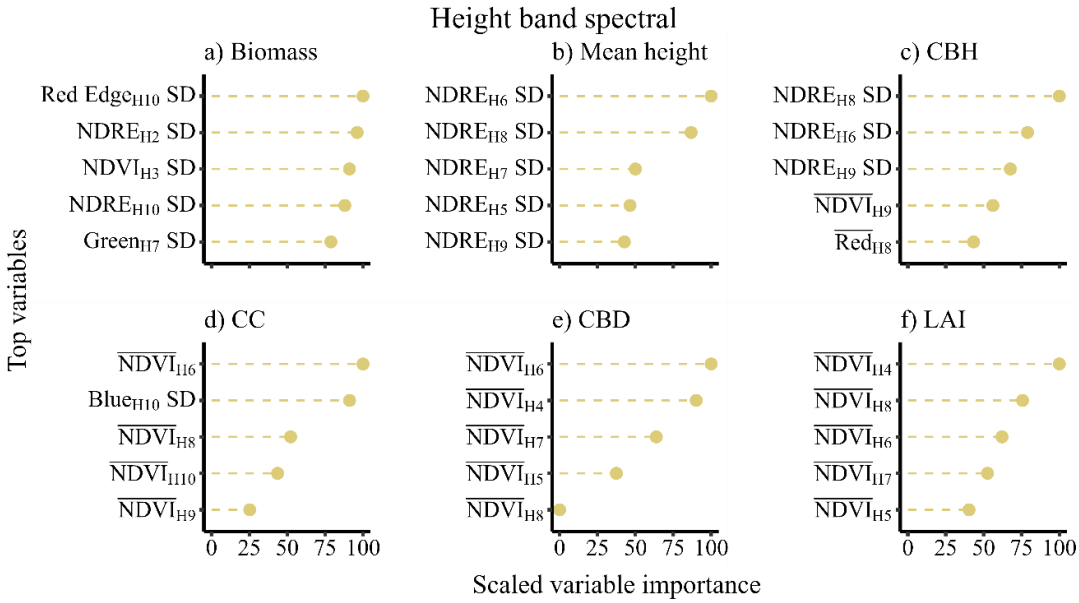


Fig. 4.S6 Random forest variable importance for height band spectral data subset models. Relative scaled importance of top five variables for random forest models produced across all sites.

For the vertical fuel parameter group, variable selection for the vertical distribution predictor subset models closely resembled that identified by the full-predictor model (Fig. 4.S4). For the horizontal fuel parameter group, the vertical distribution subset models consistently isolated a set of middle canopy height distribution variables (Fig. 4.S4).

Across all models from both parameter groups, the raster-based spectral subset models consistently identified mean NDVI as the top predictor (Fig. 4.S5). For the horizontal fuel parameter group, the raster-based spectral data subset models identified the same sets of spectral indices per canopy parameter as the full-predictor models (Fig. 4.S5).

For the vertical fuel parameter group, the height band spectral subset models relied predominantly upon the standard deviation of spectral indices, with the inclusion of some individual bands (Fig. 4.S6). For the horizontal fuel parameter group, the models for this subset utilized predominantly combinations of mean NDVI height bands (Fig. 4.S6).

Chapter 5

Preface

This final study expands the research from the previous chapter to encompass a broader range of remote sensing approaches. By so doing, I sought to explore the range of performances achievable with area-based random forest modelling and to understand the trade-offs in accuracy associated with utilizing methods with lower resolution but greater accessibility and potential spatial coverage.

This study utilized the full suite of data collected by the 3D Forests team. I did not contribute to the collection of these data. However, I did have the opportunity to observe and participate in all steps of the collection and processing workflow for these data during the initial campaign at Pepperwood. The research agenda and methods in this paper were developed in collaboration with Dr. Clark, Dr. Bentley, and Imma. I performed the data processing and analyses beyond the initial generation of plot level las files with commercial software and drafted the manuscript. My coauthors provided editing assistance. This paper has not yet been submitted to a journal.

Area-based random forest modelling of canopy fuels across the forests of California, USA: Assessment of structural and spectral remote sensing performance

Sean Reilly [1], Matthew L. Clark [2], Randi Carter [3], Lisa Patrick Bentley [3], and Imma Oliveras Menor [1,4]

[1] Environmental Change Institute, University of Oxford, Oxford OX1 3QY, UK

[2] Center for Interdisciplinary Geospatial Analysis, Department of Geography, Environment, and Planning, Sonoma State University, Rohnert Park, CA 94928, USA

[3] Department of Biology, Sonoma State University, Rohnert Park, CA 94928, USA

[4] AMAP (Botanique et Modélisation de l'Architecture des Plantes et des Végétations), CIRAD, CNRS, INRA, IRD, Université de Montpellier, Montpellier, France

Abstract

The forests of California, USA require widespread fuels reduction treatments to restore forest health and reduce the severity of future wildfires. To that end, California has committed to treating one million acres per year by 2025. Targeting these treatments through detailed data on forest fuel loads has been demonstrated to significantly decrease future fire risk compared to blanket, unguided management. Area-based remote sensing models of canopy fuels provide the primary means of obtaining these data over large regions in the complex landscape of diverse forests that characterize California. This study, therefore, seeks to assess a spectrum of structural and spectral remote sensing methods to determine the performance obtainable via these area-based models, along with the trade-offs between spatial scale, acquisition difficulty, and model accuracy. Specifically, we examined the performance of area-based random forest machine learning models using predictors from the structural remote sensing methods of terrestrial laser scanning (TLS), handheld laser scanning (HMLS), and unoccupied aerial system

Structure-from-Motion (UAS-SfM) and the spectral remote sensing methods of UAS multispectral and PlanetScope satellite imagery, along with their combinations, to model the vertical canopy fuel parameters of aboveground biomass, canopy base height (CBH), and mean height and the horizontal fuel parameters of canopy cover, leaf area index (LAI), and canopy bulk density (CBD).

Models including TLS data returned the highest performance across all fuel parameters, achieving $R^2 > 0.73$ for vertical fuel parameters and $R^2 > 0.65$ for horizontal fuel parameters. Despite its limitations, UAS-SfM models consistently returned accuracies within 10% of TLS for all parameters, including matching TLS performance for CBH. The addition of spectral data significantly improved model performance for the horizontal fuel parameters but did not affect TLS or UAS-SfM vertical structure accuracy. Models containing HMLS improved for all parameters with the inclusion of spectral data. Spectral only models performed comparably well for the horizontal fuel parameters, especially for LAI, but were unable to model the vertical structure parameters. For all three structural methods across all fuel parameters, models using voxelized predictors matched or outperformed their point cloud-based counterparts. Fusing UAS-SfM data with either lidar dataset did not improve model performance.

These findings demonstrate that accurate models of forest canopy fuel parameters across a range of forest types can be generated using area-based remote sensing random forest models. Specifically, TLS provides the highest accuracies, especially when combined with spectral data, but UAS-SfM, due to its ease of accessibility and greater potential spatial coverage, provides sufficient accuracy that allows it to be well suited for the fuel mapping needed by most land managers, landowners, and state personnel to inform landscape scale fuels reduction treatments.

Keywords

UAS, SfM, TLS, HMLS, PlanetScope, random forest, canopy fuels, biomass, California forests

1. Introduction

Wildfires drive the ecological diversity and landscape heterogeneity that characterize California, USA, and other Mediterranean climate regions around the world (Beaty and Taylor, 2008; Keeley et al., 2011; Rundel et al., 2016; Sugihara and Barbour, 2006). However, the state's fire regime, otherwise naturally self-limiting (Collins et al., 2009; Park et al., 2021), has been heavily disrupted, in part due to federal fire suppression policies since the early 1900s (Forest Climate Action Team, 2018; Stephens and Ruth, 2005). As a result of this fire exclusion, fuel loads, which are the quantities of biomass available for combustion, have accumulated significantly, leading to an increase in widespread and severe wildfires (Dennison et al., 2014; Miller et al., 2012; Miller and Safford, 2012). Consequently, an urgent need exists for proactive fuels reduction treatments, such as mechanical thinning and prescribed fire, to reduce future fire severity to presuppression levels (North et al., 2015; Stephens et al., 2023; Wu et al., 2023), with over 15 million acres of California forests requiring restoration (Forest Climate Action Team, 2018).

Fortunately, management on a portion (10-20%) of the landscape has been demonstrated to produce widespread benefits if treatment can be targeted effectively (Ager et al., 2010; Collins et al., 2013). California has committed to treating one million acres annually by 2025 (Knight et al., 2022). Modelling of this effort has demonstrated that targeting management by fuel density significantly decreases the probability of stand-replacing fires (Daum et al., 2024). This, consequently, generates a demand for data products that can provide frequent and spatially-extensive data on landscape fuel load distributions to inform these management efforts (Gale et al., 2021; Haslem et al., 2011; Hood et al., 2022; Rollins et al., 2004). In particular, mapping canopy structure, namely the vertical and horizontal composition of fuels, presents a key area of interest in management prioritization, since canopy crown torching and sustained ignition characterize high-severity fire (Agee and Skinner, 2005; Van Wagner, 1977).

California's complex landscape heterogeneity poses a significant challenge in this work since any data product must be able to extract metrics of fuel loading from a breadth of forest types, even within the

same stand or management site. These data have historically been acquired through field sampling, but this approach lacks the capacity to provide continuous coverage on the spatial scale necessary to meaningfully inform management (Arroyo et al., 2008). In contrast, remote sensing approaches, such as satellite spectral imagery, lidar, and unoccupied aerial system Structure-from-Motion (UAS-SfM), are better suited to provide continuous coverage over these larger extents (Gale et al., 2021; Szpakowski and Jensen, 2019).

Remote sensing approaches fall across spectrums of acquisition difficulty, practical limits to acquired spatial extent, and spatial, spectral, and temporal detail, which together determine the relative capability of each method for a given research or management application (Gale et al., 2021). Satellite spectral data, which are available globally at coarse resolution (meters per pixel) for no or minimal cost, lies at one end of the spectrum and has previously been employed to classify vegetation into fuel model classes over large regions (e.g., Aragoneses and Chuvieco, 2021; Shaik et al., 2022; Stefanidou et al., 2022). In contrast, lidar, or light detection and ranging, allows for the physical detection of forest structure, and therefore fuel loads, through the use of laser pulse time-distance measurements (Reutebuch et al., 2005). This sensor can be deployed on an aerial platform (ALS) or on the ground, using either a tripod mounted sensor (TLS) or a handheld mobile laser scanner (HMLS) (Andersen et al., 2005; Forbes et al., 2022; Hillman et al., 2021b; Kang et al., 2024). TLS provides the highest resolution of the listed methods at the highest acquisition expense and smallest extent, and has been demonstrated to produce extremely accurate models of canopy parameters (e.g., Bogdanovich et al., 2021; García et al., 2011; Krause et al., 2023; Rocha et al., 2023). HMLS provides lower resolution data with less spatial accuracy than TLS, but at reduced cost and effort. The utility of this technology has also been demonstrated in forestry applications (e.g., Vandendaele et al., 2022), including successful mapping of fuel types and canopy fuels in a mix of forest types (Forbes et al., 2022; Hoffrén et al., 2024; Kang et al., 2024; Skowronski et al., 2011).

UAS-SfM lies between these technologies, providing high resolution 3D data over greater extents and lower acquisition expense than either method of terrestrial lidar, and importantly, can also include

<10 cm, calibrated multi-spectral imagery when acquired with an appropriate sensor. UAS-SfM generates 3D spatial data from overlapping imagery and allows for the coincidental acquisition of structural and spectral data (Forbes et al., 2022; Reilly et al., 2021; Westoby et al., 2012). Due to the balance of cost, resolution, and spatial coverage, UAS-SfM, in theory, is well suited for management applications at stand scales (e.g., > 1 ha). In an assessment of UAS-SfM across a range of sites representative of California's forest diversity, our previous work demonstrated that random forest models, an ensemble tree-based machine learning algorithm, perform well in their ability to map the vertical structure parameters of canopy base height (CBH), mean canopy height, and aboveground biomass, but exhibit lower performance for the horizontal structure parameters of canopy bulk density (CBD), leaf area index (LAI), and canopy cover (CC) using an area-based modelling approach (Reilly et al., 2024).

This area-based approach entails extracting a suite of summary metrics from UAS-SfM point cloud and spectral data at a gridded spatial scale, such as corresponding to an underlying plot network, which are then used as model predictors. Another approach to estimate forest fuels parameters is with tree-level analysis. While tree-level models have been demonstrated to work well in some regions (e.g., Alonso-Rego et al., 2022; Rocha et al., 2023; Sun et al., 2023), current tree segmentation algorithms for UAS-SfM provide insufficient accuracy in complex forest types such as oak woodlands (Chávez-Durán et al., 2024; Grznárová et al., 2019). As a result, an area-based approach is currently better suited for the heterogenous mixed forests of California (Reilly et al., 2024). Additionally, the area-based approach eliminates the need to parameterize and assess segmentation model performance or to match segmented crowns with field individual tree measurements, facilitating model scaling across sites or between forest types (Arkin et al., 2023). Together, these attributes make this modelling approach suitable for management applications.

However, the area-based modelling approach needs to be tested using data sources across the range of remote sensing methods discussed to determine the limits of area-based random forest model performance, and the variation in accuracy across methods. UAS-SfM has limited capacity to detect below canopy structure due to the passive nature of the spectral sensor (Forbes et al., 2022; Reilly et al.,

2021; Shin et al., 2018). Therefore, assessing area-based random forest models with high resolution terrestrial lidar, and specifically TLS and HMLS, will test the upper accuracy limit of this approach and provide reference for the loss in accuracy that accompanies using remote sensing methods with greater spatial extent and lower acquisition difficulty. Due to the high fidelity of these data types, highly accurate measurements of canopy attributes can be extracted from them directly. Consequently, the use of these data for this purpose is specifically to assess the maximum possible achievable results from an area-based random forest model and are not intended to represent the optimal methods for these data types.

Furthermore, the performance of this modelling approach needs to be assessed using readily-available satellite spectral data since site accessibility, costs, and spatial scale of measurements are significant obstacles to management implementation. The process of aggregating measurements to a plot level reduces UAS-SfM spatial resolution to a comparable scale as that obtained by satellite imagery (Reilly et al., 2024). In this previous work, models for the vertical canopy fuel parameters utilized predominantly spectral indices. Consequently, spectral measurements obtained from satellite imagery have the theoretical capacity to directly model these canopy fuel parameters with comparable accuracy to UAS-SfM using area-based random forest, but this potential needs to be assessed. In particular, the capacity of higher-resolution (3.7 m) PlanetScope small satellite data, as compared to Landsat or Sentinel, to model fuel loads has not yet been assessed.

Finally, area-based random forest modelling needs to be assessed using the available combinations of data to determine if combing spectral and structural data sources, or the fusion of multiple structural data sources, can improve model performance. Both the addition of spectral data to structural predictor models and the fusion of airborne and terrestrial lidar data have been demonstrated to improve ecological model performance (Alonso-Rego et al., 2021; Alonzo et al., 2020; Qi et al., 2022), but not in all applications (Hillman et al., 2021a; Tompalski et al., 2019). Specifically, to our knowledge, the fusion of HMLS and UAS-SfM has not yet been assessed for fuels mapping. Due to the top-down and bottom-up sensing of UAS-SfM/PlanetScope and TLS/HMLS, respectively, they have opposing strengths

and limitations. Consequently, the fusion of these data sources could potentially provide a means for increasing model performance while still maintaining lower expenditure than TLS.

This paper, therefore, seeks to assess area-based random forest models of vertical and horizontal canopy fuel parameters against a range of remote sensing methods and their combinations to determine the maximum performance obtainable with this approach, and the relative loss in accuracy across methods with lower acquisition difficulty. These findings will inform the use of this method in research and management applications and provide needed data on the trade-offs between remote sensing approaches. Specifically, this study aims to:

1. Compare the structure of TLS, HMLS, and UAS-SfM point clouds and the distribution of spectral measurements between PlanetScope satellite data and UAS multispectral data.
2. Compare model performances between all combinations of structural and spectral predictors to model the wildfire fuel parameters of aboveground biomass, mean canopy height, CBH, CBD, LAI, and canopy cover.
3. Determine the optimal method of metric extraction from the structural datasets through voxelization and the fusion of lidar and UAS-SfM datasets prior to predictor extraction.
4. Compare variable selection across models by predictor type.

2. Methods

2.1 Study sites

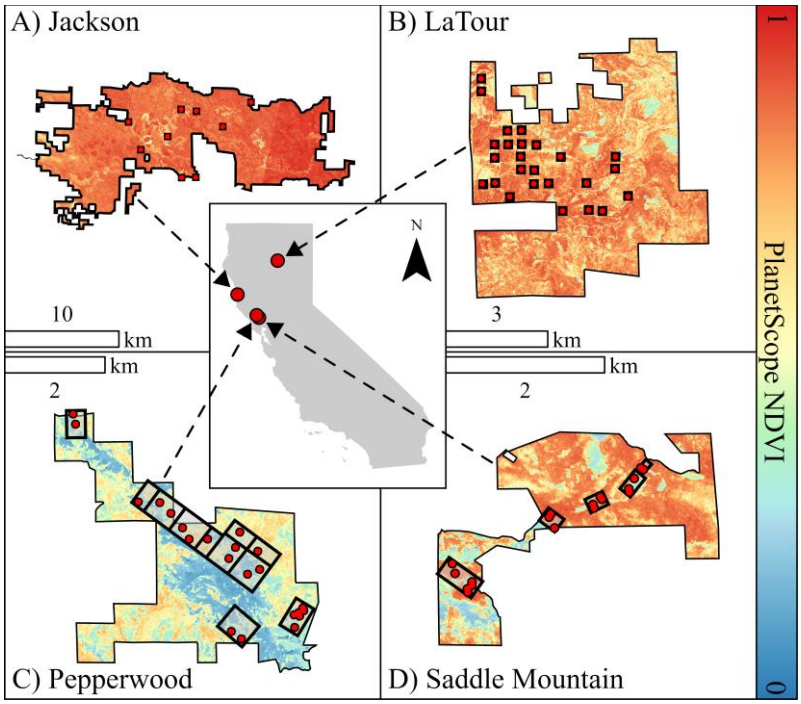


Fig. 5.1 Location of study sites within California, USA. Black boxes represent UAS flight zone perimeters and red points represent study plots. Basemap displays NDVI measurements obtained from PlanetScope satellite imagery.

From summer 2018 through 2021, we collected field measurements and remote sensing data from 79 0.04-ha forest plots from four sites across California representative of the diversity of forest types that characterize the state (Fig. 5.1). Jackson Demonstration State Forest is in the Coast Range ecoregion as is predominantly populated with second-growth coast redwood (*Sequoia sempervirens*) and Douglas fir (*Pseudotsuga menziesii*) forest (14 plots; Fig. 5.1A; Eng, 2015). LaTour Demonstration State Forest is in the Cascades ecoregion and contains mixed conifer forests, primarily white fir (*Abies concolor*) at higher elevations (25 plots; Fig. 5.1B; Berbach et al., 1995; Griffith et al., 2016). Pepperwood Preserve and Saddle Mountain both fall in the Central California Foothills and Coastal Mountains ecoregion, and support a heterogeneous landscape including Douglas fir forests, oak woodlands, chaparral, and grasslands (Pepperwood: 22 plots, Fig. 5.1C; Saddle Mountain: 18 plots, Fig. 5.1D; Ackerly et al., 2020;

Evett et al., 2013; Oldfather et al., 2016). See Reilly et al. (2024) for more detail on study sites and plot network.

2.2 Data sources

2.2.1 Field-based canopy parameter measurements

Our field sampling included all trees within each plot with a diameter at breast height (DBH) greater than 10 cm. Tree height was measured with a laser rangefinder. Individual tree lowest live crown was measured as the height above the ground of the lowest live branch within 2 m of the next branch. From these measurements, we computed plot averages for mean height and canopy base height (CBH), respectively. We modelled tree above ground biomass from these measurements using the California Air Resource's carbon offset protocols (FIA, 2014), which were then summed for each plot to derive total plot above ground biomass. We collected CBH, DBH, and height data at Saddle Mountain. We utilized preexisting CBH and height data from 2020 California Department of Forestry and Fire Protection (CAL FIRE) surveys at LaTour and Jackson and from 2018 Sentinel site data collection at Pepperwood (Ackerly et al., 2013). We supplemented these data as needed with additional field measurements. Sampling took place at Jackson between 15 June – 2 July 2020 and 8 – 12 July 2021, at LaTour between 7 – 17 July 2020, at Pepperwood between 1 Sept – 15 Oct 2019, and at Saddle Mountain between 4 – 9 Aug 2020.

In addition to tree measurements, we collected five canopy cover measurements per plot using a Forestry Suppliers spherical crown densiometer. We also collected five measurements per plot with the LI-COR LAI-2000 Plant Canopy Analyzer to determine leaf area index (LAI) and canopy gap fraction. From the canopy gap fraction measurements, we computed canopy bulk density (CBD) using the methods of Keane et al. (2005). Of note, CBD presents a challenging metric to measure through nondestructive means. Keane et al. (2005) determined their relationships through destructive sampling in western United States conifer forests and achieved a significant but modest R^2 of 0.56, and it is unclear how this model

scales to hardwood forest types. We took the average of these five canopy cover, LAI, and CBD measurements to generate one value per plot. For further details on field sampling methods, see Reilly et al. (2024).

2.2.2 ALS data

ALS data in this study served as a baseline to which the other datasets could be registered for spatial accuracy. However, we excluded ALS from our modelling analysis due to the length of time and the occurrence of significant disturbance events, namely the Tubbs Fire in 2017, between when these data were collected at Pepperwood and Saddle Mountain and the start of our field campaigns. Newer ALS was acquired in year 2022 but has not been released at the time of this analysis in year 2024. This low temporal cadence and long data latency of ALS is typical in California, and these factors are a key reason why we are exploring other remote sensors in our analysis. Watershed Science conducted ALS mapping of Pepperwood and Saddle Mountain using Leica ALS50 and ALS70 sensors between 28 Sept 2013 and 26 Nov 2013 on behalf of the 2013 Sonoma County Vegetation Mapping and Lidar Program (Watershed Sciences, 2016). Dewberry and Quantum Spatial conducted ALS mapping of Jackson using a Leica ALS70 sensor between 3 March 2017 and 24 Aug 2017 (Dewberry, 2018). Lastly, Quantum Spatial conducted ALS mapping of LaTour using a Riegl VQ1560i sensor between 11 Oct and 27 Dec 2019 (Quantum Spatial, 2020). All sensors were flown on piloted aircraft. Density of the ALS point clouds ranged from 6 to 49 points/m^2 with a mean density of 25 points/m^2. Ground points were classified by each company as part of their final data product and these ground points were used to generate ALS digital terrain models (DTMs).

2.2.3 UAS-SfM data

We flew a SenseFly eBee X fixed-wing UAS platform at Pepperwood and Saddle Mountain and onboard a DJI Matrice 200 (M200) quadcopter UAS platform at Jackson and LaTour. Flights were conducted at Pepperwood 27 Sept to 15 Oct 2019, at Saddle Mountain 4 – 5 August 2020, at Jackson 28

June to 2 July, 2020 and 8 – 12 July 2021, and at LaTour 11 – 16 July, 2020. We employed a perpendicular crosshatch flight pattern at 122-m above ground flight altitude, controlled by either SenseFly's eMotion 3 software (version 3.7) for the eBee or the Micasense Atlas app for the M200. Each platform flew with a MicaSense RedEdge-MX multispectral sensor and a MicaSense Downwelling Light Sensor (DLS) 2. The Rededge-MX sensor collects five spectral bands: blue (475 nm center, 20 nm bandwidth), green (560 nm center, 20 nm bandwidth), red (668 nm center, 10 nm bandwidth), red edge (717 nm center, 10 nm bandwidth), and near-IR (NIR, 840 nm center, 40 nm bandwidth).

Imagery was collected at 75% latitudinal and longitudinal overlap for the eBee and at 85% overlap for the M200. The eBee had to be flown at lower overlap to cover the required study area within battery flight time limitations. The DLS 2, in conjunction with a MicaSense calibration panel (RP04-1926247-OB), was used to convert raw radiance measurements to reflectance values through radiometric calibration. Using PIX4Dmapper (PIX4D, Lausanne, Switzerland, version 4.4.12), we processed this imagery into orthomosaics and SfM 3D point clouds. Orthomosaics from LaTour, Jackson, and Saddle Mountain had 5-cm resolution, while orthomosaics from Pepperwood had 15-cm resolution due to processing limitations arising from the lower imagery overlap. Density of the SfM point clouds ranged from 36 to 672 points/m^2 with a mean density of 320 points/m^2.

We used the multispectral orthomosaics to generate a set of spectral indices orthomosaics related to plant physiology (Dash et al., 2018). These consisted of the normalized difference vegetation index (NDVI, [NIR − red] / [NIR + red]), the normalized difference red edge (NDRE, [NIR – red edge] / [NIR + red edge]), and green NDVI (GNDVI, [NIR – green] / [NIR + green]) (Dash et al., 2018). We selected these indices as the set with the greatest relationship with plant physiology based on the available spectral bands from the Micasense Rededge MX (Dash et al., 2018).

Using the method and parameters from Reilly et al. (2021), we employed a cloth simulation filter in R (version 4.3.2) using the lidR package to identify an initial set of ground points from which we removed misclassified vegetation using an NDVI filter (R Core Team, 2023; Roussel et al., 2023; Zhang et al., 2016). Using these identified ground points, we registered the UAS-SfM point clouds to the ALS

DTMs. If insufficient ground points could be identified, primarily at Jackson, we registered the UAS-SfM point cloud to the complete ALS data. Finally, we used the ALS DTM to normalize the UAS-SfM point cloud. See Reilly et al. (2021) and Reilly et al. (2024) for more details on UAS-SfM data acquisition and processing.

2.2.4 TLS data

We collected TLS data using a Riegl VZ-400i (RIEGL Laser Measurement Systems GmbH) with a range of 800 m. Each plot was scanned at nine positions in an even grid, with vertical and horizontal scans conducted at each position to ensure maximum coverage (Forbes et al., 2022; Wilkes et al., 2017). Using RiSCAN PRO (Riegl Laser Measurement Systems GmbH, Horn, Austria, version 2.8.2), these individual scans were aligned to generate one plot-level scan using MultiStation Adjustment. We then registered this combined scan to the reference ALS data and height normalized the data using a DTM generated from the TLS data in Lidar360 (GreenValley International, Berkeley, California, version 4.1). Density of the TLS point clouds ranged from 41,340 to 484,016 points/m^2 with a mean density of 215,955 points/m^2. See Forbes et al. (2022) for additional details on TLS data acquisition and processing.

2.2.5 HMLS data

We collected HMLS data using a GeoSLAM ZEB-Revo (GeoSLAM, Nottingham, United Kingdom) with a range of 20 m, which we note is below the maximum canopy height for our conifer-dominated forests. The same person walked the HMLS sensor in a closed loop around the perimeter of each plot than in smaller randomized loops in the interior to ensure complete coverage, for a total scan time of 5 – 10 minutes. We used GeoSLAM software (GeoSLAM, Nottingham, United Kingdom) to convert these path data to plot point clouds, then registered this data to the processed TLS data in RiSCAN PRO. Finally, we height normalized the data using the same method as for TLS in Lidar360. Density of the HMLS point clouds ranged from 3179 to 32842 points/m^2 with a mean density of 14160 points/m^2. See Forbes et al. (2022) for additional details on HMLS data acquisition and processing.

2.2.5 Planet satellite data

PlanetScope orthorectified surface reflectance (analytic_sr) images were acquired through Planet. This data product has four spectral bands (RGB + NIR) at 3.7 m resolution (Planet Labs Inc., 2019). We downloaded all imagery obtained from each site within the date range of the corresponding UAS flight campaign. Imagery was filtered for pixels with no cloud cover using Planet's data usability mask. Like the UAS spectral data, we computed a series of spectral indices for each PlanetScope imagery band set. Due to the absence of the red edge band from the PlanetScope data, we only calculated NDVI and GNDVI for the PlanetScope data.

2.3 Data processing

2.3.1 Structural data

Table 5.1 Structural predictors. Table adapted from Reilly et al. (2024).

Predictor category	Predictor	N predictors
Upper	Max height	1
Middle	Mean height	1
	Height percentiles in 5% increments	
Upper	70% to 95%	6
Middle	35% to 65%	7
Lower	0% to 30%	7
Density	Height density bands	10
Variation	Height standard deviation	1
Variation	Height coefficient of variation	1
Variation	Height kurtosis	1
Variation	Height skewness	1
Variation	Height interquartile range (IQR)	1
Variation	Canopy relief ratio $(H_{mean} - H_{min}) / (H_{max} - H_{min})$	1
Cover	Percentage of points above 1m	1
Cover	Percentage of points above mean	1
	Total	40

We employed an area-based approach to extract predictors from the structural data sources. For each plot, we isolated the point cloud within the plot boundary and calculated 40 metrics from the distribution of the height data within that plot (Table 5.1). These metrics consisted of the same set previously utilized in Reilly et al. (2024), developed from Filippeli et al. (2019) and Marino et al. (2018). For the ten density band variables, we sliced the point cloud into ten plot-specific bands of equal height based on maximum plot height and calculated the percentage of points per band.

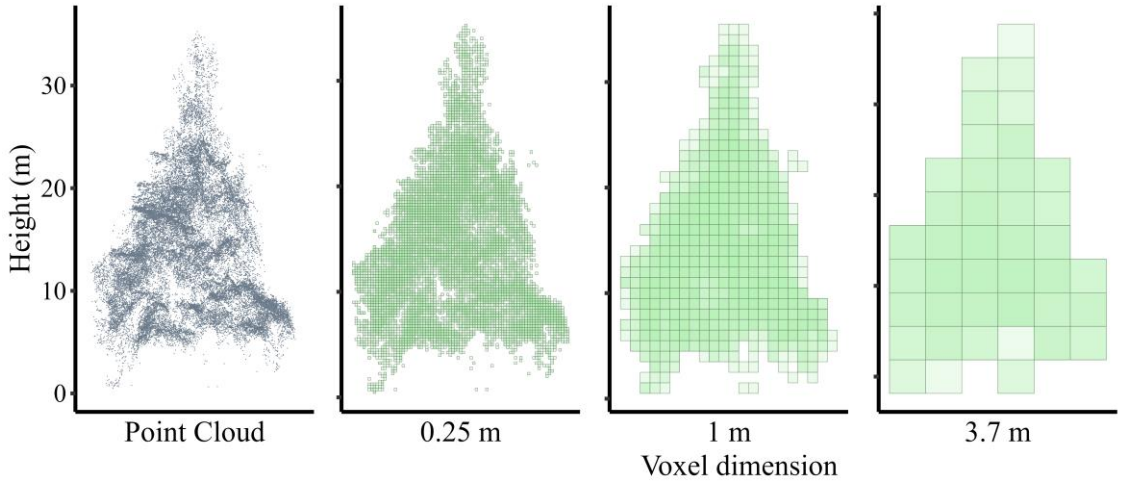


Fig. 5.2 Demonstration of the influence of dimension on voxelization for a conifer tree extracted from UAS-SfM at Pepperwood. Tree data displayed is three dimensional and darker colors denote higher density of overlapping voxels.

In addition to extracting these metrics from the point cloud directly, we also extracted the same set of predictors from voxelized versions of the data across a range of voxel dimensions (Fig. 5.2). Voxelization involves dividing the 3D space occupied by the point cloud into discrete cubic chunks and determining which of these cubes contain points (Lecigne et al., 2018). While additional statistics may be computed per voxel, for the purposes of this study, we simply identified the presence (i.e., at least one point in the voxel) or absence of each voxel. In so doing, this process serves to simplify and normalize the point cloud. Using lidR, we produced voxelized data for each plot at voxel dimensions of 0.1 m, 0.25 m, 0.5 m, 1 m, and 3.7 m (Fig. 5.2). This largest dimension corresponds to the spatial resolution of the

PlanetScope satellite data. After voxelization, metrics were extracted from the resulting plot height data as before.

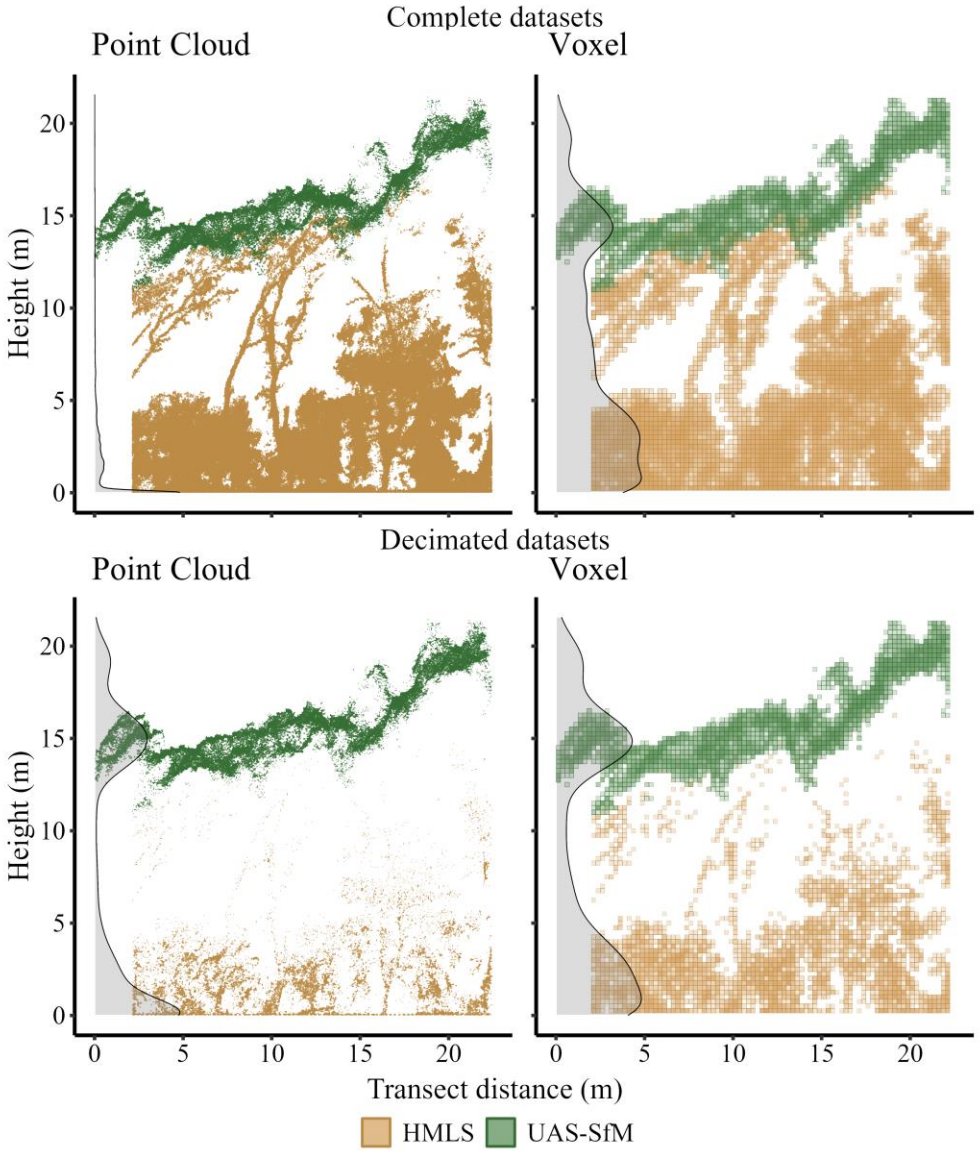


Fig. 5.3 Demonstration of fusion, decimation, and voxelization processes for a 3 m wide transect from a plot at Saddle Mountain. Left plots depict point cloud data and right plots depict voxelized versions of that data with a voxel dimension of 0.25 m. Vertical gray contour depicts density distribution of points or voxels within the transect.

In addition to extracting these metrics from each remote sensing method individually, we also extracted these metrics from fusion datasets, in which we combined one of the terrestrial lidar datasets (TLS, HMLS) with the UAS-SfM data. The point clouds from both datasets were joined using lidR, then

metrics were extracted as before from the resulting combined point cloud and its voxelized versions (Fig. 5.3 – top). Due to the significant difference in point density between the UAS-SfM and lidar data, we also produced a set of decimated fusion datasets in order to assess whether the removal of this discrepancy in point density could produce metrics with greater predictive power. For these, we extracted the densities from both point clouds and identified which was lower. We then used the homogenous decimation function within lidR with a resolution of 1 m to reduce both point clouds to this lower density prior to joining (Fig. 5.3 – bottom). After generating the decimated dataset, we voxelized and extracted the metrics as before.

All together, this process produced 42 sets of structural predictor metrics: One point cloud + five voxel metrics predictor sets for each of the three independent datasets + two complete fusion datasets + two decimated fusion datasets.

2.3.2 Spectral data

Table 5.2 Spectral predictors computed per band and spectral index

Predictor category	Predictor	N predictor UAS	N predictor PlanetScope
Spectral	Mean	8	6
Spectral	Standard deviation	8	6
Spectral	Interquartile Range (IQR)	8	6
Spectral	Max	8	6
Spectral	Min	8	6
Spectral	Range	8	6
Spectral	Skewness	8	6
Spectral	Kurtosis	8	6
	Total	64	48

For all bands and spectral indices for both spectral datasets (UAS-SfM, PlanetScope), we extracted eight summary metrics per plot (Table 5.2). These values were aggregated from all pixels from all images that overlaid the plot. For the mean and standard deviation, pixels were weighted by fraction contained within the plot boundary. From the UAS data, 64 predictor metrics were extracted: Eight summary metrics for each of the five spectral bands and three spectral indices. From the PlanetScope

satellite data, 48 predictor metrics were extracted: Eight summary metrics for each of the four spectral bands and two spectral indices. This expanded on the spectral metrics per band utilized in Reilly et al. (2024), wherein we only extracted mean and standard deviation per band. We omitted the height-based spectral predictors utilized in that study since they were not found to significantly contribute to model performance.

2.4 Random forest modelling

The sets of previously described structural and spectral predictors were used to generate random forest models for each fuel parameter. Random forest functions by generating an ensemble of tree-based classifiers, trained on bootstrap subsets of the data, and aggregating the individual tree predictions (Breiman, 2001). This method was selected following previous findings demonstrating that random forest matched or outperformed other machine learning approaches in UAS-SfM models of canopy fuel parameters (Reilly et al., 2024). Random forest models were generated using every combination of structural and spectral predictor sets for a total of 128 models per canopy fuel parameter (42 structural only, 2 spectral only, 84 combinations of structural and spectral). This was performed to allow for the testing of each data source independently, along with all combinations of structural and spectral data types.

Table 5.3 Cross validation spatially-blocked group distance thresholds from spatial variogram partial sill range. Abbreviations given for those parameters whose names are truncated in the text. Taken from Reilly et al. (2024).

Parameter	Abbreviation	Partial sill range
Aboveground Biomass	-	44 m
Mean height	-	75 m
Canopy base height	CBH	266 m
Canopy cover	CC	513 m
Canopy bulk density	CBD	487 m
Leaf area index	LAI	103 m

Modelling was performed using caret and the random forest package in R (Cutler and Wiener, 2022; Kuhn et al., 2023). Prior to training, we centered and scaled predictor variables using caret's built-in function. Each model was trained with 100 replicates of 10 spatial fold cross validation with recursive

feature elimination (RFE). From a given input predictor set (e.g., complete set of structural, spectral, or combination predictors), we identified a subset of predictors to use in model training using caret's RFE function. RFE involves training the model initially with the full suite of available predictors than progressing reducing that number to identify the smallest predictor set that retains the highest possible accuracy. To remove the influence of spatial autocorrelation on our model, we generated spatially-blocked groupings of plots for each fuel parameter (Ploton et al., 2020, Pohjankukka et al., 2017, Wadoux et al., 2021). These groups contain all plots that fall within a given radius of one another, and therefore, are retained together at every testing and training cross validation split. We set this distance as described in Reilly et al. (2024) using the partial sill range of the spatial variogram, which is the distance at which autocorrelation ceases to influence the data (Table 5.3). The root mean squared error (RMSE) of the fuel predictions was used for model optimization. During training, MTRY, or the number of variables available to a given tree at each split within the ensemble that comprise a random forest model, was allowed to iterate over all values between two and the complete number of predictors. Following training, the model corresponding to the mtry with the lowest RMSE was selected. 1000 trees were generated for each model. Model variable importance by predictor categories (Tables 5.1 & 5.2) were calculated as the sum of all individual variable importances per category, which were then scaled to collectively add to 100%. See Reilly et al. (2024) for further details about the random forest modelling process.

For the purposes of this paper, "combination" refers to models built using one structural and one spectral predictor set (e.g., TLS structural and PlanetScope spectral), while "fusion" refers to predictors obtained from UAS-SfM and lidar data joined together prior to metric extraction (e.g., UAS-SfM and TLS fusion). A combination fusion model, therefore, consists of structural predictors extracted from the fusion of UAS-SfM and lidar combined with a set of spectral predictors from a single source.

3. Results

3.1 Datasets

Field measurements of fuel parameters exhibited patterns related to the site-specific species assemblage (Fig. 5.S1). Pepperwood, with its greater extent of open woodlands, consistently had among the lowest values across parameters, while Jackson, with its dominant redwood stands, had the highest. LaTour and Saddle Mountain exhibited measurements between these extremes. In our previous work in Reilly et al. (2024), we identified strong correlations ($r > 0.75$) among the horizontal fuel parameters of LAI, CBD, and canopy cover, and among the vertical fuel parameters of aboveground biomass, mean height, and CBH, but weak relationships ($r < 0.45$) between groups. See Reilly et al. (2024) for more details on field measurements.

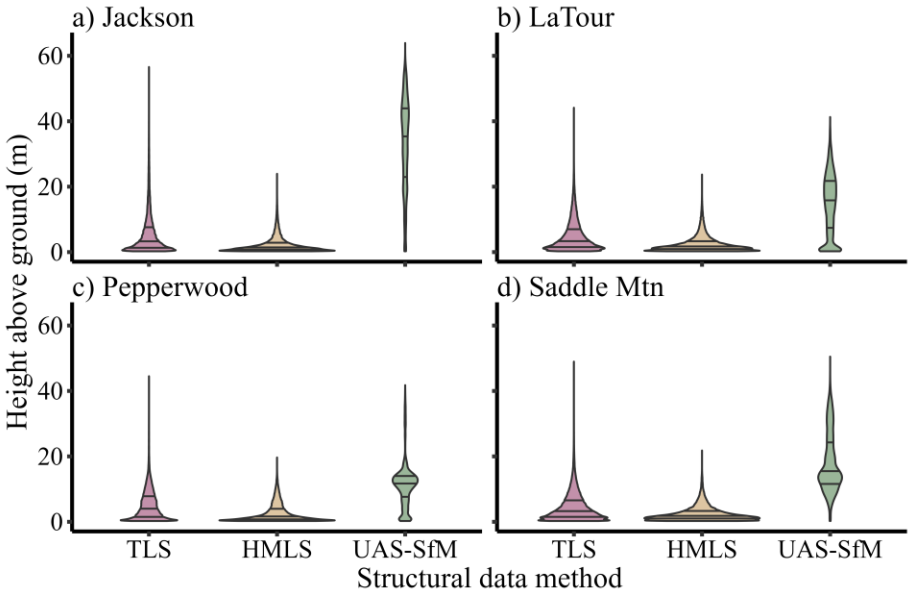


Fig. 5.4 Comparison of vertical distributions among strutural data methods. Horizontal bands represent 25th, 50th, and 75th percentiles, respectively. Violin plots scaled for equal area.

Structural data vertical distributions differed significantly among all three sensors (Fig. 5.4, Kruskal-Wallis $\chi^2 = 1.2 \times 10^6$, df = 2, $p < 0.001$). While significantly different from one another, the vertical distributions from the ground-based lidar methods of HMLS and TLS were similarly dominated by low lying points and demonstrated a consistent decay in density with increasing vertical height across

sites. The height of the respective distributions of these methods arose from their relative sensor power, with TLS able to penetrate much higher into the canopy than HMLS. In contrast, due to the difference between ground based and airborne acquisition, the vertical distribution of the UAS-SfM data reached a maximum density in the mid canopy. As a result, the UAS-SfM 25th percentile heights were higher than the 75th percentile heights for either lidar method across all sites.

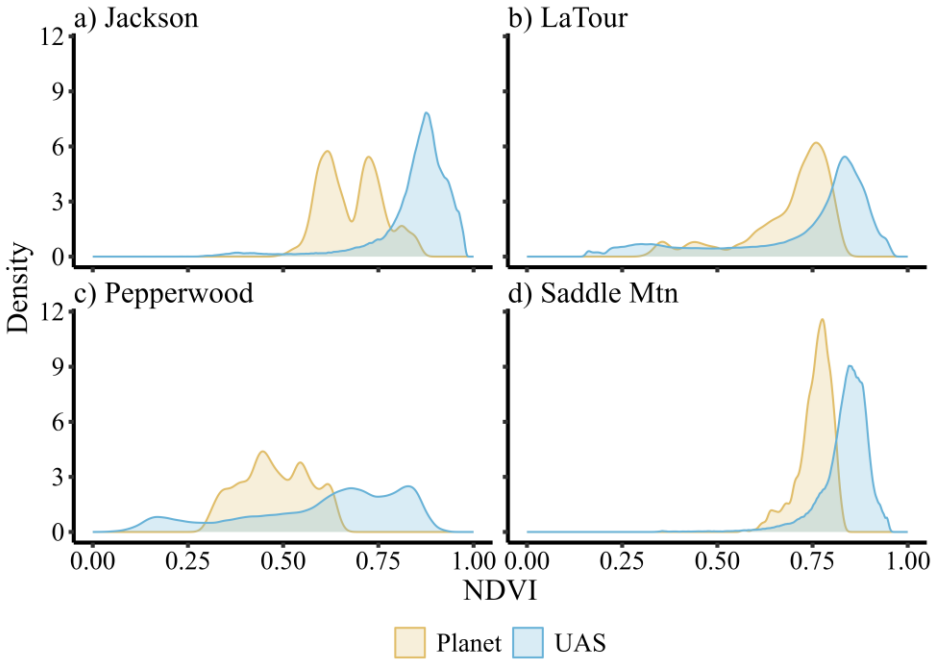


Fig. 5.5 Comparison of NDVI distributions between spectral data methods. Density values scaled such that the area under each curve sums to one.

Spectral data NDVI distributions also differed significantly between sensors (Fig. 5.5, Kruskal-Wallis $\chi^2 = 6968.2$, df = 1, $p < 0.001$). The distributions of PlanetScope NDVI measurements were consistently shifted towards lower values than those obtained from the UAS sensor. The UAS NDVI distributions from Pepperwood and LaTour, the sites with lower canopy cover, had pronounced left tails that were absent from high canopy cover sites of Jackson and Saddle Mountain. The PlanetScope NDVI distribution from LaTour had a similar left tail to the UAS distribution while the Pepperwood PlanetScope distribution did not. The PlanetScope data for Jackson displayed a bimodal distribution absent in the UAS data.

3.2 Model results

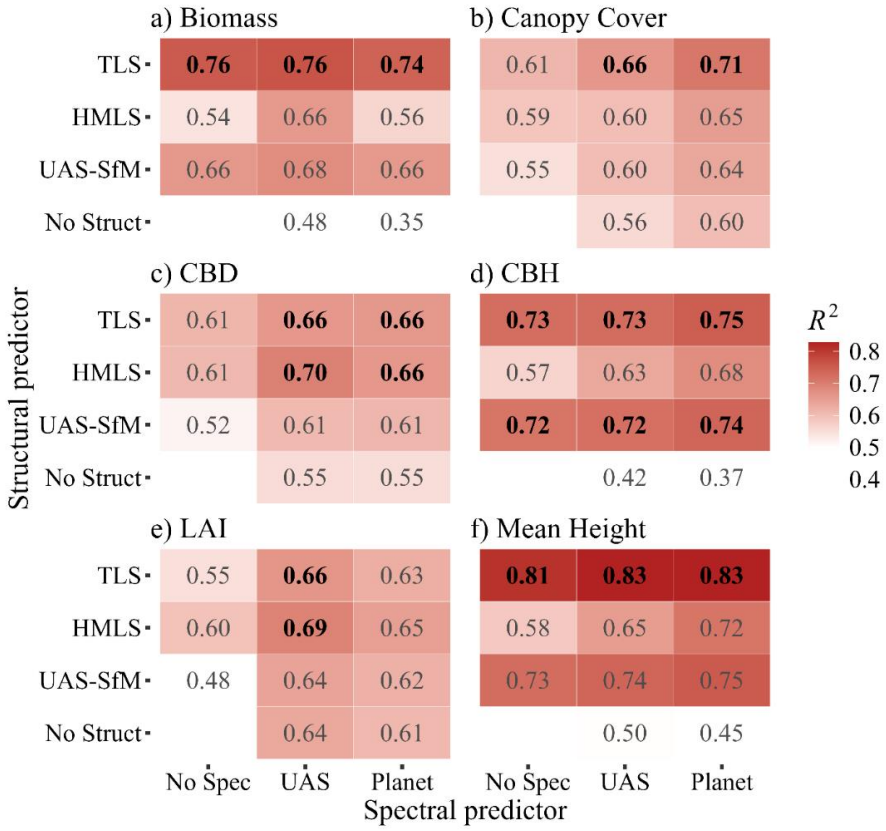


Fig. 5.7 Mean R^2 model performance metrics among structural and spectral predictor combinations. Structural predictors extracted using previously identified optimal voxel dimensions. Random forest models produced using 100 replicates of 10-fold cross validation using spatially-blocked groups. Black and bold values denote the statistically most accurate models per remote sensing method as determined by ANOVA at $\alpha = 0.05$. Multiple identified models per parameter denote statistically equivalent top performance metrics.

In comparisons between models produced using exclusively structural metrics, voxel-based models consistently matched or outperformed those models with raw point-cloud structural metrics (Fig. 5.S2). Likewise, the fusion of lidar and UAS-SfM datasets did not improve model performance beyond those obtained from single dataset structural predictors (Fig. S4). See supplement for complete analysis. Consequently, voxel-based single dataset predictors were used for all subsequent model analyses.

For the vertical fuel parameters, TLS outperformed the other structural methods for mean height and aboveground biomass, while UAS-SfM matched TLS performance for CBH (Figure 7). For mean height and aboveground biomass, UAS-SfM model performance was within 10% of that of the TLS model across all spectral combinations. The HMLS models only came within 10% of their TLS

counterpart for the structural and spectral CBH models but demonstrated a greater performance gap for all others in this parameter group. The addition of spectral data did not improve TLS or UAS-SfM model performance for any of these parameters. HMLS model accuracy, in contrast, did increase with the addition of spectral data. Spectral-only models exhibited low accuracy for all three vertical fuel parameters.

For the horizontal fuel parameters of canopy cover, CBD, and LAI, models including a combination of spectral and structural data significantly outperformed the structural or spectral only models (Fig. 5.7). For canopy cover, the combination of TLS structural data with either spectral data source returned the highest performance. Both HMLS and TLS structural with spectral models provided the highest accuracy for CBD, and there was again no difference between spectral data sources. For LAI, the top model performance was achieved by the UAS spectral predictors in combination with either the TLS or HMLS structural predictors. The PlanetScope spectral models were unable to match the UAS spectral performance for LAI. For all variations of structural predictors, including spectral only, there was less than a 5% difference in performance between UAS spectral and PlanetScope spectral models. All structural and spectral combined models returned accuracies within 11% of the top result. Spectral-only models attained accuracies within 15% of the top combined models, and within 5% for the UAS spectral LAI model. The combined UAS-SfM structure with UAS spectral model matched or outperformed the lidar structure only models across all three parameters.

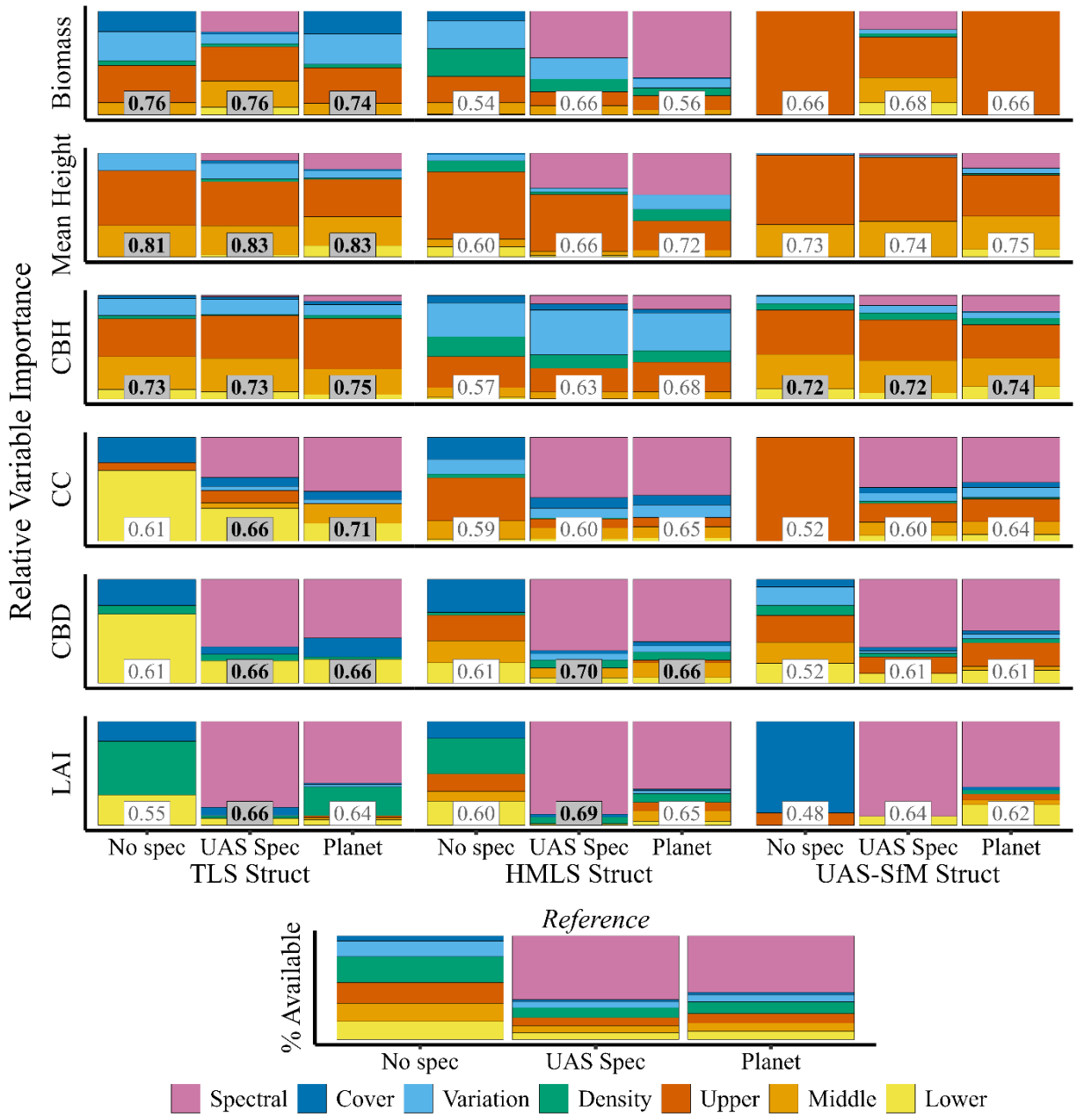


Fig. 5.8. Comparison of model relative variable performance for fuel parameters using TLS, HMLS, and UAS-SfM sensors, respectively. Box values denote mean model R^2 performance metric. Filled grey boxes with black text denote the statistically most accurate models per remote sensing method as determined by ANOVA at $\alpha = 0.05$. Multiple models per method denote statistically equivalent top performance metrics. Variable importance computed as the standardized sum of the contribution of all variables within a given category to the model. Reference diagram gives the relative distribution of variable categories if all variables weighted equally. Upper, middle, and lower categories represent height percentiles separated into thirds.

All three methods, particularly UAS-SfM and TLS, displayed distinct differences in variable selection between the vertical and horizontal fuel parameter groups (Fig. 5.8). For TLS, vertical parameter models relied predominantly upon structural predictors from the upper percentile, middle percentile, and variation categories (Fig. 5.8 – TLS Struct; Biomass, Mean Height, CBH). UAS-SfM models for vertical parameters relied almost exclusively on upper and middle height percentiles. Variable selection and performance for both sensors changed negligibly with the addition of spectral predictors. HMLS models, in contrast, utilized a wider range of predictor categories, including significant relative contributions from spectral variables for mean height and aboveground biomass, with no consistent pattern in structural predictor categories across these vertical fuel parameters (Fig. 5.7 – HMLS Struct; Biomass, Mean Height, CBH). The UAS-SfM and TLS models for CBH, the one parameter for which UAS-SfM matched TLS performance, displayed a high degree of similarity in variable selection. Despite CBH pertaining to the bottom of the canopy, models from both UAS-SfM and TLS methods utilized a mix of variables from the upper and middle percentile predictor categories. The HMLS model for CBH again differed in variable selection, utilizing predominantly variables pertaining to structural variation. This HMLS model for CBH had a lower relative variable importance of spectral predictors compared to the other vertical fuel parameters using this sensor, but the inclusion of these few spectral predictors still enhanced model performance.

In contrast, spectral variables contributed significantly to all models for the horizontal parameter group, both regarding performance and relative variable importance (Fig. 5.7 – CC, CBH, LAI). For LAI in particular, the models including UAS spectral predictors, which returned the highest model performance across all sensors, had minimal variable contributions from other predictor categories. TLS structural variable selection shifted to the lower percentile, cover, and density categories, with much smaller contributions from the upper and middle percentiles that had dominated the models for the vertical fuel parameters. Like before, HMLS models had no consistent pattern in the relative contribution of structural variable categories across horizontal fuel parameters. UAS-SfM displayed a similar variation in structural variable categories across the horizontal fuels parameter.

4. Discussion

The successful implementation of management interventions to reduce future wildfire hazard and restore fire's beneficial ecology role relies upon the availability of accurate data on fire fuel loads (Daum et al., 2024; Knight et al., 2022). Area-based machine learning models with predictors from remote sensors provide a means to meet these informational demands that is well suited to complex heterogenous forest landscapes, such as those that characterize California, USA. To this end, this study sought to explore a range of remote sensing approaches, and their combinations, to determine the limits of this approach in modelling vertical (aboveground biomass, CBH, mean height) and horizontal (canopy cover, LAI, CBD) canopy fuel parameters and quantify the reduction in accuracy associated with more accessible remote sensing methods. From these results, landowners, land managers, state personnel, and researchers can make informed decisions about which methods to employ to meet their specific project objectives and constraints.

4.1 Structural remote sensing methods

Among the structural predictors tested, models including TLS data performed the best across all vertical and horizontal fuel parameters. However, UAS-SfM models consistently returned accuracies within approximately 10% of TLS across all fuel parameters and matched the performance of TLS in modelling CBH. In contrast, HMLS models displayed greater variability, providing low accuracies for the vertical parameters but matching TLS for the horizontal parameters of LAI and CBD. For the vertical parameters, the TLS and UAS-SfM models predominantly relied upon metrics pertaining to the upper and middle canopy, especially for CBH and mean height. Consequently, the lower power of the HMLS sensor employed in this study, which had a limited range of 20 m, may have contributed to the poor performance of this method in comparison. Newer HMLS sensors extend this range to 100 m and have, therefore, demonstrated much greater performance in measuring tree height (Vandendaele et al., 2022).

In testing the optimal method for extracting predictors from the structural data, the voxel-based approach to metric extraction consistently matched or outperformed the point-based approach. This finding is consistent with prior research which identified that voxelization removes error, density variation, and artifacts from remotely sensed point cloud data (Eusuf et al., 2020; Hoffrén et al., 2024). In so doing, this approach serves to standardize the point clouds, thereby increasing the comparability among sensors (Lecigne et al., 2018). In regards to optimizing voxel size, smaller voxel dimensions are theoretically best suited for the mapping of fine-scale canopy detail (e.g., leaves, small branches), such as found in LAI, while larger voxel dimensions are better suited for capturing overall tree volume and structure (e.g., trunks, large branches), which is important in determining plot-level aboveground biomass and mean height (Lecigne et al., 2018). We found that the voxel dimensions with the highest model accuracies for both ground lidar methods align with these concepts, selecting small voxel dimensions for the horizontal parameters and larger dimensions for the vertical parameters. UAS-SfM models did not display a clear pattern in this regard but also exhibited lower variation in performance with voxel size. This is likely due to the more homogenous vertical distribution of UAS-SfM point clouds, in comparison to the ground and low vegetation dominated distribution from terrestrial lidar. Consequently, the vertical density distribution of voxels theoretically changes minimally for UAS-SfM with increasing voxel size, while the distribution from terrestrial lidar remains dominated by low elevation voxels for small voxel sizes but homogenizes at higher voxel sizes.

Fusing UAS-SfM and lidar datasets prior to predictor extraction did not improve model performance. Models built using these fused datasets returned accuracies comparable to that of the better performing constituent dataset, even for the fusion of UAS-SfM and HMLS. This aligns with the findings of Silva et al. (2023) who observed no difference in individual versus fusion TLS and ALS model performance for CBD in a pine forest. When processing the fusion datasets, voxelized predictors again matched or outperformed raw point cloud predictors. Additionally, there was minimal difference between utilizing complete datasets or decimating them to matching densities prior to joining them together. Since a voxel's presence is agnostic to the number of points that fall within that region in space, the voxelized

output of the raw and decimated fusion datasets should be meaningfully identical, especially at larger voxel sizes. This further highlights the standardization benefit of voxelization, especially across sensors.

The performance of the UAS-SfM model for CBH increased in comparison to our previous study results (Reilly et al., 2024). This change is likely due to the lower sample size in this study, constrained by the absence of TLS and HMLS scans at some plots. These missing samples predominantly came from Jackson, which, as the only redwood dominant site, has extreme values for all three parameters. Due to the consistent grouping of spatially-adjacent plots during the cross-validation assessment process, these missing plots would have always been in the same training/testing split for CBH, which has a high spatial autocorrelation distance. Since random forest is unable to extrapolate beyond the range of the training data, this group of extreme CBH values would have been poorly predicted by the model during testing in our original study, lowering model accuracy. Therefore, by removing these samples, the model performance increased markedly such that the UAS-SfM model was able to match the performance of TLS. This highlights the importance of sample range and study design, especially when investigating sites with wide ranges of parameter values.

4.2 Spectral remote sensing methods

While the spectral-only models had low accuracy for the vertical canopy fuel parameters, these models performed well for the horizontal fuel parameters in comparison to the highest accuracy achieved by the combination models. This was especially the case for LAI, for which the spectral models came within 5% of the highest performing model overall. This may be due to the fine scale nature of LAI. The aggregation of structural metrics to the plot scale likely renders this area-based structural approach poorly equipped to detect detailed canopy attributes like LAI, while spectral indices, which are directly related to plant physiology, still preserve a relationship to canopy attributes even when aggregated. For all horizontal parameter structural and spectral combination models, spectral predictors provided the greatest contribution to model performance, considering both improvement in model accuracy and overall variable importance. While the addition of spectral predictors did significantly improve the performance of HMLS

models for the vertical canopy parameters, it did not influence the performance of TLS or UAS-SfM based models for horizontal fuel parameters. The contribution of spectral metrics to HMLS model performance likely pertains to the previously discussed lower power of the HMLS sensor employed in this study, thereby providing a greater opportunity for spectral indices to contribute to the performance of a given model.

A significant difference existed between NDVI measurements obtained from the PlanetScope satellite and UAS sensors. The difference in values in likely a byproduct of the variation in band widths and overlap (Jiang et al., 2022). The PlanetScope satellite bands are significantly wider than those of the UAS Micasense RedEdge-MX sensor (MicaSense, 2020; Planet, 2019). As a result, Jiang et al. (2022) observed a ~30% RMSE difference between the PlanetScope and RedEdge-MX red bands. Despite this difference, less than a 5% difference existed between the performances of these two data sources across all models and data combinations. This suggests that, despite the differences in measured values, the two sensors were able to extract similar underlying trends and relationships across sites. Jiang et al. (2022) found higher similarities between the RedEdge-MX and data from other satellites, namely Landsat 8 and Sentinel-2, which suggests that these other instruments could be employed in a similar capacity to the PlanetScope data used in this study.

This finding of the comparability of performance between UAS-SfM and satellite spectral data presents a significant opportunity for future studies and management efforts. Satellite data from any of these sensors provides the capacity to generate fuels maps at any relevant landscape scale (e.g., Aragoneses and Chuvieco, 2021; Chuvieco et al., 2020). Since the addition of spectral data improved the models for all of the horizontal fuel parameters, regardless of structural data source, satellite data can fill a significant gap when multispectral UAS-SfM data are unattainable. Furthermore, the multispectral data from Planet satellite, let alone the even greater spectral resolution of other satellite sensors, could be used to augment UAS-SfM structural data collected with an RGB sensor, thereby mitigating the need for a more costly and rare multispectral sensor.

The UAS-SfM structural and UAS spectral combination models for the horizontal fuel parameters in this study exhibited a significant improvement in performance over our previously published model results (Reilly et al., 2024). Our previous study employed the use of height-based spectral predictors which proved to have little effect on model performance. Instead, this study employed a wider range of spectral summary statistics among the model predictor set, including the maximum and minimum values for each spectral band and index. Both the models for CBD and LAI, which demonstrated the greatest improvement in performance over the results from our previous study, utilized these end range statistics for NDVI, along with max NDRE for CBD, among the top predictor variables for the model. Future studies should explore additional indices or statistics to further improve model performance.

5. Conclusion

This study sought to assess the performance of area-based random forest models utilizing a range of remote sensing approaches for inputs to estimate horizontal and vertical canopy fuel parameters across diverse forest types in Northern California. To this end, we found that models with TLS structural predictors attained the highest performance across all fuel parameters. These TLS models attained R^2 between 0.75 and 0.83 for the vertical canopy parameters of aboveground biomass, CBH, and mean height, with no significant increase in performance with the addition of spectral predictors. In contrast, spectral data from either UAS or PlanetScope satellite sensors significantly improved TLS horizontal parameter model performance, attaining R^2 accuracies between 0.69 and 0.71 for the parameters of LAI, CBD, and canopy cover. However, due to the high labor and computational cost of TLS, it is not practical for implementation in most landscape-scale management settings and was include in this study in this way specifically to test the upper limits of this approach. Fortunately, UAS-SfM models, in combination with spectral predictors, only exhibited a maximum ~10% decline in performance, as compared to TLS, across all vertical and horizontal parameters, including matching TLS performance for CBH. Furthermore, both spectral predictors provided accuracies within ~15% of the combined models for the horizontal parameters, and within 5% for LAI.

As California scales up its restoration efforts to meet their million-acre annual goal, these remote sensing methods will become vital in informing targeted management to achieve maximum reduction in future fire hazard and in setting landscape management priorities (Daum et al., 2024; Herbert et al., 2022). Understanding the relative accuracies of these different approaches, and the costs associated with their use, can provide land managers and researchers with the tools they need to change the future of fire in California's forests. Future work should continue to expand and strengthen these models through the use of new technologies, statistical predictors, and larger sample sizes.

Authorship contribution statement

Conceptualization: S.R., L.P.B., and M.L.C.; Methodology: S.R., L.P.B., M.L.C., and I.O.; Investigation: S.R., M.L.C., L.P.B., and R.C.; Software: S.R. and M.L.C.; Formal analysis: S.R; Resources: M.L.C., and L.P.B.; Writing—original draft preparation: S.R.; Writing—review and editing: I.O., M.L.C., L.P.B., and R.C.; Visualization: S.R.; Supervision: I.O. and M.L.C.; Funding acquisition: L.P.B. and M.L.C. All authors have read and agreed to the published version of the manuscript.

Acknowledgements

Funding for this research was supported by CAL FIRE Forest Health and Forest Legacy (8GG18806) and California State University, Agricultural Research Institute (20-01-106) awards to L.P.B and M.L.C. S.R. was funded by the Rhodes Trust and through the University of Oxford Environmental Change Institute Small Grant Scheme. Pepperwood ground data collection was supported by funding from the Gordon and Betty Moore Foundation and National Science Foundation grants 1754475 and 1835086. We thank Lisa Micheli (Pepperwood Preserve), David Ackerly (UC Berkeley), Monica Delmartini (Saddle Mountain), Jason Poburko (LaTour), and Lynn Webb (Jackson) for granting us use of their sites and facilitating access to their datasets. We thank Ryan Ferrell, Michael O'Neil, Allison Kelly, Brieanne Forbes, Catherine Seel, Corbin Matley in collecting field data and Corbin Matley, Michelle Villasenor, and Natalie Hoover for their assistance in collecting UAS data. PlanetScope imagery were

acquired via the Commercial Smallsat Data Acquisition (CSDA) program through co-author Matthew Clark.

References

Ackerly, D., Oldfather, M., Halbur, M., Micheli, L., 2013. Establishment of woodland vegetation research plots at Pepperwood Preserve (Technical report for the Gordon and Betty Moore Foundation). Dwight Center for Conservation Science, Pepperwood, Santa Rosa, CA.

Ackerly, D.D., Kling, M.M., Clark, M.L., Papper, P., Oldfather, M.F., Flint, A.L., Flint, L.E., 2020. Topoclimates, refugia, and biotic responses to climate change. Front Ecol Environ 18, 288–297. https://doi.org/10.1002/fee.2204

Agee, J.K., Skinner, C.N., 2005. Basic principles of forest fuel reduction treatments. Forest Ecology and Management 211, 83–96. https://doi.org/10.1016/j.foreco.2005.01.034

Ager, A.A., Vaillant, N.M., Finney, M.A., 2010. A comparison of landscape fuel treatment strategies to mitigate wildland fire risk in the urban interface and preserve old forest structure. Forest Ecology and Management 259, 1556–1570. https://doi.org/10.1016/j.foreco.2010.01.032

Alonso-Rego, C., Arellano-Pérez, S., Guerra-Hernández, J., Molina-Valero, J.A., Martínez-Calvo, A., Pérez-Cruzado, C., Castedo-Dorado, F., González-Ferreiro, E., Álvarez-González, J.G., Ruiz-González, A.D., 2021. Estimating stand and fire-related surface and canopy fuel variables in pine stands using low-density airborne and single-scan terrestrial laser scanning data. Remote Sensing 13, 5170. https://doi.org/10.3390/rs13245170

Alonso-Rego, C., Fernandes, P., Álvarez-González, J.G., Arellano-Pérez, S., Ruiz-González, A.D., 2022. Individual-tree and stand-level models for estimating ladder fuel biomass fractions in unpruned Pinus radiata plantations. Forests 13, 1697. https://doi.org/10.3390/f13101697

Alonzo, M., Dial, R.J., Schulz, B.K., Andersen, H.-E., Lewis-Clark, E., Cook, B.D., Morton, D.C., 2020. Mapping tall shrub biomass in Alaska at landscape scale using Structure-from-Motion

photogrammetry and lidar. Remote Sensing of Environment 245, 111841. https://doi.org/10.1016/j.rse.2020.111841

Andersen, H.-E., McGaughey, R.J., Reutebuch, S.E., 2005. Estimating forest canopy fuel parameters using LIDAR data. Remote Sensing of Environment 94, 441–449. https://doi.org/10.1016/j.rse.2004.10.013

Aragoneses, E., Chuvieco, E., 2021. Generation and mapping of fuel types for fire risk assessment. Fire 4, 59. https://doi.org/10.3390/fire4030059

Arkin, J., Coops, N.C., Daniels, L.D., Plowright, A., 2023. Canopy and surface fuel estimations using RPAS and ground-based point clouds. Forestry: An International Journal of Forest Research cpad020. https://doi.org/10.1093/forestry/cpad020

Arroyo, L.A., Pascual, C., Manzanera, J.A., 2008. Fire models and methods to map fuel types: The role of remote sensing. Forest Ecology and Management 256, 1239–1252. https://doi.org/10.1016/j.foreco.2008.06.048

Beaty, R.M., Taylor, A.H., 2008. Fire history and the structure and dynamics of a mixed conifer forest landscape in the northern Sierra Nevada, Lake Tahoe Basin, California, USA. Forest Ecology and Management 255, 707–719. https://doi.org/10.1016/j.foreco.2007.09.044

Berbach, M., Cafferata, P., Schlosser, J., Eng, H., Robards, T., McDonald, S., Walters, D., Dreesmann, K., 1995. Latour Demonstration State Forest sustained yield plan. California Department of Forestry and Fire Protection.

Bogdanovich, E., Perez-Priego, O., El-Madany, T.S., Guderle, M., Pacheco-Labrador, J., Levick, S.R., Moreno, G., Carrara, A., Pilar Martín, M., Migliavacca, M., 2021. Using terrestrial laser scanning for characterizing tree structural parameters and their changes under different management in a Mediterranean open woodland. Forest Ecology and Management 486, 118945. https://doi.org/10.1016/j.foreco.2021.118945

Breiman, L., 2001. Random forests. Machine Learning 45, 5–32. https://doi.org/10.1023/A:1010933404324

Chávez-Durán, Á.A., García, M., Olvera-Vargas, M., Aguado, I., Figueroa-Rangel, B.L., Trucíos-Caciano, R., Rubio-Camacho, E.A., 2024. Forest canopy fuel loads mapping using unmanned aerial vehicle high-resolution red, green, blue and multispectral imagery. Forests 15, 225. https://doi.org/10.3390/f15020225

Chuvieco, E., Aguado, I., Salas, J., García, M., Yebra, M., Oliva, P., 2020. Satellite remote sensing contributions to wildland fire science and management. Curr Forestry Rep 6, 81–96. https://doi.org/10.1007/s40725-020-00116-5

Collins, B.M., Kramer, H.A., Menning, K., Dillingham, C., Saah, D., Stine, P.A., Stephens, S.L., 2013. Modeling hazardous fire potential within a completed fuel treatment network in the northern Sierra Nevada. Forest Ecology and Management 310, 156–166. https://doi.org/10.1016/j.foreco.2013.08.015

Collins, B.M., Miller, J.D., Thode, A.E., Kelly, M., van Wagtendonk, J.W., Stephens, S.L., 2009. Interactions among wildland fires in a long-established Sierra Nevada Natural Fire Area. Ecosystems 12, 114–128. https://doi.org/10.1007/s10021-008-9211-7

Cutler, F. original by L.B. and A., Wiener, R. port by A.L. and M., 2022. randomForest: Breiman and Cutler's Random Forests for Classification and Regression.

Dash, J.P., Pearse, G.D., Watt, M.S., 2018. UAV multispectral imagery can complement satellite data for monitoring forest health. Remote Sensing 10, 1216. https://doi.org/10.3390/rs10081216

Daum, K.L., Hansen, W.D., Gellman, J., Plantinga, A.J., Jones, C., Trugman, A.T., 2024. Do vegetation fuel reduction treatments alter forest fire severity and carbon stability in California forests? Earth's Future 12, e2023EF003763. https://doi.org/10.1029/2023EF003763

Dennison, P.E., Brewer, S.C., Arnold, J.D., Moritz, M.A., 2014. Large wildfire trends in the western United States, 1984-2011. Geophys. Res. Lett. 41, 2928–2933. https://doi.org/10.1002/2014GL059576

Dewberry, 2018. California FEMA F9 lidar report (No. G17PD00044).

Eng, H., 2015. Jackson Demonstration State Forest, California, United States of America, in: Forest Plans of North America. Elsevier, pp. 177–187. https://doi.org/10.1016/B978-0-12-799936-4.00021-7

Eusuf, M.S.R.S., Barton, J., Gorte, B., Zlatanova, S., 2020. Volume estimation of fuel load for hazard reduction burning: First results to a voxel approach. Int. Arch. Photogramm. Remote Sens. Spatial Inf. Sci. XLIII-B3-2020, 1199–1206. https://doi.org/10.5194/isprs-archives-XLIII-B3-2020-1199-2020

Evett, R.R., Dawson, A., Bartolome, J.W., 2013. Estimating vegetation reference conditions by combining historical source analysis and soil phytolith analysis at Pepperwood Preserve, Northern California Coast Ranges, U.S.A: Estimating vegetation reference conditions. Restor Ecol 21, 464–473. https://doi.org/10.1111/j.1526-100X.2012.00912.x

FIA, 2014. Regional biomass equations used by FIA to estimate bole, bark, and branches. U.S. Department of Agriculture Forest Service, Pacific Northwest Research Station.

Filippelli, S.K., Lefsky, M.A., Rocca, M.E., 2019. Comparison and integration of lidar and photogrammetric point clouds for mapping pre-fire forest structure. Remote Sensing of Environment 224, 154–166. https://doi.org/10.1016/j.rse.2019.01.029

Forbes, B., Reilly, S., Clark, M., Ferrell, R., Kelly, A., Krause, P., Matley, C., O'Neil, M., Villasenor, M., Disney, M., Wilkes, P., Bentley, L.P., 2022. Comparing remote sensing and field-based approaches to estimate ladder fuels and predict wildfire burn severity. Front. For. Glob. Change 5, 818713. https://doi.org/10.3389/ffgc.2022.818713

Forest Climate Action Team, 2018. California forest carbon plan: Managing our forest landscapes in a changing climate. Sacramento, CA.

Gale, M.G., Cary, G.J., Van Dijk, A.I.J.M., Yebra, M., 2021. Forest fire fuel through the lens of remote sensing: Review of approaches, challenges and future directions in the remote sensing of biotic determinants of fire behaviour. Remote Sensing of Environment 255, 112282. https://doi.org/10.1016/j.rse.2020.112282

García, M., Danson, F.M., Riaño, D., Chuvieco, E., Ramirez, F.A., Bandugula, V., 2011. Terrestrial laser scanning to estimate plot-level forest canopy fuel properties. International Journal of Applied Earth Observation and Geoinformation 13, 636–645. https://doi.org/10.1016/j.jag.2011.03.006

Griffith, G.E., Omernik, J.M., Smith, D.W., Cook, T.D., Tallyn, E., Moseley, K., Johnson, C.B., 2016. Ecoregions of California (Report No. 2016–1021), Open-File Report. Reston, VA. https://doi.org/10.3133/ofr20161021

Grznárová, A., Mokroš, M., Surový, P., Slavík, M., Pondelík, M., Merganič, J., 2019. The crown diameter estimation from fixed wing type of UAV imagery. Int. Arch. Photogramm. Remote Sens. Spatial Inf. Sci. XLII-2/W13, 337–341. https://doi.org/10.5194/isprs-archives-XLII-2-W13-337-2019

Haslem, A., Kelly, L.T., Nimmo, D.G., Watson, S.J., Kenny, S.A., Taylor, R.S., Avitabile, S.C., Callister, K.E., Spence-Bailey, L.M., Clarke, M.F., Bennett, A.F., 2011. Habitat or fuel? Implications of long-term, post-fire dynamics for the development of key resources for fauna and fire. Journal of Applied Ecology 48, 247–256. https://doi.org/10.1111/j.1365-2664.2010.01906.x

Herbert, C., Haya, B.K., Stephens, S.L., Butsic, V., 2022. Managing nature-based solutions in fire-prone ecosystems: Competing management objectives in California forests evaluated at a landscape scale. Front. For. Glob. Change 5, 957189. https://doi.org/10.3389/ffgc.2022.957189

Hillman, S., Hally, B., Wallace, L., Turner, D., Lucieer, A., Reinke, K., Jones, S., 2021a. High-Resolution Estimates of Fire Severity—An Evaluation of UAS Image and LiDAR Mapping Approaches on a Sedgeland Forest Boundary in Tasmania, Australia. Fire 4, 14. https://doi.org/10.3390/fire4010014

Hillman, S., Wallace, L., Lucieer, A., Reinke, K., Turner, D., Jones, S., 2021b. A comparison of terrestrial and UAS sensors for measuring fuel hazard in a dry sclerophyll forest. International Journal of Applied Earth Observation and Geoinformation 95, 102261. https://doi.org/10.1016/j.jag.2020.102261

Hoffrén, R., Lamelas, M.T., De La Riva, J., 2024. Evaluation of handheld mobile laser scanner systems for the definition of fuel types in structurally complex Mediterranean forest stands. Fire 7, 59. https://doi.org/10.3390/fire7020059

Hood, S.M., Varner, J.M., Jain, T.B., Kane, J.M., 2022. A framework for quantifying forest wildfire hazard and fuel treatment effectiveness from stands to landscapes. fire ecol 18, 33. https://doi.org/10.1186/s42408-022-00157-0

Jiang, J., Johansen, K., Tu, Y.-H., McCabe, M.F., 2022. Multi-sensor and multi-platform consistency and interoperability between UAV, Planet CubeSat, Sentinel-2, and Landsat reflectance data. GIScience & Remote Sensing 59, 936–958. https://doi.org/10.1080/15481603.2022.2083791

Kang, P., Lin, S., Huang, C., Li, S., Wu, Z., Sun, L., 2024. Revealing three-dimensional variations in fuel structures in subtropical forests through backpack laser scanning. Forests 15, 155. https://doi.org/10.3390/f15010155

Keane, R.E., Reinhardt, E.D., Scott, J., Gray, K., Reardon, J., 2005. Estimating forest canopy bulk density using six indirect methods. Can. J. For. Res. 35, 724–739. https://doi.org/10.1139/x04-213

Keeley, J.E., Bond, W.J., Bradstock, R.A., Pausas, J.G., Rundel, P.W., 2011. Fire in Mediterranean ecosystems: Ecology, evolution and management. Cambridge University Press, Cambridge. https://doi.org/10.1017/CBO9781139033091

Knight, C.A., Tompkins, R.E., Wang, J.A., York, R., Goulden, M.L., Battles, J.J., 2022. Accurate tracking of forest activity key to multi-jurisdictional management goals: A case study in California. Journal of Environmental Management 302, 114083. https://doi.org/10.1016/j.jenvman.2021.114083

Krause, P., Forbes, B., Barajas-Ritchie, A., Clark, M., Disney, M., Wilkes, P., Bentley, L.P., 2023. Using terrestrial laser scanning to evaluate non-destructive aboveground biomass allometries in diverse Northern California forests. Front. Remote Sens. 4, 1132208. https://doi.org/10.3389/frsen.2023.1132208

Kuhn, M., Wing, J., Weston, S., Williams, A., Keefer, C., Engelhardt, A., Cooper, T., Mayer, Z., Kenkel, B., R Core Team, Benesty, M., Lescarbeau, R., Ziem, A., Scrucca, L., Tang, Y., Candan, C., Hunt, T., 2023. caret: Classification and Regression Training.

Lecigne, B., Delagrange, S., Messier, C., 2018. Exploring trees in three dimensions: VoxR, a novel voxel-based R package dedicated to analysing the complex arrangement of tree crowns. Annals of Botany 121, 589–601. https://doi.org/10.1093/aob/mcx095

Marino, E., Montes, F., Tomé, J.L., Navarro, J.A., Hernando, C., 2018. Vertical forest structure analysis for wildfire prevention: Comparing airborne laser scanning data and stereoscopic hemispherical images. International Journal of Applied Earth Observation and Geoinformation 73, 438–449. https://doi.org/10.1016/j.jag.2018.07.015

MicaSense, 2020. RedEdge MX integration guide.

Miller, J.D., Safford, H., 2012. Trends in wildfire severity: 1984 to 2010 in the Sierra Nevada, Modoc Plateau, and Southern Cascades, California, USA. fire ecol 8, 41–57. https://doi.org/10.4996/fireecology.0803041

Miller, J.D., Skinner, C.N., Safford, H.D., Knapp, E.E., Ramirez, C.M., 2012. Trends and causes of severity, size, and number of fires in northwestern California, USA. Ecological Applications 22, 184–203. https://doi.org/10.1890/10-2108.1

North, M.P., Stephens, S.L., Collins, B.M., Agee, J.K., Aplet, G., Franklin, J.F., Fule, P.Z., 2015. Reform forest fire management. Science 349, 1280–1281. https://doi.org/10.1126/science.aab2356

Oldfather, M.F., Britton, M.N., Papper, P.D., Koontz, M.J., Halbur, M.M., Dodge, C., Flint, A.L., Flint, L.E., Ackerly, D.D., 2016. Effects of topoclimatic complexity on the composition of woody plant communities. AoB PLANTS 8, plw049. https://doi.org/10.1093/aobpla/plw049

Park, I.W., Mann, M.L., Flint, L.E., Flint, A.L., Moritz, M., 2021. Relationships of climate, human activity, and fire history to spatiotemporal variation in annual fire probability across California. PLoS ONE 16, e0254723. https://doi.org/10.1371/journal.pone.0254723

Planet Labs Inc, 2019. Planet imagery product specifications. Accessed 27 May 2024. https://assets.planet.com/docs/combined-imagery-product-spec-final-august-2019.pdf

Ploton, P., Mortier, F., Réjou-Méchain, M., Barbier, N., Picard, N., Rossi, V., Dormann, C., Cornu, G., Viennois, G., Bayol, N., Lyapustin, A., Gourlet-Fleury, S., Pélissier, R., 2020. Spatial validation reveals poor predictive performance of large-scale ecological mapping models. Nat Commun 11, 4540. https://doi.org/10.1038/s41467-020-18321-y

Pohjankukka, J., Pahikkala, T., Nevalainen, P., Heikkonen, J., 2017. Estimating the prediction performance of spatial models via spatial k-fold cross validation. International Journal of Geographical Information Science 31, 2001–2019. https://doi.org/10.1080/13658816.2017.1346255

Qi, Y., Coops, N.C., Daniels, L.D., Butson, C.R., 2022. Comparing tree attributes derived from quantitative structure models based on drone and mobile laser scanning point clouds across varying canopy cover conditions. ISPRS Journal of Photogrammetry and Remote Sensing 192, 49–65. https://doi.org/10.1016/j.isprsjprs.2022.07.021

Quantum Spatial, 2020. Carr Hirz Delta fires 2019 lidar processing report.

R Core Team, 2023. R: A language and environment for statistical computing.

Reilly, S., Clark, M.L., Bentley, L.P., Matley, C., Piazza, E., Oliveras Menor, I., 2021. The potential of multispectral imagery and 3D point clouds from unoccupied aerial systems (UAS) for monitoring forest structure and the impacts of wildfire in Mediterranean-climate forests. Remote Sensing 13, 3810. https://doi.org/10.3390/rs13193810

Reilly, S., Clark, M.L., Loechler, L., Spillane, J., Kozanitas, M., Krause, P., Ackerly, D., Bentley, L.P., Oliveras Menor, I., 2024. Unoccupied aerial system (UAS) Structure-from-Motion canopy fuel parameters: Multisite area-based modelling across forests in California, USA. Remote Sensing of Environment.

Reutebuch, S.E., Andersen, H.-E., McGaughey, R.J., 2005. Light detection and ranging (LIDAR): An emerging tool for multiple resource inventory. Journal of Forestry 7.

Rocha, K.D., Silva, C.A., Cosenza, D.N., Mohan, M., Klauberg, C., Schlickmann, M.B., Xia, J., Leite, R.V., Almeida, D.R.A. de, Atkins, J.W., Cardil, A., Rowell, E., Parsons, R., Sánchez-López, N., Prichard, S.J., Hudak, A.T., 2023. Crown-level structure and fuel load characterization from airborne and terrestrial laser scanning in a longleaf pine (Pinus palustris Mill.) forest ecosystem. Remote Sensing 15, 1002. https://doi.org/10.3390/rs15041002

Rollins, M.G., Keane, R.E., Parsons, R.A., 2004. Mapping fuels and fire regimes using remote sensing, ecosystem simulation, and gradient modeling. Ecological Applications 14, 75–95. https://doi.org/10.1890/02-5145

Roussel, J.-R., Auty, D., De Boissieu, F., Sánchez Meador, A., Jean-François, B., Demetrios, G., Steinmeier, L., Adaszewski, S., 2023. lidR: Airborne LiDAR Data Manipulation and Visualization for Forestry Applications.

Rundel, P.W., Arroyo, M.T.K., Cowling, R.M., Keeley, J.E., Lamont, B.B., Vargas, P., 2016. Mediterranean biomes: Evolution of their vegetation, floras, and climate. Annu. Rev. Ecol. Evol. Syst. 47, 383–407. https://doi.org/10.1146/annurev-ecolsys-121415-032330

Shaik, R.U., Laneve, G., Fusilli, L., 2022. An automatic procedure for forest fire fuel mapping using hyperspectral (PRISMA) imagery: A semi-supervised classification approach. Remote Sensing 14, 1264. https://doi.org/10.3390/rs14051264

Shin, P., Sankey, T., Moore, M., Thode, A., 2018. Evaluating unmanned aerial vehicle images for estimating forest canopy fuels in a ponderosa pine stand. Remote Sensing 10, 1266. https://doi.org/10.3390/rs10081266

Silva, C.A., Diego Rocha, K., Cosenza, D.N., Moha, M., Klauberg, C., Schlickmann, M.B., Xia, J., Leite, R.V., Almeida, D., Atkins, J.W., Cardil, A., Rowell, E., Parsons, R., Sánchez-López, N., Prichard, S.J., Hudak, A.T., 2023. Modeling crown-bulk density from airborne and terrestrial laser scanning data in a longleaf pine forest ecosystem, in: IGARSS 2023 - 2023 IEEE International Geoscience and Remote Sensing Symposium. Presented at the IGARSS 2023 - 2023

IEEE International Geoscience and Remote Sensing Symposium, IEEE, Pasadena, CA, USA, pp. 3094–3097. https://doi.org/10.1109/IGARSS52108.2023.10282833

Skowronski, N.S., Clark, K.L., Duveneck, M., Hom, J., 2011. Three-dimensional canopy fuel loading predicted using upward and downward sensing LiDAR systems. Remote Sensing of Environment 115, 703–714. https://doi.org/10.1016/j.rse.2010.10.012

Stefanidou, A., Gitas, I.Z., Katagis, T., 2022. A national fuel type mapping method improvement using sentinel-2 satellite data. null 37, 1022–1042. https://doi.org/10.1080/10106049.2020.1756460

Stephens, S.L., Foster, D.E., Battles, J.J., Bernal, A.A., Collins, B.M., Hedges, R., Moghaddas, J.J., Roughton, A.T., York, R.A., 2023. Forest restoration and fuels reduction work: Different pathways for achieving success in the Sierra Nevada. Ecological Applications e2932. https://doi.org/10.1002/eap.2932

Stephens, S.L., Ruth, L.W., 2005. Federal forest-fire policy in the United States. Ecological Applications 15, 532–542. https://doi.org/10.1890/04-0545

Sugihara, N.G., Barbour, M.G., 2006. Fire and California vegetation, in: Sugihara, N. (Ed.), Fire in California's Ecosystems. University of California Press, pp. xvi–9. https://doi.org/10.1525/california/9780520246058.003.0001

Sun, Z., Wang, Y., Ding, Z., Liang, R., Xie, Y., Li, R., Li, H., Pan, L., Sun, Y., 2023. Individual tree segmentation and biomass estimation based on UAV digital aerial photograph. J. Mt. Sci. 20, 724–737. https://doi.org/10.1007/s11629-022-7563-7

Szpakowski, D., Jensen, J., 2019. A review of the applications of remote sensing in fire ecology. Remote Sensing 11, 2638. https://doi.org/10.3390/rs11222638

Tompalski, P., White, J.C., Coops, N.C., Wulder, M.A., 2019. Quantifying the contribution of spectral metrics derived from digital aerial photogrammetry to area-based models of forest inventory attributes. Remote Sensing of Environment 234, 111434. https://doi.org/10.1016/j.rse.2019.111434

Van Wagner, C.E., 1977. Conditions for the start and spread of crown fire. Can. J. For. Res. 7, 23–34. https://doi.org/10.1139/x77-004

Vandendaele, B., Martin-Ducup, O., Fournier, R.A., Pelletier, G., Lejeune, P., 2022. Mobile laser scanning for estimating tree structural attributes in a temperate hardwood forest. Remote Sensing 14, 4522. https://doi.org/10.3390/rs14184522

Wadoux, A.M.J.-C., Heuvelink, G.B.M., de Bruin, S., Brus, D.J., 2021. Spatial cross-validation is not the right way to evaluate map accuracy. Ecological Modelling 457, 109692. https://doi.org/10.1016/j.ecolmodel.2021.109692

Watershed Sciences, 2016. Sonoma County vegetation mapping and lidar program: Technical data report.

Westoby, M.J., Brasington, J., Glasser, N.F., Hambrey, M.J., Reynolds, J.M., 2012. 'Structure-from-Motion' photogrammetry: A low-cost, effective tool for geoscience applications. Geomorphology 179, 300–314. https://doi.org/10.1016/j.geomorph.2012.08.021

Wilkes, P., Lau, A., Disney, M., Calders, K., Burt, A., Gonzalez de Tanago, J., Bartholomeus, H., Brede, B., Herold, M., 2017. Data acquisition considerations for Terrestrial Laser Scanning of forest plots. Remote Sensing of Environment 196, 140–153. https://doi.org/10.1016/j.rse.2017.04.030

Wu, X., Sverdrup, E., Mastrandrea, M.D., Wara, M.W., Wager, S., 2023. Low-intensity fires mitigate the risk of high-intensity wildfires in California's forests. Sci. Adv. 9, eadi4123. https://doi.org/10.1126/sciadv.adi4123

Zhang, W., Qi, J., Wan, P., Wang, H., Xie, D., Wang, X., Yan, G., 2016. An easy-to-use airborne LiDAR data filtering method based on cloth simulation. Remote Sensing 8, 501. https://doi.org/10.3390/rs8060501

Supplement

S1. Field data

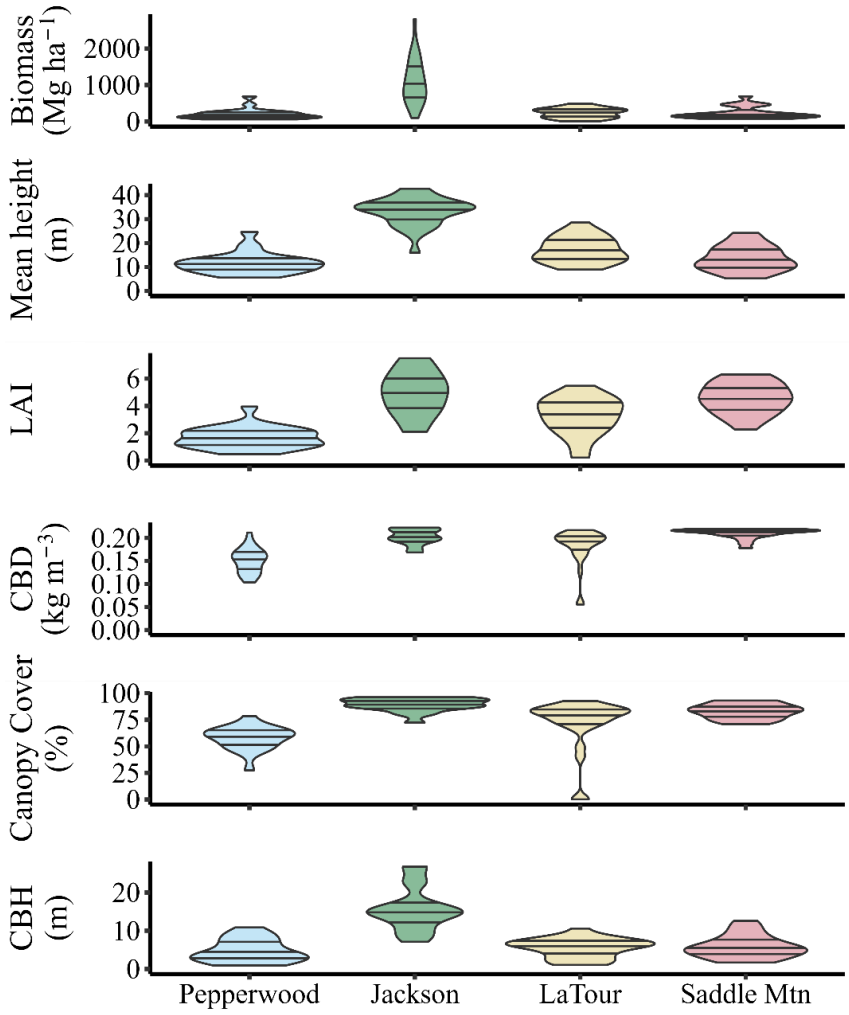


Fig. 5.S1 Distribution of field measurements of fuel parameters by site. Horizontal bands represent 25th, 50th, and 75th percentiles, respectively. Violin plots scaled for equal area within each canopy parameter comparison.

S2. Voxel vs point cloud predictor comparison

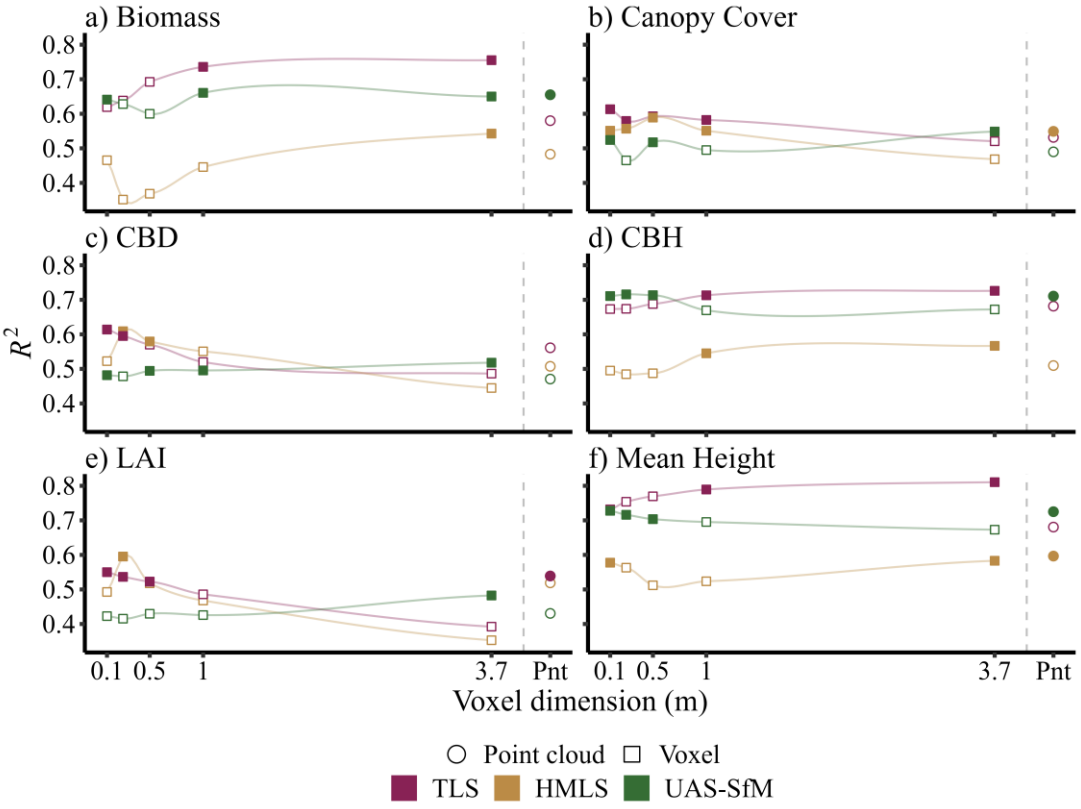


Fig. 5.S2 Comparison of point cloud (pnt) and voxel size model performance. Mean R^2 performance metrics obtained from random forest models produced using exclusively structural predictors extracted from raw point cloud and from various voxel dimensions. Models produced using 100 replicates of 10-fold cross validation using spatially-blocked groups. Solid shapes denote the statistically most accurate models per remote sensing method as determined by ANOVA at $\alpha = 0.05$. Multiple solid shapes per method denote statistically equivalent top performance metrics.

In general, optimal voxel dimension was inconsistent across fuel parameters. The voxel dimension selection for the two lidar methods consistently overlapped, while the UAS-SfM voxel selection differed.

TLS and HMLS models for the vertical parameters of aboveground biomass, CBH, and mean height performed best for larger voxel sizes, with the additional inclusion of the 0.1 m voxel model for mean height. In contrast, TLS and HMLS models for the horizontal parameters of canopy cover, CBD, and LAI performed best for smaller voxel sizes.

UAS-SfM models exhibited lower variation in model performance across voxel dimensions, especially for aboveground biomass, canopy cover, and CBD (Fig. 5.6). For all three of these metrics, both the largest and smallest voxel dimensions were statistically indistinguishable. CBH and mean height models both performed best at the smallest voxel dimensions, while LAI obtained the highest model accuracy at the largest voxel dimension.

S3. Structural data fusion

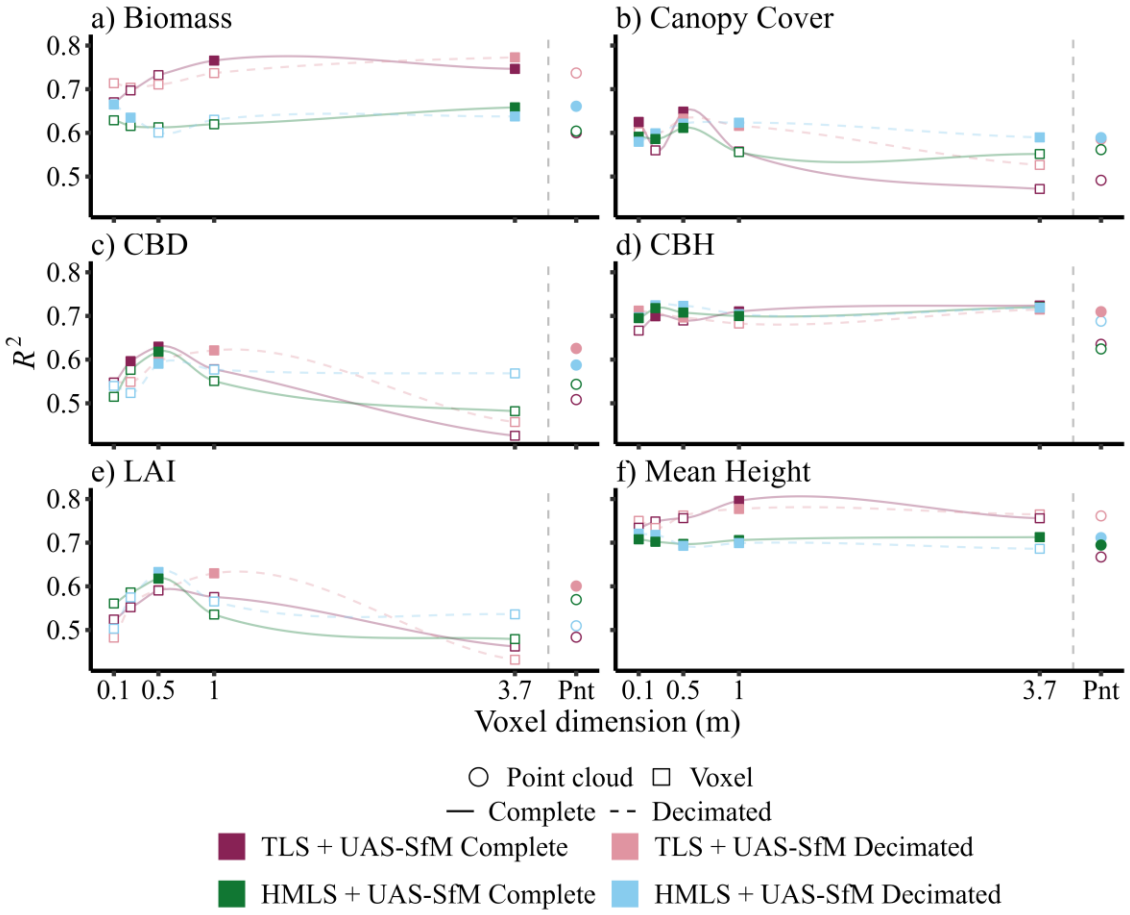


Fig. 5.S3 Comparison of point cloud and voxel size model performance for lidar and UAS-SfM fusion data. Mean R^2 performance metrics obtained from random forest models produced using exclusively structural predictors extracted from raw point cloud and from various voxel dimensions. Models produced using 100 replicates of 10-fold cross validation using spatially-blocked groups. Solid shapes denote the statistically most accurate models per remote sensing method as determined by ANOVA at $\alpha = 0.05$. Multiple solid shapes per method denote statistically equivalent top performance metrics.

As with the single dataset structural metric models, voxel-based models matched or outperformed point cloud-based models for all variations of the fusion data (Fig. 5.S3). Likewise, there were no significant differences between decimated and complete fusion data model performance for any of the canopy parameters, with the exception of TLS + UAS-SfM LAI. For this model, the decimated data outperformed its complete counterpart. On average, these models exhibited less variation with voxel size than the individual data models.

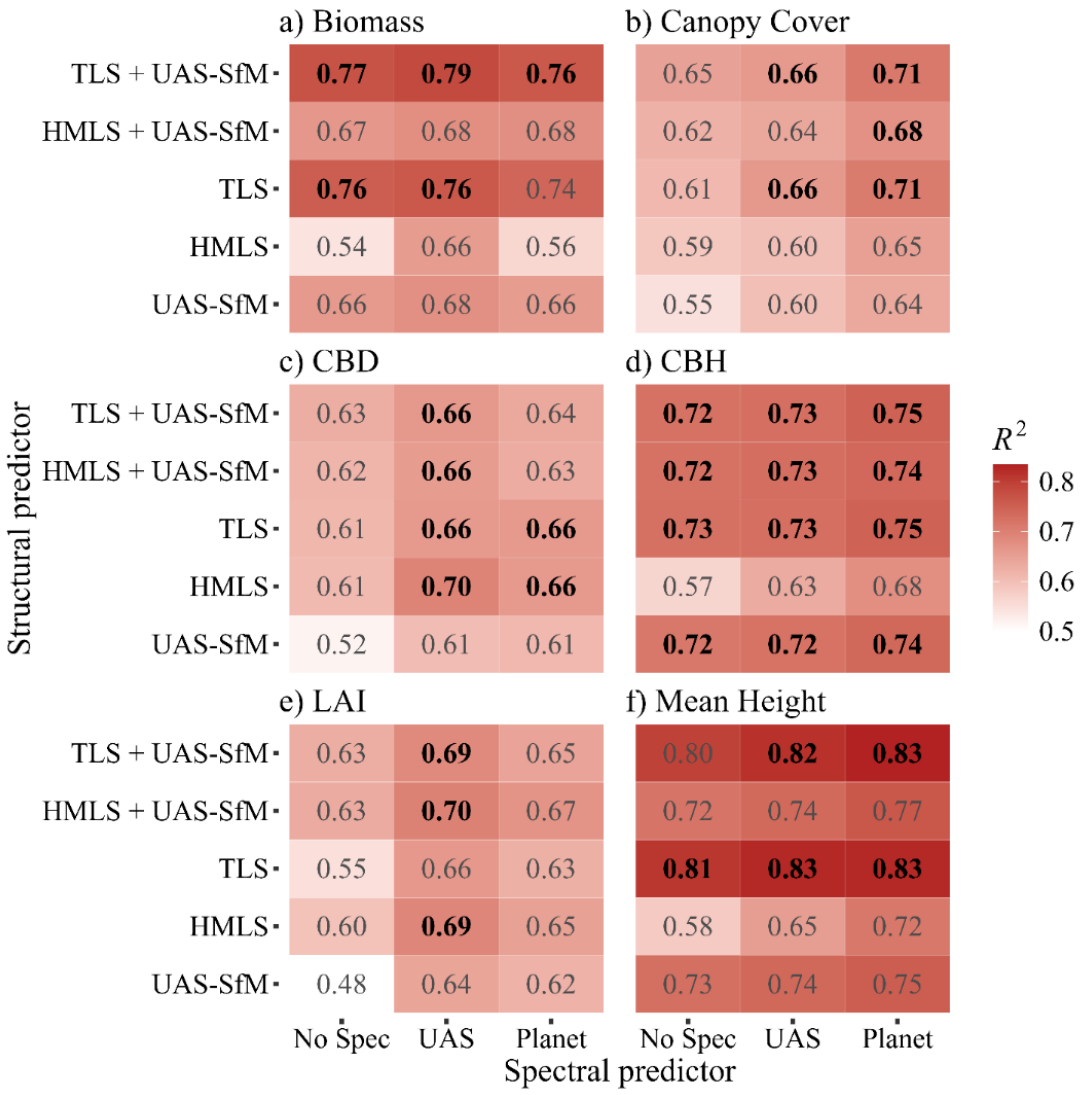


Fig. 5.S4 Mean R^2 model performance metrics among structural and spectral predictor combinations, including structural fusion datasets. Structural predictors extracted using previously identified optimal voxel dimensions. Random forest models produced using 100 replicates of 10-fold cross validation using spatially blocked groups. Black and bold values denote the statistically most accurate models per remote sensing method as determined by ANOVA at $\alpha = 0.05$. Multiple models per method denote statistically equivalent top performance metrics.

The addition of the lidar and UAS-SfM fusion data models did not substantially change the previous patterns of significance (Fig. 5.S4). The fusion data models did not outperform the single structural dataset predictor models for any of the canopy fuel parameters. These models performed comparably to whichever constituent datasets had the individual highest model performance, with the addition of the second dataset not meaningfully improving model performance. Only the HMLS + UAS-SfM structural predictor, PlanetScope spectral predictor model for canopy cover emerged as a significant model when neither of the individual structural predictors had previously been significant. Regarding models that had previously been significantly comparable to other top performance metrics, only the TLS structural, PlanetScope spectral model for aboveground biomass and the TLS structural, UAS spectral model for LAI lost significance with the addition of the structure fusion models.

Chapter 6

Synthesis

1. Thesis motivation

As has been consistently emphasized throughout this thesis, the body of work presented herein sought to address an information gap in the mitigation of wildfire hazard in California, with the goal of assisting in one portion of the work that needs to be done to restore the beneficial ecological role of fire in California's forest ecosystems. The impetus for this thesis arose from the 2018 California Climate Change Assessment which repeatedly identified the need for "bridging the gap between researchers and practitioners" and developing new tools to inform better decision making around forest management (Bedsworth et al., 2018). The methods, effectiveness, and costs of landscape fuel reduction treatments are well established (Stephens et al., 2023) and the state government has made the necessary commitments to support these efforts at scale (Knight et al., 2022). The effectiveness of this work, however, depends significantly on the ability to target these efforts systematically based on information on forest fuel loading (Ager et al., 2010; Collins et al., 2013; Daum et al., 2024). Prior to beginning this work, there was a lack of knowledge on how land managers, owners, and state personnel in California use information in fire hazard mitigation decision making and what attributes of a data source would render it operationalizable in their efforts. This thesis, therefore, sought to understand these informational needs and investigate a canopy fuel remote sensing method to address their requirements and constraints.

2. Results

Prior to investigating remote sensing methodologies for mapping fire fuel loads, I explored how land managers make decisions around treatments for fire hazard mitigation, and, specifically, the role of information within these processes. This work, presented in my first study, provides a critical framework through which any remote sensing method may be evaluated. Regardless of the accuracy of a fuel mapping method or the scientific interest it generates, it cannot meaningfully influence conditions on the ground if it does not align with the needs and limitations of the land managers who will utilize this research in guiding their efforts. To that end, this study employed a fuzzy cognitive mapping methodology to capture the perspectives of landowners, managers, and fire professionals in Napa and

Sonoma counties of California, USA. From these interviews, priority setting emerged as the key driver of management outcomes. Improving the success of these outcomes in the future hinges on collective priority setting and the reduction in barriers towards cohesive action and collaboration between disparate groups.

Within these decision-making paradigms, information and expert consultation consistently played an important role in the overall system, but there was minimal consensus between participants on what source of information they utilized. However, two themes did consistently determine the usefulness of an information source. The most significant theme was accessibility and ease of use. Landowners described feeling excluded by technical jargon or "fire world language." Likewise, participants identified needing to share and access data without a high personal technical capacity. Even professional land managers eschewed technical data collection for walking the land when working with landowners. The second significant theme that emerged was the importance of data time and scale. Information must be delivered rapidly and cover a sufficiently large spatial extent to inform management efforts attempting to keep pace with the frequency of annual fires.

While these more informal approaches for information gathering have proved serviceable until now, they cannot scale to support the significant increase in yearly treatment extent that needs to be undertaken to restore California's forests and their historical fire regime. Consequently, there is a need to bridge the gap between local land managers with limited technical capacity, both in regard to capability and resources, and the potential of landscape scale datasets to appropriately direct management efforts for maximum effectiveness. To that end, one interviewee highlighted the value of aerial imagery and mapping to create a sense of collective effort. This suggests the potential of remote sensing to provide widescale information to support decision-making, dependent upon a method's ease of collection and the delivery of results in a readily accessible format to minimize resource and capacity limitations.

Of the emerging remote sensing methods, unoccupied aerial system Structure-from-Motion (UAS-SfM) appeared to provide the greatest potential for meeting these demands. It is relatively inexpensive compared to lidar methods at a stand scale while retaining the ability to directly measure

structure, unlike satellite data. In addition, it can provide aerial imagery and continuous map outputs that ground based methods lack, thereby helping to minimize the technical barriers to understanding that preclude the use of other methods. However, the capability of this method had not yet been assessed in California

Therefore, in my second paper, I sought to assess whether UAS-SfM could provide meaningful measurements of forest attributes in the structurally complex and diverse forests that characterize California's ecosystems. Specifically, I developed and tested a processing workflow to enable the extraction of structural and spectral metrics from this method. Prior to this study, UAS-SfM had been primarily been tested in conifer forests or forests without complete canopy cover (e.g., Alonzo et al., 2018; Belmonte et al., 2019; Shin et al., 2018). The workflow developed in this study consisted of ground finding cloth simulation filter parameterization, airborne lidar (ALS) alignment, height normalization, and metric extraction using tools within the lidR R package (Roussel et al., 2023; Zhang et al., 2016). This work established that UAS-SfM cannot identify sufficient ground points in closed canopy forests for height normalization, the first stage of canopy metric extraction. Consequently, I developed a workflow for aligning and height normalizing UAS-SfM to digital terrain models (DTMs) obtained from ALS.

The UAS-SfM metrics extracted using this workflow demonstrated close similarity to ALS upper canopy measurements, and that this relationship diminished for lower or below canopy measurements. I used these findings to assess the persistent impact on forest health and structure from a major fire as a demonstration of the long-term monitoring possibilities of these data. Max height and bulk canopy height exhibited minor but significant changes. Canopy health, assessed through the proxy of the normalized difference vegetation index (NDVI), however, displayed large persistent depression with increasing burn severity. These findings highlight the additional analytical capabilities that the inclusion of spectral data with UAS-SfM provides over lidar.

The establishment of this workflow and the validation of the metrics extracted via this method paved the way for my third paper, wherein I applied UAS-SfM metrics to the machine learning modelling of fuel parameters. Due to the previous finding that UAS-SfM possessed little capability to detect below

canopy structure, I focused on canopy fuel parameters. These consisted of above ground biomass, canopy base height (CBH), mean canopy height, leaf area index (LAI), canopy bulk density (CBD), and canopy cover. Together, these represent important forest attributes for canopy torching and sustained ignition, along with metrics for monitoring and informing management interventions. The first major finding from this paper was the identification of two distinct groupings of parameters which I categorized into horizontal (LAI, CBD, cover) and vertical (biomass, CBH, mean height) fuels. These categories emerged from correlations in the field data, but persisted strongly throughout the modelling results from this paper and the next.

For the modelling, I tested a suite of machine learning algorithms to determine if there was a difference in performance across methods. While random forest performed marginally better than the alternatives, the variation in performance was minimal between random forest, support vector machine, and the forward linear models. Model accuracy did differ markedly between the two parameter groups. The vertical canopy parameters returned R^2 values between 0.69 and 0.75, while the horizontal parameters returned R^2 values between 0.49 and 0.59. Figure seven from this paper provided a demonstration of the mapping capability of this modelling approach, showcasing the output from this method that most closely satisfies the information requirements identified in the first study. Unfortunately, our attempt at transferring this model to a novel site demonstrated a significant decline in predictive performance for horizontal fuels.

The result that I found the most exciting at the time of discovery from this thesis was the variable selection differences between the two parameter groups. I did not anticipate the severity of the separation in variable selection between these groups. Machine learning receives the frequent critique of being a "black box" since it is not possible to extract the relationships between predictors and outcomes as one can with linear models. These findings, however, speak strongly to the biological underpinnings of the relationships the models discovered between attributes of the UAS-SfM data and the fuel parameters they modeled. The model for CBH, in particular, demonstrated the power of these machine learning techniques in overcoming the inherent weaknesses of a remote sensing approach. This model was able to perform

well for an attribute that UAS-SfM could not measure directly by leveraging the relationship in canopy structure between canopy base and mean heights.

While these model performances were interesting on their own, they needed to be placed in context of the suite of available remote sensing approaches to have scale. I also wished to disentangle the capability of the area-based remote sensing approach utilized in this study from the detection limitations of the UAS-SfM method. Lastly, the dominance of spectral metrics in the horizontal fuels models suggested to me that satellite spectral sensor may be able to achieve comparable results, which would be a highly significant finding due to the removal of data acquisition effort or expense.

Together, these lines of questioning led to the final paper of my thesis which sought to explore the limits of area-based random forest models across a suite of structural and spectral remote sensing methods. In this final paper, I tested random forest models built using metrics extracted from terrestrial laser scanning (TLS), handheld mobile laser scanning (HMLS), UAS-SfM, and PlanetScope satellite spectral. For the structural datasets, I extracted metrics from a range of processing workflows related to voxelization and data fusion. I then produced models using all combinations of structural and spectral data for a total of 128 models per canopy fuel parameter.

Models built using TLS returned the consistently highest performance, as expected due to the exceptionally high resolution of TLS data. However, UAS-SfM returned model accuracies within 10% of TLS for all parameters, including matching TLS performance for CBH. HMLS model performance proved highly variable and the fusion of UAS-SfM with either terrestrial lidar method did not improve model performance. The addition of spectral data did not change TLS or UAS-SfM vertical fuel parameter model accuracy but did contribute significantly to the performance of all horizontal canopy fuel models. There was less than a 5% difference between PlanetScope satellite spectral models and UAS spectral predictor models.

Together, these results suggest that area-based random forest models built using predictors extracted from UAS-SfM are well suited for meeting the informational needs of land managers and landowners in their management decision making around fuels reduction treatments. This method came

close to matching the performance of models built using TLS, the highest standard in forestry structural remote sensing, but at a fraction of the cost and with the ability to provide continuous large spatial coverage. With the advent of new UAS technologies like the Wingtra vertical takeoff fixed wing, these data will only become more accessible over larger areas in the future.

3. Limitations and future directions

3.1 Connecting research to practitioners

Despite the progress made in this thesis, a significant gap persists between the research presented herein and practitioners' access to these methods and data. Based on the results of the interviews, none of the interviewees expressed the capacity to collect or process these types of data. This study was further removed from their access by the use of a multispectral sensor, which is significantly more expensive, rarer, and difficult to process than a traditional RGB sensor. However, models built using PlanetScope satellite spectral data, in conjunction with UAS-SfM structural data, performed comparably to fully UAS-SfM models. Therefore, this suggests the results in this study could be replicated at lower cost using UAS-SfM structural data obtained using an RGB sensor and supplementing these data with satellite spectral metrics.

The gap remains, however, to connect the collection of UAS imagery, a largely automated process accessible to practitioners, with the technical processing workflow required to generate the prediction maps presented here. While this thesis used commercial PIX4D SfM software, open source SfM software does exist (OpenSfM). Valuable future work should focus on the development of easily accessible tools with an automated processing pipeline to take user supplied imagery through orthomosaic imagery generation and finally to fuels modelling and mapping.

Due to the significant decline in accuracy observed in the novel site transfer, however, the models within this tool will need to be carefully geographically constrained to prevent their misuse. This limitation can further be addressed by significantly expanding the sample size used for model training. As demonstrated in the last paper, LAI can be well modelled by spectral variables alone even at the sample

size used in this study. Kang et al. (2021) successfully modelled LAI at significantly higher accuracy (R^2 = 0.88) using Landsat across the continental United States from a dataset of 1.6 million points derived from other satellite products. Through expanding the sampling network underlying this work, similarly robust models can hopefully be developed in the future to enhance the ability of these tools when applied to novel areas.

3.2 Tree delineation



Fig. 6.1. Cluster of oak trees at Pepperwood. Note the number of trunks beneath one continuous canopy. Variation in leaf coloring due to the presence of multiple oak species within this cluster.

As discussed in the introductions of the third and forth papers, the work in this thesis employed an area-based approach due to the challenges of tree delineation in the complex forests that dominated the study sites, in particular Pepperwood and Saddle Mountain. However, this approach is inherently limited regarding maximum achievable accuracy. UAS-SfM has been demonstrated to have the capacity to generate highly accurate estimates of aboveground biomass beyond the performance achieved in this thesis when computed at the individual tree level (e.g., Alonzo et al., 2018; Navarro et al., 2020). In addition, Alonzo et al., (2018) successfully utilized UAS-SfM data with segmented tree crowns to classify tree type, a result that could not be achieved with lidar data alone. Beyond improved modelling accuracy, successful individual tree crown segmentation opens many new avenues of research that are not possible

using area-based approaches. For example, in the second study, the post-fire impact analysis was limited to examining widespread changes in a limited number of metrics related to maximum canopy height. With segmented UAS-SfM data, this analysis could be extended significantly to track individual tree and species level recovery following fire and other disturbance events. This could significantly improve managers' ability to undertake proactive management given specific long-term restoration objectives.

To my knowledge, no studies have attempted to conduct tree segmentation on UAS-SfM data from the mixed forests and woodlands of Mediterranean California. Most prior work, such as the previously mentioned research on biomass, segmented crowns from UAS-SfM data either manually or through the use of a watershed algorithm applied to a canopy height model (e.g., Alonzo et al., 2018; Mohan et al., 2017; Shin et al., 2018). This algorithm identifies local maxima in the point cloud and segments trees by descending from this point until it reaches a boundary originating from a neighboring maximum or reaches a ceiling window size. This algorithm works well in the conical conifer forests that have dominated these previous studies but is ineffectual in the undulating canopies of the oak forests of Mediterranean California and the study sites Pepperwood and Saddle Mountain in particular.

My original proposal for my final paper involved developing a four-band neural network for tree segmentation. DeepForest, a CNN model produced by researchers at the University of Florida, has demonstrated acceptable precision and recall across a wide range of forest types including oak forests (Weinstein et al., 2020). However, this model and the many others presented in the current literature utilize preexisting RGB segmentation backbones such as ResNET or U-NET or point based CNN models such as PointNet++ (e.g., Ayhan and Kwan, 2020; Gupta et al., 2020; Korznikov et al., 2021; Safonova et al., 2021). My idea was to extend the RGB model from Weinstein et al. (2020) to accept additional structural rasters extracted from the UAS-SfM point cloud (Hassan, 2019). I spent several months working on this project before having to abandon it due to data quality. Without significant time and resources, I could not find a way to generate a sufficiently large and reliable training dataset. Dr. Clark at Sonoma State University tasked his students with manually delineating tree crowns from aerial imagery while I attempted to generate a training dataset using data from the National Ecological Observatory

Network. However, even to the naked eye, the mass of oak forests defies delineation (Fig. 6.1). Eventually, I moved on to the final paper presented here after determining that I could not trust the training data we had developed. However, if, in the future, someone can develop a training dataset of sufficient quality, I believe this approach could provide a significant new avenue for research.

3.3 Subcanopy fuels and other data sources

A significant limitation to the approach explored in this thesis is the inability to measure surface and ladder fuels. This is a significant gap in the remote sensing literature as a whole due to the challenge it presents (Gale et al., 2021). While I did not test whether UAS-SfM could measure these fuel types beyond the inclusion of the ALS metric for ladder fuels in my first study, any model that claims to do so must be examined critically. Due to canopy occlusion, in high canopy cover forests these models would only be able to assess subcanopy fuels through their relationship to top of canopy structure, similar to how our model for CBH approximated this value through upper canopy metrics. However, while CBH is a parameter of the canopy and, therefore, directly linked to the upper canopy, surface fuels inherently are not. Instead, these models would be performing an approximation of the assignment of fuel class models for which there is already a significant body of research (Hoffrén et al., 2023a, e.g., 2024). I cannot envision a method by which this limitation of UAS-SfM could be circumvented. Instead, future work in modelling these fuels will likely need to explore lidar based methods.

The studies presented here did not extensively explore ALS. The cost argument for UAS-SfM pertains most significantly at plot to stand scales. At scales beyond this extent, the manual effort required to collect UAS-SfM imagery becomes prohibitively expensive and time consuming. Beyond these limits, such as at the scale of a county or a national forest, ALS becomes a more viable remote sensing option. However, the collection of these data is still extremely expensive and, therefore, faces significant barriers to its acquisition. I was unable to explore ALS more fully because, while it existed for the entire study area, the age of the data at Saddle Mountain and Pepperwood, compounded by major disturbance from the

Tubbs Fire, was such that it was no longer relevant. This speaks to the time limitation that arose during the first interview study and will always limit the utility of ALS for fuels mapping in operational contexts.

UAS lidar can provide tenfold higher point density compared to the ALS data utilized in this thesis with lower acquisition and processing times as compared to UAS-SfM (Hillman et al., 2021). In direct measurement methodologies, UAS lidar has been demonstrated to possess significantly greater capacity to detect subcanopy structures than UAS-SfM and, therefore, could provide a means to measure surface and ladder fuels (e.g., Harder et al., 2020). However, Arkin et al. (2023) found UAS-SfM based models of height and CBH outperformed their UAS lidar counterparts in Douglas fir forests. Based on how well UAS-SfM performed in relation to TLS in the final study, I would not expect UAS lidar to significantly outperform UAS-SfM models for other canopy parameters either. However, future work should explore the capacity of this method to measure surface and ladder fuels, especially considering the rapidly declining price of this technology.

Finally, and perhaps most significantly, future work should explore the capabilities of spaceborne lidar, such as the Global Ecosystem Dynamics Investigation (GEDI) sensor on the International Space Station. These data can be acquired globally for free and, therefore, would completely remove many of the acquisition barriers identified in the interview study. These data have been demonstrated to perform well at modelling LAI in conifer forests (Wang et al., 2023), fuel type classification (Hoffrén et al., 2023b), and modelling canopy heights in tropical forests (Geremew et al., 2023), among others.

4. Conclusion

This thesis established the foundation for using UAS-SfM area-based random forest models to map canopy fuel parameters. This technology is well suited to inform land managers, landowners, and fire professionals in their priority setting and, therefore, improve fuels treatment management outcomes. In this research, UAS-SfM has been demonstrated to provide a means to generate widespread area maps at high accuracy, close in performance to the highest accuracy obtained by TLS. Through the widespread implementation of these methods to guide California's extensive commitment to fuels treatment, there is

hope that future fire hazard can be reduced sufficiently to restore fire to its ecological role as a landscape shaping driver of biodiversity throughout the state.

References

Ager, A.A., Vaillant, N.M., Finney, M.A., 2010. A comparison of landscape fuel treatment strategies to mitigate wildland fire risk in the urban interface and preserve old forest structure. Forest Ecology and Management 259, 1556–1570. https://doi.org/10.1016/j.foreco.2010.01.032

Alonzo, M., Andersen, H.-E., Morton, D., Cook, B., 2018. Quantifying boreal forest structure and composition using UAV Structure-from-Motion. Forests 9, 119. https://doi.org/10.3390/f9030119

Arkin, J., Coops, N.C., Daniels, L.D., Plowright, A., 2023. Canopy and surface fuel estimations using RPAS and ground-based point clouds. Forestry: An International Journal of Forest Research cpad020. https://doi.org/10.1093/forestry/cpad020

Ayhan, B., Kwan, C., 2020. Tree, Shrub, and Grass Classification Using Only RGB Images. Remote Sensing 12, 1333. https://doi.org/10.3390/rs12081333

Bedsworth, L., Cayan, D., Franco, G., Fisher, L., Ziaja, S., 2018. Statewide summary report (No. SUMCCCA4-2018– 013). California's Fourth Climate Change Assessment.

Belmonte, A., Sankey, T., Biederman, J.A., Bradford, J., Goetz, S.J., Kolb, T., Woolley, T., 2019. UAV-derived estimates of forest structure to inform ponderosa pine forest restoration. Remote Sensing in Ecology and Conservation n/a. https://doi.org/10.1002/rse2.137

Collins, B.M., Kramer, H.A., Menning, K., Dillingham, C., Saah, D., Stine, P.A., Stephens, S.L., 2013. Modeling hazardous fire potential within a completed fuel treatment network in the northern Sierra Nevada. Forest Ecology and Management 310, 156–166. https://doi.org/10.1016/j.foreco.2013.08.015

Daum, K.L., Hansen, W.D., Gellman, J., Plantinga, A.J., Jones, C., Trugman, A.T., 2024. Do vegetation fuel reduction treatments alter forest fire severity and carbon stability in California forests? Earth's Future 12, e2023EF003763. https://doi.org/10.1029/2023EF003763

Gale, M.G., Cary, G.J., Van Dijk, A.I.J.M., Yebra, M., 2021. Forest fire fuel through the lens of remote sensing: Review of approaches, challenges and future directions in the remote sensing of biotic determinants of fire behaviour. Remote Sensing of Environment 255, 112282. https://doi.org/10.1016/j.rse.2020.112282

Geremew, T., Gonsamo, A., Zewdie, W., Pellikka, P., 2023. Extrapolation of canopy height and cover metrics of GEDI LiDAR in tropical montane forest ecosystem. African Geographical Review 1–17. https://doi.org/10.1080/19376812.2023.2164865

Gupta, A., Byrne, J., Moloney, D., Watson, S., Yin, H., 2020. Tree Annotations in LiDAR Data Using Point Densities and Convolutional Neural Networks. IEEE Trans. Geosci. Remote Sensing 58, 971–981. https://doi.org/10.1109/TGRS.2019.2942201

Harder, P., Pomeroy, J.W., Helgason, W.D., 2020. Improving sub-canopy snow depth mapping with unmanned aerial vehicles: lidar versus Structure-from-Motion techniques. The Cryosphere 14, 1919–1935. https://doi.org/10.5194/tc-14-1919-2020

Hassan, A., 2019. Transfer learning from RGB to multi-band imagery. URL https://www.azavea.com/blog/2019/08/30/transfer-learning-from-rgb-to-multi-band-imagery/

Hillman, S., Wallace, L., Lucieer, A., Reinke, K., Turner, D., Jones, S., 2021. A comparison of terrestrial and UAS sensors for measuring fuel hazard in a dry sclerophyll forest. International Journal of Applied Earth Observation and Geoinformation 95, 102261. https://doi.org/10.1016/j.jag.2020.102261

Hoffrén, R., Lamelas, M.T., De La Riva, J., 2024. Evaluation of handheld mobile laser scanner systems for the definition of fuel types in structurally complex Mediterranean forest stands. Fire 7, 59. https://doi.org/10.3390/fire7020059

Hoffrén, R., Lamelas, M.T., De La Riva, J., 2023a. UAV-derived photogrammetric point clouds and multispectral indices for fuel estimation in Mediterranean forests. Remote Sensing Applications: Society and Environment 31, 100997. https://doi.org/10.1016/j.rsase.2023.100997

Hoffrén, R., Lamelas, M.T., De La Riva, J., Domingo, D., Montealegre, A.L., García-Martín, A., Revilla, S., 2023b. Assessing GEDI-NASA system for forest fuels classification using machine learning techniques. International Journal of Applied Earth Observation and Geoinformation 116, 103175. https://doi.org/10.1016/j.jag.2022.103175

Kang, Y., Ozdogan, M., Gao, F., Anderson, M.C., White, W.A., Yang, Yun, Yang, Yang, Erickson, T.A., 2021. A data-driven approach to estimate leaf area index for Landsat images over the contiguous US. Remote Sensing of Environment 258, 112383. https://doi.org/10.1016/j.rse.2021.112383

Knight, C.A., Tompkins, R.E., Wang, J.A., York, R., Goulden, M.L., Battles, J.J., 2022. Accurate tracking of forest activity key to multi-jurisdictional management goals: A case study in California. Journal of Environmental Management 302, 114083. https://doi.org/10.1016/j.jenvman.2021.114083

Korznikov, K.A., Kislov, D.E., Altman, J., Doležal, J., Vozmishcheva, A.S., Krestov, P.V., 2021. Using U-Net-Like Deep Convolutional Neural Networks for Precise Tree Recognition in Very High Resolution RGB (Red, Green, Blue) Satellite Images. Forests 12, 66. https://doi.org/10.3390/f12010066

Mohan, M., Silva, C.A., Klauberg, C., Jat, P., Catts, G., Cardil, A., Hudak, A.T., Dia, M., 2017. Individual tree detection from unmanned aerial vehicle (UAV) derived canopy height model in an open canopy mixed conifer forest. Forests 8, 340. https://doi.org/10.3390/f8090340

Navarro, A., Young, M., Allan, B., Carnell, P., Macreadie, P., Ierodiaconou, D., 2020. The application of Unmanned Aerial Vehicles (UAVs) to estimate above-ground biomass of mangrove ecosystems. Remote Sensing of Environment 242, 111747. https://doi.org/10.1016/j.rse.2020.111747

Roussel, J.-R., Auty, D., De Boissieu, F., Sánchez Meador, A., Jean-François, B., Demetrios, G., Steinmeier, L., Adaszewski, S., 2023. lidR: Airborne LiDAR Data Manipulation and Visualization for Forestry Applications.

Safonova, A., Guirado, E., Maglinets, Y., Alcaraz-Segura, D., Tabik, S., 2021. Olive Tree Biovolume from UAV Multi-Resolution Image Segmentation with Mask R-CNN. Sensors 21, 1617. https://doi.org/10.3390/s21051617

Shin, P., Sankey, T., Moore, M., Thode, A., 2018. Evaluating unmanned aerial vehicle images for estimating forest canopy fuels in a ponderosa pine stand. Remote Sensing 10, 1266. https://doi.org/10.3390/rs10081266

Stephens, S.L., Foster, D.E., Battles, J.J., Bernal, A.A., Collins, B.M., Hedges, R., Moghaddas, J.J., Roughton, A.T., York, R.A., 2023. Forest restoration and fuels reduction work: Different pathways for achieving success in the Sierra Nevada. Ecological Applications e2932. https://doi.org/10.1002/eap.2932

Wang, Y., Fang, H., Zhang, Y., Li, S., Pang, Y., Ma, T., Li, Y., 2023. Retrieval and validation of vertical LAI profile derived from airborne and spaceborne LiDAR data at a deciduous needleleaf forest site. GIScience & Remote Sensing 60, 2214987. https://doi.org/10.1080/15481603.2023.2214987

Weinstein, B.G., Marconi, S., Aubry-Kientz, M., Vincent, G., Senyondo, H., White, E.P., 2020. DeepForest: A Python package for RGB deep learning tree crown delineation. Methods Ecol. Evol. 11, 1743–1751. https://doi.org/10.1111/2041-210X.13472

Zhang, W., Qi, J., Wan, P., Wang, H., Xie, D., Wang, X., Yan, G., 2016. An easy-to-use airborne LiDAR data filtering method based on cloth simulation. Remote Sensing 8, 501. https://doi.org/10.3390/rs8060501